In Vivo Characterisation of Ischaemic Preconditioning in Rodents and Humans

Thesis presented for the degree of Doctor of Philosophy in the Division of Medicine, University College London

William John Jenner

DECLARATION

“I, William Jenner confirm that the work presented in this thesis is my own. Where information has been derived from other sources, I confirm that this has been indicated in the thesis.”

in vivo veritas

ABSTRACT

Prolonged arterial occlusion results in ischaemic cell death. Reperfusion is necessary to prevent irreversible tissue infarction, but paradoxically contributes to some cell death. The composite ischaemia-reperfusion (IR) injury, contributes to tissue damage in common clinical conditions, and reducing IR injury remains a validated therapeutic target.

Ischaemic preconditioning (IPC) attenuates IR injury and is elicited by non-lethal periods of ischaemia in advance of a prolonged arterial occlusion. IPC also exerts a systemic protective effect, remote ischaemic preconditioning (RIPC), which is believed to occur through activation of humoral and neural pathways.

Experiments in this thesis investigated IPC and RIPC using four *in vivo* models. Firstly, in a rat model of stroke caused by transient occlusion of the middle cerebral artery, RIPC induced by limb ischaemia reduced infarct size. Secondly, in healthy volunteers *in vivo,* vascular occlusion caused endothelial IR injury of the brachial artery and this model was used to determine whether physical exercise elicited a protective phenotype similar to RIPC. In these experiments, only IPC has an effect to reduce IR injury. Thirdly, the inflammatory response to cantharidin was used in healthy volunteers to model the innate immune response, and to compare the anti-inflammatory effects of aspirin and IPC. Aspirin reduced inflammation in subjects with an early resolution phenotype, but IPC had no effect on the immune response. Fourthly, the effect of IPC on the response to exercise was investigated in healthy cyclists. IPC did not alter exercise capacity but increased skeletal muscle oxygenation in humans during an incremental exercise test. The results in this thesis complement certain previous observations and provide evidence of heterogeneity in the protective phenotype of IPC and RIPC.

ACKNOWLEDGEMENTS

The British Heart Foundation and the UCLH/UCL Comprehensive Biomedical Research Centre, for their financial support of my research.

The study volunteers, to whom I am personally indebted. Thank-you for your willing participation, despite the pins-and-needles, blisters, and cramped thighs.

Ms. Valerie Taylor, Dr. Inmaculada Villar, and Professor Mark Lythgoe, for their technical expertise in the middle cerebral artery occlusion model.

Dr. Michael Okorie, Dr. Stavros Loukogeorgakis, and Dr. Kristin Veighey for their guidance in the vascular ultrasound technique, and advice in dealing with the trials and tribulations of human research.

The British Olympic Medical Institute, Ms. Carissa Fallan, Dr. Brian Cunniffe, and Dr. Marco Cardinale for their financial support, expert assistance, and enthusiasm throughout the exercise testing.

The Gilroy research group, Dr. Alastair O'Brien, Dr. Tatsiana Audzevich, Dr. Simon Yona and Ms. Justine Newson for their welcoming nature, guidance, and constructive approach to the blister project.

The UCL students, Mr. Edgar Brodkin, Ms. Chloe Rayner, Ms. Adrienn Gyori, and Dr. Madhur Motwani, for their patience and commitment to the research.

Professor Derek Gilroy, Professor Hugh Montgomery and Professor Gordon Stewart for their intellectual input, invaluable advice, and encouragement over the past three years.

Professor Raymond MacAllister for having faith in my abilities. Without your mentorship, patience and sense of humour, I could not have achieved this goal.

Finally to my parents, family, friends and to Bernie. Throughout the PhD you have shown me unwavering support, for which I am eternally grateful.

TABLE OF CONTENTS

LIST OF FIGURES

LIST OF TABLES

LIST OF EQUATIONS

LIST OF ABBREVIATIONS

ACh	acetyl choline
Akt	protein kinase B
ANCOVA	analysis of covariance
ANOVA	analysis of variance
ADP	adenine diphosphate
α (alpha)	type I error
AMP	adenine monophosphate
ATP	adenine triphosphate
BBB	blood brain barrier
BE	base excess
BL	baseline
cAMP	cyclic adenosine monophosphate
CCA	common carotid artery
CV	coefficient of variation
EDHF	endothelium-derived hyperpolarising factor
EDTA	ethylenediaminetetraacetic acid
ELISA	enzyme-linked immunosorbent assay
eNOS	endothelial nitric oxide synthase
ExPC	exercise preconditioning
Erk	extraregulated kinase
FMD	flow mediated dilatation
FSC	forward scatter
GABA	gamma-aminobutyric acid
GLUT	glucose transporter
GMP	guanosine monophosphate
GPCR	g protein coupled receptor
Hb	haemoglobin
HCO_3^-	hydrogen bicarbonate
Hct	haematocrit
HIIT	high intensity interval training
HLA	human leukocyte antigen
HR	heart rate
ICAM-1	intercellular adhesion molecule-1
ICC	intraclass correlation coefficient
IL-	interleukin
IPC	local ischaemic preconditioning
IPostC	local ischaemic postconditioning
IR	ischaemia-reperfusion
La	lactate
L-FMC	low-flow mediated constriction
MAPK	mitogen activated protein kinases
MCA	middle cerebral artery
MDSC	myeloid derived suppressor cell
MFI	mean fluorescence intensity
MHC	major histocompatibility complex
mK_{ATP}	mitochondrial ATP-dependent potassium channel

mg	milligram
ml	millilitre
mPTP	mitochondrial permeability transition pore
NAD^+	nicotinamide adenine dinucleotide
NIRS	near-infrared spectroscopy
NO	nitric oxide
PBS	phosphate buffered solution
PKA	protein kinase A
PKC	protein kinase C
PKG	protein kinase G
RIPC	remote ischaemic preconditioning
RIPerC	remote ischaemic perconditioning
RIPostC	remote ischaemic postconditioning
RISK	reperfusion injury salvage kinase
ROS	reactive oxygen species
RPE	rating of perceived exertion
rpm	revolutions per minute
SD	standard deviation
SSC	side scatter
StO_2	saturation of tissue oxygenation
THI	tissue haemoglobin index
T_{MAX}	peak or maximal exercise
TNF-α	tumour necrosis factor-alpha
T_{SUBMAX}	end of continuous submaximal exercise
TTC	triphenyl tetrazolium chloride
TTE	time to exhaustion
$\dot{V}_{CO_2}$	carbon dioxide elimination
$\dot{V}_E$	ventilation
$\dot{V}_{O_2}$	oxygen delivery
VTI	velocity time integral
W	watt
W/min	watts per minute
WR	work rate

1. INTRODUCTION

1.1. Background

Cardiovascular disease has a high morbidity and mortality in the developed world. The 2006 death rate for cardiovascular disease in the USA was 263 per 100,000 (1), and currently accounts for 1 in 3 deaths in the UK (191,000 deaths/year) (2). Atherosclerotic cardiovascular disease often results in either total or partial arterial occlusion, and presents clinically as an acute ischaemic event such as myocardial infarction (124,000/year in the UK) or stroke (152,000/year in the UK) (3). Despite improvements in treating cardiovascular disease over the past 30 years, reducing the burden further requires improved prevention of atherosclerotic cardiovascular events, and improved treatment when these events occur.

In addition to acute ischaemic emergencies, ischaemia occurs during elective surgical procedures, such as coronary artery bypass graft surgery and organ transplantation. In both of these examples of emergency and elective cases, arterial flow to an organ or tissue is critically reduced, and this limits supply of oxygen and glucose, and removal of waste metabolites. Treatments of ischaemia, including bypass, percutaneous coronary intervention, and thrombolysis, rely on rapid restoration of oxygenated blood flow to the ischaemic tissue, which is vital in ensuring cell viability. Reperfusion however is commonly described as a "double-edged sword". Whilst vital for tissue recovery, reperfusion paradoxically contributes to cellular injury (4). The resultant damage from a combined ischaemic event and treatment by reperfusion, is known collectively as an ischaemia-reperfusion (IR) injury.

One of the most widely studied interventions to reduce IR injury is ischaemic preconditioning (IPC). Ischaemia acts as physiological hormesis; whilst a prolonged episode causes cellular injury, brief non-lethal bouts are well tolerated, and can induce a protective phenotype against subsequent ischaemic injury. During IPC, a tissue or organ

is exposed to brief periods of non-lethal intermittent ischaemia and reperfusion prior to the prolonged ischaemic event (5). Furthermore IPC is believed to induce a systemic protective effect, such that tissues distant to the site of IPC also become protected against IR injury (6). IPC and variants thereof are currently undergoing human clinical trials for a variety of ischaemic conditions (7).

The pathophysiology of IR injury involves a complex interaction between numerous mechanisms, and hence results from *in vitro* studies are often not replicated *in vivo*. Furthermore findings in animal experiments often fail to provide sufficient efficacy and safety when studied in human clinical trials (8). This highlights the importance of well-designed animal models, and the necessity for human *in vivo* models to ensure that early findings have the potential to contribute as useful clinical treatments.

My PhD comprises an investigation into the mechanisms of IPC. I have utilised four *in vivo* models (one rat model, three human models) to describe the effects of IPC on stroke, the vascular endothelium, acute inflammation, and muscle oxygenation. This thesis describes two years and five months of research.

1.2. Ischaemia-reperfusion injury

The injury resulting from a prolonged arterial occlusion and subsequent reperfusion is termed ischaemia-reperfusion (IR) injury. Below are described the mechanisms which contribute to the pathophysiology of IR injury, firstly during ischaemia, and secondly during reperfusion.

1.2.1. Ischaemic injury

Arterial occlusion reduces the delivery of oxygen to tissues, and the removal of toxic waste metabolites. The cellular response to ischaemia is to reduce energy consumption, and to switch towards oxygen-independent energy pathways. From the onset of acute

ischaemia cells become reversibly injured. As ischaemia is prolonged, cellular injury becomes irreversible, resulting in a complete tissue infarction, which can be lethal to the organ.

Given that ischaemic heart disease has a high worldwide mortality, and that several well-categorised *in vitro* and *in vivo* animal models of myocardial IR injury exist, most of the mechanistic changes understood to occur during ischaemia are based upon observations from myocardial experiments. In describing the mechanism of injury this report primarily details cells in the ischaemic myocardium, before specifically reporting the endothelial, cerebral, and skeletal musculature response to ischaemia.

1.2.1.1. Mechanism of ischaemic injury

Cells with a high metabolic demand, such as cardiomyocytes, have poor tolerance to ischaemia. The degree of injury is dependent on the totality of the occlusion, the duration of the occlusion, and the volume of tissue supplied by the occluded vessel. Animal studies have shown that after forty minutes of coronary artery occlusion, 28% of the area at risk is irreversibly injured, rising to 70% after three hours (9). The mechanism by which ischaemia induces cell death involves a series of intracellular changes (see Figure 1.1).

Healthy cardiomyocytes use oxidative phosphorylation of fatty acids and carbohydrates to supply energy in the form of adenine triphosphate (ATP). During ischaemia, insufficient oxygen supply leads to a series of downstream effects which are detrimental to cell viability. During early coronary ischaemia (15-20 seconds from onset), any oxygen available as oxyhaemoglobin in capillaries is exhausted, $NADH_2$ / NAD^+ ratio increases (10), and ATP and phosphocreatine are depleted (11). Anaerobic metabolism is required to generate additional ATP (12).

To compensate for a halting of oxidative phosphorylation, ATP demand is reduced by decreasing membrane potential and cessation of cardiomyocyte contractions. Nonetheless demand outstrips supply. Additional ATP is provided as NADH is oxidised to NAD^+, and by lactate dehydrogenase catalysing the reduction of pyruvate to lactate. The ATP-dependent phosphorylation of fructose-6-phosphage to fructose-1,6-diphosphate is necessary for continued glycolysis, but stops when ATP becomes critically low (11).

Lack of blood flow during ischaemia also prevents the removal of waste metabolites from tissue. This increases concentration of several glycolytic products including glucose-6-phosphate, alpha glycerol phosphate, and glucose-1-phosphate. In addition intracellular accumulation of adenine diphosphate (ADP) is detrimental to cell survival. ADP is converted to ATP and adenosine monophosphate (AMP), and AMP to hypoxanthine. Hypoxanthine along with lactate, acyl carnitine, CoA and H^+ accumulate and contribute to structural changes that result in cellular necrosis (10).

The catabolism of ATP, creatine phosphate and glycogen in the ischaemic cell rapidly increases the number of molecules within it, increasing the osmotic load (10). Water moves along the osmotic gradient, and causes cell swelling. Osmolar load changes alter intracellular ion concentrations, notably resulting in potassium ions being exported extracellularly, potentially contributing to ischaemic cardiac arrhythmias.

Lactate produced during glycolysis lowers intracellular pH and further disrupts the ionic balance within the cell. Reduced activity of the ATP-sensitive Ca^{2+} channel, causes subsequent increase in intracellular calcium. The ATP-dependent Na^+ / K^+ exchanger slows, possibly due to reactive oxygen species (ROS) accumulation (13), resulting in an increase in intracellular Na^+ (14).

During the initial 30-40 minutes of myocardial ischaemia, alterations to intracellular chemistry lead to changes in cell structure. By this point many cells will have suffered irreversible injury, primarily due to mitochondrial swelling, loss of glycogen stores, aggregation of nuclear chromatin, and sarcolemmal disruption. Sarcolemmal injury occurs due to the cytoskeletal and membrane disruption that follows catabolite accumulation. This is believed to be a trigger of cardiomyocyte death, because the sarcolemma releases critical intracellular enzymes into the extracellular space (10).

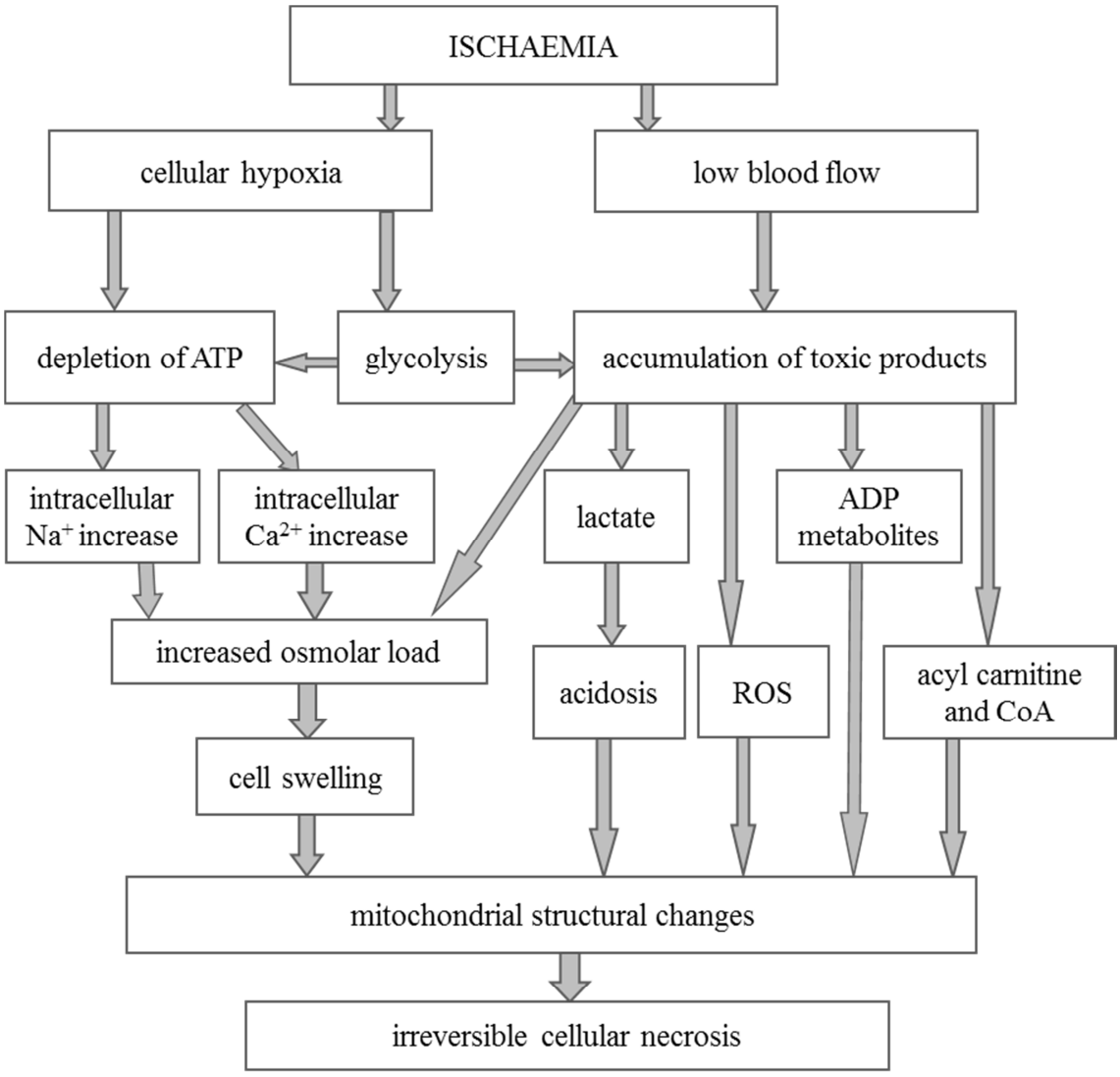

Figure 1.1 Mechanism of ischaemic injury. Ischaemia causes hypoxia and a low flow state. This results in rapid depletion of adenine triphosphate (ATP), the development of anaerobic metabolic pathways, and an accumulation of toxic metabolites. The depletion of ATP disrupts ATP-dependent ion channels, resulting in an increase in intracellular Na^+ and Ca^{2+}, and hence cell swelling. This in combination with toxic reactive oxygen species (ROS), adenine diphosphate (ADP) metabolites, acyl carnitine, CoA and an acidosis, causes structural changes in the mitochondria, leading to irreversible cellular necrosis.

1.2.1.2. Endothelial ischaemic injury

The cellular response to ischaemia in the endothelium resembles that in the myocardium. It appears that in the myocardial microvasculature, the endothelium is more tolerant of ischaemia than cardiomyocytes, most likely due to a reduced energy demand when compared with surrounding cells (10). As such during myocardial ischaemia, endothelial destruction does not occur until substantial irreversible cardiomyocyte injury has occurred (10). The resistance to ischaemia by endothelial cells is supported by human studies showing that endothelial dysfunction induced by IR injury is transient, and restored by 60 minutes of reperfusion (15). In peripheral conduit arteries the exact changes during ischaemia are less well characterised than the myocardium, but endothelial cells are known to suffer from metabolic and ionic imbalance, structural damage, and cell swelling in a similar manner to cardiomyocytes (14).

The endothelium is crucial in the maintenance of vascular tone by release of endogenous mediators. In response to ischaemia there is a reduced production of vasodilator and cytoprotective substances, such as nitric oxide (NO) and prostacyclin; an increase in vasoconstrictors, such as thromboxane A2 and endothelin-1; and an increase in pro-inflammatory mediators such as cytokines and adhesion molecules (16). Prolonged ischaemia can cause structural alterations to endothelial cells, resulting in endothelial protrusions that may contribute to myocardial no-reflow, a phenomenon associated with reperfusion injury (17).

1.2.1.1. Cerebral ischaemic injury

Cerebral neurons and glia, like cardiomyocytes, have a high demand for glucose and oxygen. Cells undergo changes similar to those described above, with the addition of some specific neuronal alterations. Cerebral artery occlusion is characterised by two

ischaemic regions. Firstly, a core of absolute no-flow that undergoes a rapid irreversible necrotic cell death. Secondly, an ischaemic penumbra, a region of low flow around the ischaemic core that retains partial blood supply through the collateral vasculature, and therefore undergoes a slower progression to cell death (18).

In the ischaemic core, lactate and other metabolites accumulate, resulting in acidosis, ionic imbalance, oedema, and necrosis. In addition the energy deficit causes neurons to depolarise, which activates voltage-gated ion channels. Channels release excitatory neurotransmitters, such as glutamate, into the extracellular space, which cause stimulation of glutamate receptors on other neurones. This process is known as excitotoxicity, and results in a considerable increase in intracellular Na^+, Cl^- and Ca^{2+} concentrations, and subsequent cytotoxic oedema (19). As extracellular glutamate concentration increases, it moves into the penumbral regions, and propagates a wave of peri-infarct depolarisation (18).

1.2.1.2. Exercise-induced ischaemia

Some of these changes during ischaemia are mimicked by the effects of physical exercise of muscle. Exercise increases the requirement for high energy phosphate within myocytes. An increase in oxidative phosphorylation using the mitochondrial electron transport chain accounts for this, but relies on adequate oxygen supply. When exercise is performed at an increasing work rate, a mismatch occurs between oxygen demand and supply, such that aerobic metabolism alone can no longer maintain sufficient supply of ATP, and anaerobic metabolism is required to contribute to ATP requirements. This point is known as the anaerobic threshold, and is characterised by an exponential increase in carbon dioxide elimination, despite a constant increase in oxygen consumption. Anaerobic metabolism occurs by the splitting of phosphocreatine and anaerobic glycolysis. During high-intensity exercise this results in a number of

detrimental intracellular pathways, which are comparable to those occurring during low-flow ischaemia.

If glycolysis occurs at a rate which is faster than the tricarboxylic acid cycle can process pyruvate, then lactate will accumulate intracellularly in proportion relative to pyruvate production (20). The fundamental advantage of lactate production is that it allows for the reoxidation of NADH and H^+ to NAD^+, and thereby continues ATP production despite anaerobic conditions. However lactate production increases H^+ ions, which require intracellular buffering from circulating hydrogen bicarbonate (HCO_3^-). As work rate continues to increase, a threshold is reached whereby the buffering capacity of HCO_3^- is no longer sufficient to prevent the increase in intracellular H^+. This results in a number of adaptive physiological changes, including an increase in ventilatory drive, consumption of muscle glycogen, plasma electrolyte concentration, and a metabolic acidosis.

As in low-flow ischaemia, exercise-induced anaerobic metabolism results in an increased production of metabolic intermediates, such as alanine, alpha-glycerol phosphate, and pyruvate. These contribute to muscular fatigue obtained from exercising above the anaerobic threshold, and result in a reduction in power output (21). The mechanism that governs the halting of intense exercise varies between individuals is highly contentious, but believed to be a combination of central fatigue governed by the central neuronal response to intense exercise, and peripheral fatigue due to intracellular changes in the musculature (22). Place et al. summarised four major causes of peripheral muscular fatigue: an increase in intracellular inorganic phosphate concentration, an increase in reactive oxygen and nitrogen species (ROS), an increase in extracellular potassium, and a decrease in pH (21). This peripheral fatigue is comparable to low-flow ischaemia, because as described in 1.2.1.1, acidosis, altered

osmolar load, and ROS also contribute to the cellular dysfunction attributed to ischaemic injury. The metabolic effects of exercise differ in one important way from those of ischaemia, in that there is continual washout of metabolites.

1.2.1.3. Treatment of ischaemic injury

Treatment of ischaemia relies on rapid restoration of blood flow prior to irreversible injury. This is achieved clinically by thrombolysis, arterial bypass, or percutaneous intervention. Despite improvements in reducing the duration from onset of ischaemia to treatment, it is often the case that by the point of revascularisation, patients have already suffered substantial ischaemic injury. Treatment with reperfusion is crucial in the prevention of irreversible changes, but a paradoxical reperfusion injury inhibits recovery.

1.2.2. Reperfusion injury

The theory that reperfusion might contribute to the overall injury was first proposed by Jennings et al. who observed that a short duration of ischaemia followed by reperfusion induced a greater infarct than a longer duration of ischaemia without reperfusion (23). It is further supported by the reduction in infarct size caused by a variety of interventions timed to occur at reperfusion and hence unable to influence ischaemia, such as ischaemic postconditioning (IPostC) (24). Numerous therapeutic options have been developed to reduce reperfusion injury, yet despite promising results in preclinical studies, in clinical trials none have shown sufficient efficacy and safety to be incorporated into recommended revascularisation therapy (25–27).

Below are described the mechanisms of reperfusion injury. Again, the majority of evidence is from cardiac studies, but comparisons are drawn between these observations, and the cerebral and endothelial response to reperfusion.

1.2.2.1. Mechanism of reperfusion injury

Reperfusion injury might be considered as a flood following a drought: despite having all the necessary ingredients for recovery, their presence is overwhelming, and accentuates injury in an already fragile cell population. During reperfusion, rapid oxygen flux activates a number of detrimental pathways, and exaggerates components of cellular injury suffered during ischaemia (Figure 1.2). Dysfunctional cardiomyocytes release ROS from their mitochondria, which result in the denaturing of critical enzymes, membrane failure, nucleic acid damage, reduced NO bioavailability (28), and opening of the mitochondrial permeability transition pore (mPTP).

Other factors also play a role in promoting cellular injury during reperfusion. The Na^+ overload during ischaemia causes Na^+ / Ca^{2+} exchange during reperfusion, and results in a rise in intracellular calcium (29). Calcium causes a rapid attraction of actin and myosin molecules, inducing myofibrillar hypercontraction and ATP depletion (28), contributing to the breakdown of mitochondrial structure (30). In addition, the rapid restoration of physiological pH appears to exaggerate injury; given that reperfusion with an acidic buffer can reduce mPTP opening, and some protective techniques slow the return to a normal pH (28).

Reperfusion causes the opening of the mPTP, which is widely regarded as a crucial step in irreversible cellular injury (4). The opening of the mPTP causes uncoupled oxidative phosphorylation, mitochondrial swelling and rupture (28). Loss of mitochondria will quickly result in necrotic cell death, whereas inhibition of mPTP opening during reperfusion reduces injury (31).

Reperfusion injury causes cell death by three methods. This is primarily by necrosis, following mitochondrial rupture. Recent evidence has also suggested that cell death by autophagy and apoptosis may be important during reperfusion. Apoptosis is an ATP-

dependent programmed cell death, and follows extracellular activation of a caspase pathway by membrane receptors, or intracellular activation through the mPTP (30). The finding that inhibiting caspase pathways reduces infarct size supports a role for apoptosis in reperfusion injury (32). Autophagy and the ubiquitin proteasome system target proteins for degradation as part of regular protein renewal in cells, a process shown to be upregulated in reperfusion (33).

Another pathological process that complicates reperfusion is the no-reflow phenomenon; despite conduit vessel reperfusion, blood flow does not always return to the microvasculature, and ischaemia persists (34). Cells remaining in these ischaemic zones will continue to progress towards necrosis. The cause of no reflow is in part due to the previously described ischaemia-induced endothelial disruption. However, it is likely to be heavily influenced by the plugging of capillaries by the infiltration of the microcirculation of neutrophils, platelets, and mixed cell aggregates. Furthermore, the production of vasoconstrictors such as endothelin-1 by dysfunctional endothelial cells is likely to restrict return of flow.

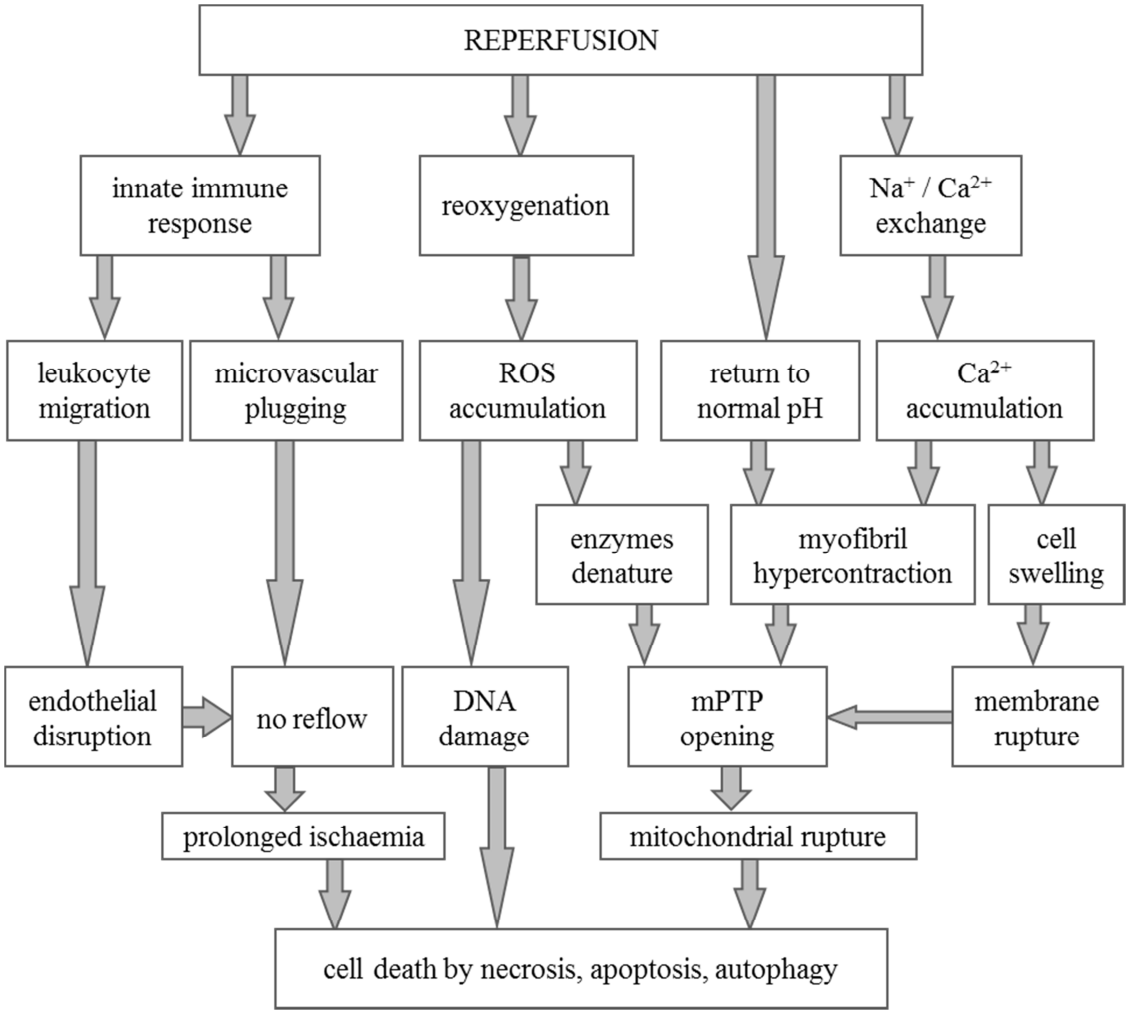

Figure 1.2 Mechanism of reperfusion injury. Reperfusion induces a rapid reoxygenation, resulting in production of reactive oxygen species (ROS), which lead to deoxyribonucleic acid (DNA) damage and protein degradation. This, in combination with rapid changes in pH, cell swelling following ion imbalance, and hypercontraction of myofibrils, leads to the opening of the mitochondrial permeability transition pore (mPTP), a trigger for subsequent cell death. There is a contribution of the innate immune response, which results in disruption of endothelial cells and microvascular plugging. This contributes to the no-reflow phenomenon and subsequent cell death.

1.2.2.2. Inflammatory response to reperfusion

During IR, tissues develop a proinflammatory state and an immune response similar to that designed for killing invading pathogens. Cytokines, complement, lipid mediators and ROS are released during ischaemia and early reperfusion, and promote endothelial rolling, adherence, and transmigration of neutrophils into reperfusing tissue (35). This occurs by an increased expression of P-selectin and intercellular adhesion molecule-1 (ICAM-1) on endothelial cells. Increased rolling promotes neutrophil adhesion molecule expression, such as the CD11b/CD18 glycoprotein complex. Our group has previously shown that limb IR injury increases expression of CD11b on circulating neutrophils (15).

Neutrophils are believed to contribute to tissue injury by release of enzymes and ROS within the extracellular space, by plugging the microvasculature and contributing to no-reflow, and promoting further neutrophil infiltration and activation. Enzymes released by neutrophils include elastases, collagenase, gelatinase, and acid hydrolases, which catalyse the degradation of the extracellular matrix comprising collagen, elastic, and glycoproteins (36).

Furthermore leukocytes release pro-inflammatory cytokines including IL-1ß, IL-8, and TNF-α. These cytokines act in a positive feedback, encouraging further leukocyte trafficking. Cytokines also act upon resident cells to activate apoptotic and necrotic pathways. Complement pathways are also activated during reperfusion, contributing to further leukocyte trafficking and cell death (37).

Recently, interest has grown into a high molecular weight protein complex, known collectively as the inflammasome. This is believed to govern the sterile inflammatory response to reperfusion by influencing cytokine release and activation of caspases. Kawaguchi et al. emphasised an important role for cardiac fibroblasts in governing the

response to myocardial IR injury (38). They then showed that ROS and K^+ efflux in fibroblasts causes the activation of IL-1ß, a process dependent on the inflammasome.

1.2.2.3. Endothelial reperfusion injury

Reperfusion injury reduces both receptor-dependent and receptor-independent endothelial function. Experiments in isolated animal coronary arteries show that following reperfusion, there is a reduction of endothelium-dependent vasodilatation, but not endothelium-independent vasodilatation, suggesting that the endothelium is much more susceptible to IR than surrounding smooth muscle (39,40).

Human *in vivo* studies from our group have shown that limb IR reduces endothelium-dependent dilatation in response to intra-arterial ACh (41). This dysfunction appears to be transient, with recovery by 60 minutes (15). Indeed, endothelial cells from canine coronary arteries appear to take much longer to recover from IR (42).

The cause of transient endothelial dysfunction in humans remains uncertain. This may be attributable to a reduced substrate bioavailability in the nitric oxide pathway, supported by evidence that administration of L-arginine preserves endothelial function following myocardial infarction in dogs (43). Alternatively organ bath studies have suggested that neutrophil adhesion and migration contributes to dysfunction (44). Reperfusion stimulated neutrophil migration disrupts the binding of the endothelium to the basement membrane, and causes inter-endothelial cell gap formation, increasing the permeability of the vasculature (28).

ROS are also likely to be a key contributor to post-IR endothelial dysfunction. ROS are known to substantially increase following reperfusion, and their inhibition can prevent experimental endothelial dysfunction (45). Chronic granulomatous disease patients have a genetic mutation in NADPH oxidase subunits, and subsequently have negligible oxidase activity in neutrophils. A recent study showed that these patients are resistant to

endothelial IR injury, when compared to matched controls, supporting a role for ROS in mediating endothelial IR injury (46).

1.2.2.1. Cerebral reperfusion injury

Reperfusion following cerebral ischaemia results in similar changes to those in the heart. Intracellular ROS concentration increases, damaging neuronal organelles, causing the opening of the mPTP and a release of proapoptotic molecules and critical intracellular enzymes. Inflammation is also likely to contribute to reperfusion injury in stroke. As in the heart, leukocytes are activated and infiltrate the cerebral parenchyma to subsequently release pro-inflammatory cytokines and chemokines. Inhibiting tumour necrosis factor (TNF)-α, a pro-inflammatory cytokine, with TNF binding protein can reduce experimental infarct size following middle cerebral artery occlusion (47).

In addition to the neuronal changes, reperfusion of the cerebral vasculature can cause destruction of the blood-brain barrier (BBB). The BBB is a cellular matrix comprised of tight junctions between endothelial cells, and is crucial in providing homeostatic control within the brain by restricting movement of high molecular weight proteins. During cerebral IR injury, the BBB degrades, primarily due to the detrimental effect of matrix metalloproteases, oxidative stress, thrombin and bradykinin on the tight junctions (48). This allows for a subsequent movement of high molecular weight proteins into the brain parenchyma, causing a vasogenic oedema. Furthermore, BBB destruction allows for the movement of leukocytes into the tissue. The now fragile vascular wall is also at an increased risk of reperfusion-induced haemorrhage.

1.2.2.2. Reperfusion following high intensity exercise

Following intense exercise, subsequent power output is reduced. This is supported from studies on individual myocytes, which show that following continued stimulation, maximal force will decline (49). The drop in function following intense exercise is

comparable to the post-ischaemic loss of cellular function attributable to reperfusion injury. Following the cessation of exercise, the cellular demand for high energy phosphate is dramatically reduced. As with post-occlusive reperfusion, the metabolic changes that contribute to peripheral muscular fatigue during exercise, such as metabolic acidosis, presence of waste metabolites, and increased extracellular potassium, are rapidly reversed (50). However despite this, force generation in recovering muscles remains reduced.

The cause of decreased force generation, as with classical reperfusion injury, appears due to the rapid ROS production in recovering myocytes (21). This is supported by evidence from Bruton et al. (51). They showed that mice overexpressing superoxide dismutase, which converts superoxide to hydrogen peroxide, had decreased sensitivity to calcium concentration. The lower sensitivity to calcium results in a decreased force output, suggesting that the presence of highly-reactive peroxide molecules contribute to muscular fatigue. Further studies have suggested that a range of ROS might contribute to exercise fatigue, without causing changes in calcium sensitivity (49). These results suggest that, as in classical reperfusion, the post-exercise delay in force recovery could be attributable to the detrimental effects of ROS on intracellular mechanisms.

1.2.2.3. Treatment of reperfusion injury

A large number of therapeutic interventions to treat reperfusion injury have been trialled in both animal and human studies. These have been summarised in several reviews (4,28,30), and include ROS scavengers, inhibitors of Na^+/H^+ exchange (52), NO donors (53), and mPTP inhibitors (26). Unfortunately, none have successfully shown sufficient efficacy and safety to be incorporated into current revascularisation therapy, and additional therapies are needed to tackle this clinical conundrum.

Another protective phenomenon is ischaemic conditioning. Application of intermittent non-lethal ischaemia applied prior to (preconditioning), during (perconditioning), or immediately following (postconditioning) a prolonged ischaemia is believed to induce a protective state against reperfusion injury. Ischaemic preconditioning, the intervention of interest in my PhD, is discussed in more detail below.

1.3. Ischaemic preconditioning

Unlike specifically targeted therapies, ischaemic preconditioning (IPC) is a protective phenomenon that influences multiple factors involved in the pathogenesis of IR injury. IPC was first observed by Murry et al., who exposed canine hearts to brief, intermittent episodes of IR (four cycles of five minutes ischaemia followed by five minutes of reperfusion) prior to a sustained (40 minutes) ischaemic insult, reperfusion and 4 days of recovery (5). IPC substantially reduced infarct size, and this effect has since been replicated in many mammalian species, and more recently in a number of clinical trials (7).

IPC was originally believed to target ischaemic injury, given that IPC reduced the rate of ATP depletion, and H^+ and lactate accumulation in the ischaemic myocardium (54). However, recent studies have shown that if intermittent ischaemia is applied at the point of reperfusion (IPostC), this also reduces infarct size. Given that IPostC can have no effect on cell behaviour during ischaemia, and yet reduces infarct size, it suggests that reperfusion injury is also a likely target for IPC (24). Furthermore inhibition of adenosine and bradykinin receptors at the point of reperfusion prevents IPC without influencing ischaemia. There remains uncertainty in the exact mechanism of IPC, but current theory is described below.

1.3.1. Local ischaemic preconditioning

Local ischaemic preconditioning (IPC) is the most widely studied type of conditioning stimulus. It is defined as the application of intermittent IR to an organ or tissue that will subsequently undergo a prolonged IR injury. IPC takes effect during an initial or early window, lasting for one to two hours after the stimulus; and a second or late/delayed window of protection, emerging 12 hours after the stimulus, and lasting for up to and over 72 hours (55).

The mechanism of early IPC can be described as having three phases: an initial trigger phase stimulated by the binding of endogenous autacoids to G-protein coupled receptors (GPCRs); a second mediator phase where intracellular pathways transfer the protective signal from membrane receptors to sites within the cell; and finally end effectors, which render the cell tolerant to IR injury (Figure 1.3). The second window of protection is believed to recruit similar pathways as the early window, and is associated with synthesis of protective proteins following gene transcription.

1.3.1.1. Triggers of ischaemic preconditioning

Intermittent ischaemia is believed to stimulate the release of a number of endogenous factors including adenosine, bradykinin and opioids, which bind to GPCRs on the cell surface membrane, namely adenosine A_1, bradykinin B2, and δ-opioid receptors. GPCRs are coupled to G proteins, which cause cyclic adenosine monophosphate (cAMP) production, or activate phospholipase C and protein kinase C (PKC) (56). Following adenosine receptor activation, phospholipase C generates diacylglycerol, which activates PKC. Bradykinin and opioid receptors activate phosphatidyl inositol-3 kinase (PI3 kinase). Protein kinase B (Akt) is then phosphorylated, activating endothelial nitric oxide synthase (eNOS), which forms NO. This stimulates guanylyl cyclase to produce cyclic GMP, which in turn stimulates protein kinase G (PKG) (56).

In addition, α and ß adrenoceptors may also trigger IPC, which is supported by evidence that α adrenoceptor agonists confer protection against subsequent IR injury using a PKC dependent mechanism (57). Adrenoceptors are GPCRs, and activate similar G protein coupled effects to those described above. There is therefore much redundancy in the pathway, and many of the components are targeted by drugs in clinical use for other indications.

1.3.1.2. Mediators of ischaemic preconditioning

Protein kinase A (PKA), PKC and PKG are key intracellular mediators of IPC, though the exact mechanism of action is uncertain. PKG is involved in the opening of the mitochondrial ATP-dependent potassium (mK_{ATP}) channel (58). ROS are believed to mediate IPC by increasing the opening of mK_{ATP} channels in a positive feedback loop with mitochondrial PKC-ε, and also by inhibiting the opening of the mPTP (56). In addition IPC activates the reperfusion injury salvage kinase (RISK) pathway, which involves a number of survival kinases such as PI3 kinase, Akt, Jun N-terminal kinases (JNKs), and mitogen-activated protein kinases (MAPK) including p38MAPK, extraregulated kinase 1/2 (Erk 1/2), and MAPK-activated protein kinase-2 (59). The role for the RISK pathway is supported by evidence showing that inhibiting kinase phosphorylation prevents IPC-induced cardioprotection (60).

1.3.1.3. End effectors of ischaemic preconditioning

The RISK pathway and other mediators effect protection by targeting several elements of the detrimental IR cascade. This includes preventing the opening of the mPTP through inhibition of GSK-3β, activation of PI3 kinase, or eNOS stimulation with NO release (31,61). Again, there is redundancy in these pathways, but it is generally accepted that central to the effector mechanism of IPC is the prevention of reperfusion-induced closure of the mitochondrial K_{ATP} channels and subsequent opening of the

mPTP. Whilst there remains gaps in the mechanism, it is known that IPC limits Ca^{2+} accumulation in the mitochondria (62), inhibits GSK-3β (63), activates the RISK pathway, and recruits eNOS (64), which are individually known to reduce mPTP opening. Mitochondrial K_{ATP} channels are involved in the prevention of membrane uncoupling and stabilisation of the mitochondrial membrane (65), ROS production (56), and inhibition of mPTP opening (56). PI3K and p38 MAPK activate glucose transporter 4 (GLUT4), resulting in an improved glucose uptake.

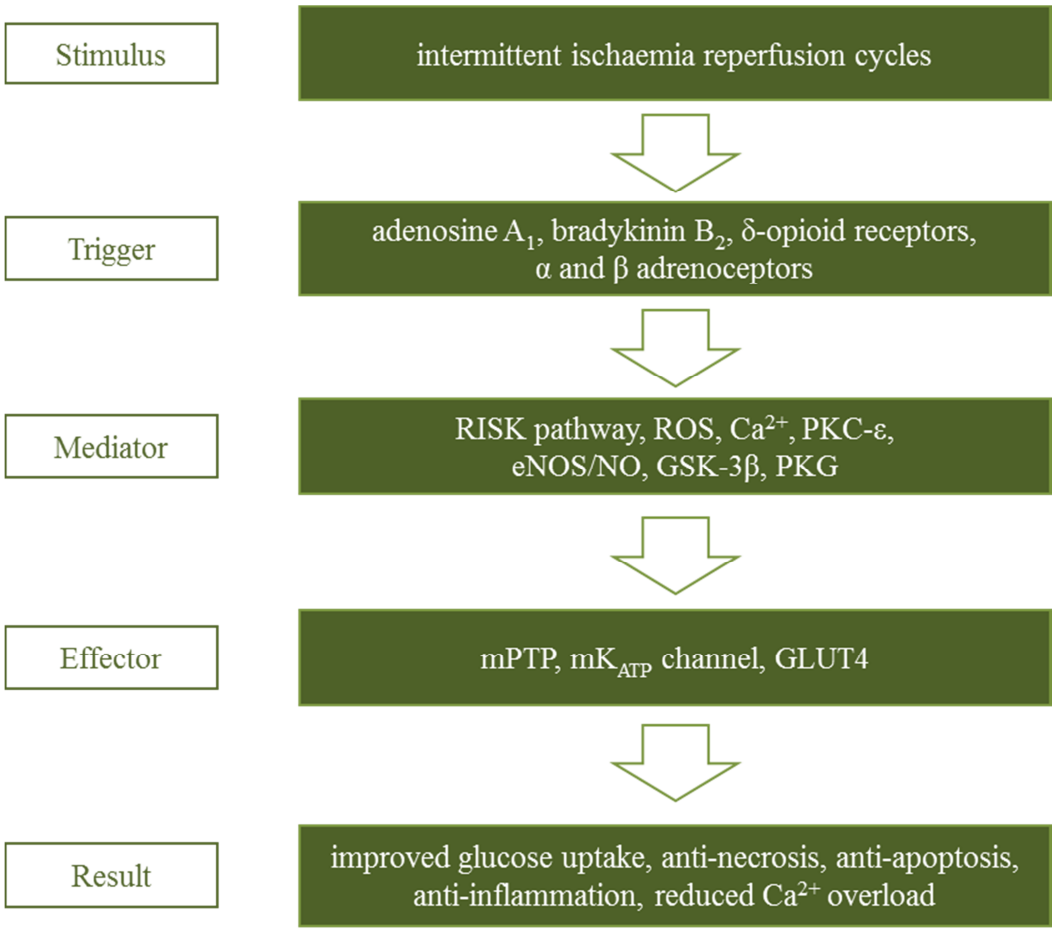

Figure 1.3 Mechanism of local ischaemic preconditioning. Intermittent cycles of ischaemia and reperfusion stimulate G-protein coupled receptors including adenosine A_1, bradykinin B_2, δ-opioid, and α and β adrenoceptors. These trigger intracellular mediators, in particular the reperfusion injury salvage kinase (RISK) pathway, reactive oxygen species (ROS), calcium ions (Ca^{2+}), endothelial nitric oxide synthase (eNOS), and other kinases (PKC-ε, GSK-3ß, PKG). The effect is a reduction in the opening of the mitochondrial permeability transition pore (mPTP), increased opening of the mitochondrial potassium (mK_{ATP}) channel, and activating the GLUT-4 transporter. These factors enhance tolerance to subsequent IR injury, by improving glucose uptake, and inhibiting cell death and inflammation.

1.3.1.4. Anti-inflammatory effects of ischaemic preconditioning

As discussed, reperfusion is associated with an acute, sterile inflammatory response. If IPC acts primarily on reperfusion, it is reasonable to hypothesise that IPC may alter the immune responses associated with reperfusion. Stimulation of eNOS, a mediator of IPC, results in the production of nitric oxide (NO), which is known to be anti-inflammatory.

The hypothesis that IPC is anti-inflammatory is supported by evidence from animal studies. Szabo et al. found that IPC prevents the IR-induced increase in leukocyte rolling and adhesion in rat tibial microcirculation, and prevents the increase in CD11b and ICAM-1 expression on leukocytes and peripheral tissue respectively (66). Erling et al. observed that IPC prevented the increase in leukocyte activation, and expression of selectins and ICAM-1, induced by mesenteric IR injury (67). Inhibiting chemosensitive C–fibres or calcitonin gene-related peptide receptors can prevent these anti-inflammatory effects of IPC (68).

In humans, the evidence for IPC influencing leukocyte trafficking is limited to observations made from *in vitro* neutrophil studies. Our group has previously shown that following upper limb IR injury, CD11b expression is increased in circulating neutrophils, and is prevented by IPC (15). The mechanism behind this might be due to interaction between neutrophils and endogenous autacoids, notably opioids and bradykinin (69,70). There is also evidence that IPC may prevent the no-reflow phenomenon by attenuating circulating monocyte-platelet aggregates (71).

Shimizu et al. performed an *in vitro* study phenotyping circulating human neutrophils following application of IPC (72). They observed a reduced adhesion of neutrophils to wells coated in fetal bovine serum, 24 hours after IPC stimulation. IPC also reduced neutrophil apoptosis, and increased in N-formyl-methionyl-leucyl phenylalanine-

stimulated CD63 and CD66b expression. However there were no changes in neutrophil CD11b expression, NADPH oxidase activity, phagocytosis, and cytokine expression following IPC. To date no study has investigated whether IPC modulates the human inflammatory response *in vivo*.

1.3.2. Remote ischaemic preconditioning

IPC also confers a systemic protective effect against IR injury. Przyklenk et al. observed in dogs that the region of myocardium supplied by the left anterior descending coronary artery could be protected from IR injury by IPC applied to the territory supplied by the circumflex artery (6). This result has been reproduced by several groups, and it is now understood that IPC applied to one tissue can prevent another from prolonged IR injury, a property known as remote ischaemic preconditioning (RIPC) (6). RIPC has since been shown to protect against IR injury in the heart (6), brain (73), kidney (74), skeletal muscle (75) and liver (76).

The observation that RIPC could be induced by intermittent IR of the limb (41), gave an opportunity to translate this systemic protective effect into human clinical trials (77). Intermittent limb ischaemia as a stimulus for RIPC is appealing as an intervention because it is non-invasive, simple to administer, and inexpensive.

1.3.2.1. Transferring the protective stimulus

In effecting protection, RIPC is believed to recruit similar intracellular pathways to local IPC, involving signalling kinases that act upon K_{ATP} channels and the mPTP to render the cell resistant to IR injury (78). The most intriguing element of RIPC is the pathway that transfers protection from the ischaemic stimulus to the site of injury. The current literature supports three hypotheses: that transfer of protection is mediated by neural, humoral and immunological mechanisms. The evidence supporting each hypothesis is described below.

The release of adenosine and bradykinin at the site of RIPC stimulus are believed to activate neural mechanisms. Evidence that the autonomic ganglion blocker trimetaphan can inhibit RIPC suggests the autonomic nervous system is involved (79). Recently Mastitskaya et al. have shown that the cardioprotection afforded by RIPC relies on intact activity of vagal pre-ganglionic neurones (80). They showed that RIPC as a therapy against rat myocardial IR injury was abolished by systemic muscarinic blockade using atropine, or by specific inhibition of vagal pre-ganglionic neurones. Another group have shown that protection afforded by limb RIPC can be prevented by femoral nerve transection (81).

The evidence for a humoral pathway is based on the observation that transfusing the blood of a preconditioned animal into that of a non-preconditioned animal can transfer the protective effect (82). Furthermore the dialysate of plasma from preconditioned rabbits or humans can effect protection against an experimental cardiac IR injury (83). This effect is abrogated by naloxone, suggesting that endogenous opioids are important in the humoral pathway.

As described, IPC modifies the inflammatory response to IR injury. Given that both IPC and RIPC reduce leukocyte rolling, it is possible that circulating leukocytes might transfer the protective effect (67). The modified neutrophil function observed by Shimizu et al. was from leukocytes acquired from the contralateral arm to that receiving intermittent ischaemia (72). RIPC also upregulates the pro-resolution cytokine interleukin-10 (84). Inhibition of cyclooxygenase 1 and 2 by SC-560 and rofecoxib respectively can inhibit RIPC in a model of gastric IR injury (85).

It is therefore possible that RIPC uses a multifaceted approach, with neural, humoral and anti-inflammatory factors overlapping to confer protection against IR. This is supported by evidence that inhibition of several alternative pathways can attenuate

RIPC. As with IPC there may also be mechanistic differences in the two windows of protection. Furthermore, it is likely that differences exist between the transfer of protection in RIPC between rodents and higher mammals.

1.3.2.2. Remote ischaemic preconditioning in experimental stroke

Preconditioning has been shown to protect against experimental rodent stroke (86). Initially this was evident using local IPC, by non-lethal occlusions of the middle cerebral artery (MCA) prior to prolonged IR (87). More recently it has been shown that RIPC induced by iliac or femoral artery occlusion, can reduce infarct size during cerebral ischaemia, in both a four-vessel occlusion method (88), and a permanent MCA occlusion (73). However, it is uncertain whether RIPC is effective in a transient model, which as described is more representative of human stroke.

The mechanism of cerebral protection is similar to that described in cardiac studies. Firstly there are two windows of protection (86,89). Secondly RIPC involves neural and humoral pathways, given that both ganglion blockade by hexamethonium, and antagonism of adenosine receptors inhibits cerebral protection by RIPC (90). Furthermore inhibition of NOS, a mediator of the preconditioning pathway, by L-NAME abrogates cerebral protection (88). Further work is required to investigate how RIPC modifies the MCA model in varying experimental conditions, including the occlusion strategy (permanent vs transient), anesthetic regime (inhaled vs injectable), and strength of RIPC stimulus.

1.3.3. Exercise as a preconditioning stimulus

In humans, performing regular physical exercise is associated with reduced mortality from cardiovascular events (91,92). This was believed to be related to exercise-induced reduction in traditional risk factors, such as obesity, hypertension, hypercholesterolaemia, and insulin resistance. More recently however, exercise has

been shown to protect against myocardial IR injury irrespective of these risk factors (93).

McElroy et al. reported that after 5 weeks of swim training, infarct size was reduced by 30% in rodent myocardial IR injury (93). This observation has been reproduced in several studies using alternative exercise training programs (94,95). The mechanism of training-induced preconditioning as a protective stimulus involves increased heat shock proteins, NO production, antioxidants, endoplasmic reticulum stress proteins, cyclooxygenase-2, development of collateral vasculature, and mitochondrial adaptation (reviewed by Kavazis et al. (96) and Powers et al. (97)).

1.3.3.1. Acute exercise preconditioning

A single bout of exercise increases heart rate, activates the sympathetic nervous system, and releases endogenous factors, including opioids, nitric oxide, α-adrenoceptor agonists, and bradykinin. High intensity exercise causes high flow ischaemia of exercising muscle, where oxygen supply is insufficient to meet metabolic demand. In animal models evidence suggests that exercise-induced preconditioning (ExPC) to reduce IR injury can be achieved by just a few days of exercise training (98), or even from a single exercise bout (99,100).

That ExPC activates IPC pathways is supported by results from Domenech et al., who found that 5 cycles of 5 minutes exercise followed by 5 minutes of rest can reduce canine myocardial IR injury, and like IPC it offered two windows of protection (99). Acute ExPC, like IPC, appears to involve mK_{ATP} channels and PKC (100,101).

In humans, studies have shown that exercise-induced myocardial ischaemia causes preconditioning, which is known as the “warm up phenomenon” (102). It has been documented for over 50 years that angina patients have fewer ischaemic symptoms in the second of two consecutive exercise stress tests, where exercise is limited by

myocardial pain or ECG changes (103). This exercise-induced high flow ischaemia has been shown to exhibit protection against interventional myocardial ischaemia over a comparable time window to IPC (104,105).

Moreover IPC can be compared to high-intensity interval training (HIIT). Brief, intermittent, high intensity exercise performed regularly reduces the risk of cardiovascular death in men and women (106). HIIT is known to increase intracellular kinase activity (such as p38 MAPK) (107), which is comparable to the intracellular mechanisms of IPC.

Like IPC, ExPC confers a systemic protective effect. Exercise induces protection in organs which are known to have minimal response to acute exercise, such as the brain. Jia et al. showed that 3 weeks of exercise training improves rat cerebral tolerance to IR (108). Evidence for systemic ExPC effects in humans is limited. Tyldum et al. showed that intake of a high fat meal induces endothelial dysfunction in healthy volunteers (109). This was prevented by an intense lower limb exercise protocol, performed 12-16 hours prior to the meal.

Brief exercise as a preconditioning stimulus is of interest in clinical settings, such as elective surgery. The long term health benefits of exercise in reducing cardiovascular risk factors have been widely reported (92), but if ExPC is known to reduce humans IR injury, this could promote the uptake of exercise in the wider population, and help to lower the burden of cardiovascular disease.

1.3.4. Ischaemic preconditioning as a treatment for IR injury in humans

In the past 10 years, IPC and RIPC have been suggested as treatments for IR injury in humans. Evidence for this is supported by experimental *in vivo* studies and randomised controlled clinical trials, which are described below.

1.3.4.1. Human ischaemia reperfusion injury studies

Our research group has developed a model of limb IR injury, by using vascular assessment tools to ascertain the effects of IR on endothelial function *in vivo* (15,41,79,110–112). Prolonged upper arm cuff inflation to a suprasystolic pressure followed by reperfusion induces a transient endothelial dysfunction in conduit and resistance vessels. Endothelial function has been assessed in two ways, firstly as a reduction in endothelium-dependent dilatation of resistance vessels in response to intra-arterial administration of acetylcholine (41). Secondly as a reduction in endothelium-dependent dilatation of conduit vessels in response to a hyperaemic stimulus, a phenomenon known as flow mediated dilatation (FMD) (15). This model has served to identify a number of interventions that reduce human IR injury, including IPC (15), RIPC (79), local and remote IPostC (111), nitrates (113) and HMG CoA reductase inhibitors (114).

1.3.4.1. Clinical trials of local ischaemic preconditioning

Local IPC has been trialled in a number of clinical conditions including cardiac surgery (7), liver transplantation (115) and lower limb orthopaedic surgery (116). A meta-analysis of randomised controlled trials of IPC in coronary surgery (23 trials, 933 patients) found a significant reduction in the number of ventricular arrhythmias, inotrope use, and length of intensive care stay in patients compared with controls (7). However a Cochrane review and meta-analysis of the benefits of IPC in liver resections (4 trials, 271 patients) found insufficient evidence to support a protective effect (117). Unfortunately meta-analyses of small trials cannot account for publication bias, and large, randomised controlled trials demonstrating clinically useful effects of IPC are needed before it can be adopted in clinical practice.

1.3.4.2. Clinical trials of remote ischaemic preconditioning

As described, the non-invasive nature of limb RIPC is appealing for use in patients. To date several small clinical trials have shown an improvement in clinical endpoints by RIPC, in coronary artery bypass graft surgery (118) aortic aneurysm repair (119), and acute kidney injury (120). However a meta-analysis of vascular or endovascular trials (4 trials, 115 patients) up to July 2011 found no difference between RIPC and control (121). Once again, large randomised trials are necessary to clarify the presence of a clinical benefit. A search of *www.clinicaltrials.gov* in August 2012 for *remote ischemic preconditioning* found 26 trials currently recruiting, suggesting that these questions will be answered within the next few years.

1.3.5. Ischaemic preconditioning and skeletal muscle function

Skeletal muscles are tolerant of brief low-flow ischaemia, most likely due to the necessity to readily perform anaerobic metabolism during intense exercise. Studying how IPC influences skeletal muscles can act as a proxy for how IPC affects vital organs such as the heart, during IR injury. Saito et al. found that IPC can improve the oxygen supply to the musculature during sciatic nerve stimulation of the gastrocnemius of rats (122). In addition muscle re-oxygenation following occlusion is improved by prior IPC in rats (123) and humans (124).

Methods for improving muscle function are of great interest in sport science. This is especially true for novel interventions that take advantage of the innate physiology. The oxygen transport system during exercise is critical in determining athletic performance, and interest has grown into interventions that can legally modify the rate-limiting steps, such as high-altitude training. Oxygen delivery is dependent on arterial oxygen saturation, haemoglobin concentration, arterial partial pressure of oxygen, muscle blood

flow, and muscle oxygen extraction (22), and studies use assessments of oxygen delivery ($\dot{V}_{O_2}$) and consumption as outcomes to relate to exercise performance.

Blood flow restriction in combination with exercise (known as KAATSU training) is known to encourage training effects on skeletal muscles, and to improve cardiovascular response to an orthostatic stimulus (125). Until recently however, no published studies had investigated whether IPC alone can improve muscle function in humans. Groot et al. recorded that IPC improves human exercise performance on an exhaustive cycling exercise (126). They observed that suprasystolic cuff inflations consisting of three cycles of 5 minutes ischaemia followed by 5 minutes reperfusion on both lower limbs, improved exercise performance in a subsequent incremental exercise test. IPC improved maximal oxygen delivery ($\dot{V}_{O_2\ max}$) by 3% and maximal power output (WR_{max}) by 1.6% in 15 well trained cyclists (126).

Crisafulli et al. performed a similar experiment, whereby subjects were randomised to control, IPC or a submaximal exercise and IPC combination, prior to an incremental exercise test (127). Both IPC and the exercise and IPC combination increased maximal power output (4%), total exercise time, maximal ventilation, and maximal heart rate, when compared to control. Unlike the previous study, they did not observe any change in $\dot{V}_{O_2\ max}$ with IPC. Further evidence suggests that upper limb IPC can improve performance in a standardised swimming test (128). However Clevidence et al. found no effect with IPC on either submaximal or maximal testing for ventilatory or performance outcomes (129). Whilst evidence suggests that IPC may improve muscular function, differences exist in the literature as to whether this is reflected in an improved exercise performance.

1.4. Scope of thesis

In this thesis I plan to investigate the mechanisms of IPC using *in vivo* models of IR injury. Firstly, by using a rat model to study the effects of RIPC on a cerebral IR injury caused by transient occlusion of the middle cerebral artery following reperfusion. Secondly, by using a human vascular model to study the effects of IPC, RIPC and ExPC on endothelial IR injury. Thirdly, by using a human skin blister model to study the anti-inflammatory effects of IPC. Finally, by using a human exercise test to investigate the effects of IPC on muscular oxygenation and exercise performance.

1.5. Hypotheses

- Remote ischaemic preconditioning protects against cerebral ischaemia-reperfusion injury in rats.

- Exercise and ischaemic preconditioning protect against endothelial ischaemia-reperfusion injury in humans.

- Ischaemic preconditioning reduces leukocyte trafficking to an inflammatory stimulus in humans.

- Ischaemic preconditioning increases skeletal muscle oxygenation and improves exercise performance in humans.

2. GENERAL METHODS

2.1. In vivo assessment of cerebral ischaemia-reperfusion injury in rats

2.1.1. Background

Human ischaemic stroke is typically associated with thromboembolism, which results in arterial occlusion within the cerebral circulation. To identify and characterise novel therapies for human stroke, it is crucial to begin with an adequate animal model. Stroke models allow researchers to investigate potential treatments for efficacy and safety prior to human clinical trials. However, as with many animal *in vivo* models, stroke studies are often limited by being unrepresentative of the disease in question and by exhibiting a large within-population variability.

Studying stroke in rodents has become increasingly popular since the development of genetically modified mice, and the general trend towards conducting fewer experiments in higher mammals. However despite a variety of therapies showing promise in murine stroke models, the majority have failed to translate to clinical practice in humans, and currently the only licensed therapeutic agents to treat ischaemic stroke in the UK are the recombinant tissue plasminogen activator alteplase, the thienopyridine clopidogrel, and aspirin (130).

Two factors that differ between human and experimental animal stroke continue to hamper the translation of therapies from animals to human. Firstly, most human strokes will undergo a period of occlusion, followed by reperfusion, either due to thrombolytic therapy (131) or the development of collateral flow (132), whereas many experimental stroke models consist of ischaemia only. Secondly, human strokes are usually less than 10% of the hemispheric volume, whereas animal studies often tend to involve at least 30% of the hemispheric volume (133).

Research to date using animals has had three main objectives. Firstly, to improve the understanding of the pathophysiology of stroke, the cellular changes which occur during it and in particular the elements that contribute to cell death or towards cell preservation. Secondly to understand which risk factors contribute to stroke. Finally, to test novel interventions that aim to develop new treatments against human stroke. These objectives have been studied in a variety of stroke models, which others have comprehensively reviewed (see Durukan & Tatlisumak, 2007 (134) and Carmichael, 2005 (133)). To investigate the role of ischaemic preconditioning in stroke a focal ischaemia-reperfusion model was used, that involved the temporary occlusion of the middle cerebral artery.

2.1.1.1. Middle cerebral artery occlusion

A number of different methods exist for inducing a murine ischaemic stroke, including craniectomy, embolic, endothelin-1 induced, photothrombosis and middle cerebral artery (MCA) occlusion stroke models (134). The current study, used an intraluminal suture MCA occlusion method (135), which has become the most widely used stroke model (136). It is less traumatic than alternatives, has a low within-population variability, and by allowing for reperfusion is more representative of human ischaemic stroke, which itself regularly involves occlusion of the MCA (137). The intraluminal suture model involves the insertion of a monofilament into the internal carotid artery, such that it occludes the MCA. This can be manipulated using occlusion of the contralateral carotid artery to reduce flow within the circle of Willis whilst the patent vertebral arteries ensure flow is maintained to the contralateral hemisphere.

2.1.1.2. Histological analysis

An assessment of infarct size can be determined by magnetic resonance imaging, or by histological staining. Given the necessity to rapidly produce results during method

development, and the logistical challenge of using magnetic resonance imaging, this study used a common histological method. Brain slices were stained using 2,3,5-triphenyltetrazolium (TTC). TTC identifies live tissue by producing a red precipitate in cells with active mitochondria. This results in a distinct contrast between infarcted and non-infarcted tissue, which can be measured by imaging software (Figure 2.2).

Histological variables include the number and thickness of the slices, the duration of dye exposure, the scanning hardware, the imaging software and the outlining technique. In addition, previous murine stroke experiments have observed that a cerebral infarct is associated with extensive vasogenic oedema within the tissue, which can introduce bias within the data, and should be accounted for when interpreting infarct size (138). Several equations have been suggested for calculating the infarct size (138,139), the majority of which use a correcting factor for oedema.

2.1.2. Experimental set up

All procedures were carried out in the UCL Centre for Advanced Biomedical Imaging, in a temperature controlled surgical facility. All surgical procedures were conducted by a UCL research technician, who has over twenty years of experience in performing *in vivo* animal research. I conducted the study design, provided technical support during the procedures, and performed all image analysis. All research was conducted according to the UK Home Office Guidelines under the 1986 Animals (Scientific Procedures) Act, and all procedures were outlined in the Home Office project license 70/6919. Experimental protocols are described in section 3.2.

2.1.2.1. Animal preparation

Male, Sprague Dawley rats (aged 10-12 weeks; Charles River Ltd, Margate, UK) were housed in filter cages in diurnal conditions for at least 24 hours prior to surgery. Rats weighed 180-220 g immediately prior to surgery, to reduce variability in cerebral artery

luminal diameters. Rats of smaller size were at risk of the filament piercing the cerebral vasculature, and in those of a larger size it was more likely that blood would flow around the filament.

2.1.2.2. Surgical procedure

Experimental stroke was induced using an intraluminal filament to cause a unilateral stroke of the region of the cerebral hemisphere supplied by the MCA. Rats were maintained using injectable anaesthesia in the majority of studies. Anaesthesia was induced with a mixture of 0.24 mg/kg fentanyl and 7.5 mg/kg fluanisone (Hypnorm, Vetaphama, UK), and 1.5 mg/kg midazolam hydrochloride (Hypnovel, Roche Products Ltd, UK) given in a 300 µl fluid volume as an intra-peritoneal (i.p.) injection. Midazolam, a short acting benzodiazepine, enhances the action of gamma-aminobutyric acid (GABA), the primary inhibitory neurotransmitter, on the GABA receptors in the neurones. Fentanyl, an opioid, primarily acts upon µ opioid receptors, and is used as an analgesic and anaesthetic agent. Fluanisone, a butyrophenone, is an antipsychotic and used to sedate the animal, and for maintenance of anaesthesia with fentanyl, to potentiate the anaesthetic and analgesic effect. Continued anaesthesia was maintained with 0.12 mg/kg fentanyl and 3.75 mg/kg fluanisone, administered as an i.p. injection every 30-60 minutes. Throughout surgery the body temperature was maintained at 37°C by use of a feedback regulated heating pad and the animals were carefully monitored to ensure suitable anaesthesia and respiratory function.

The surgical procedure is demonstrated in Figure 2.1. Firstly the neck flap was shaved, followed by a ventral midline neck incision, and the left and right common carotid arteries (CCA) were identified. The bifurcation of the right CCA into the internal and external carotid arteries was located, followed by the bifurcation of the pterygopalatine artery from the right internal carotid artery. A vascular clip was attached just proximally

to the first bifurcation of the right CCA, and a tie placed at the proximal end, to inhibit blood flow to the site of filament entry. The right CCA was then opened using vascular scissors, and a silicon rubber-coated monofilament (size 4-0, diameter with coating 0.35 ± 0.02 mm, filament length 30 mm, Doccol Corporation, USA) was advanced into the arterial lumen and directed into the internal carotid artery, such that the silicone tip of the filament rested within the circle of Willis, and blocked the entry of blood into the MCA. To aid positioning over the MCA, the monofilament had been pre-marked with a silver line 13 mm from the tip, such that the filament was assumed to be correctly positioned when the silver line reached just superiorly to the bifurcation of the pterygopalatine artery. At this point the filament was secured, and maintained in position for 60 minutes. In studies requiring a contralateral occlusion the left CCA was occluded using a vascular clip, and then released when necessary.

Reperfusion of the MCA was achieved by retracting the monofilament and by releasing the right CCA. This returned flow to the cerebral circulation, and the neck was closed up and animals recovered from anaesthesia in a temperature controlled (37°C) recovery box. Following recovery animals were returned to their filter cage, and monitored for evidence of recovery and neurological symptoms.

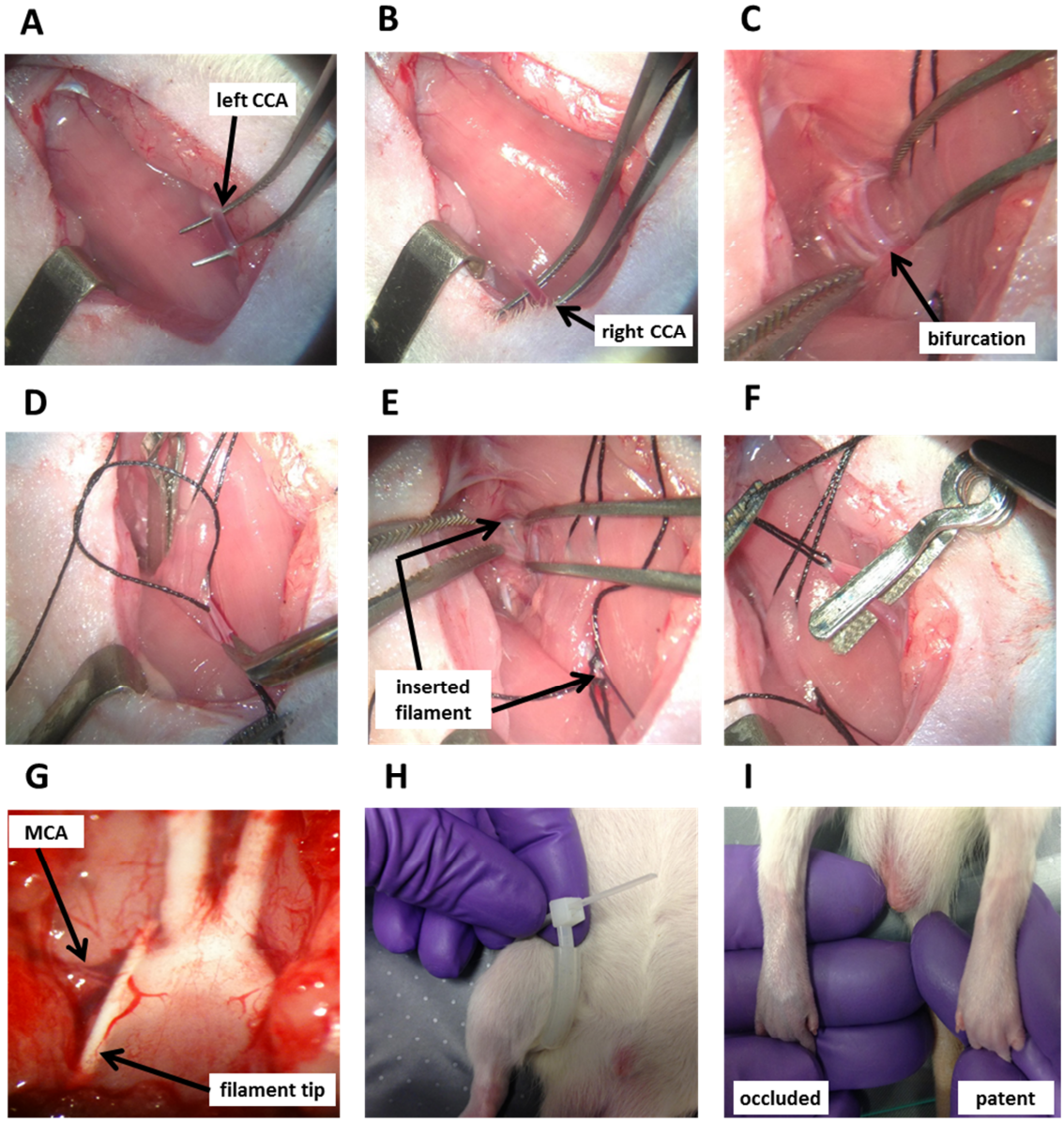

Figure 2.1 Experimental procedures for middle cerebral artery occlusion surgery. Initially the left (A) and right (B) common carotid arteries (CCA) were identified and isolated. A vascular clip was then placed just inferiorly to the bifurcation of the right CCA into the internal and external carotid artery (C). The right CCA was tied and a small incision made in the arterial wall (D) to allow for monofilament insertion. The filament was advanced into the internal carotid artery, and the position checked above the bifurcation of the pterygopalatine artery (E). The left CCA was occluded using a vascular clip (F). Dissection of the palate and viewing the ventral aspect of the brain confirmed that the filament occluded the MCA (G). RIPC was induced by tightening of a cable tie (H) at the top of the right thigh, and occlusion confirmed by a colour change in the ischaemic right paw (I).

2.1.2.3. Brain isolation

After 24 hours of recovery, animals were anesthetised (0.16 mg/kg fentanyl, 5 mg/kg fluanisone, 1 mg/kg midazolam hydrochloride i.p.) and culled by a schedule 1 procedure before decapitation. The skin around the head was extended back over the eyes, and the skull washed with water to remove blood and hair. The skull was opened using straight iris scissors from the entrance of the spinal cord to the eye sockets. A coronal cut was made between the eye sockets, and the crown of the skull was removed. The lateral edges of the skull were held back using a rongeur, and the brain was excised along the ventral aspect from caudal to rostral, to release the cranial nerves and vasculature. The brain was immediately placed on a 4 cm diameter filter paper disc, and two to three drops of lubricating oil (3 in 1, USA) were dropped on the top of the brain to aid slicing.

2.1.2.4. Histological staining of infarcted tissue

The brain was sliced from caudal to rostral into 1 mm slices using a tissue slicer (McIlwain Tissue Chopper, Mickle Laboratory Engineering Co. Ltd, UK). The sliced brain was immediately transferred to plate containing the staining dye (2% w/v TTC solution, Sigma Aldrich, USA) for 20 minutes at room temperature, where the slices were separated in a caudal to rostral fashion, ensuring that the slices arranged with the rostral side facing superiorly. Slices were then transferred to a fixing solution (formaldehyde 4% aqueous solution, VWR, USA) for 20 minutes. Slices were briefly dried using an absorbent paper, arranged vertically on a clear plastic sheet, and scanned (PIXMA MX700 2400 dpi, Canon, Japan) using a black background in preparation for image analysis.

2.1.2.5. Remote ischaemic preconditioning

Remote ischaemic preconditioning (RIPC) was induced by use of a cable tie to inhibit arterial flow to the right lower limb (Figure 2.1). The cable tie was tightened at the level of the hip to ensure that a large volume of thigh muscle received RIPC. Cable tie tightening initially resulted in neuromuscular injury in some cases, as animals were observed to be limping during recovery. This was avoided by passing a thin plastic tube through the cable tie, such that during tightening the pressure was spread evenly across the limb. Vascular occlusion was confirmed by observing that the skin became blue during cuff tightening.

2.1.2.6. MK-801

MK-801, ((+)-5-methyl-10,11-dihydro-5H-dibenzo(a,d) cyclohepten-5,10-imine maleate) is a known neuroprotective agent (140,141), which was used as a positive control in this study. It is a noncompetitive antagonist for the N-methly-D-aspratate (NMDA) receptor, which inhibits the release of glutamate into the extracellular space during ischaemia (see 1.2.1.1). Glutamate accumulation causes excitotoxicity and is associated with cell swelling and neuronal death. MK-801 has been shown to reduce infarct size in several rat stroke models, though it is associated with side effects including sedation and respiratory depression. MK-801 (Sigma-Aldrich, USA) was administered as a 3 mg/kg i.p. injection 15 minutes prior to monofilament insertion occlusion.

2.1.3. Image analysis

Brain slice images were saved in the tagged image file format (TIFF) and analysed using a public domain Java-based image processing program (Image J v1.44, National Institutes of Health, USA). Images were initially zoomed to 300%, and the images were adjusted to ensure that the maximal contrast between the infarcted and the non-infarcted

tissue was observed. Three outlines were drawn on each slice: around the infarcted territory, the entire ipsilateral hemisphere, and the entire contralateral hemisphere. Care and attention was taken to ensure that the exact outline of each slice was followed, and the area was saved. All analyses were performed by myself, to avoid potential inter-analyser variability.

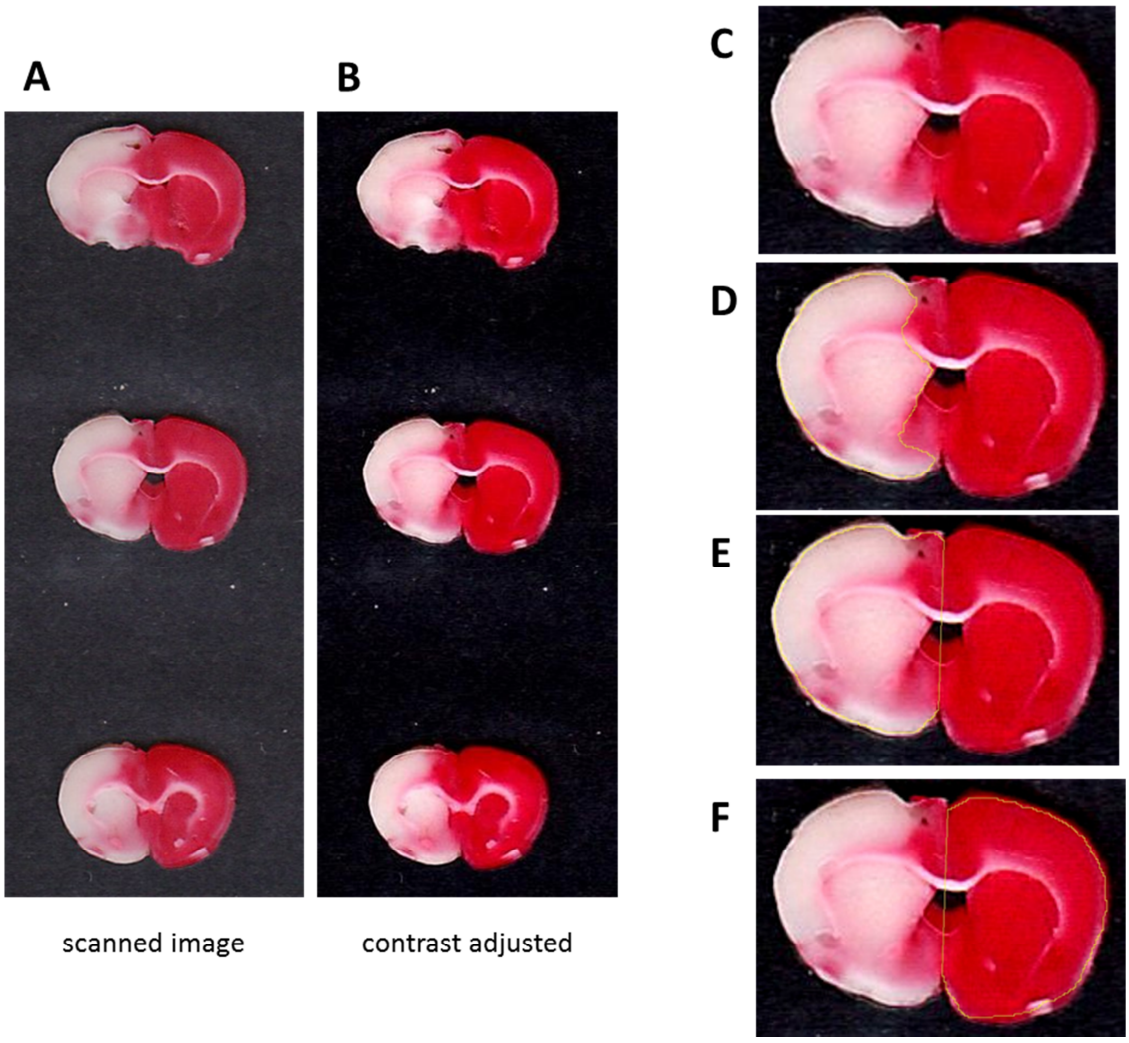

Figure 2.2 Image analysis technique for rodent brain slices. Slices were arranged vertically and scanned with a black background (A), before the contrast was adjusted (B). Each slice (middle cerebral artery territory slice shown) is then zoomed to 300% (C), and the areas of the infarcted territory (D), the entire ipsilateral hemisphere (E) and the entire contralateral hemisphere (F) are measured free hand using imaging software. Yellow line indicates measured area.

2.1.4. Interpretation of results

Analysis of acquired data was performed using graphing software (GraphPad Prism, GraphPad Inc, USA). Equation 2.1 was used to calculate the hemispheric lesion volume and to account for oedema (139,142,143). Briefly a correction factor was applied to the lesion area, and then expressed as a percentage of the contralateral hemisphere. Lesion size is expressed as an area of a single slice in the MCA territory (see Figure 2.2 C-F), and as a volume to establish infarct volume throughout the cerebral hemispheres, by calculating the mean of 8-10 slices. Coefficient of variation was calculated using Equation 2.2. Sample sizes were calculated using statistical software (Power and Sample Size Calculations, Dupont & Plummer, v3.0, (144)).

$$\%\, L_M = \frac{L_m \times \left\{ 1 - \left[\frac{I_m - C_m}{C_m} \right] \right\}}{C_m} \times 100$$

where:

$\%\, L_M$ = modified lesion area
L_m = measured lesion area
C_m = measured contralateral hemisphere area
I_m = measured ipsilateral hemisphere area

Equation 2.1 Calculation to account for oedema within the infarcted territory.

$$\text{coefficient of variation} = \frac{\text{standard deviation}}{\text{mean}} \times 100$$

Equation 2.2 Calculation of coefficient of variation.

2.2. In vivo assessment of endothelial function in humans

2.2.1. Background

The endothelium is a dynamic organ, consisting of a single layer of cells lining the vasculature, which play a crucial role in maintaining homeostasis. Endothelial cells release endogenous vasodilators, inhibit thrombosis and regulate the movement of leukocytes from the circulation into peripheral tissues. In a number of clinical conditions the endothelium is known to become dysfunctional, which is associated with a reduction in the release of endogenous mediators, and the development of a pro-thrombotic state. Endothelial dysfunction is associated with progression of atherosclerosis (145) and may be of value in predicting cardiovascular events in some patient groups (146,147).

In response to shear stress, endothelial cells release factors including nitric oxide, dilator prostaglandins and endothelium-derived hyperpolarizing factor, which cause smooth muscle relaxation and hence vasodilatation. Researchers have attempted to quantify this dilatation for use as an additional prognostic tool in atherosclerosis, and to assess endothelial function *in vivo* for other diseases. Several *in vivo* assessments currently exist, including invasive techniques such as resistance vessel dilatation in response to intra-arterial acetylcholine as assessed by venous plethysmography (148), quantitative coronary angiography (149); and non-invasive methods such as flow mediated dilatation (150), peripheral arterial tonometry (151), laser Doppler flowmetry (152) and pulse wave velocity (153).

2.2.1.1. Flow mediated dilatation

Celermajer et al. showed that measuring the increase in brachial artery diameter in response to hyperaemia (flow mediated dilatation, FMD) might be a valid measure of endothelial function in humans (150), which studies in this PhD have utilised. FMD is a

non-invasive, reproducible ultrasound technique, which assesses change in peripheral conduit artery diameter (2-5 mm, typically brachial, radial or femoral artery) in response to a transient hyperaemia. Reactive hyperaemia that follows brief distal limb arterial occlusion, results in a 7-fold increase in brachial artery flow and causes vasodilatation (154). FMD is primarily dependent on NO production, given that L-NMMA, an inhibitor of nitric oxide synthase, almost entirely abolishes FMD with no effect on blood flow (155). Other endogenous vasodilators such as endothelium-derived hyperpolarizing factor (EDHF) and prostacyclin may also contribute to FMD (154,156).

The technique requires a high degree of ultrasonographer skill, and a number of groups have reviewed the technical aspects of FMD, and have agreed on guidelines that should be followed during the assessment (157–159). This is needed to achieve a low within-subject variability (160,161). FMD is typically performed by ultrasound of the brachial or radial artery in a longitudinal plane, using a high frequency ultrasound probe. Vessel diameter is recorded before and after a five minute arterial occlusion, usually distally to the arterial section of interest. FMD is expressed as the difference between baseline and the maximum dilatation following hyperaemia, with respect to baseline diameter. Alternative assessments include absolute dilatation, the time required to reach maximal dilatation, and the area under the diameter-time curve (161).

FMD is the most commonly used assessment of endothelial function because it is inexpensive, repeatable, and non-invasive. For this reason it has lent itself well to large population-based studies (162), and to repeated studies on healthy volunteers (15). FMD is reduced in patients with endothelial dysfunction such as diabetes mellitus (163,164), and in recent years FMD has also been used as a surrogate marker for cardiovascular disease in clinical trials (reviewed by Charakida et al. (165)).

To investigate the mechanisms of preconditioning, our research group has developed a non-invasive human *in vivo* model using endothelial function as the primary outcome (15). We have previously shown that twenty minutes of upper limb ischaemia, followed by twenty minutes of reperfusion causes a reduction in endothelial function in conduit and resistance vessels, quantified by a reduction in FMD in the brachial (79) and radial (15) artery, and in the acetylcholine-stimulated increase in forearm blood flow (112). Given the low within-subject variability and practicality associated with FMD, this technique was used to assess endothelial function in the current investigation.

2.2.1.2. Low-flow mediated constriction

During distal occlusion, conduit arterial flow is reduced by approximately 70%, and the artery vasoconstricts (low-flow mediated constriction, L-FMC) (154). This was originally believed to only occur in patients with hypercholesterolaemia, and not in a healthy population (166). However Spieker et al. showed in a healthy population, that a significant constriction occurs in the radial artery, and is of a similar degree to the dilatation (167). Recent interest has developed from the observation that radial artery L-FMC is as repeatable as FMD, and like FMD, is reduced in patients with coronary artery disease. It has been suggested that L-FMC may complement FMD, possibly by providing an estimate of basal endothelial function (154).

If L-FMC is repeatable and related to FMD, then it supports the notion that L-FMC could have an additive role in the *in vivo* assessment of endothelial function. Recently groups have shown that FMD and L-FMC correlate (168,169), and thus L-FMC may represent the flip-side of FMD, whereby a reduction in flow causes an endothelium-dependent reduction in diameter; the opposite to the dilatation seen in response to hyperaemia. However at present this remains speculation. Unlike FMD, L-FMC is not abolished by L-NNMA (155), and variably dependent on prostaglandins, EDHF and

endothelin-1 (154,167). Alternatively L-FMC could be a myogenic or neurogenic response to arterial occlusion or a composite of several pathways. Further work is required to assess whether L-FMC, like FMD, is an endothelium dependent phenomenon. One way of addressing this question is to investigate how L-FMC is modified by IR injury.

2.2.2. Experimental set up

Experimental protocols are described in 3.2.2 and 4.2.3. Studies were approved by the Joint UCL/UCLH Committees on the Ethics of Human Research (Committee A), with the reference 09/H0714/67, and conducted within the guidelines of the Declaration of Helsinki. All studies were conducted in a temperature controlled laboratory (24-26°C) in the Clinical Research Facility, University College Hospital. Healthy males (aged 18-45 years) were recruited by using an advertising email directed to students at UCL and by word of mouth. Females were not included due to the potential variation of endothelial function with the menstrual cycle (170), and the necessity to repeat studies more often than once every 28 days. Participants were excluded if they were younger than 18 years old, or older than 45 years old. All current or previous smokers, those taking regular medication, and subjects with a recent history of a vascular or inflammatory disorder were excluded. Participants were asked to refrain from moderate exercise and alcohol intake for at least 24 hours, and caffeine and high fat meals for at least four hours prior to each study. Subjects provided written consent prior to experimental procedures.

2.2.2.1. Brachial artery flow mediated dilatation

International guidelines for FMD have been followed for experimental studies (157). Training was given by two experienced vascular scientists. FMD in the brachial artery was assessed as described previously (79). Experimental set up is shown in Figure 2.3.

Briefly participants were positioned supine on an adjustable hospital bed for at least 10 minutes prior to the start of ultrasound recording, and were asked to remain still throughout the study. The right arm was rested in an arm holder, with the forearm slightly raised using a foam pad to aid comfort. An 8.5 cm wide pneumatic cuff was placed 2 cm distal to the medial epicondyle of the right forearm. Right index finger skin temperature was maintained between 28-32°C, using a heated bean bag to warm the hand if necessary.

A B-mode ultrasound scan of the brachial artery was obtained in a longitudinal section between 5 and 10 cm proximal to the antecubital fossa. The ultrasound probe was a 13.0 MHz linear-array transducer connected to an Aloka SSD-5000 ultrasound system (Aloka Hitachi, Japan). For repeated tests previous subject recordings were reviewed prior to image acquisition, and both ultrasound probe position and baseline diameter were matched where possible.

Image quality was maintained using an adjustable probe holder (Vascular Imaging, Netherlands). Fine adjustments with the probe holder in the coronal and sagittal plane maintained a constant, focused image of the upper and lower walls, and counteracted any movement caused by cuff inflation. Longitudinal, ECG-gated, end-diastolic images were acquired, and recorded onto DVD.

For each FMD protocol, recording lasted 11 minutes in duration. Following one minute of rest, the distal cuff was inflated to 300 mmHg using an automatic cuff inflator (Logan Research Ltd, UK), which caused a low-flow state within the arterial lumen. After five minutes of occlusion the cuff was released. This resulted in a reactive hyperaemia and a subsequent dilatation. The arterial diameter was measured for a further five minutes. Blood flow velocity was continuously monitored by pulsed-wave

Doppler. Blood pressure was assessed immediately prior to each ultrasound recording using an automated blood pressure cuff on the left arm (Dinamap, GE Healthcare, UK).

2.2.2.1. Radial artery flow mediated dilatation

To assess FMD in the radial artery, the distal cuff was placed on the wrist, and the right forearm was fixed in position using a compression pillow (PRA Plastics & Development Ltd, UK) to reduce arterial movement during cuff inflation. A B-mode ultrasound scan was then obtained in a longitudinal section between 5 and 15 cm distal to the antecubital fossa for the radial artery assessment. For repeated tests the previous participant recordings were again reviewed prior to image acquisition, and both ultrasound probe position and baseline diameter were matched where possible. The timing protocol, and cuff pressures were identical for radial and brachial FMD.

2.2.2.2. Ischaemia-reperfusion injury

For the induction of IR injury, a 6.5 cm wide cuff was applied to the right upper arm, and inflated to 200 mmHg using an automated cuff inflator (Hokanson, USA). Ischaemia was confirmed by an absence of a flow signal at the level of the brachial or radial artery. For the IR injury protocols refer to section 4.2.3.3.

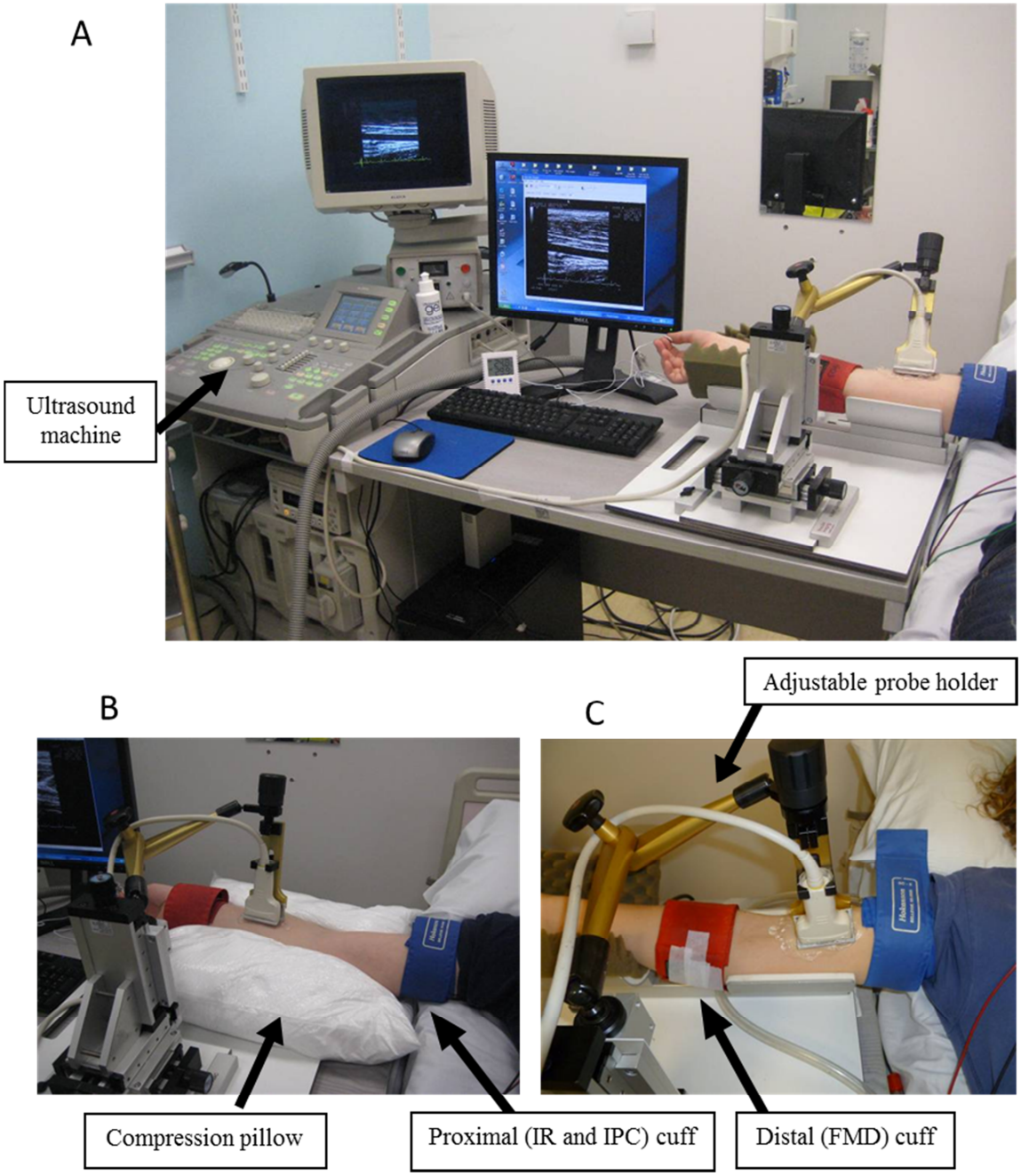

Figure 2.3 Experimental set up for vascular ultrasound studies. Subjects laid supine whilst the right arm was imaged (A). The FMD cuff was applied below the medial epicondyle for the FMD protocol. A proximal cuff was fitted below the shoulder for inducing IR and IPC. In the radial studies a compression pillow maintained arm stability (B), whilst in the brachial studies the arm was supported by an arm holder and foam pad (C).

2.2.2.3. Local ischaemic preconditioning

For the induction of IPC a 6.5 cm wide cuff was applied to the right upper arm, and inflated to 200 mmHg using an automated cuff inflator (Hokanson, USA). Ischaemia was confirmed by an absence of a flow signal at the level of the brachial or radial artery. For IPC protocols refer to section 5.2.3.2.

2.2.2.4. Remote ischaemic preconditioning

For the induction of RIPC a 6.5 cm wide cuff was applied to the left upper arm, and inflated to 200 mmHg using an automated cuff inflator (Hokanson, USA). Ischaemia was confirmed by the absence of a radial pulse. For RIPC protocols refer to section 5.2.3.1.

2.2.2.5. Exercise preconditioning

To assess the effect of exercise preconditioning (ExPC) on IR injury, subjects performed a ramp exercise protocol using an electronically braked cycle ergometer (Lode, Netherlands). Following a four minute warm up of unloaded cycling (0 W), an exercise protocol based on weight and age was used to steadily increase cycle resistance (20-40 W/min, Equation 2.3) (20), whilst cycling at a constant cadence (60 revolutions per min, rpm). Exercise continued until physical exhaustion, or until subjects were unable to maintain a cadence of above 50 rpm despite encouragement. Heart rate was recorded throughout. For ExPC protocol refer to section 5.2.3.3.

$$\text{work rate increments} = \frac{\text{weight x } [50.72 - (0.372 \text{ x age})]}{100}$$

where: work rate increments (watts per minute)
weight (kilograms)
age (years)

Equation 2.3 Calculation of work rate increments for exercise preconditioning study.

2.2.3. Analysis of acquired ultrasound images

2.2.3.1. Analysis of diameter changes

Images were acquired in real-time during FMD recording using automated software (Brachial Tools, Medical Imaging Applications, USA). The software obtained images once every 3 seconds across a 3 cm longitudinal section. Data analysis was performed using specialist software (Brachial Analyser, Medical Imaging Applications, USA). Initially, a region of interest was chosen with an optimum image quality, defined by an obvious definition between the arterial intima and the lumen, which was free from anatomical artefacts (see Figure 2.4A). During analysis FMD traces were scrutinised, and were excluded if necessary due to poor image quality or the presence of artefacts (see Figure 2.4B&C). Furthermore studies were excluded if, post hyperaemia, the vessel failed to return to within 0.2 mm of the baseline diameter, or if there was a difference in baseline diameter of greater than 0.2 mm between scans performed before and after the IR injury intervention.

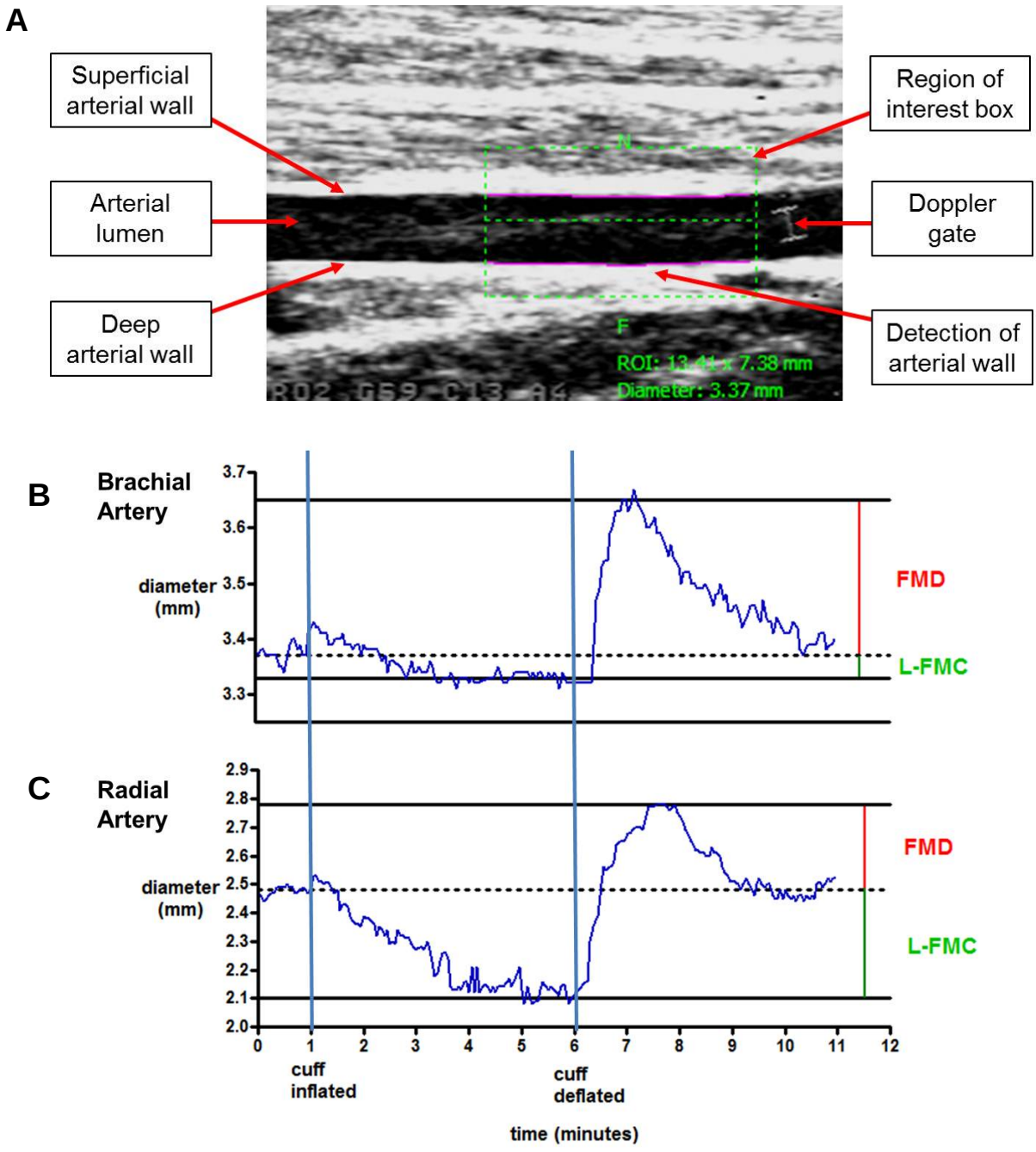

Figure 2.4 Typical ultrasound image and brachial and radial artery diameter responses during flow mediated dilatation protocol. Vessel diameter was measured in a longitudinal section every three seconds, using edge-detection software (A). This produced graphs for the 11 minute recording period in the brachial (B) and radial arteries (C). The radial artery was narrower, and had a greater mean L-FMC% that the brachial artery, whilst FMD is similar.

2.2.3.2. Analysis of the velocity-time integral

Arterial blood flow velocity was analysed from the pulsed wave Doppler flow signal. Each cardiac cycle produced a velocity-time profile, displayed as a spectral Doppler curve. Calculating the area under the curve gives a velocity-time integral (VTI), which is approximately the distance covered by a pulse of blood in one cardiac cycle. Given a constant heart rate and arterial diameter, VTI can be considered as proportional to flow (flow = velocity x π r^2). Thus VTI was used as a convenient proxy for flow, consistent with previous studies (111,112).

For this thesis, VTI was calculated at baseline, during low flow and during high flow (Figure 2.5). Images collected during recording were retrospectively analysed for VTI. Individual images were identified, and envelopes were manually traced using the free-hand function in commercially available imaging software (Image J v1.44, National Institutes of Health, USA). Baseline VTI was calculated as the mean of three consecutive velocity-time profiles, 30 seconds prior to distal cuff inflation. Low-flow VTI was calculated as the mean of three consecutive velocity-time profiles, taken 30 seconds prior to distal cuff deflation. High-flow VTI was calculated as the mean of the three greatest velocity-time profiles, which occurred within the first 10 seconds of cuff release.

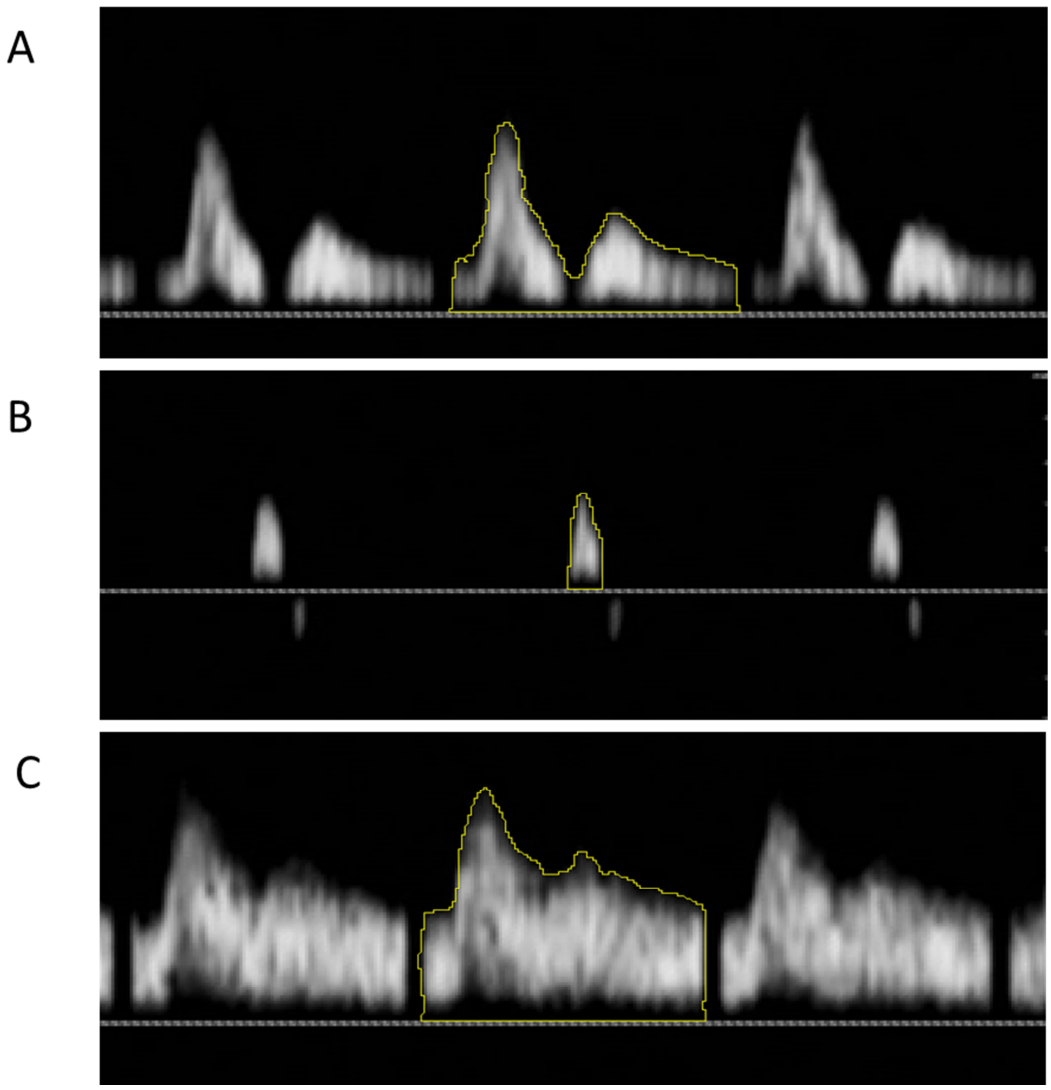

Figure 2.5 Image analysis technique for velocity-time integral assessment. Representative image is shown of the Doppler velocity-time envelope in the brachial artery. Profiles were displayed for each cardiac cycle during flow mediated dilatation recording. Imaging software was used to free-hand (yellow line) outline the envelope during rest (baseline, A), distal cuff occlusion (low flow, B), and following cuff release (high flow, C). Area under the curve measurements were expressed as the velocity-time integral (VTI) in meters.

2.2.3.3. Variability of the image analysis

Repeated recordings were made to assess the variability of the diameter and flow analysis techniques. To assess the variability associated with the image analysis technique, I analysed 11 brachial artery ultrasound scans on two occasions (Figure 2.6). FMD, L-FMC, baseline diameter and velocity time integral (VTI) were highly

repeatable. There was no evidence of systematic bias between the repeated analyses, given that the differences were evenly spread around 0 on Bland-Altman plots.

To assess between-analyser variability, I then analysed 18 brachial artery ultrasound scans that were also analysed by an experienced ultrasonographer (Figure 2.7). The coefficient of variation indicated that analysis of baseline diameter, FMD and L-FMC are more variable when assessed by two investigators instead of one. Furthermore there was some evidence of systematic bias between analysers for baseline diameter, though this had no effect on FMD or L-FMC. This was most likely due to a calibration differences between analysers. Given this, results in this thesis were analysed by myself as a single investigator, to limit analysis variability.

	BL diameter (mm)	FMD (%)	L-FMC (%)	BLVTI (m)	LF VTI (m)	HF VTI (m)
mean	3.62	8.38	2.29	0.071	0.019	0.316
between subject SD	0.33	2.36	2.87	0.023	0.006	0.047
within subject SD	0.01	0.29	0.14	0.003	0.001	0.006
Mean CV (%)	0.2	3.4	6.1	3.7	3.29	2.01
ICC	1.00	0.99	1.00	0.99	0.99	0.98
mean difference	0.00	-0.07	0.03	-0.004	0.000	0.004
difference SD	0.02	0.57	0.26	0.005	0.001	0.017
n	11	11	11	11	11	11

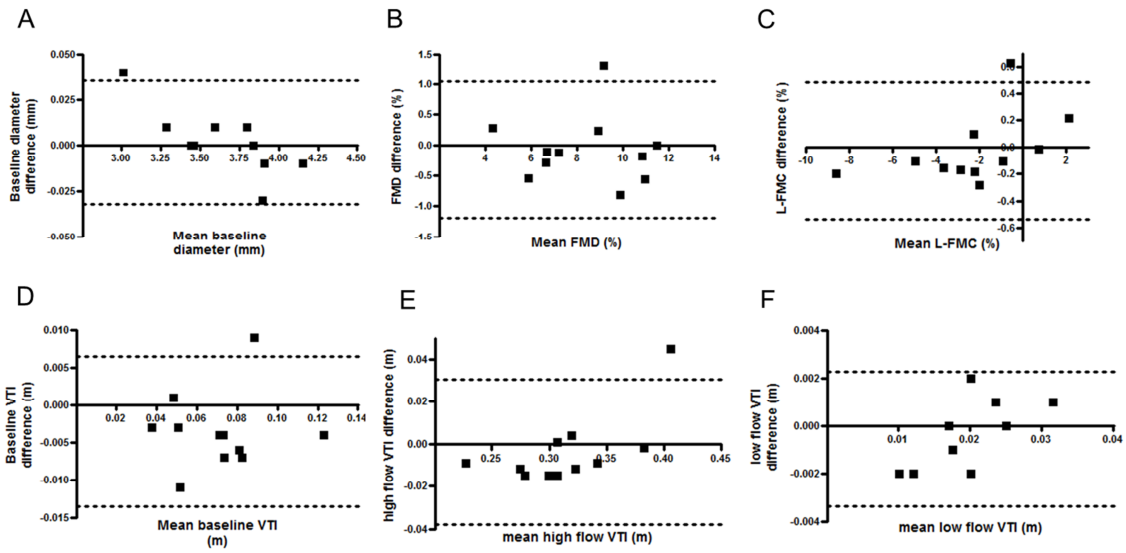

Figure 2.6 Within-analyser variability of ultrasound images. 11 brachial artery flow mediated dilatation scans were analysed on two separate occasions. Table summarises statistical results. Bland-Altman plots are shown for baseline diameter (A), flow mediated dilatation (FMD) (B), low-flow mediated constriction (L-FMC) (C), baseline velocity-time integral (VTI) (D), high flow VTI (E) and low flow VTI (F). There was no evidence of systematic bias. Dotted lines represent 95% limits of agreement.

	BL diameter (mm)	FMD (%)	L-FMC (%)
Mean	3.90	6.12	2.87
between subject SD	0.32	3.37	2.01
within subject SD	0.06	0.54	1.09
Mean CV (%)	1.5	8.8	38.1
ICC	0.97	0.98	0.77
mean difference	-0.08	0.02	-0.08
difference SD	0.08	1.06	2.09
n	18	18	14

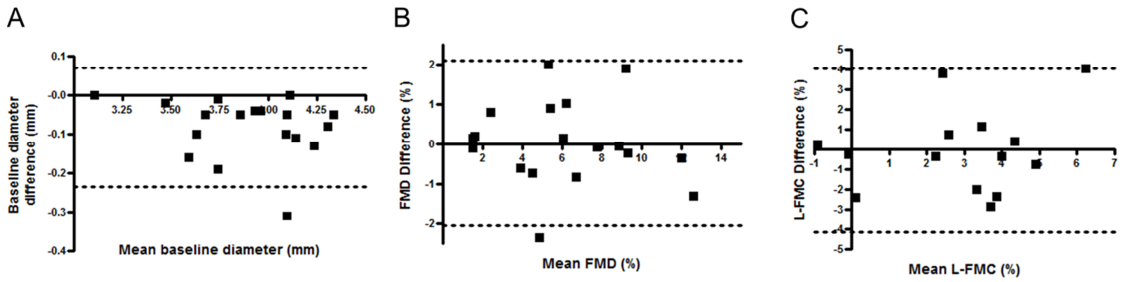

Figure 2.7 Between-analyser variability of ultrasound images. 18 brachial artery flow-mediated dilatation scans were analysed by two investigators. Table summarises statistical results. L-FMC could not be measured in 4 images. Bland-Altman plots are shown for baseline diameter (A), flow mediated dilatation (FMD) (B) and low-flow mediated constriction (L-FMC) (C). There was some evidence of bias for baseline diameter. Dotted lines represent 95% limits of agreement.

2.2.4. Interpretation of results

Data were analysed by myself using analysis software (GraphPad Prism, Graph Pad Inc, USA). FMD was calculated as the difference between baseline diameter, and the highest three consecutive values following cuff release. L-FMC was calculated as the difference between baseline diameter and the final 30 seconds prior to cuff deflation. Both FMD and L-FMC were expressed as the percentage change from baseline. Baseline, high flow and low flow VTI are expressed as absolute values in metres. High and low flow VTI included a correction for heart rate.

2.3. In vivo assessment of acute inflammation in humans

2.3.1. Background

To investigate the effect of IPC on the human inflammatory response it was necessary to use a quantitative assessment of acute inflammation. As discussed, IPC influences human leukocyte function *in vitro*, but it remains uncertain whether altering immune function occurs *in vivo*, and thus whether this is an important part of the mechanism by which IPC reduces IR injury. A number of human *in vivo* models of acute inflammation exist, which include the negative pressure skin blister model (171), the systemic inflammatory reaction following endotoxin inhalation (172), and the cantharidin-induced skin blister model (173).

As an experimental technique for categorising inflammation, the cantharidin skin blister is advantageous in that, unlike endotoxin inhalation, it assesses a local response. In addition our group has previously shown it is non-invasive, has a low within-person variability, and can be maintained to categorise both the acute and resolving inflammatory response in healthy volunteers (174). It also has few side effects, and a retrospective analysis of topical cantharidin administration identified erythema (37%), mild to moderate pain (14%), a transient burning sensation (10%), and a post-inflammatory hypo or hyperpigmentation (8%) as being the major unwanted side effects (175).

Cantharidin, a protein phosphatase inhibitor (3,6 epoxy-1,2-dimethylcyclohexane-1,2-dicarboxylic anhydride), is obtained from beetles of the order *Coleoptera* and the family *Meloidae*, which induce skin blistering on contact with skin. Cantharidin has been used historically as a treatment for helminths and ulcers, and as an aphrodisiac (176). However when swallowed it induces pharyngeal blistering, vomiting, and haematemesis (177). Cantharidin is currently used as a treatment for plantar warts (178), and has been

suggested as a novel therapy for acquired perforating dermatosis (179). When applied topically to the skin, cantharidin is absorbed into the epidermis by the lipid layers of the cellular membranes (176). This results in an initial suprabasal acantholysis, followed by an extensive acantholysis down to the level of the sebaceous glands (180).

In cantharidin blister studies to date, leukocytes that enter the fluid-filled space have been enumerated, and a differential acquired by histologically staining cells, or by labelling cells with fluorescent antibodies and performing flow cytometry. Furthermore cytokines, chemokines and inflammatory lipids that accumulate in the fluid may be assessed by performing an enzyme-linked immunosorbent assay (ELISA). This study has investigated blisters at two time points, 24 and 72 hours. At 24 hours inflammatory blister leukocytes are primarily neutrophils, but by 72 hours the neutrophils are reduced, which coincides with an increase in macrophages (181).

2.3.2. Experimental set up

The study was approved by the UCL ethics committee, reference 2907/02, and conducted within the guidelines of the Declaration of Helsinki. Healthy males (aged 18-45 years) were recruited from researchers within the UCL Division of Medicine and from UCL students using an advertising poster and by word of mouth. Participants provided written consent prior to experiments. Subjects were excluded if they had a history of an acute or chronic inflammatory, vascular or gastrointestinal disorder, recent immunisation, or had any known adverse response to aspirin. Participants were asked to avoid non-steroidal anti-inflammatory medication for at least 72 hours, to avoid all medication (including caffeine and alcohol) for at least 24 hours, and intense exercise for at least 24 hours prior to each blister application. Following blister application, participants were asked to avoid alcohol, caffeine, medication and moderate intensity exercise until the final blister was aspirated.

2.3.2.1. Blister induction

Table 2.1 lists the materials required to induce two cantharidin blisters. Blisters were induced as previously described by our group (Figure 2.8) (174,181). Initially the skin was prepared by choosing two parallel sites approximately 30-70 mm from the elbow crease on the ventral aspect of the forearm. The sites had 20-40 mm between them, depending on forearm width. Any hairs in a 3 cm diameter of the area chosen were trimmed, and the area cleaned with 70% alcohol. Two 10 mm diameter filter paper discs were positioned in the centre of each blister site. 12.5 µl of 0.1% cantharidin was then pipetted onto each disc. The paper discs were then covered with 16 mm diameter film discs, and then the foam pads were positioned superiorly, such that each film disc was protected by two foam pads. The pads were covered with an adhesive dressing, which was applied at a constant pressure and without extensive forearm skin depression to minimise blister volume variability. Participants were advised to keep the dressing dry by covering during bathing.

Table 2.1 Materials required for each participant to receive forearm skin blisters. Below are shown materials required for application and aspiration of two cantharidin skin blister, at 24 and 72 hours.

Material		Supplier
Filter paper punched into 10 mm diameter discs (Whatman® grade 1)	2 discs	Whatman International Ltd, Maidstone, UK)
Laboratory film punched into 16 mm diameter discs (Parafilm™)	2 discs	Alpha Laboratories, Eastleigh, UK
Foam pads cut into 30 mm diameter discs (Activheal® Non-adhesive foam pad, 10 x10 cm)	4 discs	Advanced Medical Solutions Ltd, Winsford, UK
0.1% cantharidin (0.7% Cantharone® diluted in acetone)	25 µl	Dormer Laboratories Inc., Toronto, Canada
Adhesive dressing (IV 3000™, 10x14 cm)	1 dressing	Smith & Nephew, Hull, UK
Film dressing (Mepore® Film & Pad, 9x10 cm)	2 dressings	Mölnlycke Heath Care, Gothenburg, Sweden
Ulcer dressing (Comfeel® Plus, Ulcer Dressing, 10x10 cm)	1 dressing	Coloplast, Peterborough, UK
Cap from 30 ml Specimen Tube	1 cap	Sterilin, Newport, UK
Support bandage (Tubigrip® size C, medium elbow)	15cm	Mölnlycke Heath Care, Gothenburg, Sweden
Surgical tape cut into 10 cm strips (Micropore™)	10 strips	3M Healthcare, Loughborough, UK
Alcohol wipe	3 wipes	UHS, Enfield, UK
Disposable Haemocytometer (C-Chip)	2 slides	Digital Bio, Seoul, Korea
0.4% trypan blue stain	20 µl	Life Technologies Ltd, Paisley, UK
3% sodium citrate, dissolved in 0.9% sodium chloride	100 µl	Sigma Aldrich, Gillingham UK
26 gauge sterile needle	2 needles	Sigma Aldrich, Gillingham UK
1 ml syringe	2 syringes	Terumo, Egham, UK
Roswell Park Memorial Institute (RPMI) media (Gibco®)	2 ml	Life Technologies Ltd, Paisley, UK
1.5 ml microcentrifuge tubes	4 tubes	Appleton Woods, UK

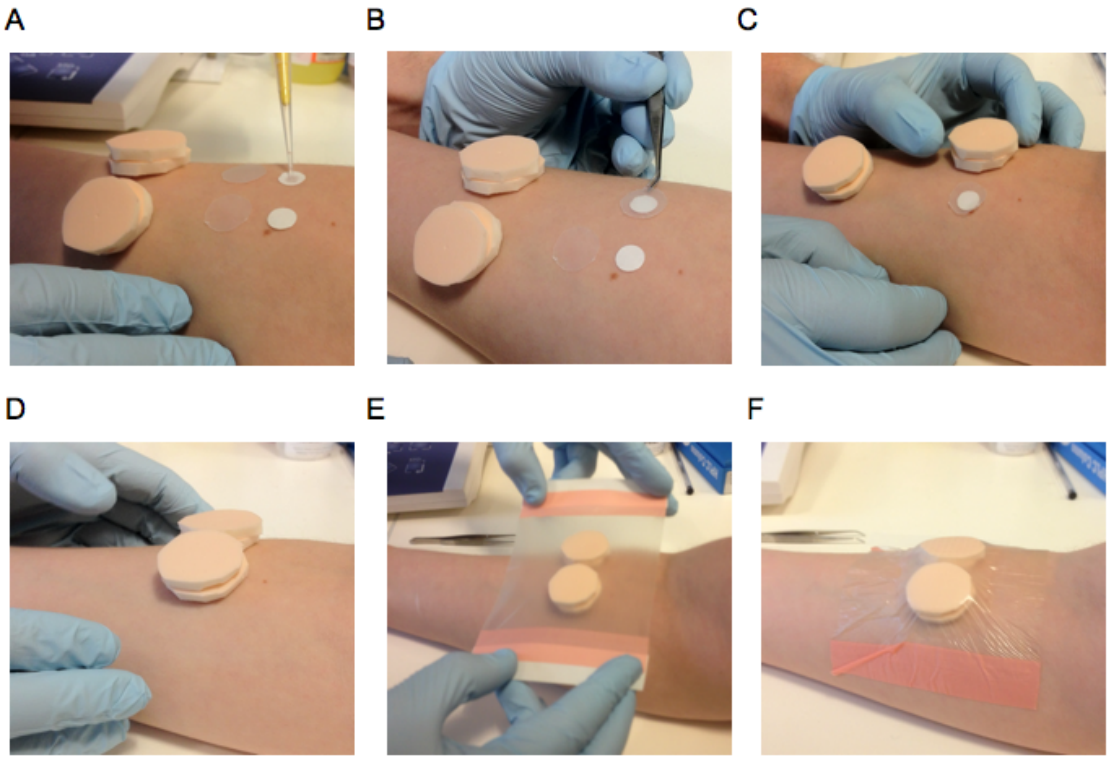

Figure 2.8 Induction of cantharidin blister. Photos show experimental set up for induction of cantharidin skin blisters (182). Initially 12.5 µl of 0.1% cantharidin were pipetted onto filter paper discs (A). These were covered by film discs and foam pads (B–D). Finally an adhesive dressing was used to fix the position (E-F). Dressings were then kept in position for 24 hours.

2.3.2.2. Blister aspiration at 24 and 72 hours

Participants returned to the laboratory at 24 and 72 hours following blister patch application for blister aspiration (Figure 2.9). The adhesive dressing, followed by the foam, film and paper discs were carefully removed, the integrity of blisters was assessed, and the diameter recorded. The blister that had been assigned to aspiration at 24 hours was then pierced at the lateral border with a sterile needle, and a syringe was rolled across the blister pushing the fluid onto the skin. The fluid was aspirated from the skin, and transferred to a centrifuge tube containing 50 µl of 3% sodium citrate. The tube was immediately weighed, and centrifuged (2000 *g.* , 5 minutes, 10°C). The

supernatant was removed and aliquoted, before being frozen at -80°C for further analysis. The cell pellet was resuspended in 0.1-1 ml of RPMI buffer, depending on the size of the pellet.

Following blister aspiration, the area was cleaned with a 70% alcohol swab, and covered with a sterile dressing. The remaining intact 72 hour blister was then given a protective cover so that it was secured for the remaining 48 hours (Figure 2.10). Initially a 2 cm hole was cut into an ulcer dressing, which was shaped to fit around the remaining blister. A thin strip of the ulcer dressing was cut to cover the rim of a specimen tube cap, which was secured over the blister using medical tape. Finally the cap and dressings were covered with a support bandage. At 72 hours, participants returned to the laboratory. The bandage, cap and dressings were removed, and again the blister was inspected for integrity, before being aspirated as at 24 hours.

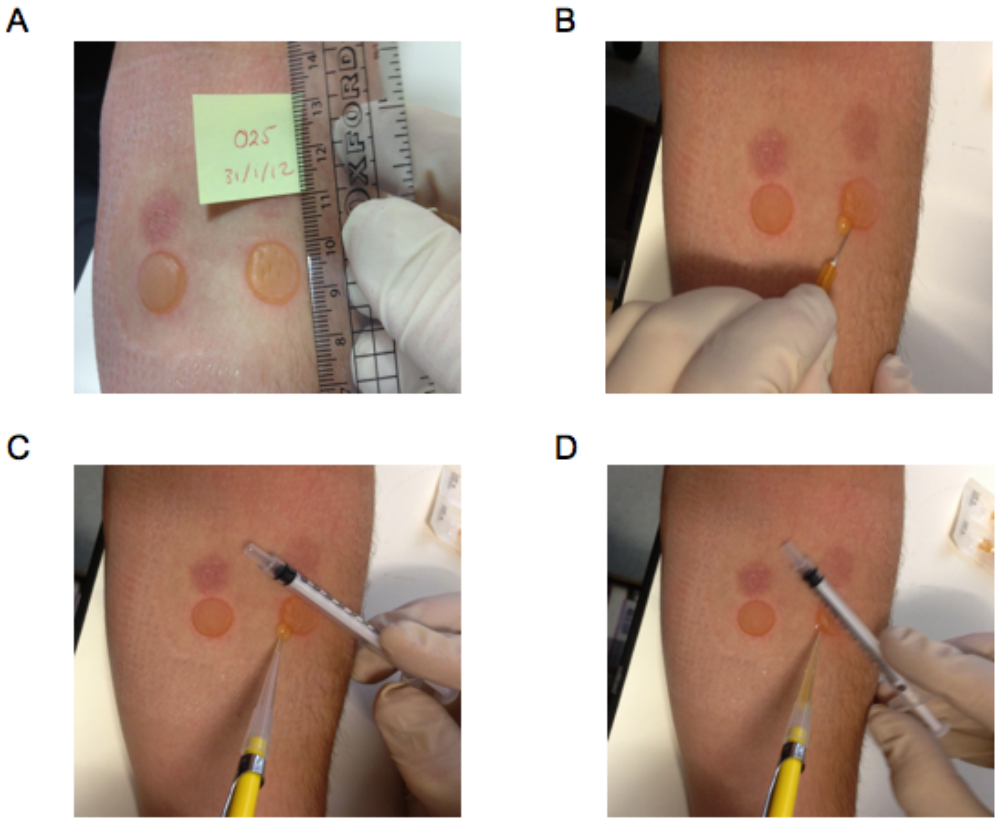

Figure 2.9 Aspiration of cantharidin blister. Blisters were aspirated at 24 and 72 hours following application (182). Initially blisters were inspected for integrity and measured for size (A). Blisters were then aspirated at the lateral border using a sterile needle (B). A syringe was rolled across the blister to push out the contents, whilst the fluid was aspirated using a pipette (C and D).

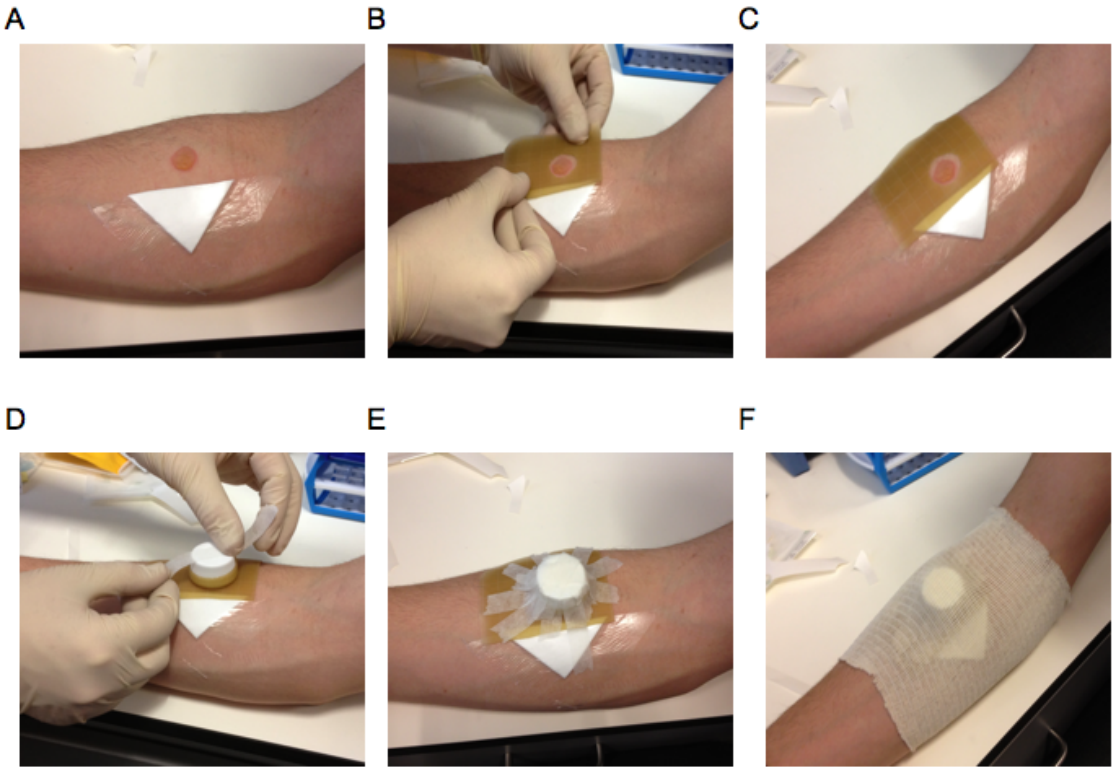

Figure 2.10 Protecting the cantharidin blister from 24 to 72 hours. Aspirated 24 hour blisters were cleaned and covered with a sterile dressing (A) (182). Then an ulcer dressing is fitted around the remaining intact blister (B and C), before it is secured by a protective cap (D and E), and finally by a support bandage (F). The remaining blister was aspirated at 72 hours.

2.3.2.3. Cell counting

To enumerate blister leukocytes and assess viability, 10 µl of the cell suspension was mixed with 10 µl 0.4% trypan blue solution (Sigma Aldrich, UK). Trypan blue is not absorbed by cells with an intact cell membrane, and hence is used to exclude dead cells. 10 µl of this mixture was then pipetted into the enclosed chamber of a disposable manual haemocytometer (Digital Bio, Korea) and cells were enumerated using a light microscope (Primo Vert, Zeiss, Germany). The total blister cell count was calculated using Equation 2.4.

$$TCC = \text{cells in } 1mm^2 \text{ box} \times 10^4 \times 2 \times \text{cell suspension volume}$$

$$\text{cell concentration} = \frac{TCC}{\text{oedema}}$$

where

TCC = absolute total cell count (n)
oedema = blister oedema volume (ml)

Equation 2.4 Calculation of total blister cell count. Cells are expressed as the absolute total cell count or as the cell concentration within the blister fluid.

2.3.2.4. Collection and preparation of human peripheral blood

Peripheral blood was drawn from the antecubital vein of participants using a 21G butterfly needle (Vacuette®, Greiner, Austria), and collected in tubes containing ethylenediaminetetraacetic acid (EDTA), which when blood was added formed an EDTA concentration of 1.8 mg per ml, to prevent the sample from clotting. Plasma was isolated by centrifuging blood collection tubes at a high velocity (3000 *g.*, 10 min, 10°C). Plasma supernatant was then aliquoted and immediately stored at -80°C for later analysis.

To isolate leukocytes, venous blood was exposed to a hypotonic solution, followed by a hypertonic correction to induce red cell lysis, whilst maintaining the integrity of the peripheral blood leukocytes. To achieve this 5 ml of venous blood were added to 45 ml of distilled water (1:10) for 17 seconds only. Then, 5 ml of 9% NaCl solution were added, immediately returning the blood mixture to an isotonic solution, and preventing leukocytes from losing membrane integrity. After 5 minutes the mixture was centrifuged (500 *g.* , 5 min, 10°C), followed by aspiration of the supernatant, and the remaining cell pellet was resuspended in 500 µl hypotonic ACK lysing buffer (Lonza,

Switzerland) for 3 minutes, to ensure lysis of the remaining red blood cells. After 3 minutes 1 ml of flow cytometry buffer (1% fetal calf serum, 2 mM EDTA in 1 x phosphate buffered solution, PBS) was added, and the mixture was centrifuged (500 *g.* , 5 min, 10°C). Cells were then resuspended in 2 ml of flow cytometry buffer, resulting in an approximate leukocyte concentration of 12.5 x 10^6 cells/ml.

2.3.3. Flow cytometry

2.3.3.1. Background

Fluorescent labelling of cells using flow cytometry allows researchers to quantify relative expression of specific receptors on cell populations. This is of particular use in the setting of the cantharidin blister, because it provides a rapid, accurate differential of leukocytes, and can be compared with circulating leukocytes. One previous cantharidin blister study has used flow cytometry for cell identification (181). However this study planned to make use of modern equipment using the BD LSR Fortessa™ system, to label each cell mixture with seven antibodies. This allowed for cell differentiation in every blister and venous sample, and to determine cell activation by using major histocompatibility complex class II (MHC class II) expression. Training was given by an experienced post-doctoral research fellow.

2.3.3.2. Leukocyte preparation for flow cytometry

Blister leukocytes were prepared for flow cytometry by centrifuging cells (2000 *g.* , 5 min, 10°C), and resuspending cell pellets in flow cytometry buffer. 40 µl of cell suspension were used at each time point, and given an approximate concentration of 0.05 – 0.5 x 10^6 cells / 40 µl.

Working dilutions of each antibody was determined by titration and assessment of expression on circulating leukocytes. The list of antibodies used, including information on the fluorescent conjugate, concentration, and population of labelled cells are given in

Table 2.2. 40 µl of cell suspension was incubated with 60 µl antibody mixture on a 96-well plate for 25 minutes on ice in the dark. Samples were then washed 3 times by adding 150 µl flow cytometry buffer, centrifuged (800 *g.* , 3 min, 10°C), before being resuspended in 400 µl fixing buffer (0.1% paraformaldehyde in PBS), and transferred to a 1.1 ml microtube. Samples were analysed using the LSRFortessa™ flow cytometer (BD, USA) within 7 days of cells being fixed.

Table 2.2 Antibodies used to characterise leukocyte populations. Antibodies were acquired from bioscience manufacturers. [1] BD, [2] AbD Serotec, [3] eBioscience, all USA.

Antigen	Clone	Fluorescent conjugate	Volume (µl / test)	Stock concentration (µg/ml)	Cell population labelled
CD3[1]	UCHT1	APC	10	3	T-lymphocytes
CD14[1]	M5E2	Alexa Fluor® 700	2.5	200	Monocytes/Macrophages
CD16[1]	3G8	FITC	20	50	Granulocytes
CD19[1]	SJ25C1	PE-Cy™7	2.5	6	B-lymphocytes
CD56[1]	B159	PerCP-Cy™5.5	2.5	25	Natural-killer cells
CD163[1]	M130	PE	20	6.25	Monocyte/Macrophages
HLA-DR[1]	L243	V450	2.5	50	MHC Class II$^+$ cells
CD33[2]	WM53	PE	10	100	All myeloid lineage cells
CD11b[3]	ICRF44	PE-Cy™7	2.5	200	Myeloid lineage cells
CD15[1]	H198	PerCP-Cy™5.5	5	25	Granulocytes

2.3.3.3. Flow-assisted cell sorting

In three subjects, cells were sorted for histological staining and morphological assessment. Samples were prepared as previous, except that the final resuspension was in 400 µl of flow cytometry buffer. The resuspended cell suspension was analysed using the FACS Aria flow cytometer (BD, USA) within 2 hours of preparation. Cells were sorted according to the standardised gating strategy (see 2.3.3.5).

2.3.3.4. Histological staining and slide preparation

Sorted populations were processed for microscopy. Slides were prepared by centrifuging the sorted cell suspension using a cytospin and subsequently staining using a modified Wright's staining procedure (Shandon Kwik-Diff, Thermo Fisher, UK). Stained cells were viewed by microscopy (200 x, Olympus BX41, Olympus, Japan), and photographed using imaging software (Image Pro 6.3, MediaCybernetics, USA).

2.3.3.5. Data analysis

Data were analysed using the FlowJo software (FlowJo v7.6.1, Tree Star Inc, USA). Briefly cell populations were identified within dot plots based upon size, granularity and fluorescence. Due to the lack of published data on blister cell differentiation by flow cytometry, a novel gating strategy was designed to identify individual cell populations. The gating was almost identical for both circulating and blister populations. Positive antibody expression was identified by performing florescence-minus-one (FMO) controls, which contain all antibodies except for one. FMO controls are typically used to identify populations that are positive and negative for the antibody of interest (183). Gating strategy is described in section 6.3.2. Populations are labelled according to relative fluorescence intensity, indicated by superscript text i.e. x^{hi} = high expression, x^{dim} = medium expression, x^{lo} = low or no expression.

2.3.4. Tumour-necrosis-factor-alpha and interleukin-10 assay

To assess the concentration of tumour-necrosis-factor-alpha (TNF-α) and interleukin-10 (IL-10) in the blister fluid and plasma, a series of enzyme linked immunosorbent assays (ELISAs) were performed. TNF-α assay (Human TNF-alpha DuoSet, R&D Systems, USA) and IL-10 assay (Human IL-10 ELISA Set, BD OptEIA^{TM}, BD, USA) were performed according to manufacturer's protocol. Initially each well of a 96-well flat bottom plate (Costar®, Corning Life Sciences, USA) was coated with 50 µl capture

antibody (anti-human TNF-α; anti-human IL-10). The plate was then sealed and incubated overnight at room temperature. The following day the wells were aspirated, and washed twice with addition of 200 µl wash buffer (0.05% Tween 20 in 1 x PBS). The plate was then blocked by adding 150 µl reagent diluent (TNF-α, 1% bovine serum albumin in 1 x PBS; IL-10, 1% fetal calf serum in 1 x PBS), and then incubated at room temperature for one hour, before two additional washes.

Blister and plasma samples were removed from -80°C, and thawed at room temperature. Samples were then vortexed and centrifuged (100 *g*. , 2 min, 20°C) to collect all the fluid. Samples were diluted 1.5-2 times with reagent buffer. Samples and standards were added to wells of the plate, and incubated for 2 hours at room temperature. Plates were washed twice, and 50 µl of detection antibody (biotinylated anti-human TNF-α; biotinylated anti-human IL-10 monoclonal antibody) were added to each well. Plates were incubated for 2 hours at room temperature, before two wash steps. Next 50 µl of Streptavidin-horseradish peroxidase conjugate (SAv- HRP) were added to each well. Plates were covered and incubated for 20 minutes at room temperature, before two additional washes. 50 µl of freshly prepared substrate solution (1:1 mixture of hydrogen peroxide and tetramethylbenzidine) were added to each well, and incubated for 20 minutes at room temperature. 25 µl of stop solution (2N H_2SO_4) were then added to each well, and plates were gently tapped to ensure mixing. Optical density was assessed using a plate reader and results were exported into an excel spreadsheet.

2.3.5. Adverse events

During this study there was a single adverse event. One subject received a single 24 hour forearm blister on the right arm. 6 days following blister aspiration the subject reported to the research group a 48 hour history of pain, swelling and redness in several locations on the arm. He also reported that he had been swimming in an outdoor pond

within the 48 hours window. On examination there were three sites on infection on the right arm, with evidence of lymphangitis both distal and proximal to the blister (Figure 2.11). The participant was reviewed as an outpatient in University College Hospital and prescribed a single course of antibiotics. By 24 hours the lymphangitis was resolving, and the participant had made a complete recovery after completing the course of antibiotics. This was the only adverse event in this study (total: 186 blisters), but previous reports have observed lymphangitis second to cantharidin (184,185).

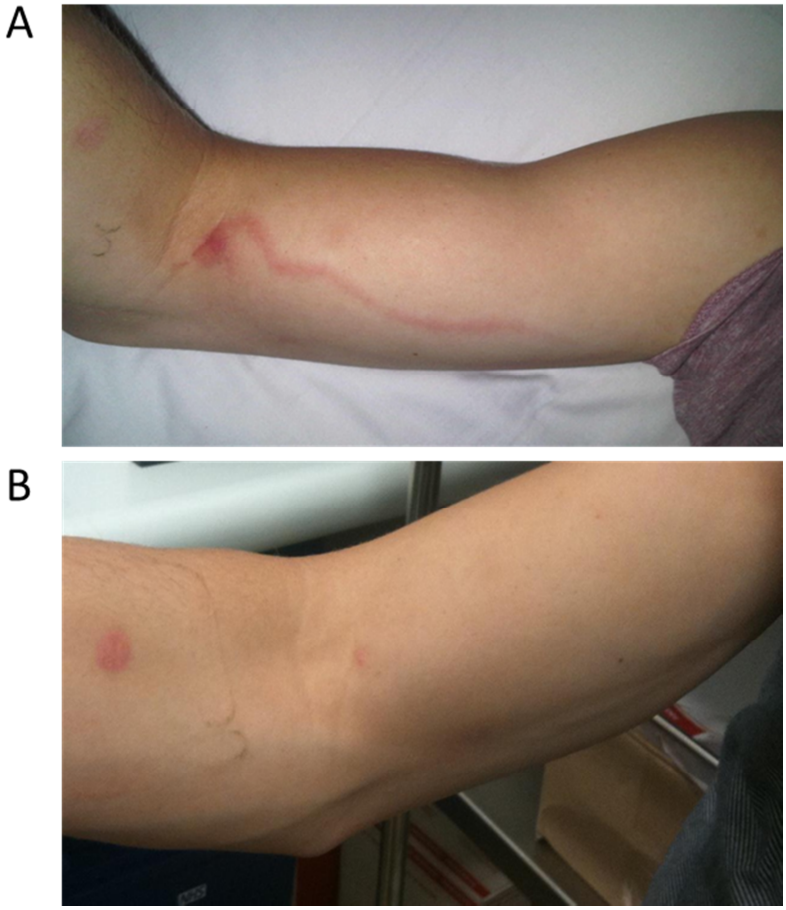

Figure 2.11 Lymphangitis second to cantharidin exposure. 6 days following blister aspiration the subject showed evidence of an infective lymphangitis (A). After one week of antibiotic treatment the participant had made a complete recovery (B).

2.4. In vivo metabolic assessment during exercise in humans

2.4.1. Background

Recent studies have suggested that IPC can improve aspects of endurance exercise performance, principally an increased maximal oxygen delivery ($\dot{V}_{O_2\ max}$) (126), an increased maximal power output (WR $_{max}$) (127), and an improved swimming time (128). The first two of these studies were using graded exercise tests. Graded or incremental exercise tests to exhaustion are commonly performed to assess general aerobic fitness and performance, and to identify the lactate and respiratory thresholds. These types of exercise test have recently identified improvements in performance following administration of nitrate supplements (186) and ß-alanine (187). Graded exercise tests have been routinely used to study the effectiveness of various interventions as well as to assess endurance capacity and aerobic power in athletes following training interventions (126,188).

To determine the effect of IPC on aspects of human performance, it was important to design an experiment that would adequately measure several parameters involved in the metabolic pathways. As discussed, it remains uncertain whether IPC influences aerobic or anaerobic metabolism during exercise, and therefore both of these elements should be considered for investigation. This was achieved by measurements of systemic oxygen delivery, carbon dioxide elimination, ventilation, skeletal muscle oxygenation, heart rate response, blood gases, and recovery measurements (see protocol in section 8.2.3). Below are discussed the methods used to perform this investigation.

2.4.2. Experimental set up

This project was approved by the UCL ethics committee, reference 2907/001, and conducted within the guidelines of the Declaration of Helsinki. All measurements were

conducted in the British Olympic Medical Institute in a temperature (21-23ºC) controlled research laboratory.

Healthy well-trained males (aged 18-45 years) were recruited from local amateur cycling and triathlon clubs by advertising email. Inclusion criteria were as follows: participants were training for at least 4 hours per week, were members of a cycling or triathlon club, and competed in cycling or triathlon events at least once every two months. All subjects provided written consent, and completed a standard health screen questionnaire. Participants were excluded if they had any known history of disease or injury which might pose a contraindication for the testing as defined by the American College of Sports Medicine guidelines (189), or were taking any regular medication. Participants taking dietary supplements were not excluded, but were advised to continue with the same supplement dosing throughout testing. Prior to each study subjects avoided all competitive events for at least 72 hours, all training for 48 hours, and all exercise for 36 hours. In additional participants remained free from alcohol and all medication for 24 hours and caffeine for 12 hours. To standardise for hydration participants drank a large glass of water upon waking. All testing sessions began between 6 am and 11 am to account for known variation in circadian rhythm, and subjects arrived in a fasting state. At least seven days were left between visits to allow for a period of washout. This study followed a randomised controlled cross-over design.

2.4.3. Baseline measurements

2.4.3.1. Blood pressure and heart rate

Resting blood pressure and heart rate were recorded on the right arm using an automatic blood pressure cuff (Omron, Japan) after sitting at rest for 10 minutes, and calculated as the mean of three recordings.

2.4.3.2. Anthropometric measurements

Subcutaneous fat is proportional to total body fat, and this gives an estimate of training and nutritional status. In this project mid-thigh skinfold thickness was also necessary to aid interpretation of the near-infrared spectroscopy results (see section 2.4.5). Calipers were used to assess the body composition by skinfold thickness measurements. Height and weight were assessed by a height chart and scales respectively.

Training was given by an International Society for the Advancement of Kinanthropometry accredited sport scientist. Skinfold thickness measurements were made in duplets at fixed anatomical locations: biceps, triceps, subscapularis, iliac crest, supraspinale, abdomen, mid-thigh, and medial calf. If there was greater than a 5% difference between the two skinfolds at each site, then it was repeated. Percentage body fat was calculated using a standard 7-site formula (190).

2.4.4. Local ischaemic preconditioning

Preliminary studies demonstrated that receiving a preconditioning stimulus to the lower limbs is less tolerable that on the upper limbs. The present study was subsequently designed such that the pressure during the IPC protocol was both tolerable to the participant, and sufficient to induce a vascular occlusion. Given known heterogeneity in arterial occlusion pressure, a pre-determined occlusion pressure was established on an individual basis.

2.4.4.1. Baseline assessment of peripheral flow

Flow was assessed using a pocket Doppler probe (Dopplex MD2, Huntleigh Diagnostics, UK), and vascular occlusion was confirmed by a loss of both audio and visual outputs. To determine the occlusion pressure of the femoral artery, a blood pressure cuff (20x86 cm XXL cuff, Heine, Germany) was gradually inflated on the left thigh, until the flow was lost over the dorsalis pedis artery. Identification of the dorsalis

pedis artery was via the pulse on the dorsal aspect of the foot, immediately lateral to the extensor halluces longus tendon.

2.4.4.2. Application of intervention cuffs

The IPC intervention during this study was induced by inflating two blood pressure cuffs (20x86 cm XXL cuff, Heine, Germany) at the top of the thighs using an automated cuff inflator (Hokanson, USA). IPC was induced by cuff inflation to 20-30 mmHg above the pressure required to induce arterial occlusion. Sham cuff inflations were set to a pressure of 20 mmHg below resting diastolic blood pressure.

2.4.5. Near infrared spectroscopy

2.4.5.1. Background

Near-infrared spectroscopy (NIRS) has developed through the necessity to non-invasively monitor cerebral and muscular oxygenation in the clinical and research settings. In recent years this has developed in the exercise medicine and sport science field, especially given the availability of small, portable devices, which can be used to relate muscle oxygenation to oxygen delivery ($\dot{V}_{O_2}$) (191).

NIRS is based upon the principle that when light of the near infrared range (typically 700-1000 nm) is shone on a tissue, it is either reflected or absorbed. These wavelengths are chosen to enable assessment of haemoglobin, and in particular to quantify the ratio between concentration of oxygenated haemoglobin ([HbO_2]) and total haemoglobin ([HbT]), which absorb light of different wavelengths (peaks at 750 nm for haemoglobin, and 900 nm for oxyhaemoglobin). The absorption spectra for [HbT] and [HbO_2] are graphed in Figure 2.12. Absorption at these specific wavelengths are proportional to concentration and described by the Beer-Lambert law (see Equation 2.5).

$$A = \log_{10} [I_0/I] = a \text{ x } c \text{ x } l$$

Where A = attenuation measured in optical densities

I_0 = intensity of incident light

I = intensity of transmitted light

a = specific extinction coefficient

c = concentration of absorbing material

l = length of light path through the material

Equation 2.5 The Beer Lambert Law for assessing level of absorption through a material. This equation is the basis for calculating the concentration of oxyhaemoglobin by NIRS. From Horecker 1943 (192).

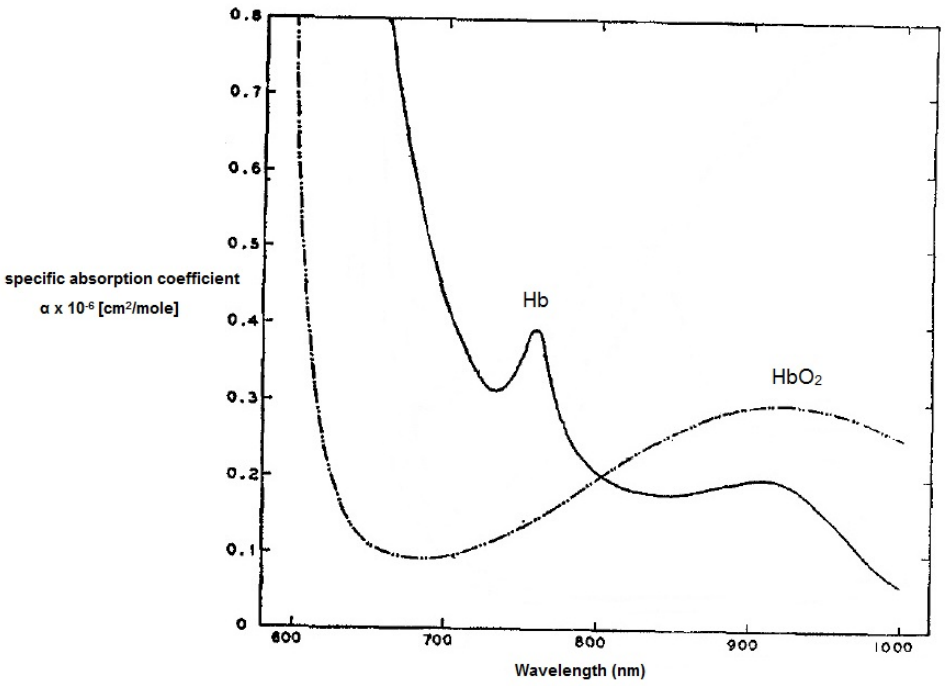

Figure 2.12 Absorption spectra of haemoglobin and oxyhaemoglobin. Graph shows the specific absorption spectra for haemoglobin (Hb) and oxyhaemoglobin (HbO_2), which is used to derive the concentration using Equation 2.5. Modified from Horecker 1943 (192).

Several limitations exist with the use of NIRS, including the difficulty distinguishing the contribution of myoglobin and cytochrome C to the [HbO_2] and [HbT] signals. Whilst NIRS can quantify haem oxidation, is cannot distinguish between this in haemoglobin or myoglobin. However myoglobin and cytochrome C are believed to account for less than 15% of the light absorption signal (193), and the current study employed a crossover design so that small variations are unlikely to pose a confounding factor.

2.4.5.2. Measurement of muscle oxygenation during exercise

A number of groups have used NIRS to assess muscle oxygenation during exercise protocols, and in sporting performances tests (194–196). During an incremental exercise protocol NIRS has shown that muscle oxygenation relates to $\dot{V}_{O_2}$ values (191), and has a good agreement with respiratory measurements to identify the anaerobic threshold (197). The protocol in the current study has employed NIRS to assess the changes in oxygenation in the vastus lateralis muscle during both cuff inflations and exercise, as our group has recently performed in a group of elite speed skaters (195).

2.4.5.3. InSpectra^{TM} near infrared spectroscopy device

The InSpectra^{TM} 650 device (Hutchinson Technology, USA) is a single-distance continuous-wave NIRS device. It consists of a main display unit and a disposable probe attachment, which contains an emitter and a receiver unit. Recordings were made once every two seconds, producing two values at each time point, the tissue haemoglobin oxygen saturation (StO_2) and the tissue haemoglobin index (THI). Values were available and recorded in real-time, and analysed following data acquisition. The distance between the emitter and the receiver was fixed at 15 mm, and it is suggested that this corresponds to a mean signal depth of 7.5 mm, with the maximum signal depth

being 15 mm (198). Using a group of well-trained subjects aimed to ensure that this signal depth corresponded to skeletal muscle and not adipose tissue.

2.4.5.3.1. Tissue haemoglobin oxygen saturation

StO_2 is the ratio of oxygenated haemoglobin to deoxygenated haemoglobin, expressed as a percentage. The algorithm to calculate the StO_2 is described in Myers et al. 2005 (198), and is attained from attenuation measurements at 680, 720, 760 and 800 nm, whereby second derivative spectroscopy is applied to account for light scattering effects, movement artefacts, baseline drift, and chromophores with constant absorption.

2.4.5.3.2. Tissue haemoglobin index

The THI corresponds to the total haemoglobin within the amount of tissue covered by the optical path length (199). However this volume of tissue is uncertain, and hence the index is in arbitrary units. Highly vascular tissues, such as the muscles, exhibit a higher THI than poorly vascularised tissues, such as adipose tissues. It has also been reported that during venous occlusion, the rise in blood volume results in an increase in THI, whereas during arterial occlusion there is no change, or a small decrease (199).

2.4.5.4. Near infrared spectroscopy set up

The InSpectra^{TM} device consists of a skin probe and a main display unit. In the current study the probe was positioned on the left thigh, two thirds of the distance between the greater trochanter and the lateral epicondyle, and 2–8 cm medially, such that the probe rested on the lower third of the belly of the vastus lateralis muscle (Figure 2.13). This area had been shaven and marked prior to probe application. Preliminary work showed that during exercise, the probe suffered from extensive movement if not secured. To account for this, the probe and attached wire were secured using black cloth tape (Grays, UK), a plastic cap, a crepe bandage, and a support bandage (Tubigrip®, Mölnlycke Heath Care, Sweden).

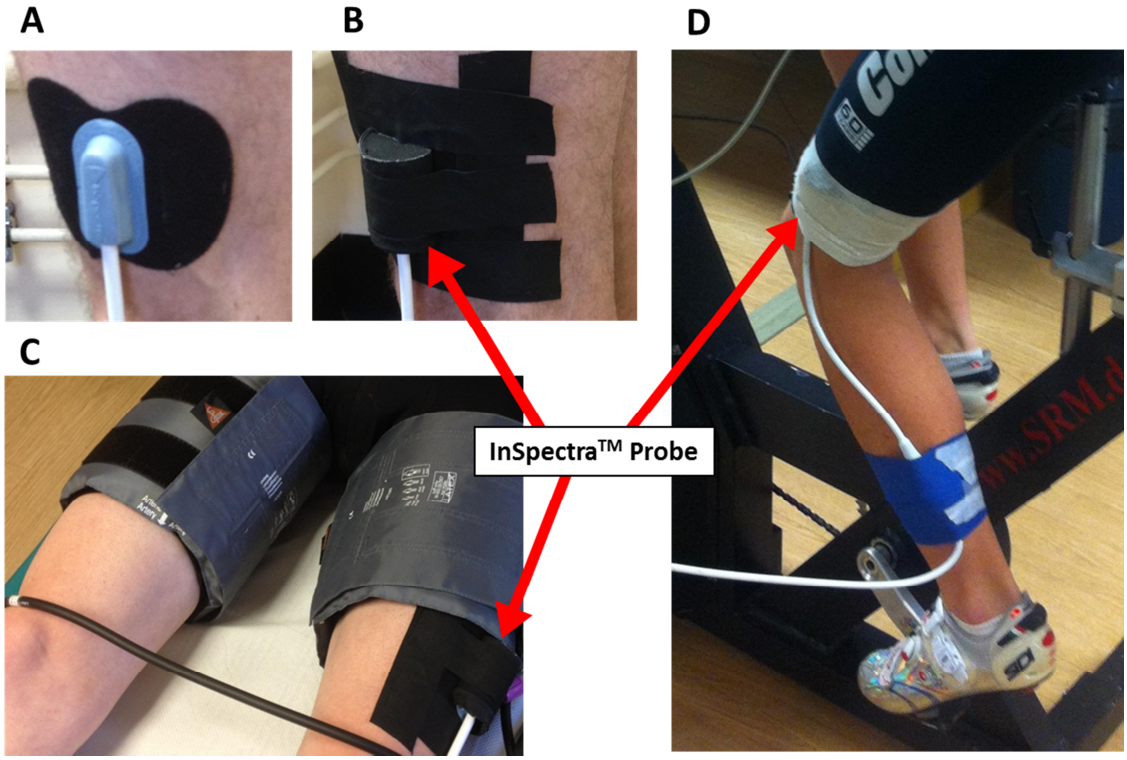

Figure 2.13 Experimental set up of near-infrared spectroscopy recording. Initially the NIRS probe was positioned at the base of the belly of the vastus lateralis muscle (A), before being secured with tape and a cap (B). This allowed for sufficient space above the probe for cuff application when necessary (C). The probe is further secured by a support bandage during exercise testing (D).

2.4.5.5. Data analysis

Values for StO_2 and THI were recorded every two seconds throughout all the testing, and transferred to a spreadsheet for post-test analysis. For each time point, StO_2 and THI were expressed as the mean value of the previous twenty seconds. This was an optimal window of investigation to account for the noise associated with recording during exercise, based upon results in the preliminary studies.

2.4.6. Assessment of cardiorespiratory variables

The K4b^2 system (Cosmed, Italy) was used to perform respiratory gas analysis during exercise and recovery. The system consists of a portable unit and a mask, which was fixed to the participant during testing. The portable unit contains CO_2 and O_2 analysers,

the electronics controlling the sampling pump, and barometric sensors. Power is supplied by a battery pack, which was positioned on the participants back. The portable unit was connected to a low resistance turbine by a gas sampling line. Inspired and expired air passing through the mask was directed into the turbine. As the turbine spins it interrupts infrared light passing through the optoelectronic reader. Gas collected in the sampling line was rapidly assessed for O_2 and CO_2 within the portable unit. The K4b^2 system has been validated against the Douglas bag method, and was deemed acceptable over a range of exercise intensities (200). In the current study it was used to measure O_2 delivery ($\dot{V}_{O_2}$), CO_2 elimination ($\dot{V}_{CO_2}$) and ventilation ($\dot{V}_E$).

2.4.6.1. Gas analyser experimental set up

The K4b^2 was prepared for study according to the manufacturers guidelines. In all studies the main unit was turned on to equilibrate for at least 45 minutes prior to calibration. Sequential calibration of the unit followed. Firstly the system was calibrated at room air to adjust the gain of the O_2 analyser and to adjust the baseline on the CO_2 analyser. Secondly the unit was calibrated by providing known fixed concentrations of O_2 and CO_2 (16.00% and 5.00% respectively) from a gas cylinder (Cosmed, Italy), to update the gain and the baseline of the analysers. A delay calibration was performed to update the software with the duration required for gas samples to pass from the turbine to the portable unit. Finally, the turbine was calibrated using a 3 litre gas syringe to adjust for volume gain and match the predicted value.

Participants were asked to position themselves on a cycle ergometer, and a heart rate strap (Polar, Finland) was applied to the chest, followed by a secure harness containing the main unit and battery pack (see Figure 2.14). A mask was then fitted to the face of each subject, and checked for a tight seal. Having confirmed this, the mask was secured and the turbine attached to the front of the mask. Participant preparation on the

ergometer was approximately five minutes in duration. The main unit was connected to a laptop (Lenova, China) and monitored in real-time using the K4b^2 software.

Figure 2.14 Experimental set up for breath by breath gas analyser during exercise testing. A harness secures the portable unit and battery pack to the subject, whilst inspiratory and expiratory gases pass through the turbine. This in turn is secured by a mask and head-net.

2.4.6.2. Data analysis

All heart rate and respiratory data were collected breath-by-breath ($\dot{V}_{O_2}$, $\dot{V}_{CO_2}$ and $\dot{V}_E$) and analysed using specialist software (Cosmed, Italy). Results were calculated from data acquired at the end of a constant submaximal exercise bout of 150 W (T_{SUBMAX}) and at peak exercise (T_{MAX}) (see protocol in Figure 2.15). Results at T_{SUBMAX} for all parameters were calculated as the mean value during the final minute of cycling at a power of 150W. Maximal heart rate (HR_{max}) was taken as the mean of the final 20 seconds of exercise. In some instances erroneous flattening of respiratory graphs occurred during the final 1-3 minutes of exercise. Therefore maximum $\dot{V}_{O_2}$, $\dot{V}_{CO_2}$ and $\dot{V}_E$ values were estimated by extrapolation from linear regression above the anaerobic threshold, but below peak values.

2.4.7. Exercise protocols and design

To evaluate both the aerobic and anaerobic metabolic pathways during exercise, an incremental exercise test to volitional exhaustion was employed. Participants began cycling at a submaximal power output of 150W. This was followed by incremental increases in resistance (50 W/min), whilst maintaining a constant cadence (80–100 revolutions per minute, rpm). Given the well trained nature of the study population, increments were set to 50 W.

Exercise testing was carried out on an electronically braked cycle ergometer (SRM, Germany). The seat and handlebar height and position were adjusted for each subject during the first visit, and remained constant for subsequent visits. The attached Powermeter (SRM, Germany), and accompanying software allowed for the application of an incremental protocol, such that resistance increased to give a specific power output, given that cadence remained constant throughout the test.

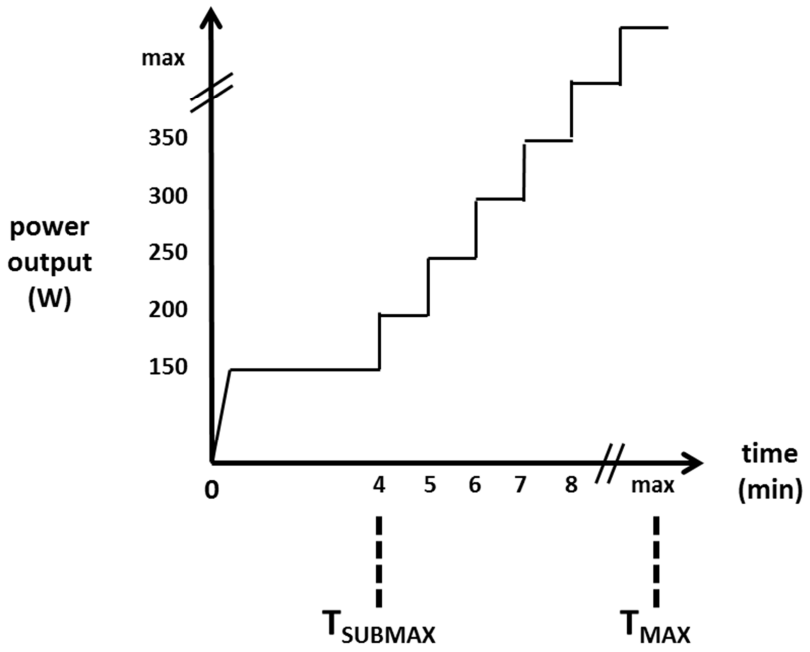

Figure 2.15 Incremental protocol using during exhaustive exercise test. Subjects began by cycling at 150 W at a self-selected cadence for 4 minutes. At this point (T_{SUBMAX}) power output was increased by 50 W/min until volitional exhaustion (T_{MAX}).

2.4.8. Rating of perceived exertion

In order to assess the subjects perceived rating of exertion, a modified Borg scale was used (OMNI Perceived Exertion Scale, 0 – 10) (201). Subjects were asked to rate their exertion using this scale every minute during exercise.

2.4.9. Blood pressure monitoring

Blood pressures are measured during exercise testing as a rapid, non-invasive method to monitor systemic cardiovascular function, in combination with heart rate. At maximum exercise intensity blood pressure increases, often to a systolic pressure of 200 mmHg and a diastolic pressure of approximately 100 mmHg (20). Blood pressure was assessed on the right arm during rest, exercise, and recovery using an automated blood pressure cuff (Omron, Japan). Manual blood pressures were impractical due to the number of other outcomes that were measured during and following the exercise test.

2.4.10. Assessment of blood lactate

Exercise above the anaerobic threshold increases circulating lactate (La) and hydrogen ion (H^+) concentration, causing a metabolic acidosis, which contributes to a muscular fatigue and physical exhaustion. Lactate measurements from capillary blood samples are commonly used during exercise testing to allow athletes to calculate their anaerobic threshold, to modify training strategies, and to test subject responses to a single exercise regime. Following an exhaustive period of exercise, circulating [La] is often greater than 10 mmol/L.

In the current study a Lactate Pro^{TM} (Arkway, Japan) device was used to offer a rapid, method for assessing blood [La] during rest, exercise and recovery (Figure 2.16). Following blood drawing with a sterile lancet, a disposable test strip was held to the finger tip, which used capillary action to take up the sample, such that only 5 µl of blood were required per sample. In the device, blood lactate combined with lactate

oxidase and potassium ferricyanide to form potassium ferrocyanide and pyruvate (202). When a voltage was applied, ferrocyanide was oxidised, creating a current proportional to the concentration of lactate, and measured amperometrically. The Lactate Pro™ device is accurate and repeatable, having been validated against gold-standard blood gas machines (203).

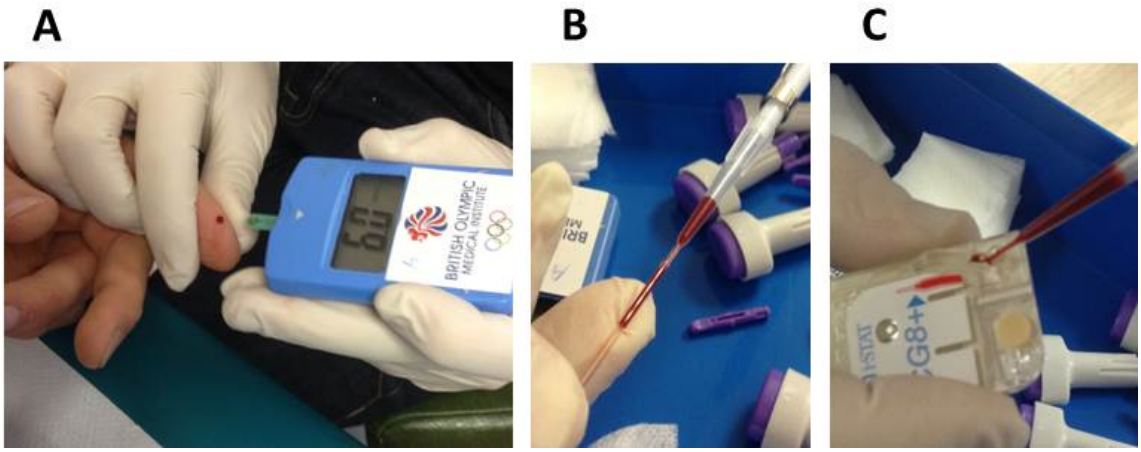

Figure 2.16 Capillary sampling during exercise testing. Following blood drawing, lactate concentration was measured from a drop of capillary blood (A). A capillary tube was then used to acquire a sufficient blood sample (B), which was transferred by pipette into the well of an iSTAT cartridge for blood gas and electrolyte measurement (C).

2.4.11. Assessment of blood gases and electrolytes

An exhaustive cycling test induces profound changes to blood gases and biochemistry (20). To account for exercise-induced metabolic acidosis, circulating bicarbonate (HCO_3^-) buffers the acid, and the resulting CO_2 is then expired. Blood gases at the end of an exhaustive test are associated with a high [La] and a low [HCO_3^-]. As the acidosis progresses, the [H^+] stimulate the carotid bodies, such that $\dot{V}_E$ increases more rapidly than $\dot{V}_{CO_2}$, and decreases arterial partial pressure of CO_2 ($PaCO_2$) (20).

Plasma electrolytes increase above the anaerobic threshold. This is most likely due to the increased intracellular osmolality due to accumulation of lactate and other metabolites during exercise (20). The increase in intracellular osmolality causes water to move into the cell along the osmotic gradient, and thus causing an increase in concentration in plasma electrolytes.

Blood gases are typically measured using a standard blood gases machine, such as the Radiometer ABL 700 (Radiometer, Denmark). However with the growing necessity for point-of-care testing, novel devices have been developed which allow for rapid detection of gases, whilst maintaining a high sensitivity to aid clinical diagnostics. One such device is the i-STAT® system (Abbott Laboratories, USA). The iSTAT® allows for different analyses to be made on the same sample. The current study has used $CG8^+$ cartridges, which provide plasma concentrations for pH, partial pressure of carbon dioxide (PCO_2), partial pressure of oxygen (PO_2), oxygen saturation (sO_2), total carbon dioxide ($TCO_{2)}$, bicarbonate (HCO_3^-), base excess (BE), sodium (Na^+), potassium (K^+), ionised calcium (iCa^{2+}), glucose, haematocrit (Hct) and haemoglobin (Hb). The methods used to perform each analysis are summarised in Table 2.3.

The cartridges were filled and processed according to manufacturer guidelines. Briefly capillary samples were taken from the finger tips during the exercise testing studies (Figure 2.16). A disposable lancet was held over the fingertip, and pressed onto the skin. Capillary blood was collected using two heparinised capillary tubes per sample (Na heparinised microhaematocrit capillary tubes, Hawksley, UK), and then immediately transferred to the cartridge by sterile pipette. The cartridge was transferred to the handheld unit and results were acquired within two minutes of sample acquisition.

Table 2.3 Analysis methods performed by iSTAT® CG8+ cartridges. Details obtained from manufacturer website (204).

Factor	Method of analysis	Range of values
pH	Direct potentiometry	6.50 – 8.20
pCO_2	Direct potentiometry	5 – 130 mmHg
pO_2	Amperometrically (similar to a conventional Clark electrode)	5 – 800 mmHg
TCO_2	Based upon Henderson-Hasselbalch equation	5-50 mmol/L
HCO_3	Calculated from pH and PCO2	N/A
BE	Calculated from pH and PCO2	N/A
sO_2	Function of PO_2	N/A
Na^+	Ion-selective electrode potentiometry	100-180 mmol/L
K^+	Ion-selective electrode potentiometry	2-9 mmol/L
iCa^{2+}	Ion-selective electrode potentiometry	0.25– 2.50 mmol/L
Glucose	Amperometrically	1.1-38.9 mmol/L
Haematocrit	Conductometrically	10-75%
Haemoglobin	Function of Hct	N/A

2.4.12. Assessment of blood haemoglobin and haematocrit

Haemoglobin is often assessed during exercise testing; it increases during an intense exercise bout to improve the delivery of oxygen during exercise (205). This study utilised the HemoCue® Hb 201^+ haemoglobin system (HemoCue® AB, Sweden), which provides a rapid point of care assessment of haemoglobin using a modified azidemethemoglobin reaction (206). Within each microcuvette a reagent containing sodium deoxycholate, sodium nitrite and sodium azide nitrite induces blood lysis, and converts haemoglobin to azide methamoglobin. Haemoglobin concentration is then assessed by a photometer, where the absorbance is measured at 570 and 880 nm, to

compensate for turbidity. The HemoCue® offers good agreement with a gold standard measure of haemoglobin, even at low concentrations (207).

Venous blood was collected using a 21-G butterfly needle (Becton Dickinson, USA) from the left antecubital vein, into 6 ml EDTA tubes which were kept at room temperature. All haemoglobin measurements were taken in duplets. Haematocrit was assessed by filling sodium heparinised micro-haematocrit capillary tubes with EDTA venous blood samples. Tubes were then spun (14000 *g*. , 5 min, room temperature) using a desktop microcentrifuge (HaematoSpin 1400, Hawksley, UK), and the haematocrit was measured in duplicate using a tube reader.

3. THE EFFECT OF ISCHAEMIC PRECONDITIONING ON CEREBRAL ISCHAEMIA-REPERFUSION IN RATS

3.1. Introduction

Human stroke currently accounts for 53,000 deaths per year in the UK (208). Thrombolysis, induced by infusion of tissue plasminogen activator, is the only widely used specific therapy for the treatment of acute stroke, but it is limited by a small treatment effect and risk of intracranial haemorrhage (209).

To reduce the burden of stroke, *in vivo* animal models are needed both to develop our understanding of stroke pathophysiology, and to identify novel treatments. Acute stroke in humans is characterised by an arterial or arteriolar occlusion that causes cerebral ischaemia, and is often followed by endogenous or exogenous thrombolysis and subsequent reperfusion. Modelling this in animals requires a method to cause a transient occlusion, allowing for reperfusion of the cerebral circulation, and therefore more representative of human stroke than permanent occlusion models. However *in vivo* stroke models are often limited by large between-animal variability, and as such stroke studies designed for testing novel therapies are often underpowered.

Recently groups have suggested that remote ischaemic preconditioning (RIPC) protects the brain from permanent cerebral arterial occlusion and ischaemia occurring after total circulatory arrest (88,210). This chapter describes the methodology for the development of a rat IR stroke model that uses a transient middle cerebral artery (MCA) occlusion. The initial experiments characterised the stroke model. Following this I sought to investigate whether MK-801, a known neuroprotective agent, reduces infarct size in this model. Finally studies investigated several RIPC protocols as potential neuroprotective strategies.

3.2. Methods

3.2.1. Experimental set up

Animal preparation and surgical procedures are described in section 2.1.2.

3.2.2. Experimental protocols

Seventy-one male, Sprague Dawley rats (aged 10-12 weeks, weight 180-200 g) were used to perform the experimental protocols detailed below.

3.2.2.1. Characterising the rat cerebral ischaemia-reperfusion model

The protocols used to characterise the model investigated two factors (see Figure 3.1). Firstly, whether a contralateral common carotid artery (CCA) occlusion applied during MCA occlusion influenced infarct size and between-animal variability. In protocol A the contralateral CCA was patent throughout the study; in protocol B the contralateral CCA was occluded for the first 30 minutes of the MCA occlusion; in protocol C the contralateral CCA was occluded for the full 60 minutes of the MCA occlusion. Secondly whether the duration of recovery influenced the infarct size and variability. In protocol D the duration of recovery was extended from 24 to 72 hours.

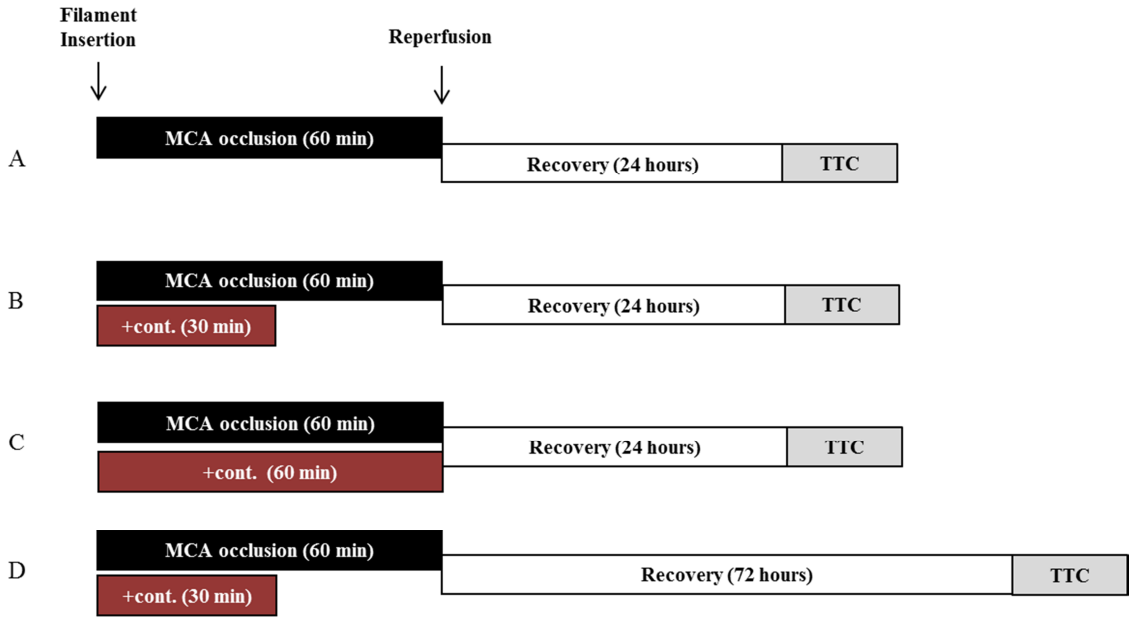

Figure 3.1 Experimental protocols to characterise the rat stroke model. This consisted of 60 minutes of MCA occlusion followed by 24 hours recovery (A), 60 minutes of MCA occlusion with 30 minutes contralateral CCA occlusion followed by 24 hours recovery (B), 60 minutes of MCA occlusion with 60 minutes contralateral CCA occlusion followed by 24 hours recovery (C), and 60 minutes of transient MCA occlusion with 30 minutes contralateral CCA occlusion followed by 72 hours recovery (D). +cont, contralateral CCA occlusion; MCA, middle cerebral artery; TTC, triphenyltetrazolium chloride staining analysis.

3.2.2.2. Effect of MK-801 and remote ischaemic preconditioning on cerebral ischaemia-reperfusion injury

MK-801 was used as a positive control (see section 2.1.2.6); it was administered 15 minutes prior to filament insertion (dose = 3 mg/kg i.p.) (Figure 3.2E). To determine the effect of RIPC, rats received 4 cycles of 5 minutes ischaemia followed by 5 minutes reperfusion on the right lower limb, immediately prior to filament insertion. This was performed with protocols consisting of a contralateral CCA occlusion of both 30 (Figure 3.2F) and 60 minutes duration (Figure 3.2G).

.

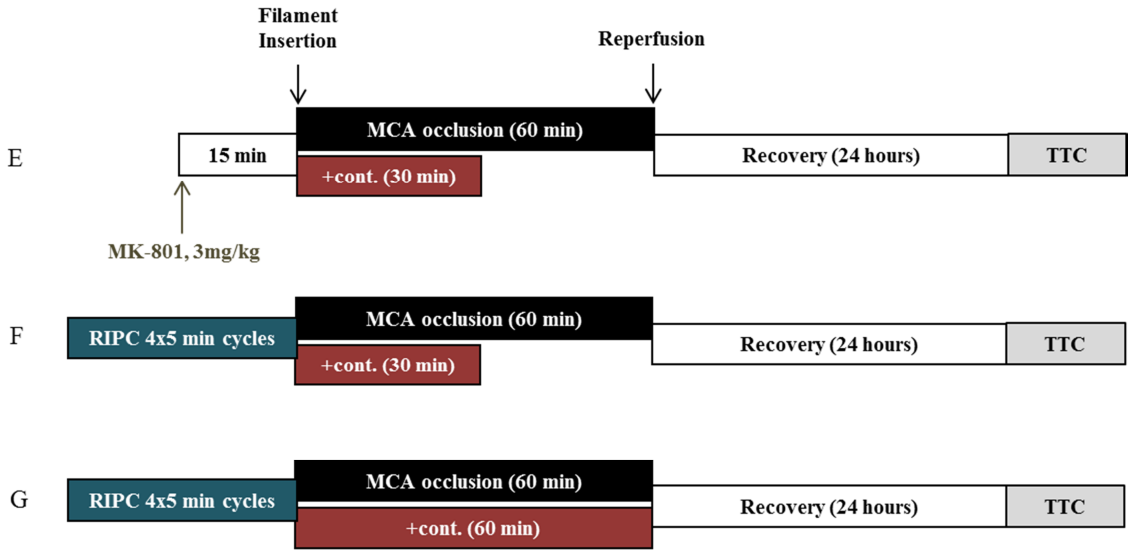

Figure 3.2 Experimental protocols to investigate the effect of MK-801 and RIPC on rodent stroke. MK-801 was administered 15 minutes prior to filament insertion (E). RIPC consisted of 4 cycles of 5 minutes occlusion followed by 5 minutes reperfusion, with both 30 (F) and 60 (G) minutes contralateral occlusion. +cont. denotes contralateral CCA occlusion. MCA, middle cerebral artery; TTC, triphenyltrazolium staining analysis.

RIPC was investigated further using additional protocols. Firstly the total duration of limb occlusion and reperfusion was extended to 90 minutes (3 RIPC cycles of 15 minutes occlusion and 15 minutes reperfusion, Figure 3.3H). Secondly the effects of anaesthesia on RIPC were investigated, by replacing injectable anaesthetics with inhaled anaesthesia (5% isoflurane for induction, 2% isoflurane for maintenance) (Figure 3.3J). Due to the extended duration of anaesthesia during these RIPC protocols, sham controls were used to mimic the revised schedule of the experiments (Figure 3.3I&K).

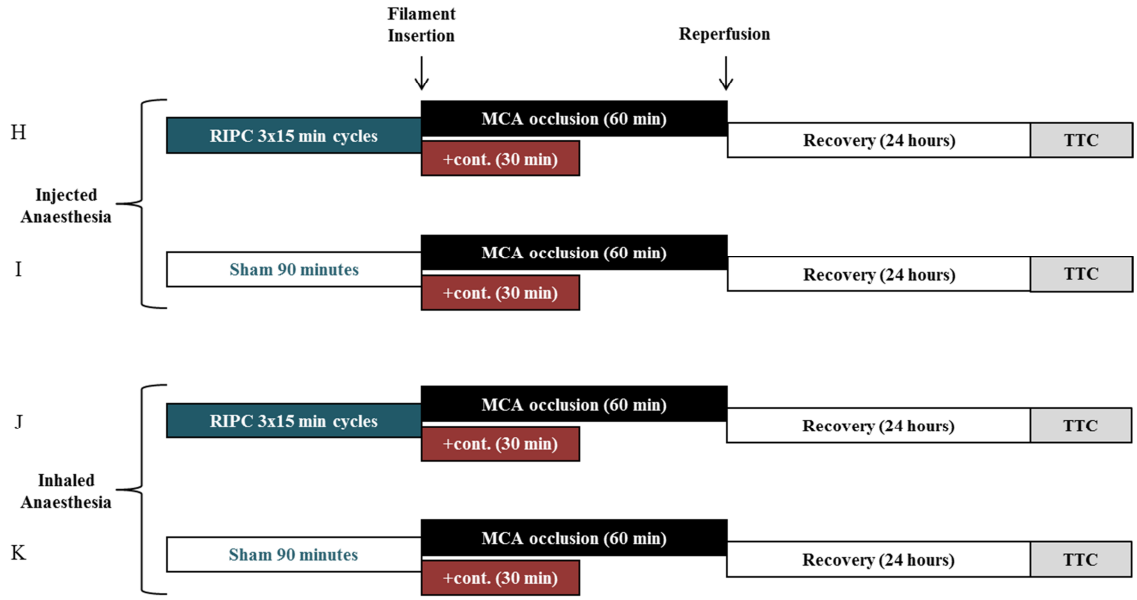

Figure 3.3 Experimental protocols to investigate the effects of duration and anaesthesia on RIPC-induced neuroprotection. The cycles of RIPC were extended to 3 cycles of 15 minutes occlusion and reperfusion (H). A sham control had matched anaesthetic dosing but without limb occlusions (I). Both of these protocols were repeated with inhaled isoflurane replacing injected anaesthesia (J & K). +cont. denotes contralateral CCA occlusion. MCA, middle cerebral artery; TTC, triphenyltrazolium staining analysis.

3.2.3. Image analysis

All images were analysed as described in section 2.1.3.

3.2.4. Calculations and statistics

Results are presented as the modified lesion area, as the percentage of the total hemispheric volume, and as the percentage of the area of the single MCA slice (see section 2.1.4). Group data are given as the mean ± SD. Results from RIPC protocols were matched with respective controls from the characterisation protocols, and were compared by unpaired *t* test or one-way ANOVA with a post-hoc Bonferroni multiple comparison test where appropriate. Within-group variation was expressed using the coefficient of variation (CV). Sample sizes were calculated using statistical software (Power and Sample Size Calculations, Dupont & Plummer, v3.0, (144)). $p < 0.05$ was deemed statistically significant.

3.3. Results

3.3.1. Contralateral occlusion increases infarct size and reduces between animal variability

MCA occlusion for 60 minutes caused a cerebral infarct (lesion volume, 45.9 ± 11.2%, n = 5). Contralateral CCA occlusion during MCA occlusion resulted in an increase in hemispheric lesion volume (30 min contralateral, 58.3 ± 8.9%, n = 6; 60 min contralateral, 71.7 ± 8.6%, n = 9; one-way ANOVA: 0 vs 60 min $p < 0.001$, 30 vs 60 min $p < 0.05$, Figure 3.4A). The increase in infarct size was associated with a reduction in within-protocol variability (no contralateral, CV = 24.5%; 30 min contralateral occlusion, CV = 15.2%; 60 min contralateral occlusion, CV = 12.0%).

Similar conclusions were drawn when data were analysed by single slice; lesion size increased after contralateral occlusion (no contralateral, 63.5 ± 8.2%, n = 5; 30 min contralateral, 73.0 ± 7.5%, n = 6; 60 min contralateral, 85.0 ± 4.8%, n = 9; one-way ANOVA: 0 vs 60 min $p < 0.001$, 30 vs 60 min $p < 0.05$; Figure 3.4B) and variability was reduced (no contralateral occlusion, CV = 12.9%; 30 min contralateral occlusion, CV = 10.3%; 60 min contralateral occlusion, CV = 5.7%).

In the group that received 60 minutes of contralateral CCA occlusion, 4 out of 9 (44%) showed evidence of a mild subcortical contralateral infarction, with none observed in the two remaining groups. Contralateral infarctions might confound the oedema correction in the lesion size calculation, so the majority of the intervention studies used 30 minutes of contralateral occlusion, at the expense of a greater within-protocol variability, but without confounding contralateral infarctions. A power calculation showed that 5 rats were needed to detect a 30% reduction in lesion size, and hence all intervention protocols had no fewer than 5 rats.

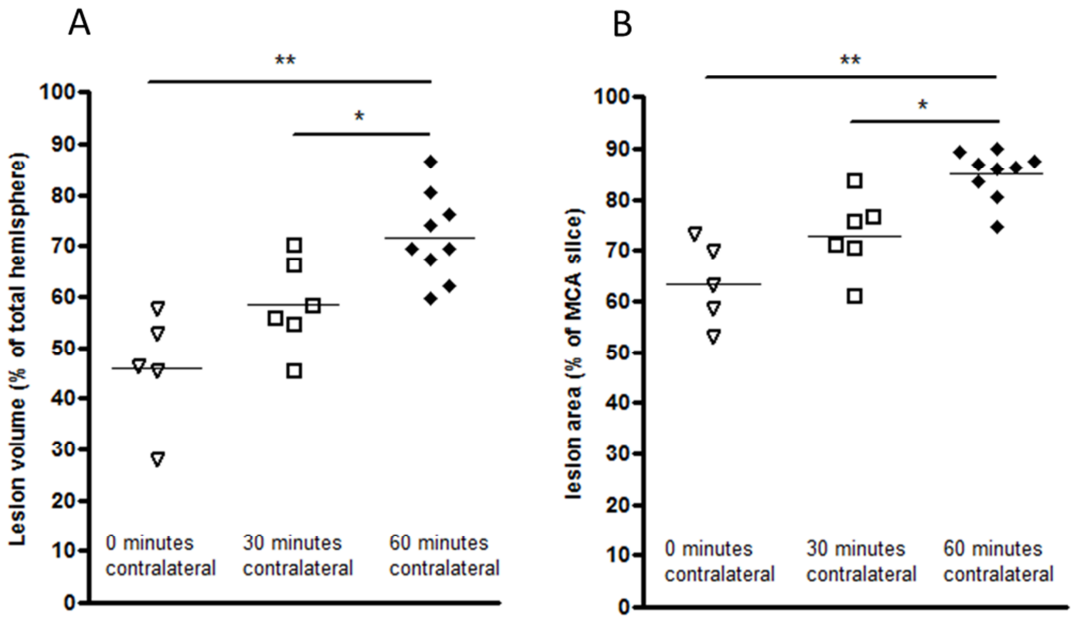

Figure 3.4 Effect of contralateral common carotid artery occlusion on lesion size. Increasing the duration of contralateral CCA occlusion in the rat stroke model resulted in an increase in lesion volume and a decrease in variability (A). These observations were consistent when the single slice analysis approach was used (B). Each point represents one animal, lines are group means. Triangles, 0 minutes of contralateral occlusion (n = 5); squares, 30 minutes of contralateral occlusion (n = 6); diamonds, 60 minutes of contralateral occlusion (n = 9); ** , $p < 0.01$; * , $p < 0.05$.

3.3.2. Extending the duration of recovery has no effect on infarct size, but increases between-animal variability

Further characterisation included extending the duration of reperfusion from 24 to 72 hours. This had no effect on hemispheric lesion volume (24 hours, 58.3 ± 8.9%, n = 6; 72 hours, 56.9 ± 15.1%, n = 7; unpaired *t* test, $p = 0.83$; Figure 3.5A). There was, however, an increase in variability (24 hours, CV = 15.2%; 72 hours, CV = 26.6%). The single slice analysis gave a similar result for both lesion size (24 hours, 73.0 ± 7.5%, n = 6; 72 hours, 72.3 ± 9.2%, n = 7; unpaired *t* test, $p = 0.89$; Figure 3.5B), and variability (24 hours, CV = 10.3%; 72 hours, CV = 12.8%).

Results show that the stroke model with 30 minutes of contralateral CCA occlusion and 24 hours of recovery has a low between-animal variability, irrespective of whether the whole brain or the single slice analysis method is used. Subsequent protocols used only the hemispheric lesion volume analysis method.

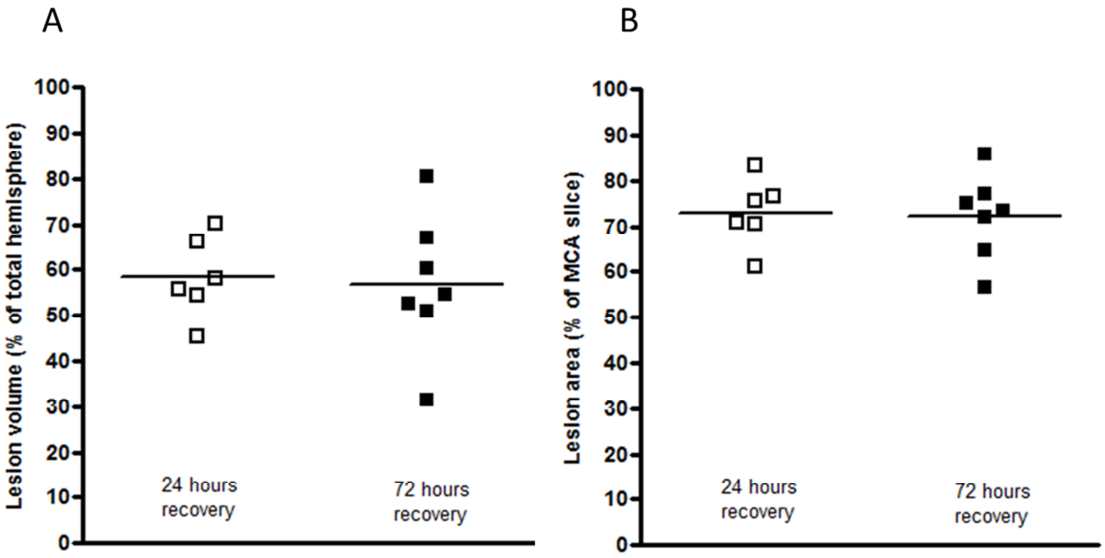

Figure 3.5 Effect of increasing the duration of recovery on lesion size. Increasing the duration of reperfusion had no effect on hemispheric lesion volume, but increased the variability (A). This observation was matched when the single slice analysis approach was used (B). Each point represents one animal, lines are group mean. White squares, 24 hours recovery (n = 6); black squares, 72 hours recovery (n = 7).

3.3.3. MK-801 reduces rat cerebral ischaemia-reperfusion injury

MK-801 conferred neuroprotection against cerebral infarction resulting in a significantly reduced hemispheric lesion volume when compared to control (control 58.3 ± 8.9%, n = 6; MK-801 48.0 ± 6.6%, n = 6; unpaired *t* test, $p < 0.05$; Figure 3.6).

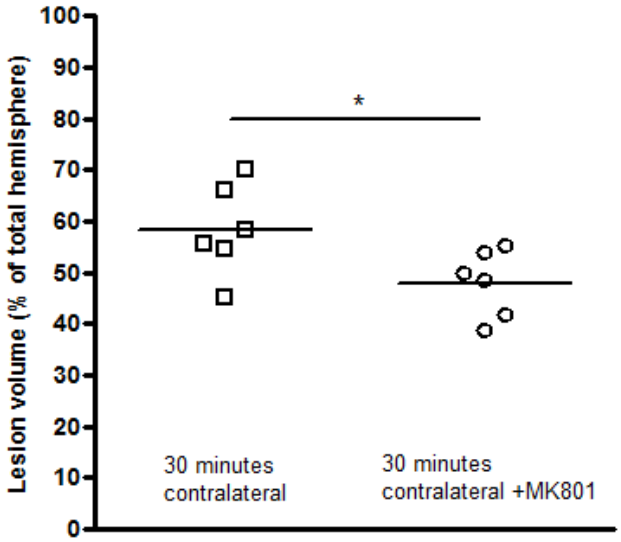

Figure 3.6 Effect of MK-801 on lesion size. MK801 was administered as a 3 mg/kg i.p. dose 15 minutes prior to filament insertion, and this significantly reduced the infarct size of the whole hemisphere. Each point represents one animal, lines are group mean. Squares, control with 30 minutes contralateral occlusion (n = 6); circles, MK801 with 30 minutes contralateral occlusion (n = 6). * , $p < 0.05$.

3.3.4. Remote ischaemic preconditioning using four 5-minute cycles does not protect against rat cerebral ischaemia-reperfusion injury

RIPC was initially studied using protocols consisting of 4 cycles of 5 minutes lower limb occlusion and 5 minutes of reperfusion. There was no difference between control and RIPC with 30 minutes (control, 58.3 ± 8.9%, n = 6; RIPC, 66.3 ± 12.1% n = 7; unpaired *t* test, $p = 0.21$; Figure 3.7) or 60 minutes of contralateral occlusion (control, 71.7 ± 8.6%, n = 9; RIPC, 76.1 ± 6.1%, n = 7; unpaired *t* test, $p = 0.27$; Figure 3.7).

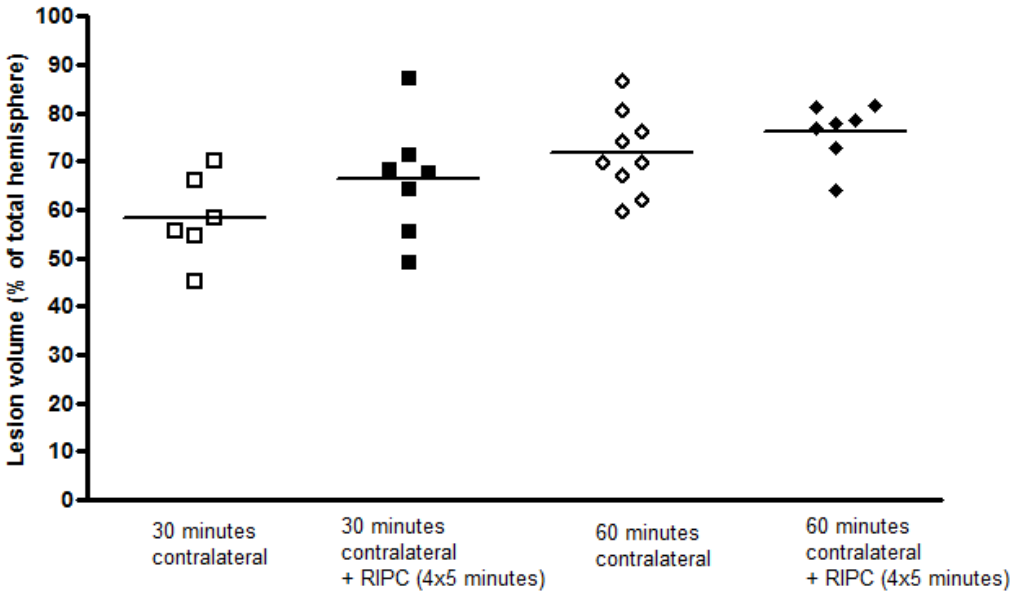

Figure 3.7 Effect of 4 cycles remote ischaemic preconditioning of 5 minutes on lesion size. RIPC had no effect on hemispheric infarct volume with either 30 or 60 minutes of contralateral CCA occlusion. Each point represents one animal, lines are group mean. White squares, control with 30 minutes contralateral occlusion (n = 6); black squares, RIPC with 30 minutes contralateral occlusion (n = 7); white diamonds, control with 60 minutes contralateral occlusion (n = 9); black diamonds, RIPC with 60 minutes contralateral occlusion (n = 7).

3.3.5. Remote ischaemic preconditioning protects against cerebral IR injury with inhaled, but not injectable anaesthesia

A final set of protocols examined whether a stronger stimulus of RIPC was required to induce protection against cerebral infarction, and whether the type of anaesthesia influenced the protective effect. Three RIPC cycles of an increased duration of 15 minutes occlusion, followed by 15 minutes of reperfusion, caused a non-significant reduction in infarct size when compared to the sham control (sham, 47.2 ± 6.0%, n = 5; RIPC, 41.8 ± 13.3%, n = 7; unpaired *t* test, $p = 0.42$; Figure 3.8). When repeated using inhaled anaesthesia, there was significant protection by RIPC to reduce stroke volume (sham, 38.3 ± 9.3%, n = 6; RIPC, 18.3 ± 5.3%, n = 6; unpaired *t* test, $p = 0.001$; Figure 3.8).

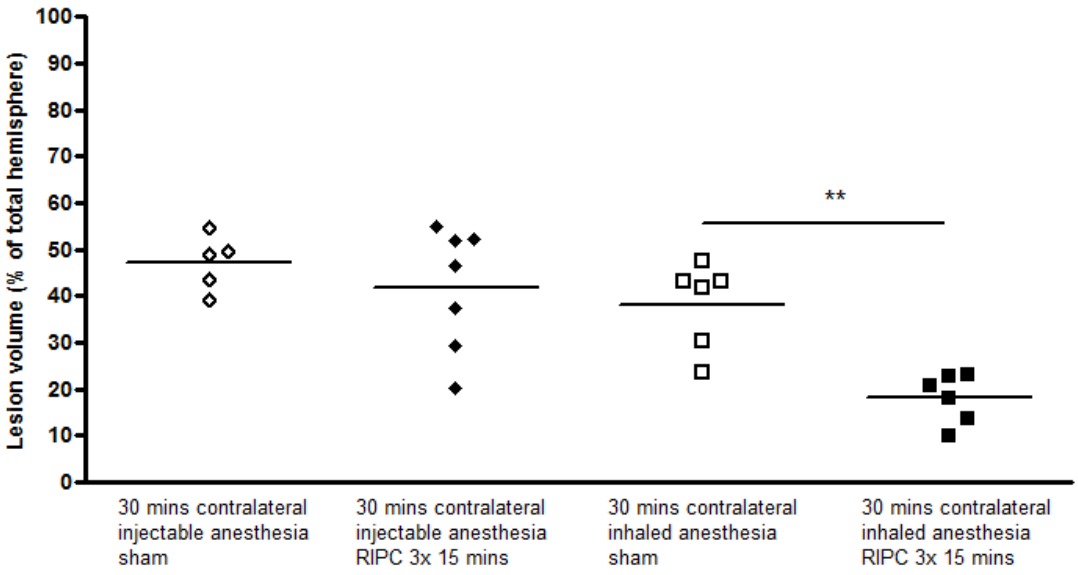

Figure 3.8 Effect of injected and inhaled anaesthesia on remote ischaemic preconditioning-induced neuroprotection. Increasing RIPC to 3 cycles of 15 minutes ischaemia and 15 minutes of reperfusion caused a non-significant reduction in infarct volume. Significant protection was observed when the anaesthetic was switched from injected to inhaled anaesthesia. RIPC studies were compared with time matched controls, and data analysed in a blinded fashion. Each point represents one animal, lines are group mean. White diamonds, sham control with injectable anaesthetic (n = 5); black diamonds, RIPC with injectable anaesthetic (n = 7); white squares, sham control with inhaled anaesthesia (n = 6); black squares, RIPC with inhaled anaesthesia (n = 6). ** , $p < 0.01$.

3.4. Discussion

The initial characterisation experiments presented in this chapter showed that the between-animal variability within the transient MCA occlusion model can be reduced using a contralateral CCA occlusion. Intervention studies initially supported previous observations that MK-801, a non-competitive antagonist of NMDA, reduces infarct volume, and thereby acted as a positive control for the model. Investigations of RIPC observed that it reduced infract size, but only to a significant extent when using inhaled, rather than injected anaesthesia.

3.4.1. Contralateral occlusion reduces variability in the middle cerebral artery occlusion model

To achieve a repeatable stroke model several factors were controlled in the methodology that might otherwise have increased variability (see section 2.1.2). These included the strain of the animal, age, sex and weight. Technical factors included the anesthetic regime, animal temperature during surgery and the size of the filament. However several factors were difficult to account for, such as the between-animal variability in collateral flow, which may differ considerably even within animal strain (211).

One way to reduce the effects of collateral flow was to reduce the flow throughout the cerebral circulation during MCA occlusion. This was achieved by occluding the contralateral CCA, whilst the patent vertebral arteries ensured the some cerebral blood flow was maintained. This resulted in a small increase in lesion size, and a decrease in the between-animal variability. However 60 minutes of contralateral CCA occlusion reduced cerebral flow to the extent that a small contralateral subcortical infarct developed in some animals. The presence of a contralateral infarct will induce contralateral oedema, and might confound the correction employed for ipsilateral

oedema. Therefore 30 minutes of contralateral CCA occlusion was chosen as the control for subsequent protocols.

Extending the duration of reperfusion had no effect on the mean infarct volume, but was associated with an increase in variability. Cell death in the infarcted territory is believed to occur during the arterial occlusion and initial 24 hours following reperfusion, and thus 24 hours of recovery were suitable for this study, matching protocols in the published literature (212,213).

3.4.2. Injectable anaesthesia inhibits the protective effect of remote ischaemic preconditioning

In the initial experiments using 4 cycles of 5 minutes RIPC did not reduce cerebral infarction, whereas the NMDA-receptor antagonist MK-801 showed significant protection. This was surprising, given that 3 or 4 cycles of 5 minutes occlusion and reperfusion is the gold standard RIPC protocol most commonly used in animal and human IR injury studies (5). The RIPC protocol was modified to match that performed in a recent rat stoke study; Ren et al. showed that 15 minute cycles of ischaemia and reperfusion were sufficient to induce a substantial protective effect (210). Using this protocol, there was a trend towards a reduced infarct size, but this was not significant.

One major experimental difference between my protocol and that by Ren et al., was the use of isoflurane to achieve anaesthesia, compared to the regime used in the present studies (a mixture of midazolam, fentanyl and fluanisone). When RIPC was induced using three 15-minute cycles, in the presence of isoflurane-based anaesthesia, a substantial protective effect of RIPC was identified. This suggests that the injected anaesthetic mixture inhibited RIPC. Of the three agents, only the opiate fentanyl is known to modulate preconditioning pathways, with most studies demonstrating that

opiates induce ischaemic protection (214). Further work is required to investigate the inhibitory action of these agents.

3.4.3. Remote ischaemic preconditioning as a treatment for human stroke

Since the start of this project several papers have been published, reporting the protective effects of RIPC using MCA models (212,213,215). Hahn et al. showed that RIPC reduces infarct size in a transient model of cerebral IR injury using a 4 cycles of 5 minutes occlusion protocol (212). Others have shown that RIPC may be abolished by inhibiting the adenosine A1 receptor (213), and by sensory nerve inhibition (215). All of these studies used an inhaled anaesthetic, further supporting the hypothesis that the lack of protective effect observed in my initial protocols was due to inhibition by the injected anaesthetic regime.

The onset of human stroke is unpredictable, and thus preconditioning is not plausible in this setting. However, future studies might aim to investigate whether intermittent cuff inflation applied during (RIPerC), or immediately following (RIPostC), a cerebral vessel occlusion, can afford protection. Whilst it has been suggested that both RIPerC (212), and RIPostC induce effective experimental neuroprotection (216), the mechanistic pathways are less well documented than RIPC. If RIPerC and RIPostC demonstrate sufficient efficacy and safety profile, it justifies a clinical trial. Indeed, Hougaard et al. have recently reported the study design for a phase III trial to validate the benefit of RIPerC in thrombolysed stroke patients, whereby intermittent limb ischaemia is started in the ambulance prior to hospital admission (217), using a similar study design to another trial that demonstrated efficacy of RIPerC in myocardial infarction (218).

3.5. Conclusion

My results describe the characterisation of an *in vivo* rat model of transient MCA occlusion, and identified an optimal schedule of vascular occlusion and reperfusion to generate the most consistent data. There are neuroprotective effects of RIPC, though stronger stimuli may be needed than appear effective in other organs. The effect of RIPC is masked by certain anaesthetic schedules. Further work aims to investigate the efficacy of RIPC in humans using an in vivo IR injury model.

4. CHARACTERISING A HUMAN IN VIVO VASCULAR MODEL OF ISCHAEMIA-REPERFUSION INJURY

4.1. Introduction

Flow mediated dilatation (FMD) has been used for nearly 20 years as a measure of endothelial function in humans *in vivo*. It is believed to be primarily nitric oxide mediated, and patients with endothelial dysfunction exhibit a reduced FMD. Importantly FMD exhibits a low within-subject variability when assessed by trained ultrasonographers, which has been documented by several research groups (154,161,219). Our research group has pioneered a human *in vivo* model of endothelial ischaemia-reperfusion (IR) injury over the past 10 years, using FMD as a marker of endothelial function. This model has been used to investigate therapeutic interventions for safety and efficacy against IR injury (15), prior to clinical trials in patients (118).

Despite the years of research, some uncertainty still exists regarding the physiological mechanisms regulating vascular diameter during basal, low, and high flow states. Most recently interest has developed in the arterial constriction that occurs during cuff occlusion, with Gori et al. demonstrating that this constriction (low-flow mediated constriction, L-FMC) is repeatable, is reduced in patients with atherosclerosis, and is correlated with FMD (154), consistent with it being a flow mediated phenomenon similar to FMD.

Our group has previously shown that upper limb IR injury induced by 20 minutes of proximal cuff inflation followed by reperfusion and subsequent recovery, reduces brachial artery FMD by 44–65% with no effect on baseline arterial diameter, blood pressure and heart rate, baseline arterial flow, or the hyperaemic flow stimulus (79,110,111). The IR-induced FMD reduction in the radial artery appears more profound, ranging from 55-87%, despite shorter durations of ischaemia and reperfusion (15,113,114,220).

The aim of this chapter was to explore the effect of IR injury on L-FMC, to validate L-FMC as a flow-dependent phenomenon. Here I report a characterisation of a human IR injury model in the brachial and the radial arteries. Initially within-subject variability was quantified for a number of vascular parameters including FMD and L-FMC. Secondly, the relationships between diameter and flow were investigated, during both low flow and transient high flow. Finally the response of these factors to IR injury is reported.

4.2. Methods

One hundred and sixty-seven studies were performed on 54 healthy male subjects aged 24 ± 6 (mean ± SD).

4.2.1. Subject preparation

Subjects were recruited and prepared for the study as outlined in section 2.2.2. All study participants were healthy males (aged 18-45 years).

4.2.2. Experimental set up

The FMD technique and IR experiments were set up according to section 2.2.2. Acquired images were analysed according to section 2.2.3.

4.2.3. Experimental protocols

4.2.3.1. Variability of the endothelial function test

To assess the within-subject variability of the ultrasound technique, subjects underwent imaging on two occasions of the brachial artery (n = 13) and the radial artery (n = 9). To assess between-analyser variability subjects were scanned by myself and an experienced sonographer (n = 6). Ultrasound images were analysed for baseline diameter, FMD, L-FMC, baseline velocity time integral (VTI), high flow VTI, and low flow VTI. At least 24 hours elapsed between scans on the same subjects.

4.2.3.2. Relationship between diameter and flow

To analyse the relationships between vessel diameter and flow, single ultrasound scans were performed on subjects in the brachial (n = 48) and radial (n = 24) artery. All scans were analysed for baseline diameter, FMD, L-FMC, baseline VTI, high flow VTI and low flow VTI.

4.2.3.3. Effect of limb ischaemia-reperfusion injury on endothelial function

The effect of IR on endothelial function was assessed using the protocols described in Figure 4.1. Brachial artery protocols were initially based upon previous results by our group which used 20 minutes of ischaemia, followed by reperfusion and 20 minutes of recovery (n = 20) (79,110–112). Results observed in section 4.3.3.1 led to additional brachial artery studies with the duration of post-reperfusion recovery extended by 5 minutes (n = 21). Radial artery protocols were carried out with 15 minutes of ischaemia and recovery, consistent with studies in the published literature, which have reported that this significantly reduces FMD (113,114).

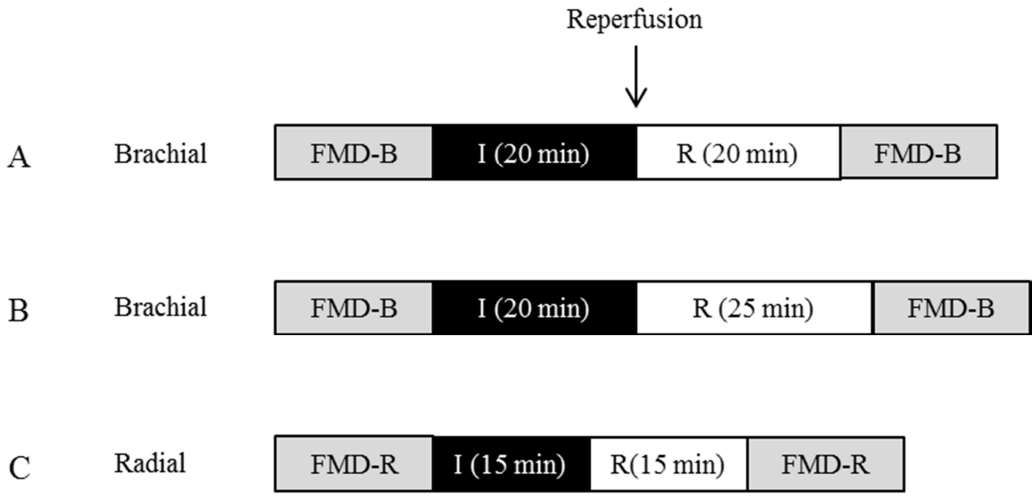

Figure 4.1 Experimental protocols for characterising a human vascular ischaemia-reperfusion injury model. Brachial artery studies were initially based upon 20 minutes ischaemia and 20 minutes of reperfusion (A) before being extended to 25 minutes of reperfusion (B). Radial artery studies consisted of durations of 15 minutes ischaemia and 15 minutes reperfusion (C). FMD-B, brachial artery flow mediated dilatation; FMD-R, radial artery flow mediated dilatation; I, ischaemia; R, recovery following reperfusion.

4.2.4. Calculations and statistics

FMD and L-FMC are expressed as absolute delta change (mm) or as a percentage of baseline (%). VTI at baseline, low-flow and high-flow are expressed as absolute values (m) or as absolute delta change (m) (see 2.2.4). FMD and L-FMC were corrected for baseline diameter, and VTI was corrected for heart rate. Results were excluded if there was a difference in baseline diameter of greater than 0.2 mm between scans performed before and after IR injury. Variability results are presented using the coefficient of variation (CV) and the intraclass correlation coefficient (ICC). Results are displayed using Bland-Altman plots, which include the mean difference, the standard deviation of the differences, and the 95% limits of agreement. Sample sizes were calculated using statistical software (see 3.2.4). Relationships between diameter changes and flow are presented using scatter plots including a linear regression with Pearson's *r* and a

correlation to assess whether the slope differs from 0. Pre and post-IR data were analysed for baseline diameter, FMD, L-FMC and VTI. Results are given as mean ± SD, and within group results were compared using paired *t* tests, given that baseline values fulfill normality criteria. $p < 0.05$ was deemed statistically significant.

4.3. Results

Consistent with experimental protocols, results are described firstly for testing variability, secondly to investigate relationships between variables, and finally to investigate the effect of IR injury on the responses to low and high flow stimuli. All studies were carried out with no adverse events.

4.3.1. Variability of endothelial function testing

The variability of changes in diameter and flow was assessed in the brachial and the radial arteries, and are described below.

4.3.1.1. Within-subject variability

In the brachial artery L-FMC (CV = 80.3%) was considerably more variable than FMD (CV = 12.1%) with no evidence of systematic bias in any outcome measure (Figure 4.2). This is primarily due to L-FMC having a lower mean value compared to FMD with a similar within subject SD (FMD, 8.50 ± 1.03%; L-FMC 1.74 ± 1.40%). Compared to the brachial artery, the radial artery had a higher CV for FMD (brachial, 12.1%; radial, 22.8%), but a lower ICC (brachial, 0.76; radial, 0.84) (Figure 4.3). For L-FMC the radial artery had a lower CV (brachial, 80.3%; radial, 28.9%), and a lower ICC (brachial, 0.66; radial, 0.71). VTI variability was similar in both arteries.

	BL diameter (mm)	FMD (%)	L-FMC (%)	BL VTI (m)	LF VTI (m)	HF VTI (m)
Mean	3.64	8.50	1.74	0.062	0.017	0.306
between subject SD	0.34	1.81	1.96	0.022	0.006	0.044
within subject SD	0.08	1.03	1.40	0.008	0.002	0.016
Mean CV (%)	2.1	12.1	80.3	12.7	12.8	5.20
ICC	0.95	0.76	0.66	0.88	0.88	0.88
mean difference	0.03	-0.97	0.41	-0.002	-0.001	-0.020
difference SD	0.13	1.47	2.46	0.022	0.005	0.037
n	13	13	13	13	13	13

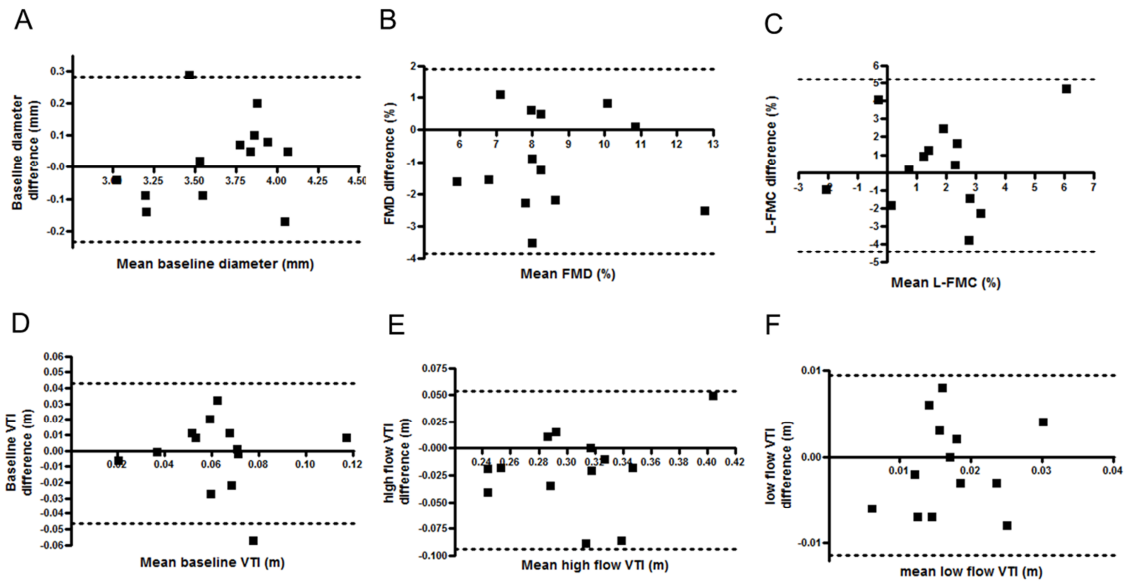

Figure 4.2 Within-subject variability of brachial artery outcome variables. Brachial artery flow mediated dilatation (FMD) scans were performed on 13 subjects on two occasions. Table summarises statistical results. Bland-Altman plots are shown for baseline diameter (A), FMD (B), low-flow mediated constriction (L-FMC) (C), baseline velocity time integral (VTI) (D), high flow VTI (E) and low flow VTI (F). Dotted lines represent 95% limits of agreement. Each point represents one subject.

	BL diameter (mm)	FMD (%)	L-FMC (%)	BL VTI (m)	LF VTI (m)	HF VTI (m)
Mean	2.12	8.37	6.55	0.076	0.011	0.290
between subject SD	0.22	4.40	2.97	0.051	0.003	0.075
within subject SD	0.10	1.90	1.89	0.009	0.002	0.023
Mean CV (%)	4.6	22.8	28.9	12.1	15.5	7.8
ICC	0.83	0.84	0.71	0.97	0.80	0.92
mean difference	-0.02	0.87	-1.28	0.007	0.000	-0.040
difference SD	0.18	3.18	3.50	0.027	0.004	0.052
n	9	9	9	8	8	8

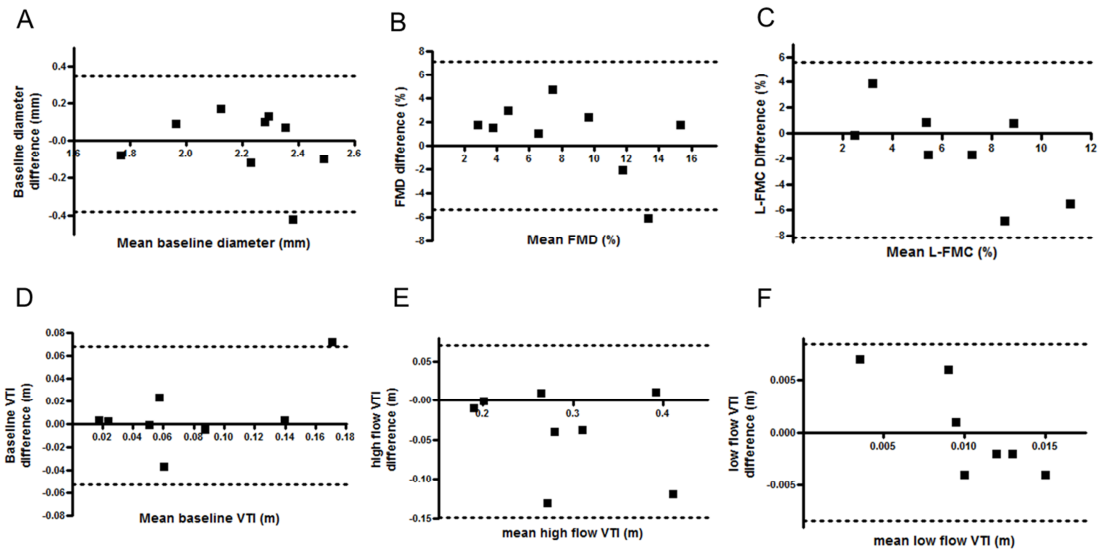

Figure 4.3 Within-subject variability of radial artery outcome variables. Radial artery flow mediated dilatation (FMD) scans were performed on 9 subjects on two occasions. Table summarises statistical results. Bland-Altman plots are shown for baseline diameter (A), FMD (B), low-flow mediated constriction (L-FMC) (C), baseline velocity-time integral (VTI) (D), high flow VTI (E) and low flow VTI (F). Dotted lines represent 95% limits of agreement. Each point represents one subject.

4.3.1.2. Between-sonographer variability

There was some evidence of systematic bias for L-FMC, but not diameter of FMD for between-sonographer studies (Figure 4.4). Brachial artery between-sonographer variability was similar to within-sonographer variability for baseline diameter (BL diameter, 1.8 vs 2.1; FMD, 18.1 vs 12.1; L-FMC, 52.9 vs 80.3).

	BL diameter (mm)	**FMD (%)**	**L-FMC (%)**
Mean	3.57	7.81	2.41
between subject SD	0.36	1.80	2.06
within subject SD	0.06	1.42	1.27
Mean CV (%)	1.8	18.1	52.9
ICC	0.97	0.62	0.72
mean difference	0.05	0.19	-1.80
difference SD	0.09	2.69	2.65
n	6	6	6

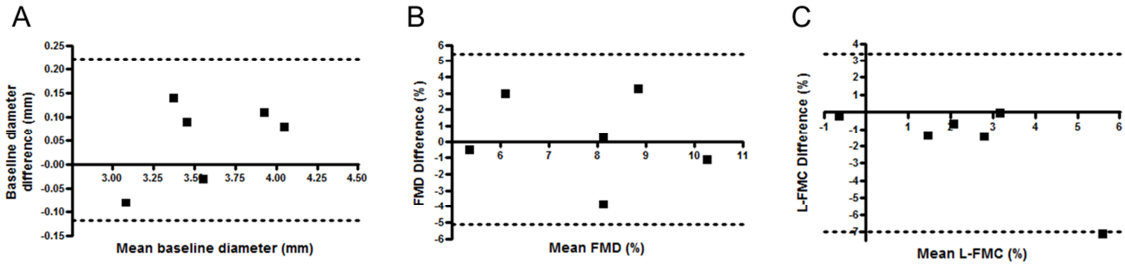

Figure 4.4 Between-sonographer variability of brachial artery flow mediated dilatation outcome variables. Brachial artery flow mediated dilatation scans were performed on 6 subjects on two occasions by two investigators. Table summarises statistical results. Bland-Altman plots are shown for baseline diameter (A), flow mediated dilatation (FMD) (B) and low-flow mediated constriction (L-FMC) (C). Dotted lines represent 95% limits of agreement. Each point represents one subject.

4.3.2. Relationships between changes in diameter and flow

4.3.2.1. Flow mediated dilatation and low-flow mediated constriction are correlated with baseline diameter.

The relationships between resting baseline diameter, FMD and L-FMC are shown in Figure 4.5. FMD had a negative correlation with baseline diameter in both the brachial and radial arteries (brachial, r = -0.391, p = 0.006, n = 48; radial, r = -0.408, p = 0.048, n = 24; linear regression). L-FMC was positively correlated with baseline diameter in the brachial and radial arteries (brachial, r = 0.260, p = 0.075, n = 48; radial, r = 0.603, p = 0.002, n = 24; linear regression). There was a trend of negative correlation between L-FMC and FMD in both arteries, but this did not reach statistical significance (brachial, r = -0.092, p = 0.534, n = 48; radial, r = -0.376, p = 0.070, n = 24; linear regression).

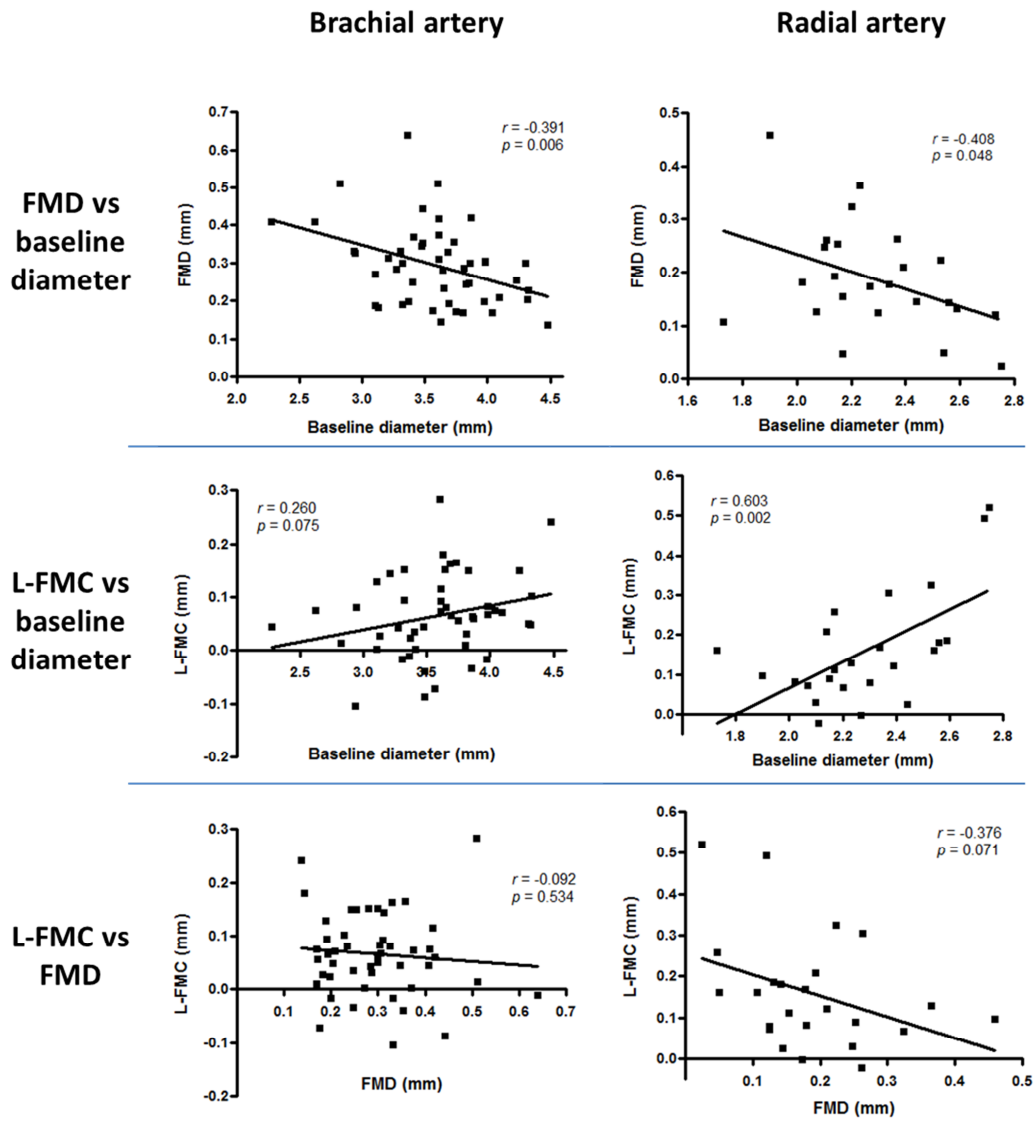

Figure 4.5 Relationships between flow mediated dilatation, low-flow mediated constriction and baseline diameter. Resting ultrasound recordings were made on healthy male subjects in the brachial (n = 48) and radial (n = 24) artery. Calculations were made of flow mediated dilatation (FMD), low-flow mediated constriction (L-FMC), and baseline diameter. FMD was negatively correlated with baseline diameter in both arteries. L-FMC was positively correlated with baseline diameter in both arteries, though this did not reach statistical significance in the brachial artery. FMD and L-FMC tended towards a negative correlation in both arteries, but this did not reach statistical significance in either artery. Each point represents one subject. Lines show linear regression.

4.3.2.2. Diameter changes are weakly associated with flow

The relationship between FMD and the change in VTI during the transient high flow ($\Delta VTI_{high\text{-}flow}$), and L-FMC and the change in VTI during the low flow ($\Delta VTI_{low\text{-}flow}$), are shown in Figure 4.6. FMD had a weak positive correlation with $\Delta VTI_{high\text{-}flow}$ in both arteries (brachial, r = 0.155, p = 0.293, n = 48; radial, r = 0.285, p = 0.177, n = 24; linear regression). L-FMC was positively correlated with $\Delta VTI_{low\text{-}flow}$ in both arteries (brachial, r = 0.309, p = 0.033, n = 48; radial, r = 0.466, p = 0.022, n = 24; linear regression).

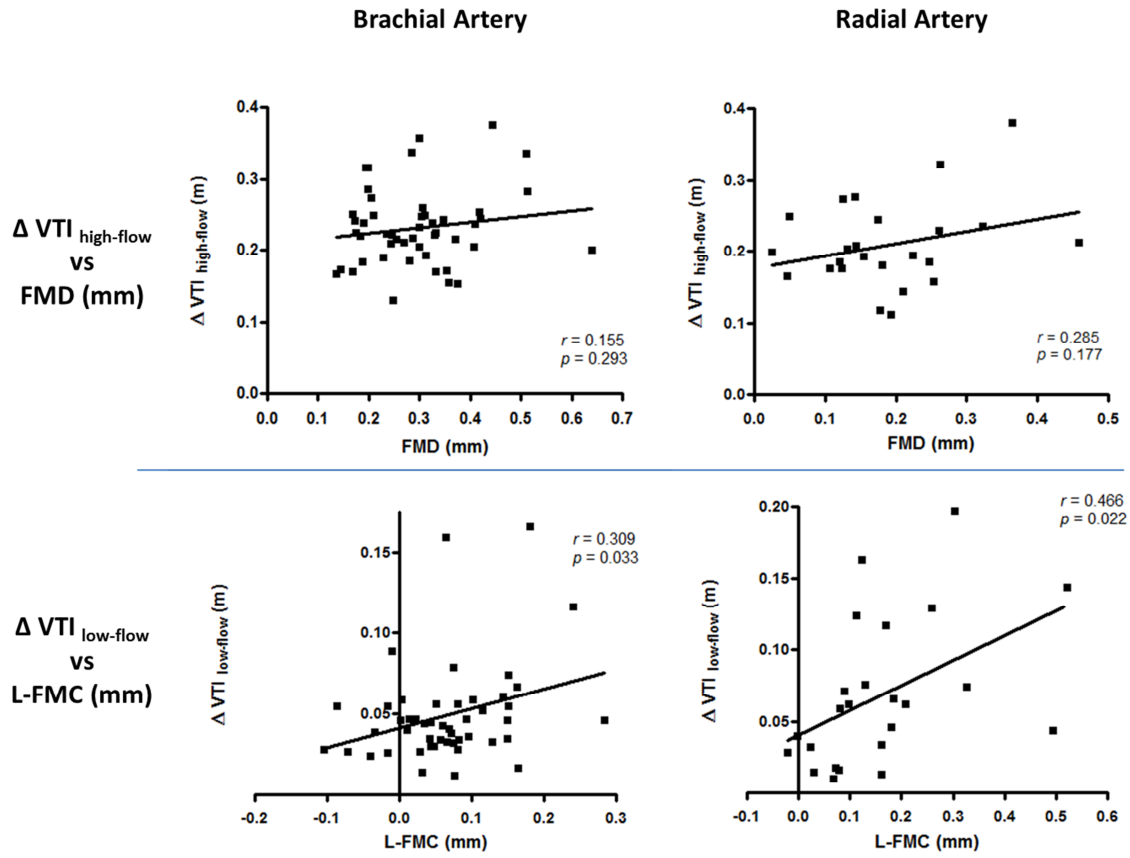

Figure 4.6 Relationship between arterial diameter and velocity time integral. Resting ultrasound recordings were made on healthy male subjects in the brachial (n = 48) and radial (n = 24) artery. Calculations were made of flow mediated dilatation (FMD), low-flow mediated constriction (L-FMC), and the change in velocity-time integral (ΔVTI). $\Delta VTI_{high\text{-}flow}$ and FMD were weakly correlated in both arteries, but this did not reach statistical significance in either artery. $\Delta VTI_{low\text{-}flow}$ was correlated with L-FMC in both arteries. Each point represents one subject. Lines show linear regression.

4.3.3. Effect of ischaemia-reperfusion injury on endothelial function

Results are summarised in table Table 4.1 and described below.

4.3.3.1. Twenty minutes of recovery is insufficient duration for arterial diameter to return to baseline

Following 20 minutes of recovery following reperfusion, resting arterial diameter remained dilated when compared to baseline (BL, 3.62 ± 0.32; post IR 3.69 ± 0.38; p = 0.001, paired t test; n = 20; Figure 4.7A). By extending the duration of recovery to 25 minutes, the vessel was no longer significantly dilated (BL, 3.60 ± 0.37; post IR 3.63 ± 0.36; p = 0.105, paired t test; n = 21; Figure 4.7B). After 15 minutes of recovery in the radial artery, the vessel was dilated, but did not reach statistical significance (BL, 2.34 ± 0.15; post IR, 2.38 ± 0.17; p = 0.083, paired t test; n = 10; Figure 4.7C).

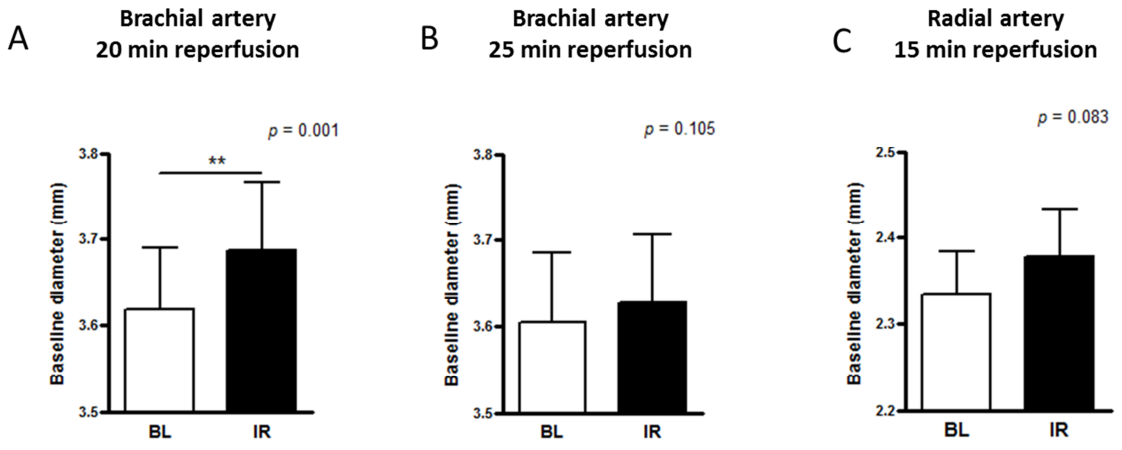

Figure 4.7 Effect of ischaemia-reperfusion injury on baseline diameter. Flow mediated dilatation recordings were made on healthy male subjects. This was followed by IR, and a second recording. Brachial artery baseline diameter was significantly increased 20 minutes following reperfusion (n = 20, A). Brachial artery baseline diameter was increased at 25 minutes of reperfusion, but this was not significant (n = 21, B). Radial artery baseline diameter was increased at 15 minutes reperfusion, but this was not significant (n = 10, C). Bars show mean ± standard error. ** , p < 0.01

4.3.3.2. Ischaemia-reperfusion injury reduces flow mediated dilatation and increases low-flow mediated constriction

FMD and L-FMC values were corrected for differences in baseline diameter, using baseline correlations (Figure 4.5). IR reduced brachial artery FMD at 20 minutes (BL, 7.64 ± 2.06%; post IR, 5.09 ± 1.90%; $p < 0.0001$, n = 20) and 25 minutes of reperfusion (BL, 8.05 ± 2.49%; post IR 6.53 ± 3.08%, $p = 0.004$, n = 21), and in the radial artery (BL, 9.36 ± 2.91%; post IR, 5.96 ± 4.93%, $p = 0.017$, n = 10; paired *t* test) (Figure 4.8). IR increased brachial artery L-FMC at 20 minutes (BL, 2.50 ± 2.54%; post IR 3.49 ± 2.10%, $p = 0.025$, n = 20) and at 25 minutes of reperfusion (BL, 1.85 ± 2.17%; post IR 2.80 ± 1.85%, $p = 0.041$, n = 21), and in the radial artery (BL, 5.46 ± 4.60%; post IR 8.71 ± 4.64%, $p = 0.055$, n = 10; paired *t* test) (Figure 4.8).

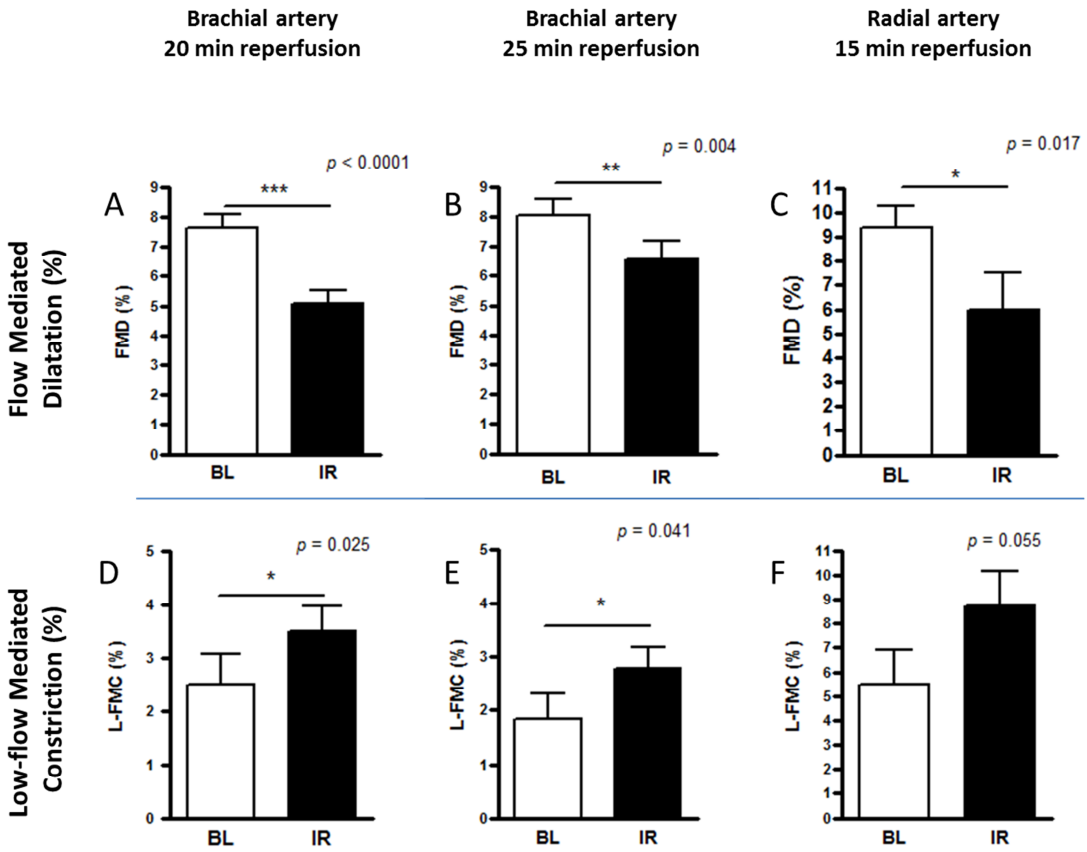

Figure 4.8 Effect of ischaemia-reperfusion injury on flow mediated dilatation and low-flow mediated constriction. FMD recordings were made on healthy male subjects. This was followed by IR, and a second recording. IR caused a reduction in FMD in the brachial artery 20 minutes following reperfusion (n = 20, A), 25 minutes following reperfusion (n = 21, B), and in the radial artery at 15 minutes following reperfusion (n = 10, C). IR caused an increase in L-FMC in the brachial artery 20 minutes following reperfusion (n = 20, D), 25 minutes following reperfusion (n = 21, E), and in the radial artery at 15 minutes following reperfusion (n = 10, F). Bars show mean ± standard error. ***, p < 0.001; ** , p < 0.01; * , p < 0.05

4.3.3.3. Ischaemia-reperfusion injury results in a complex alteration to arterial flow

There was a slight decrease in heart rate (HR) during IR injury studies (see Table 4.1), and hence velocity-time integral (VTI) was HR-adjusted according to baseline correlations. IR resulted in a decrease in the baseline VTI, however this was only significant in the brachial artery with 25 minutes of reperfusion (brachial 20 min, BL 0.071 ± 0.020 m, post IR 0.066 ± 0.029 m, $p = 0.377$, n = 20; brachial 25 min, BL 0.075 ± 0.025 m, post IR 0.063 ± 0.018 m, $p = 0.042$, n = 21; radial 15 min, BL 0.090 ± 0.065 m, post IR 0.077 ± 0.047 m, $p = 0.368$, n = 10; paired *t* test; Figure 4.9A-C). IR resulted in an increase in high flow VTI (brachial 20 min, BL 0.321 ± 0.046 m, post IR 0.361 ± 0.056 m, $p < 0.001$, n = 20; brachial 25 min, BL 0.300 ± 0.052 m, post IR 0.326 ± 0.052 m, $p = 0.001$, n = 21; radial 15 min, BL 0.299 ± 0.090 m, post IR 0.318 ± 0.092 m, $p = 0.191$, n = 10; paired *t* test; Figure 4.9D-F). IR had no effect on low flow VTI (brachial 20 min, BL 0.019 ± 0.006 m, post IR 0.020 ± 0.006 m, $p = 0.566$, n = 20; brachial 25 min, BL 0.025 ± 0.010 m, post IR 0.025 ± 0.010 m, $p = 0.544$, n = 21; radial 15 min, BL 0.013 ± 0.005 m, post IR 0.014 ± 0.004 m, $p = 0.856$, n = 10; paired *t* test; Figure 4.9G-I).

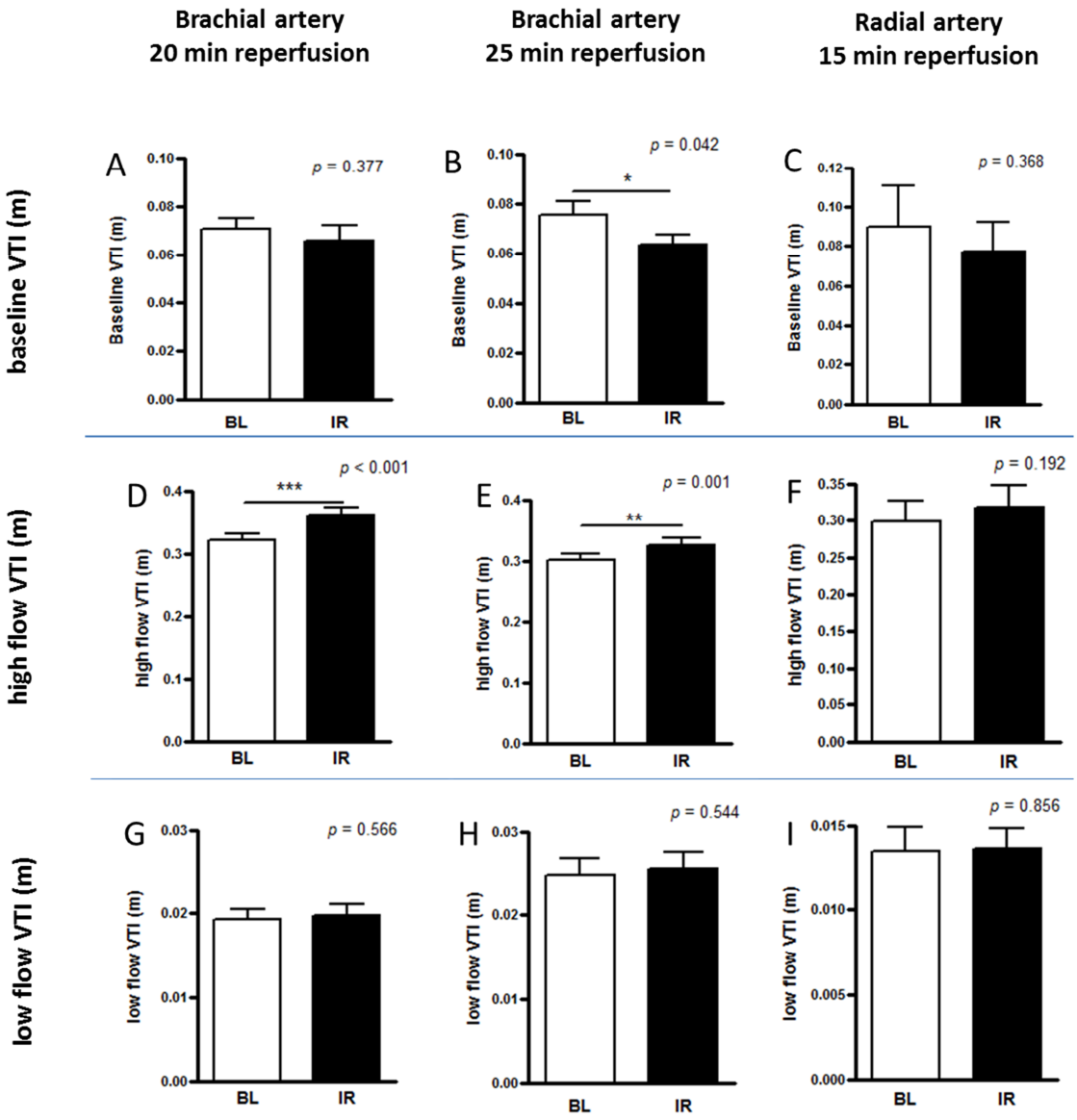

Figure 4.9 Effect of ischaemia-reperfusion injury on arterial flow. FMD recordings were made on healthy male subjects. This was followed by IR, and a second recording. IR caused a small decrease in baseline velocity time integral (VTI), which reached statistical significance in the brachial artery with 25 minutes of reperfusion (n = 21, B) but not with 20 minutes of reperfusion (n = 20, A) or in the radial artery with 15 minutes (n = 10, C). IR increased arterial high flow VTI, but this did not reach significance in the radial artery (F). IR had no effect on low flow VTI in any artery. Bars show mean ± standard error. ***, p < 0.001; ** , p < 0.01; * , p < 0.05

Table 4.1 Summarised results of the effect of ischaemia-reperfusion injury on endothelial function in humans.

	Brachial IR(20) n = 20			Brachial IR(25) n = 21			Radial IR(15) n = 10		
	BL	post IR	*p*	BL	post IR	*p*	BL	post IR	*p*
BL Diam (mm)	3.62 ± 0.32	3.69 ± 0.38	0.001	3.60 ± 0.37	3.63 ± 0.36	0.105	2.34 ± 0.15	2.38 ± 0.17	0.083
FMD (%)	7.64 ± 2.06	5.09 ± 1.90	<0.001	8.05 ± 2.49	6.53 ± 3.08	0.004	9.36 ± 2.91	5.96 ± 4.93	0.017
L-FMC (%)	2.50 ± 2.54	3.49 ± 2.10	0.025	1.85 ± 2.17	2.80 ± 1.85	0.041	5.46 ± 4.60	8.71 ± 4.64	0.055
SBP (mmHg)	115 ± 8	114 ± 8	0.416	114 ± 7	116 ± 9	0.115	114 ± 8	112 ± 9	0.285
DBP (mmHg)	62 ± 6	61 ± 5	0.658	60 ± 5	63 ± 7	0.009	58 ± 5	60 ± 6	0.052
HR (bpm)	62 ± 11	57 ± 9	0.019	64 ± 9	59 ± 7	0.033	59 ± 7	57 ± 6	0.141
baseline VTI (m)	0.071 ± 0.020	0.066 ± 0.029	0.377	0.075 ± 0.025	0.063 ± 0.018	0.042	0.090 ± 0.065	0.077 ± 0.047	0.368
high flow VTI (m)	0.321 ± 0.046	0.361 ± 0.056	<0.001	0.300 ± 0.052	0.326 ± 0.052	0.001	0.299 ± 0.090	0.318 ± 0.092	0.191
low flow VTI (m)	0.019 ± 0.006	0.020 ± 0.006	0.566	0.025 ± 0.010	0.025 ± 0.010	0.544	0.013 ± 0.005	0.014 ± 0.004	0.856

4.4. Discussion

The results in this chapter have characterised the FMD and L-FMC phenomena, their relationship to resting arterial diameter and VTI, and their response to IR injury. The within-subject variability and agreement for repeated tests for this technique has been reported by several groups (154,161,221,222). In the current study brachial artery coefficient of variation (FMD, 12.1%; BL diameter, 2.1%) was comparable to that of Donald et al. (FMD, 10.6%; BL diameter, 2.6%) (161), and Hijmering et al., (FMD, 13.9%) (222). In the radial artery intraclass correlation coefficient (FMD 0.84; L-FMC

0.71) was similar to that of Gori et al. (FMD 0.68; L-FMC 0.80) (154). This reassures that the current ultrasound technique is comparable with the published literature. Furthermore, given that analysis itself (see 2.2.3.3) is attributable to some of this variability (FMD 3.4%; BL diameter 0.2%), this shows that my ultrasound methodology provides a repeatable measure of FMD and L-FMC. The between-sonographer variability was similar to a single analyser, verifying this technique with previous experienced sonographers in our research group.

4.4.1. Assessment of endothelial function by flow mediated dilatation and low-flow mediated constriction

Using the ultrasound technique, baseline studies were performed on subjects at the brachial and radial artery. Results show similar relationships between FMD, L-FMC and resting arterial diameter for both arteries. The brachial artery has a smaller mean L-FMC than the radial artery, for reasons which remain uncertain.

Since its initial description FMD is known to be dependent on baseline diameter (150), however it has been unknown whether this is also the case for L-FMC. Results in this chapter identified a positive correlation between baseline diameter and L-FMC in both arteries. In contradiction, two previous papers reported that no relationship exists between brachial artery L-FMC and baseline diameter (166,223). Their findings may be due to a weak correlation in the brachial artery, attributable to a low mean L-FMC, and subsequently a higher within-subject variability (current study, CV = 80.3%). Lower variability in the radial artery (current study, CV = 28.9%), allows the relationship between L-FMC and baseline diameter to be more apparent. Results in this chapter also show a weak negative correlation between FMD and L-FMC in both arteries. In the literature to date, this relationship has been uncertain, with studies reporting a negative (168), positive (224), and no correlation (223). My data contribute to this uncertainty,

and additional studies of greater sample sizes are required to finalise associations between these variables.

There was a stronger relationship between blood flow (using VTI as a proxy) and L-FMC that there was between VTI and FMD. One explanation for this is that blood flow is in a steady state during L-FMC, whereas the flow stimulus changes rapidly during reactive hyperaemia.

4.4.2. Ischaemia-reperfusion injury reduces dilator endothelial function

Prolonged upper limb cuff inflation inducing ischaemia, followed by reperfusion has been used as a model to induce a transient endothelial dysfunction in our research group for over 10 years. Kharbanda et al. were the first to show that 20 minutes of ischaemia resulted in a reduction in radial artery FMD at 15 minutes following reperfusion, but that the vessel had recovered by 60 minutes (15). The reduction in FMD was independent of changes in baseline diameter or flow. More recent brachial studies have an extended duration of reperfusion of 20 minutes (110–112).

In the current study subjects received durations of IR that was identical to previous studies; 20 minutes of ischaemia followed by 20 minutes of recovery. However in my studies 20 minutes of reperfusion were insufficient to allow the brachial artery to return to baseline following the post-ischaemic vasodilatation (BL, 3.62 mm; post IR, 3.69 mm). An additional protocol extended reperfusion to 25 minutes, such that vessels were no longer significantly dilated at the start of the second recording (BL, 3.60 mm; post IR, 3.63 mm). In addition, a protocol was carried out in the radial artery using 15 minutes of ischaemia and 15 minutes of reperfusion, based upon studies of other groups (113,114,220).

Results in this chapter showed that IR reduces FMD, and increases L-FMC. IR is known to reduce endothelium-dependent vasodilatation in response to acetyl choline in

animals and humans (40,41). Furthermore, IR reduces bioavailability of vasodilators such as NO, and increases vasoconstrictors such as endothelin-1 and pro-inflammatory mediators (16). The mechanism of IR-induced endothelial dysfunction may include an increase in reactive oxygen species and a reduced bioavailability of NO. Were L-FMC merely the flip-side of FMD, then one would expect that it too would diminish after IR injury. That it increased suggests that it has a different mechanism from FMD, and this could include a role for local accumulation of vasoconstrictors including endothelin-1 (167) and thromboxane (154).

4.5. Conclusion

This chapter used an *in vivo* vascular function test to describe the variability characteristics, correlations and response to IR injury, for FMD, L-FMC, resting diameter and VTI. Correlations exist between FMD, L-FMC and baseline diameter in both the radial and brachial artery. Given the negative correlation between FMD and L-FMC, and that IR injury reduces FMD but increases L-FMC, it is suggested that the two are mechanistically different. Using this model I plan to investigate ischaemic preconditioning as a protective phenomenon against *in vivo* IR injury in humans.

5. THE EFFECT OF ISCHAEMIC AND EXERCISE PRECONDITIONING ON ISCHAEMIA-REPERFUSION INJURY IN HUMANS

5.1. Introduction

Arterial occlusion results in tissue ischaemia, cellular hypoxia, and an accumulation of waste metabolites, contributing to irreversible injury secondary to necrotic cell death. Reperfusion, whilst necessary for recovery, contributes to injury. Preventing ischaemia-reperfusion (IR) injury has been the focus of extensive research, but few therapies have successfully developed from "bench to bedside". Human *in vivo* models can act as a bridge between animal studies and clinical trials in patients; a convenient proxy to facilitate the identification of novel interventions that are safe and have a therapeutic potential in humans.

In chapter 4 a human *in vivo* model of endothelial IR injury was characterised. IR induced endothelial dysfunction, defined as a decrease in flow mediated dilatation (FMD). This was consistent with previous observations by our group and others (15,113), and complemented animal studies investigating the effect of IR on endothelial biology (39). IR also resulted in an increase in low-flow mediated constriction (L-FMC), a phenomenon only recently described, but may offer additional information of the behaviour of the arterial endothelium.

In chapter 3 a rat stroke model was described, which demonstrated that remote ischaemic preconditioning (RIPC) protects the brain from a subsequent IR injury. Previous studies by our group have observed that non-lethal, intermittent bouts of local (IPC) or remote (RIPC) ischaemic preconditioning applied prior to a prolonged limb IR protect against a reduction in FMD (15,41,79,111). IPC and RIPC have also afforded protection against IR in early phase clinical trials (see section 1.3). However, to date no studies have investigated the effect of IPC and RIPC on L-FMC following IR injury. I have speculated that, like FMD, L-FMC is an endothelium dependent phenomenon, and hypothesise that IPC and RIPC prevent the IR-induced increase in L-FMC.

Animal experiments suggest that exercise too might confer protection against IR injury (exercise preconditioning, ExPC) (section 1.3.3). Brief, intense exercise reduces experimental cerebral infarct size (108), and stimulate cellular pathways that are comparable to components of the IPC mechanism (100,101). This has not been demonstrated in a human IR injury model to date.

This chapter initially investigates the effect of RIPC on brachial artery IR injury. Secondly it describes IPC as a therapeutic intervention against IR injury in both the brachial and the radial artery. Finally ExPC is investigated as a novel therapeutic intervention against IR injury.

5.2. Methods

Fifty-nine studies were performed on 20 subjects aged 22 ± 3 years (mean ± SD).

5.2.1. Subject preparation

Subjects were recruited and prepared for study as outlined in section 2.2.2. All study participants were healthy males (aged 18-45 years).

5.2.2. Experimental set up

FMD and IR injury experiments were set up according to section 2.2.2. Acquired images were analysed according to section 2.2.3.

5.2.3. Experimental protocols

Experimental protocols designed to identify the effects of RIPC, IPC and ExPC on IR injury are detailed below.

5.2.3.1. Effect of remote ischaemic preconditioning on ischaemia-reperfusion injury

Initially studies investigated RIPC using a standard protocol, identical to that described in previous publications by our group (Figure 5.1) (79,111). After an initial brachial

artery FMD measurement on the right arm, RIPC was induced by 3 cycles of 5 minutes of left upper arm ischaemia and reperfusion. This was followed by 20 minutes of right upper limb ischaemia, reperfusion, and 20 minutes of recovery (Figure 5.1A).

Results in section 4.3.3.1 observed that 20 minutes of recovery were insufficient to allow the brachial artery to return to its resting baseline diameter following reperfusion. Therefore studies were carried out using an identical RIPC protocol, but with an extended recovery of 25 minutes (Figure 5.1B). Furthermore, to investigate whether an increased "dose" of RIPC could induce a more robust protective effect, the RIPC protocol was extended to 4 cycles (Figure 5.1C).

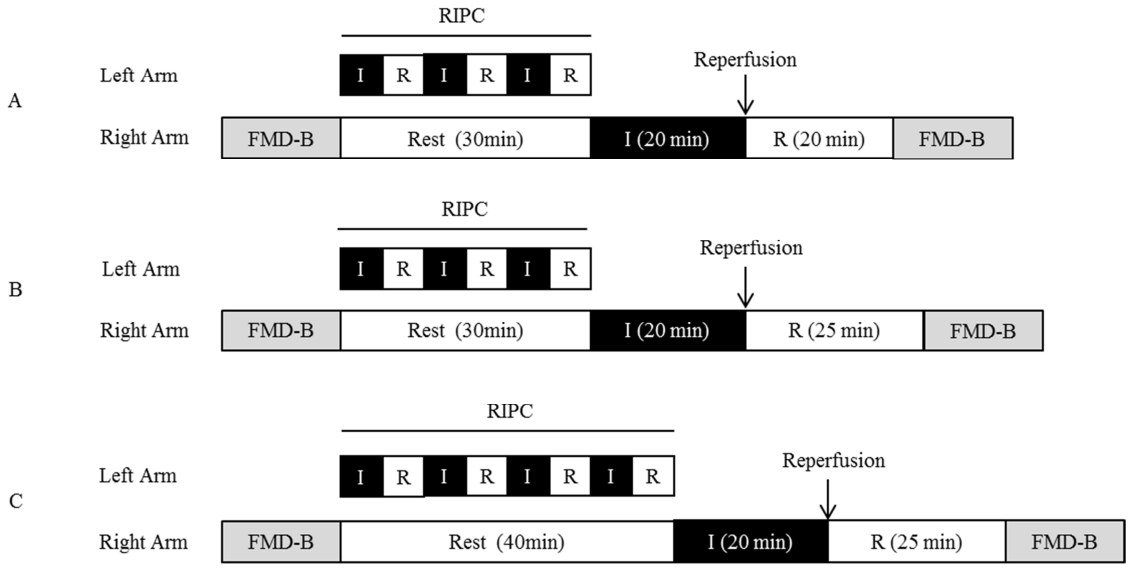

Figure 5.1 Experimental protocols to investigate the effect of remote ischaemic preconditioning on ischaemia-reperfusion injury. The initial protocol consisted of a brachial artery FMD recording on the right arm, three RIPC cycles of 5 minutes ischaemia and 5 minutes reperfusion on the left arm, 20 minutes of right arm ischaemia, reperfusion, and recovery of 20 minutes, and a second FMD recording (A). The second protocol was identical bar an extended recovery duration of 25 minutes (B). The third protocol was identical to B, with an additional cycle of RIPC (C). FMD-B , brachial artery FMD recording; I , ischaemia; R , recovery.

5.2.3.2. Effect of local ischaemic preconditioning on ischaemia-reperfusion injury

Studies then investigated the effect of IPC on IR injury using a standard protocol (Figure 5.2). After an initial brachial artery FMD recording, the right upper arm was submitted to an IPC protocol identical to those of previous studies, with three cycles of 5 minutes ischaemia and 5 minutes of reperfusion (15). This was followed by 20 minutes of ischaemia, reperfusion, and 25 minutes of recovery, and a final recording (Figure 5.2D).

Further studies investigated the effect on IPC on radial artery IR injury. Following a radial FMD recording, the same IPC protocol was used as in the brachial artery. IR injury consisted of 15 minutes of ischaemia, reperfusion, and 15 minutes of recovery, before a final recording (Figure 5.2E).

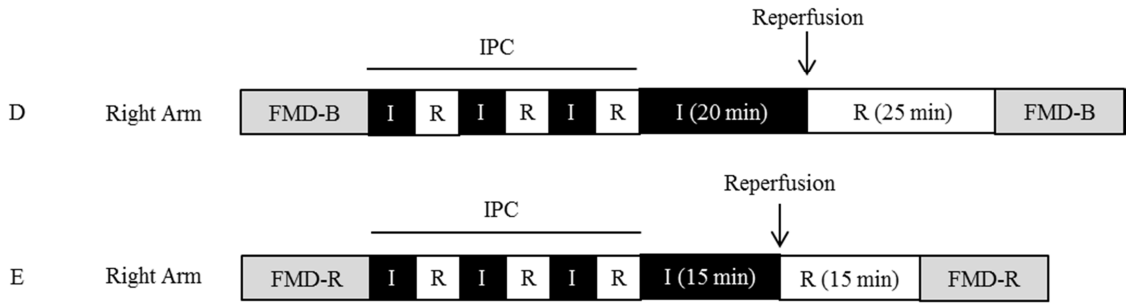

Figure 5.2 Experimental protocols to investigate the effect of local ischaemic preconditioning on ischaemia-reperfusion injury. All procedures took place on the right upper limb. The initial protocol consisted of an FMD recording, followed by three IPC cycles of 5 minutes ischaemia and 5 minutes reperfusion, 20 minutes of limb ischaemia, recovery of 20 minutes, and a second recording (D). The second protocol was in the radial artery, consisting of a recording, an identical IPC protocol, followed by 15 minutes of ischaemia and 15 minutes of reperfusion, and a final recording (E). FMD-B, brachial artery FMD; FMD-R, radial artery FMD; I , ischaemia; R , recovery.

5.2.3.3. Effect of exercise preconditioning on ischaemia-reperfusion injury

To determine whether acute exercise induced a preconditioning effect (ExPC) against upper limb IR injury, subjects underwent exercise testing prior to IR injury (Figure 5.3). After an initial brachial artery FMD recording, subjects were moved onto a stationary cycle ergometer and performed an exhaustive incremental exercise test (see section 2.2.2.5). This was followed by 35 minutes of rest to allow for heart rate recovery, and then by 20 minutes of ischaemia, 20 minutes of reperfusion, and a final recording (Figure 5.3F).

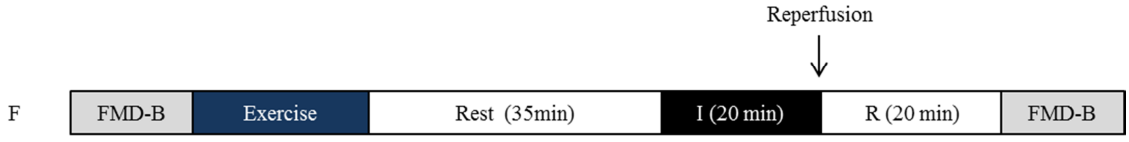

Figure 5.3 Experimental protocols to investigate the effect of exercise preconditioning on ischaemia-reperfusion injury. An FMD recording was followed by an incremental exercise test until physical exhaustion. Subjects then rested in a supine position for 35 minutes, before 20 minutes of ischaemia. After 20 minutes of reperfusion a final FMD was assessed.

5.2.4. Calculations and statistics

FMD, baseline diameter, and L-FMC were analysed from all recordings. Post IR values were corrected for differences in baseline diameter. Within protocol data were analysed using paired *t* tests. Comparisons were performed between preconditioning and control studies, firstly by using analysis of covariance (ANCOVA) to adjust for baseline FMD, providing a correlation existed between post IR values. Post IR values were matched with IR control results from section 4.3.3, and compared using a paired *t* test. A minimum sample size of 5-6 subjects was used based upon calculations from statistical

software (Power and Sample Size Calculations, Dupont & Plummer, v3.0, (144)) using an α of 0.05 and a power of 0.8. Within-subject SD for brachial artery FMD was from Figure 4.2, and complete prevention of the IR-induced reduction in FMD was assumed, based upon previous results (79). Values are expressed as mean ± SD, and correlations by Pearson r. $p < 0.05$ was deemed statistically significant.

5.3. Results

Protocols were tolerated well by all subjects, with no adverse events.

5.3.1. Remote ischaemic preconditioning has no effect on flow mediated dilatation following ischaemia-reperfusion injury

Results are displayed in Figure 5.4 and Table 5.1. Three cycles of RIPC applied immediately prior to IR did not preserve FMD at 20 minutes or 25 minutes of recovery. Increasing the stimulus to four RIPC cycles did not preserve FMD. A significant correlation existed between baseline FMD and post IR FMD for three cycles of RIPC at 20 minutes ($r = 0.75$, $p < 0.001$), 25 minutes of reperfusion ($r = 0.81$, $p < 0.0001$), and for 4 cycles of RIPC ($r = 0.87$, $p = 0.001$). These correlations justified an adjustment to post IR values using baseline FMD as the covariate. No difference existed between post IR and post RIPC+IR for all protocols.

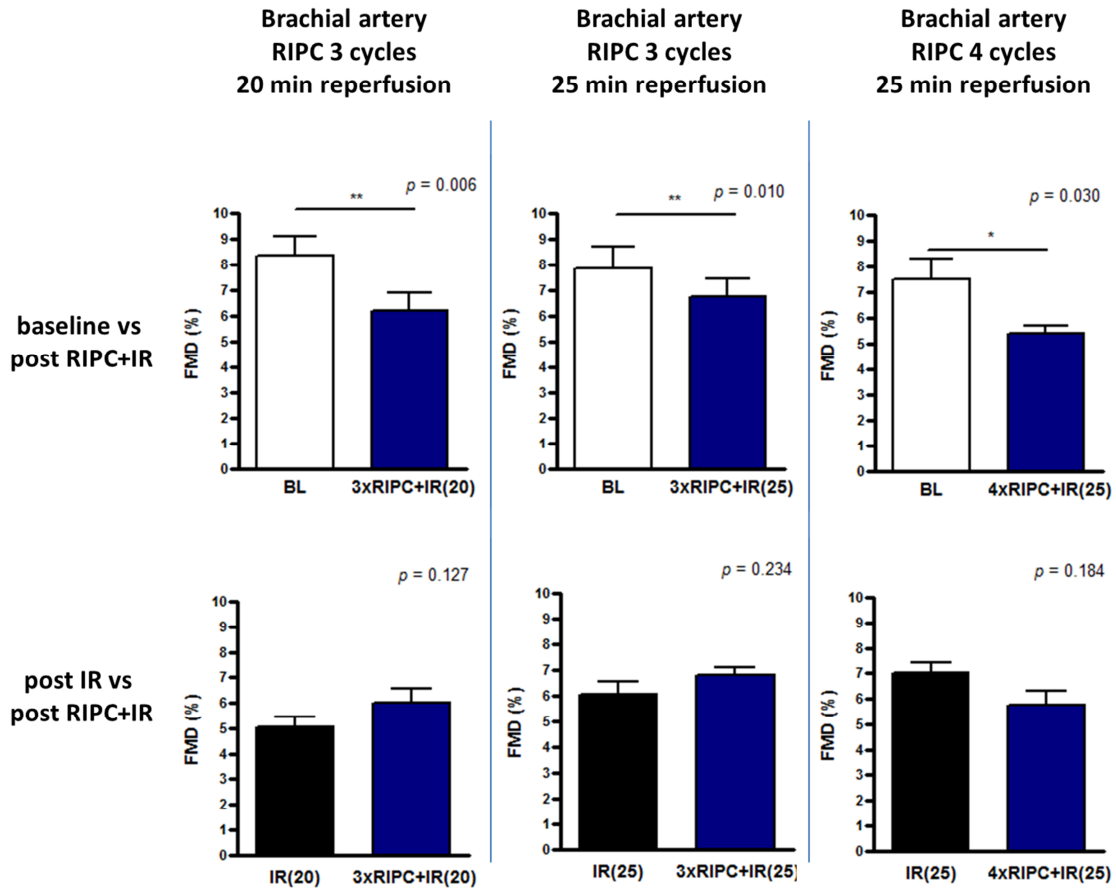

Figure 5.4 Effect of remote ischaemic preconditioning on flow mediated dilatation following ischaemia-reperfusion injury. Subjects underwent brachial artery FMD recording, followed by cycles of RIPC, prolonged limb IR, and a final recording. Results were adjusted for baseline diameter. RIPC did not prevent the IR-induced decrease in FMD, irrespective of whether the duration of recovery from reperfusion was 20 minutes (n = 11), 25 minutes (n = 14), or whether the RIPC stimulus was increased to 4 cycles (n = 5). Post IR and post RIPC+IR results were matched and adjusted for baseline FMD. There were no significant difference in post IR values between IR alone and RIPC+IR in all protocols. Groups were compared by paired *t* tests, and adjustments were made according to linear regressions. Bars and error bars are mean and standard error.

5.3.1. Remote ischaemic preconditioning has no effect on low-flow mediated constriction following ischaemia-reperfusion injury

Results are displayed in Figure 5.5 and Table 5.1. RIPC applied immediately prior to IR injury did not prevent the increase in L-FMC with 20 minutes of recovery. RIPC with 25 minutes of recovery prevented this increase; however this trend was not reproduced when increasing the number of RIPC cycles. A significant correlation existed between baseline L-FMC and post IR L-FMC for three cycles of RIPC at 20 minutes ($r = 0.64$, $p = 0.001$), for 4 cycles of RIPC ($r = 0.85$, $p = 0.001$), and almost reached significance for 3 cycles at 25 minutes of reperfusion ($r = 0.35$, $p = 0.065$). These correlations justified an adjustment to post IR values using baseline L-FMC as the covariate. No significant difference existed between post IR and post RIPC+IR for all protocols. There was a trend towards a difference for 3 cycles RIPC and 25 minutes reperfusion, but this observation was not maintained when the stimulus was increased to 4 cycles.

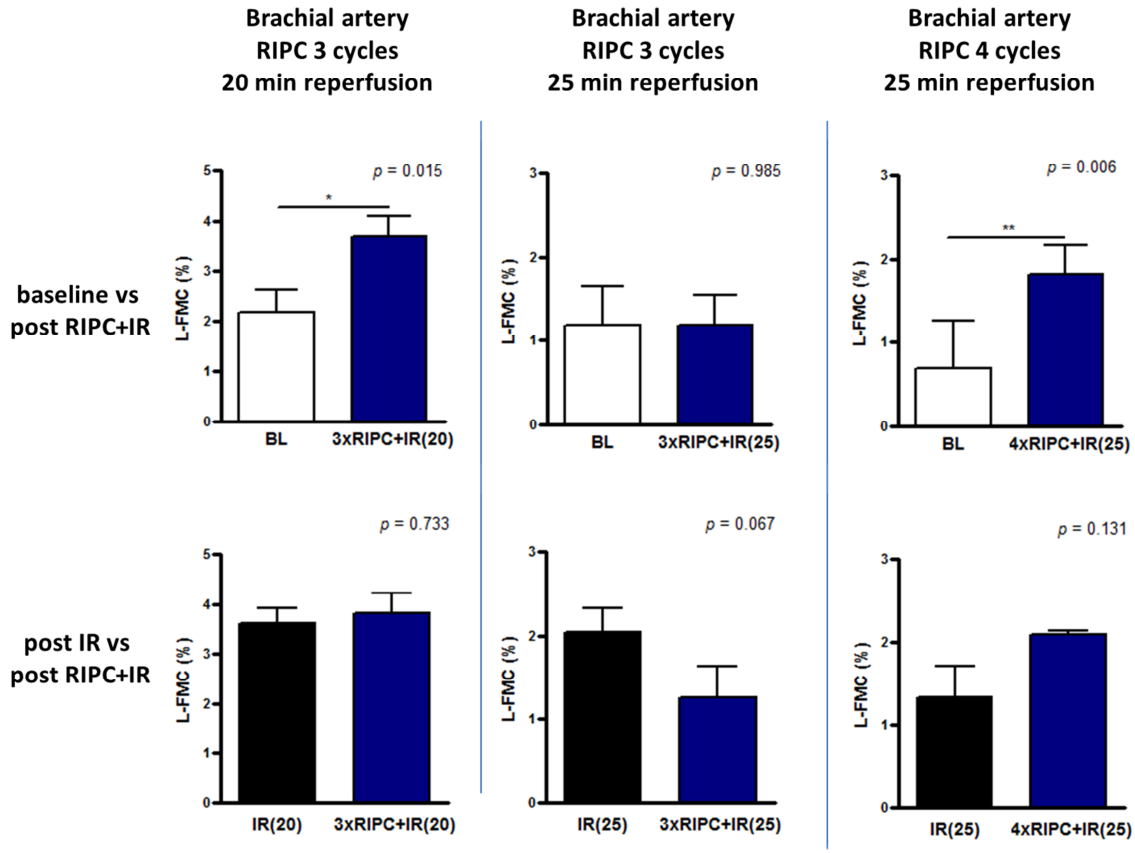

Figure 5.5 Effect of remote ischaemic preconditioning on low-flow mediated constriction following ischaemia-reperfusion injury. Subjects underwent baseline brachial FMD recording, followed by cycles of RIPC, prolonged limb IR, and a final recording. Results were adjusted for baseline diameter. RIPC did not prevent the IR-induced increase in L-FMC when the duration of recovery was 20 minutes (n = 11). When reperfusion was extended to 25 minutes, there was no increase in L-FMC (n = 14), however these results were not replicated when the RIPC stimulus was increased from 3 to 4 cycles (n = 5). Post IR and post RIPC+IR results were matched and adjusted for baseline FMD. There were no significant differences in post IR values between IR alone and RIPC+IR in all protocols. Groups were compared by paired *t* tests, and adjustments were made according to linear regressions. Bars and error bars are mean and standard error.

Table 5.1 Summarised results of the effect of remote ischaemic preconditioning on ischaemia-reperfusion injury in humans.

	3 cycles RIPC IR(20)			3 cycles RIPC IR(25)			4 cycles RIPC IR(25)		
	n = 11			n = 14			n = 5		
	BL	post RIPC+IR	*p*	BL	post RIPC+IR	*p*	BL	post RIPC+IR	*p*
BL Diam (mm)	3.62 ± 0.36	3.70 ± 0.35	0.003	3.64 ± 0.33	3.69 ± 0.37	0.137	3.64 ± 0.26	3.67 ± 0.31	0.485
FMD (%)	8.37 ± 2.37	6.20 ± 2.24	0.006	7.87 ± 3.07	6.76 ± 2.54	0.010	7.52 ± 1.54	5.42 ± 0.53	0.030
L-FMC (%)	2.18 ± 1.42	3.71 ± 1.22	0.015	1.18 ± 1.71	1.19 ± 1.26	0.985	0.69 ± 1.15	1.82 ± 0.73	0.006
SBP (mmHg)	108 ± 9	112 ± 11	0.073	116 ± 9	117 ± 9	0.199	118 ± 7	120 ± 5	0.554
DBP (mmHg)	57 ± 4	61 ± 7	0.009	58 ± 6	62 ± 7	0.004	60 ± 2	63 ± 4	0.012
HR (bpm)	61 ± 7	58 ± 8	0.161	56 ± 7	58 ± 7	0.276	58 ± 8	59 ± 8	0.683

5.3.2. Local ischaemic preconditioning protects against the ischaemia-reperfusion induced reduction in flow mediated dilatation in the brachial artery

Results are displayed in Figure 5.6 and Table 5.2. IPC applied immediately prior to IR injury preserved FMD in the brachial artery but not in the radial artery. A significant correlation existed between FMD at baseline and post IR values in the brachial ($r = 0.75$, $p < 0.001$) and in the radial ($r = 0.80$, $p < 0.001$). These correlations justified an adjustment to post IR values using baseline FMD as the covariate. A significant difference existed between IPC+IR and IR alone in the brachial but not in the radial artery.

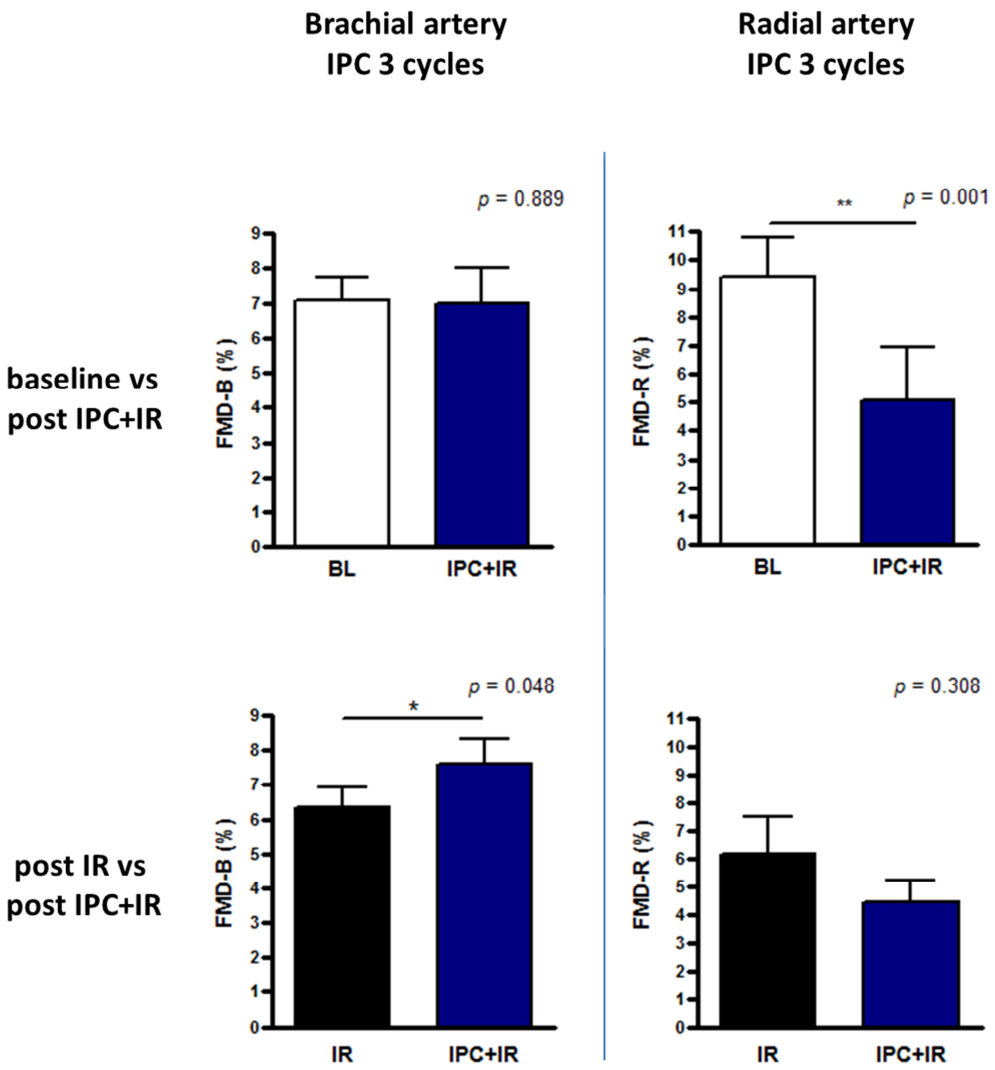

Figure 5.6 Effect of local ischaemic preconditioning on flow mediated dilatation following ischaemia-reperfusion injury. Subjects underwent baseline brachial or radial FMD recording. This was followed by cycles of IPC, prolonged limb IR, and a final recording. Results were adjusted for baseline diameter. IPC preserved FMD following IR injury in the brachial (n = 14), but not the radial artery (n = 8). Post IR and post IPC+IR results were matched and adjusted for baseline FMD. Brachial FMD following IPC+IR was significantly increased compared to IR alone. There were no significant differences between radial FMD for IPC+IR and IR alone. Groups were compared by paired *t* tests, and adjustments were made according to linear regressions. Bars and error bars are mean and standard error.

5.3.3. Local ischaemic preconditioning has no effect on low-flow mediated constriction following ischaemia-reperfusion injury

Results are displayed in Figure 5.7 and Table 5.2. IPC applied immediately prior to IR injury prevented a significant increase in L-FMC in both the brachial and radial artery. A significant correlation existed between L-FMC at baseline and post IR for values in the brachial ($r = 0.55$, $p = 0.002$) and in the radial ($r = 0.65$, $p = 0.006$). These correlations justified an adjustment to post IR values using baseline L-FMC as the covariate. There was no significant difference between IPC+IR and IR alone for the brachial or radial artery.

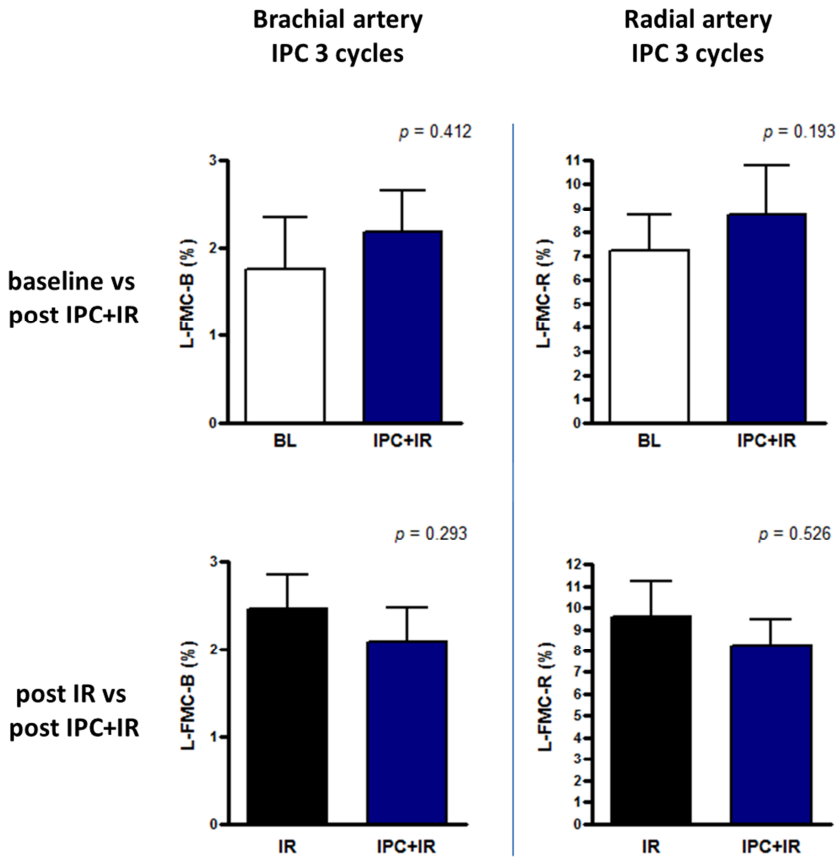

Figure 5.7 Effect of ischaemic preconditioning on low-flow mediated constriction following ischaemia-reperfusion injury. Subjects underwent baseline FMD recording in the brachial and radial artery. This was followed by cycles of IPC, a prolonged limb IR, and a final recording. Results were adjusted for baseline diameter. L-FMC was increased following IPC+IR in the brachial (n = 14) and the radial artery (n = 8), but this did not reach significance. Post IR and post IPC+IR results were matched and adjusted for baseline L-FMC. L-FMC during IPC+IR was not significantly different to IR alone in either artery. Groups were compared by paired *t* tests, and adjustments were made according to linear regressions. Bars and error bars are mean and standard error.

Table 5.2 Summarised results of the effect of local ischaemic preconditioning on ischaemia-reperfusion injury in humans.

	Brachial IPC IR			Radial IPC IR		
	n = 14			n = 8		
	BL	post IPC+IR	*p*	BL	post IPC+IR	*p*
BL Diam (mm)	3.53 ± 0.31	3.47 ± 0.30	0.017	2..42 ± 0.22	2.43 ± 0.23	0.807
FMD (%)	7.09 ± 2.44	6.99 ± 3.77	0.889	9.41 ± 3.66	5.08 ± 4.95	0.001
L-FMC (%)	1.76 ± 2.07	2.17 ± 1.77	0.412	7.22 ± 3.97	8.72 ± 5.49	0.193
SBP (mmHg)	114 ± 9	117 ± 10	0.079	113 ± 10	116 ± 10	0.196
DBP (mmHg)	59 ± 3	64 ± 7	0.010	59 ± 4	64 ± 6	0.028
HR (bpm)	59 ± 7	57 ± 7	0.141	61 ± 11	61 ± 9	0.927

5.3.4. Exercise preconditioning has no effect on flow mediated dilatation, but prevents the increase in low-flow mediated constriction following ischaemia-reperfusion injury

Results are displayed in Figure 5.8 and Table 5.3. ExPC prior to IR did not prevent the IR-induced reduction in FMD. ExPC did prevent the IR-induced increase in L-FMC. A correlation existed between baseline and post IR values, which tended towards significance for FMD (r = 0.38, p = 0.185), and was significant for L-FMC (r = 0.66, p = 0.021). These correlations justified an adjustment to post IR values using baseline FMD as the covariate. ExPC+IR was not significantly different to IR alone for FMD, but was for L-FMC.

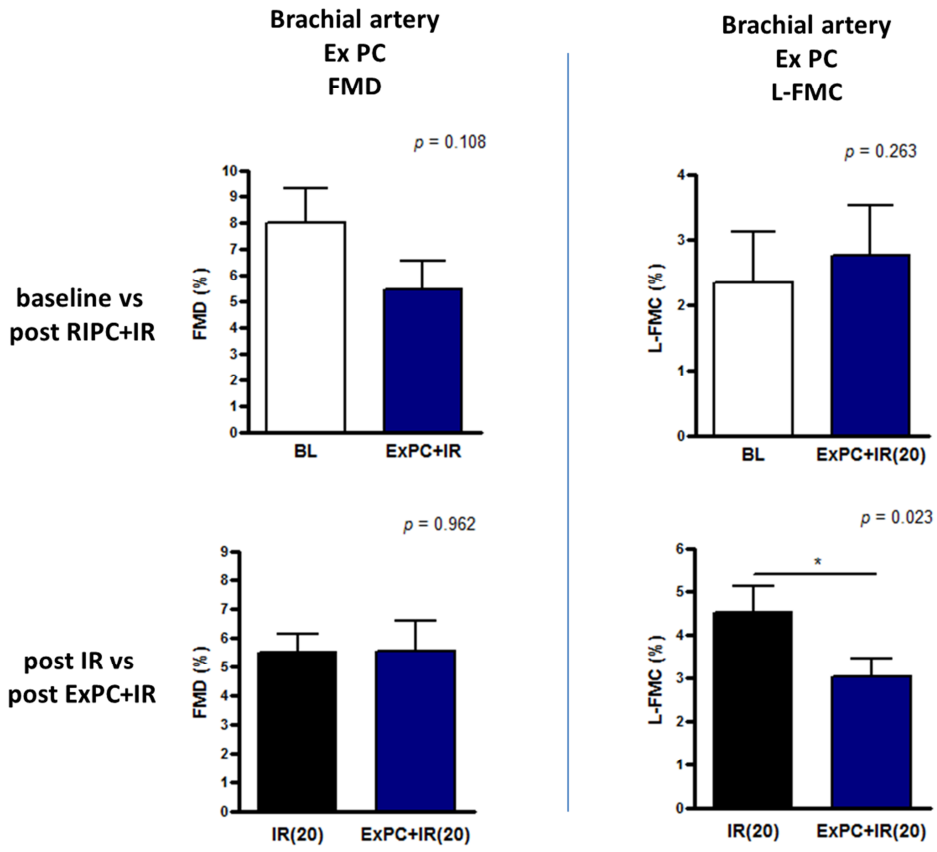

Figure 5.8 Effect of exercise preconditioning on flow mediated dilatation and low-flow mediated constriction following ischaemia-reperfusion injury. Subjects underwent baseline FMD recording in the brachial artery. This was followed by a cycling test whereby subjects cycled against an increasing resistance (20-40 W/min) for 8-12 minutes until exhaustion. After 35 minutes rest subjects received limb IR, and a final recording. Results were adjusted for baseline diameter. FMD was reduced and L-FMC was increased following ExPC+IR in the brachial artery (n = 7), but neither reached statistical significance. Post IR and post ExPC+IR results were matched and adjusted for baseline FMD / L-FMC. FMD was not different between ExPC+IR and IR alone. L-FMC was preserved by ExPC+IR compared to IR alone. Groups were compared by paired *t* tests, and adjustments were made according to linear regressions. Bars and error bars are mean and standard error.

Table 5.3 Summarised results for the effect of exercise preconditioning on ischaemia-reperfusion injury in humans

	ExPC IR		
	n = 7		
	BL	post ExPC+IR	*p*
BL Diam (mm)	3.85 ± 0.27	3.99 ± 0.24	<0.001
FMD (%)	7.99 ± 3.19	5.44 ± 2.71	0.108
L-FMC (%)	2.35 ± 1.74	2.76 ± 1.72	0.263
SBP (mmHg)	115 ± 7	113 ± 8	0.601
DBP (mmHg)	58 ± 4	59 ± 4	0.722
HR (bpm)	60 ± 8	67 ± 8	< 0.001

5.4. Discussion

Results demonstrate that RIPC does not protect against the IR induced decrease in FMD. In contrast, IPC exerts a degree of protection against IR injury in the brachial but not the radial. ExPC protected against the increase in L-FMC but had no effect on FMD.

5.4.1. Lack of protection by remote ischaemic preconditioning

In contradiction to previous studies, my results show that RIPC has no effect on post IR endothelial dysfunction defined as FMD. Observations by our group have shown that limb RIPC exhibits a robust protective phenotype against experimental IR in healthy subjects. Loukogeorgakis et al. demonstrated that 20 minutes of ischaemia and reperfusion induced a 44% reduction in FMD, but preceding IR with RIPC limited this reduction to just 15% (41). Further studies observed that when correcting for baseline FMD, this difference became highly significant ($p < 0.0001$) with 9 subjects in the RIPC group (111).

In the current studies an identical protocol observed a 33% reduction in FMD by IR alone in 20 subjects, and a 26% reduction with IR was preceded by RIPC in 11 subjects. The reason for the lack of a protective effect is unclear. Given that 20 minutes of recovery were of insufficient duration to return arterial diameter to baseline, both IR and RIPC+IR studies were conducted with an extended recovery of 25 minutes. The extended duration had no effect on RIPC, which remained when the "dose" was increased to 4 RIPC cycles. The difference in observations is potentially attributable to 1.) subject population, 2.) image analysis, 3.) experimental set up or 4.) experimental technique, which are discussed in more detail below.

The subject population in the current study was similar to previous experiments, consisting of healthy young males (aged 18 – 24 years) who were requested to adhere to dietary restrictions as previously. The subject age previously was 28.9 ± 7.7 (mean ± SD) (79) and 24.9 ± 5.4 (111), slightly older than subjects in my study (22 ± 3). However this small age difference seems unlikely to account for the inconsistencies between my data and previous studies. The sample sizes in the current study (n = 11 & n = 14) were comparable with the previous RIPC studies (n = 13, (79); n = 9, (111)).

Image analysis technique was verified by the strong agreement between analysers for baseline FMD data (section 2.2.3.3). To account for potential analyser bias, RIPC and control ultrasound scans were reanalysed in a blinded fashion by a senior researcher, and almost identical values were observed, with no effect by RIPC (data not shown). Furthermore individual recorded traces were thoroughly scrutinised by members of the research group, but were confident that the results were not attributable to movement artefacts, or to vascular spasm.

Thirdly experiment set up was investigated. In the months prior to starting experiments, the research laboratory had moved, and during this time the ultrasound recording

equipment was upgraded to a newer machine with a higher frequency probe than previously used by our group (10.0 vs 7.0 MHz respectively). This resulted in an improvement in image resolution. In addition a fully adjustable ultrasound probe holder was used in the current studies to reduce the likelihood of movement artefacts during the study. These equipment upgrades are unlikely to account for the null effect observed in my studies. Environmental conditions (24-26°C) were matched to previous studies.

Finally, differences in experimental technique could explain a null finding. No major systematic error was evident when directly observed. My ultrasound technique was heavily scrutinised and. Senior researchers within our group expressed a high level of confidence in my sonography, and that the images acquired were suitably representative of arterial diameter. In addition a fellow PhD student performed an identical set of RIPC studies with appropriate controls, and obtained similar results to my own (personal communication).

To date no satisfactory explanation has emerged to explain why the current study has failed to demonstrate a protective effect of RIPC on endothelial injury. Further studies are required using RIPC and IR with a greater sample size, and with multiple blinded analysers to verify the observations.

5.4.2. Protection with local ischaemic preconditioning

Results in this study identified a significant protective phenotype of IPC in the brachial artery against the IR-induced reduction in FMD. However this effect was not present in the radial artery, and had no effect on L-FMC. The difference between the arterial responses is uncertain, but unlikely to be attributable to experimental technique, image analysis, or study population, as these were almost identical for brachial and radial studies.

Differences between brachial and radial arteries may be explained by the study protocols. The radial protocol used 15 minutes ischaemia and reperfusion, which other groups have shown is sufficient to induce a reduction in FMD (113). In the brachial studies, ischaemia lasted 20 minutes with 25 minutes reperfusion. Chapter 4 observed that these IR in these protocols exerted similar reductions in FMD (radial, 36%; brachial, 19%), suggesting that it is unlikely that a timing difference can account for the altered response to IPC.

Alternatively the factors which control resting and stimulated endothelial function could differ between vessels. Chapter 4 made direct comparisons between responses in both the brachial and radial artery. The most obvious difference is that mean L-FMC is greater in the radial that the brachial artery, which suggests a different balance of endogenous vasodilators and vasoconstrictors (such as NO, EDHF, prostacyclin and endothelin-1) may govern control of the two vessels. Differences in the release of vasoactive mediators controlling tone could reasonably influence the lack of response to IPC in the radial artery.

5.4.3. Exercise as a preconditioning stimulus

Results in this chapter showed that unlike IPC, exercise was unable to prevent the IR-induced reduction in FMD. Whilst evidence supporting acute exercise as a preconditioning stimulus exists (section 1.3.3), there are several reasons why exercise might not have complemented these findings in the current model. Firstly there are fundamental differences between IPC and exercise. Whilst cellular hypoxia occurs in exercise above the anaerobic threshold, the maintenance of blood flow ensures that glycolytic metabolites are unlikely to accumulate. This continual washout may prevent the accumulation of endogenous autacoids to a sufficient concentration to activate G-protein coupled receptors, and the subsequent intracellular protective kinases.

IPC is stimulated by intermittent ischaemia and reperfusion, whereas the ischaemia during the current exercise protocol was brief and continuous. It is possible that the exercise stimulus differs from IPC because it did not have the same intermittent nature as IPC. Evidence suggests that repeated reperfusion may be a prerequisite for IPC, most likely so that cells can adapt to repeated non-lethal concentrations of reperfusion injury mediators. One study observed vascular protection using an exercise protocol that involved subjects exercising intermittently above and below the anaerobic threshold (109).

Alternatively the reason for a lack of protection could be that exercise does not exert systemic protection. As has been described in this chapter, RIPC is unable to exert a systemic protective effect against IR injury. Given that the aim was to observe a remote ExPC effect (lower limb exercise, upper limb IR) this may explain the results. Further studies would aims to use intermittent arm exercise to protect against IR injury in the same limb.

5.4.4. Low-flow mediated constriction following ischaemic and exercise preconditioning

The IR-induced increase in L-FMC was unaffected by IPC and RIPC, but attenuated by ExPC. Data in chapter 4 indicated that there were similarities between FMD and L-FMC in their relationship to baseline diameter, but also differences in their response to IR. Results in this chapter have identified that FMD and L-FMC have differing responses to preconditioning stimuli in that IPC prevented the IR-induced reduction in FMD, but did not attenuate the increase in L-FMC. The opposite effect was seen with ExPC. The biological significance of these observations is uncertain.

5.5. Conclusion

This chapter has suggested that local ischaemic preconditioning induces protection against the IR-induced reduction in endothelial function, as assessed by IPC. The protective effect of IPC in humans is supported by evidence in early phase clinical trials (7). Further studies in this thesis aim to investigate IPC in other models of IR injury. This will include a model of the IR injury induced sterile inflammatory response, and the muscle deoxygenation and resaturation which occurs during intense exercise.

This chapter has observed that IPC, but not RIPC or ExPC can protect against human endothelial IR injury using an *in vivo* model. The reason for the discrepancy between the results for RIPC and previous experiments remain uncertain. Further studies in this thesis aim to investigate the mechanistic properties of IPC in humans.

6. CHARACTERISING A HUMAN IN VIVO SKIN BLISTER MODEL OF ACUTE INFLAMMATION

6.1. Introduction

Growing evidence suggests that ischaemic preconditioning (IPC) might protect against IR injury by dampening the acute inflammatory response, in particular by reducing leukocyte trafficking (66). Assessing acute inflammation in healthy humans however is challenging. *In vitro* experiments are often performed to investigate individual elements of the immune system. However given the complex overlapping of innate immune pathways, such as leukocyte trafficking and complement, *in vitro* studies are often unrepresentative. The cantharidin skin blister is a non-invasive *in vivo* model, which allows for assessment of the inflammatory response by quantifying leukocyte trafficking, and has previously been used to document the anti-inflammatory effects of low and high dose aspirin (181). Thus, in collaboration with Professor Derek Gilroy's research group, the blister model was characterised, to enable its use in a crossover trial for investigating the effect of IPC on leukocyte trafficking.

To assess whether IPC reduces the human inflammatory response, a randomised crossover study was designed using a forearm skin blister model to quantify leukocyte trafficking. The protocol and results from this study are reported in chapter 7. In the current chapter the characterisation of the cantharidin skin blister model is reported. Initially a preliminary study was performed to assess the within-subject variability of the 24 hour skin blister, for a sample size calculation in the subsequent intervention study. A novel strategy to identify cell populations by flow cytometry is then described, both for circulating venous and blister leukocytes. This is followed by a report on the changes in individual cell populations, and HLA-DR and CD19 receptor expression that occur in the blister between 24 and 72 hours. By investigating two time points, this provides a picture of the cell kinetics that govern the human innate immune response, both during the onset of inflammation, and during inflammatory resolution.

6.2. Methods

6.2.1. Study participants

Participants were prepared as outlined in section 2.3.2.

6.2.2. Experimental protocol

6.2.2.1. Variability of cantharidin skin blister

A preliminary study was designed to calculate the within-subject variability of the cantharidin skin blister at 24 hours, and thus perform a sample size calculation. 10 healthy male participants (age 22 ± 2 years, mean ± SD) received two cantharidin skin blisters over two weeks. Subjects received a blister on one forearm, which was aspirated after 24 hours. At least 6 days following aspiration, a second blister was applied to the contralateral forearm, which was again aspirated after 24 hours. Blisters were induced and aspirated as described in section 2.3.2. Blisters were analysed for volume and total leukocyte count.

6.2.2.2. Leukocyte analysis in the 24 and 72 hour blisters

To characterise the cell composition in the 24 and 72 hour skin blisters, a retrospective analysis was performed on the results from the control protocol of the crossover study described in chapter 7 (see section 7.2.2). Briefly, 17 healthy male participants (age 22 ± 4 years, mean ± SD) received two blisters to the same forearm at the same time. Skin blisters were induced and aspirated at 24 hours and 72 hours (section 2.3.2). Circulating leukocytes were isolated from venous blood by a flash lysis (section 2.3.2.4). Both blister and circulating leukocytes were analysed by flow cytometry for the expression of CD3, CD14, CD16, CD19, CD56 and HLA-DR (section 2.3.3). 3 additional participants were investigated for expression of CD11b, CD15 and CD33 in the 72 hour blister.

6.2.3. Calculations and statistics

Cantharidin skin blister variability was assessed using coefficient of variation (CV) and intraclass correlation coefficient (ICC). Results are presented as total cell count (n) and cell concentration (n/ml). Total cell count and cell concentration were non-parametric, and hence presented on a logarithmic scale, with results reported as the median ± interquartile range. Given the large number of data points and the skewed distributions, results are presented as box and whisker plots, showing the median, interquartile range, and the minimum and maximum values. Sample sizes were calculated by performing a log transformation and using statistical software (Power and Sample Size Calculations, Dupont & Plummer, v3.0, (144)).

Populations identified by flow cytometry are expressed as the percentage of the total cells (linear scale, mean ± SD) and as the absolute number of cells (logarithmic scale, median ± interquartile range). Between time-point differences were assessed by paired *t* test for the percentage of the total cells, or by Wilcoxon matched pairs test for absolute cell number.

Mean fluorescence intensity (MFI) varies between cytometers and settings, and is hence expressed in arbitrary units (logarithmic scale, median ± interquartile range). Between time-point differences for blood and blister leukocyte MFI was assessed by a repeated measures Friedman test and a Dunn's post-test.

6.3. Results

6.3.1. The cantharidin skin blister has a low within-person variability

Results from the preliminary study show that the total cell count was a repeatable measure of the leukocyte trafficking (CV = 5.3%, ICC = 0.82) (Figure 6.1). The within-subject variability was reduced when expressed as cell concentration (CV = 3.2%, ICC

= 0.92). There was no difference between week 1 and week 2 in the total cell count (week 1, 328,000 ± 897,000 cells; week 2, 314,000 ± 1,161,000 cells; p = 0.389, paired t test; n = 10; Figure 6.1A) or the cell concentration (week 1, 2,827,000 ± 4,624,000 cells/ml; week 2, 1,740,000 ± 6,761,000 cells/ml; p = 0.333, paired t test; n = 10; Figure 6.1B). Sample size calculations determined the number of subjects required to show a 30, 50 and 70% reduction in the total leukocyte count.

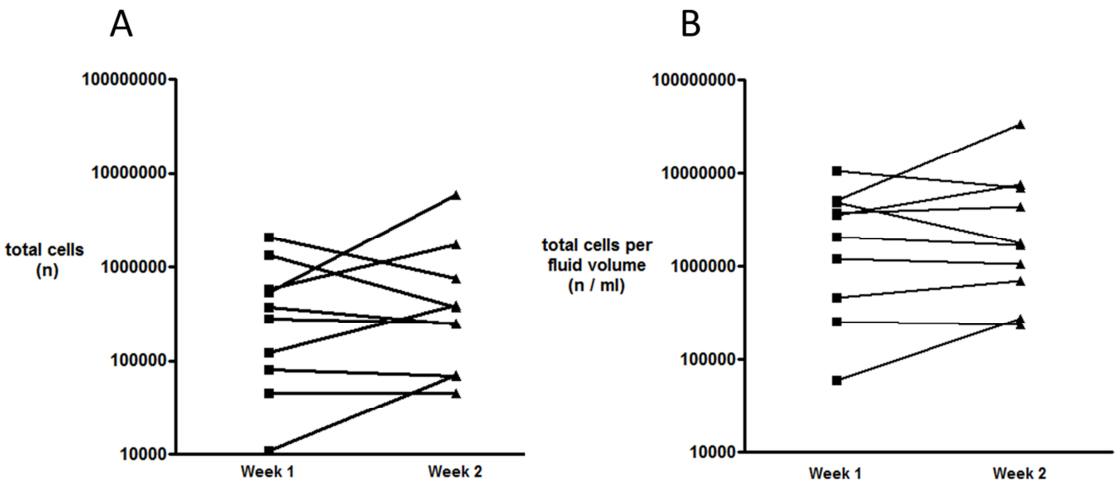

cell count reduction	sample size (total cells)	sample size (cell conc.)
30%	93	49
50%	25	13
70%	8	4

Figure 6.1 Results from preliminary 24 hour blister study. 10 healthy males received two skin blisters on two weeks, with both aspirated at 24 hours. Cells were isolated by centrifugation and enumerated by haemocytometer. Charts show results from repeated blisters, with each line representing one subject. Infiltration of leukocytes into the blister was repeatable, whether expressed as total cells (A) or as total cells per oedema volume (B). Table shows sample size results for given reductions in cell count (total cells) and cell concentration (cell conc.), using an α = 0.05 and a power of 0.8.

6.3.2. Gating strategy to differentiate individual cell populations

Using the panel of antibodies (section 2.3.3) a gating strategy was designed that could identify the populations of leukocytes present in circulating venous blood, and in the skin blister. Receptor expression, in combination with size (forward scatter, FSC) and granularity (side scatter, SSC) allowed for the identification of specific cell types. The strategy was based upon published literature for differentiating human circulating leukocytes (225,226), and following advice from experienced cytometry researchers within our research group. Flow chart in Figure 6.2 explains the gating strategy, and representative dot plots for venous and blister leukocytes are shown in subsequent figures (Figure 6.3 - Figure 6.5). FMO controls are provided in the appendix (Figure 10.1 - Figure 10.4).

Briefly, leukocytes were isolated from erythrocytes and cell debris by size and granularity. Cell doubles were removed using a FSC-height versus FSC-area plot. Lymphocytes were then identified as $CD3^{hi}$ (T lymphocytes), $CD19^{hi}$ (B lymphocytes) or $CD56^{hi}$ (natural killer cells) (see Figure 6.3). Remaining cells were split according to their expression of HLA-DR and CD16, into a.) HLA-$DR^{lo/dim}$ $CD16^{dim/hi}$ cells and b.) HLA-DR^{hi} cells (Figure 6.4 and Figure 6.5 respectively). This considerably reduced the contamination by neutrophils of the monocyte and macrophage population, and is based upon a gating strategy described recently (227).

Within the HLA-$DR^{lo/dim}$ $CD16^{dim/hi}$ gate; granulocytes and a myeloid derived suppressor-like cell (MDSC) population were differentiated by CD14 and CD16 expression (Figure 6.4). $CD16^{hi}$ $CD14^{lo}$ cells were identified as granulocytes, with the remainder being a mixed cell population, believed to be primarily MDSCs. $CD16^{hi}$ $CD14^{lo}$ cells were separated into neutrophils (FSC^{mid} SSC^{mid}) and eosinophils (FSC^{hi}

SSC^{hi}). MDSCs were differentiated into FSC^{lo} $CD14^{hi}$ cells and $FSC^{lo/mid/hi}$ $CD14^{dim/lo}$ cells.

In the HLA-DR^{hi} population, monocytes were identified as $FSC^{lo/mid}$ SSC^{lo}, with macrophages the remaining cells. Both the monocyte and macrophage subpopulations were determined by CD14 and CD16 expression. Monocytes were separated into classical ($CD14^{hi}$ $CD16^{dim}$), intermediate ($CD14^{dim}$ $CD16^{dim}$), and non-classical ($CD14^{dim}$ $CD16^{hi}$) monocytes, and a myeloid precursor population ($CD14^{dim}$ $CD16^{dim}$). Circulating macrophages were similarly differentiated by CD14 and CD16 expression.

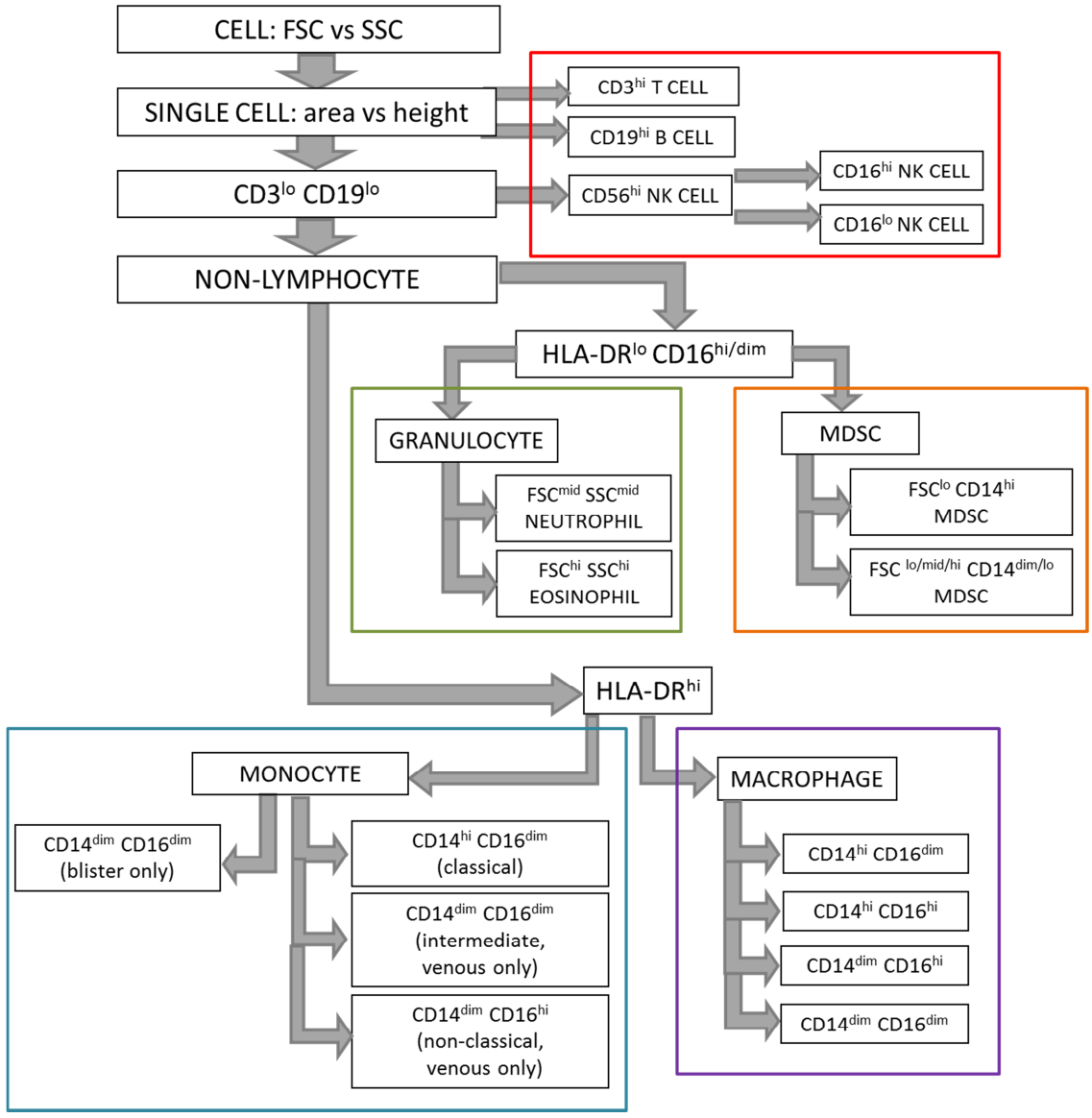

Figure 6.2 Flow chart describing the gating strategy employed to identify inflammatory and venous leukocyte populations by flow cytometry. Boxes show the different cell types separated in this manner, with arrows showing the direction in which the gating was applied. Firstly single cells were identified, and were separated into different types of lymphocyte (red box, see Figure 6.3). The remaining cells were separated by HLA-DR and CD16 expression, with HLA-DR^{lo} CD16$^{hi/dim}$ cells identified as granulocytes (green box, see Figure 6.4) and myeloid derived suppressor-like cells (MDSC) (orange box, see Figure 6.4). HLA-DR^{hi} cells were identified as monocytes (blue box, see Figure 6.5) or macrophages (purple box, see Figure 6.5). Coloured boxes match boxes in subsequent figures.

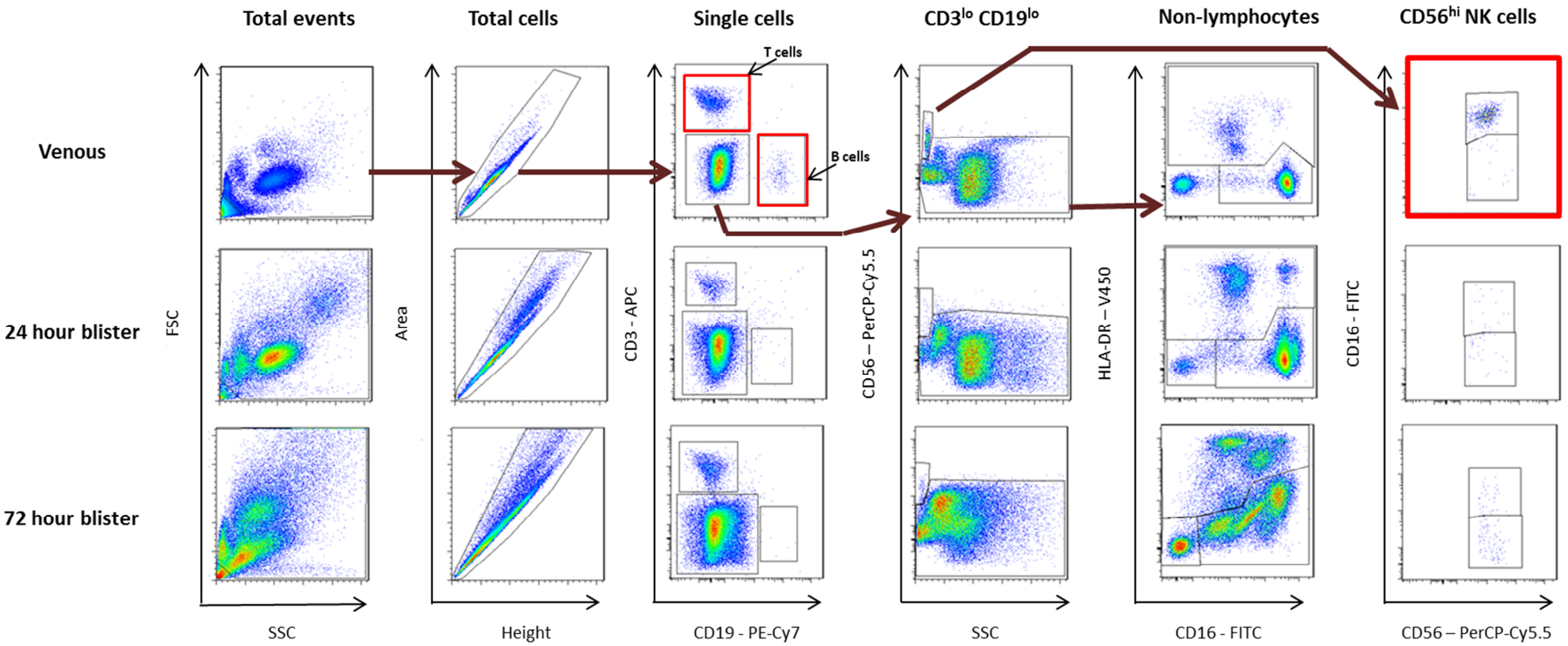

Figure 6.3 Lymphocyte gating strategy for venous and inflammatory leukocytes. Above are representative dot plots for the flow cytometry gating strategy to isolate CD3^{hi} T lymphocytes, CD19^{hi} B lymphocytes, and CD56^{hi} natural killer cells. Circulating leukocytes were obtained from venous blood and following a flash lysis to remove erythrocytes. Inflammatory leukocytes were obtained from cantharidin skin blisters in healthy males. Single cells were isolated using a forward (FSC) vs side scatter (SSC) plot, and an area vs height plot. T, B and NK cells were then isolated (red boxes), with the remaining non-lymphocytes separated into HLA-DR ^{hi} cells and HLA-DR$^{lo/dim}$ CD16$^{hi/dim}$ cells. The strategy was almost identical for venous (top row), 24 hour blister (middle row) and the 72 hour blister (bottom row) leukocytes. Arrows indicate gating strategy.

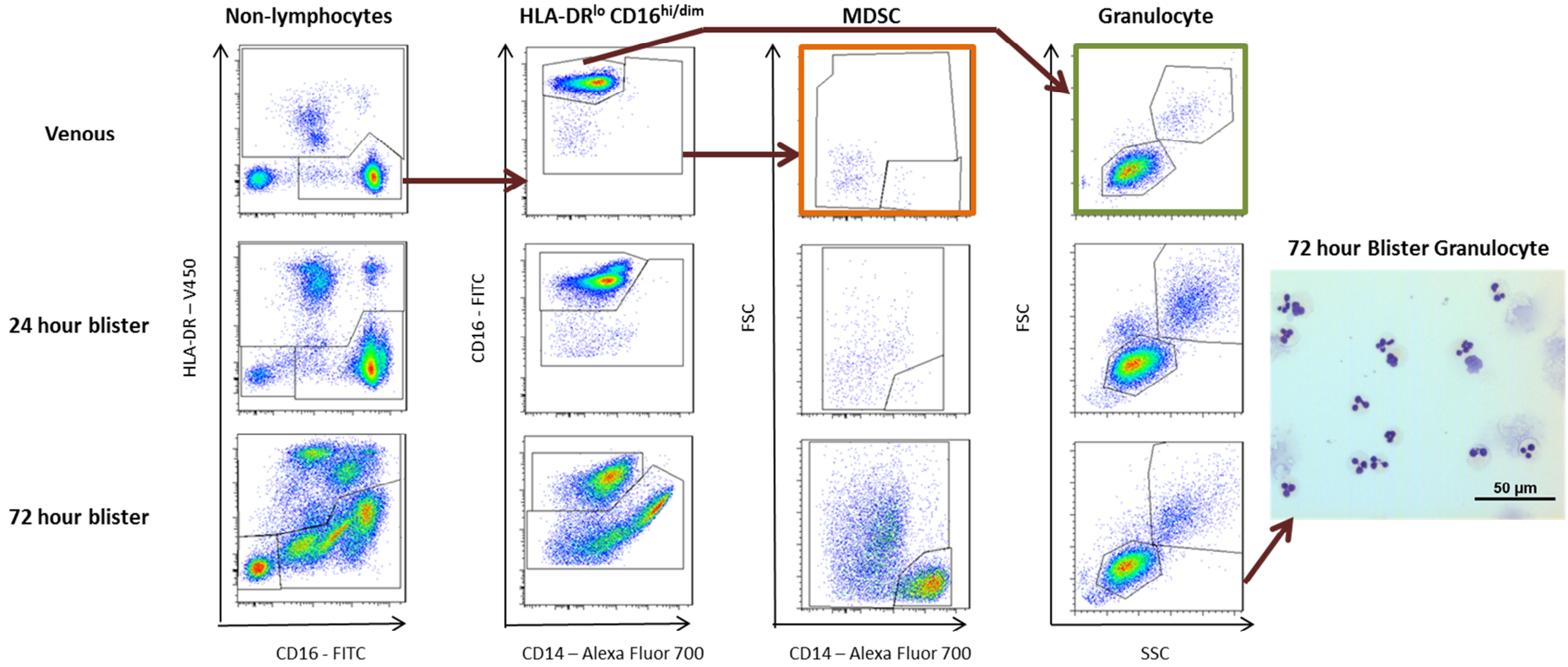

Figure 6.4 Granulocyte and myeloid derived suppressor cell gating strategy for venous and inflammatory leukocytes. Above are representative dot plots for the flow cytometry gating strategy. Circulating leukocytes were obtained from venous blood and following a flash lysis to remove erythrocytes. Inflammatory leukocytes were obtained from cantharidin skin blisters in healthy males. Following removal of lymphocytes, HLA-DR $^{lo/dim}$ CD16$^{hi/dim}$ cells were differentiated into CD16^{hi} granulocytes (green box) and CD16^{dim} MDSCs (orange box). MDSCs were differentiated into CD14^{hi} and CD14^{lo} cells. CD16^{hi} cells were differentiated into neutrophils (FSC^{mid} SSC^{mid}) and eosinophils (FSC^{hi} SSC^{hi}). The strategy was almost identical for venous (top row), 24 hour blister (middle row) and the 72 hour blister (bottom row) leukocytes. Arrows indicate gating strategy.

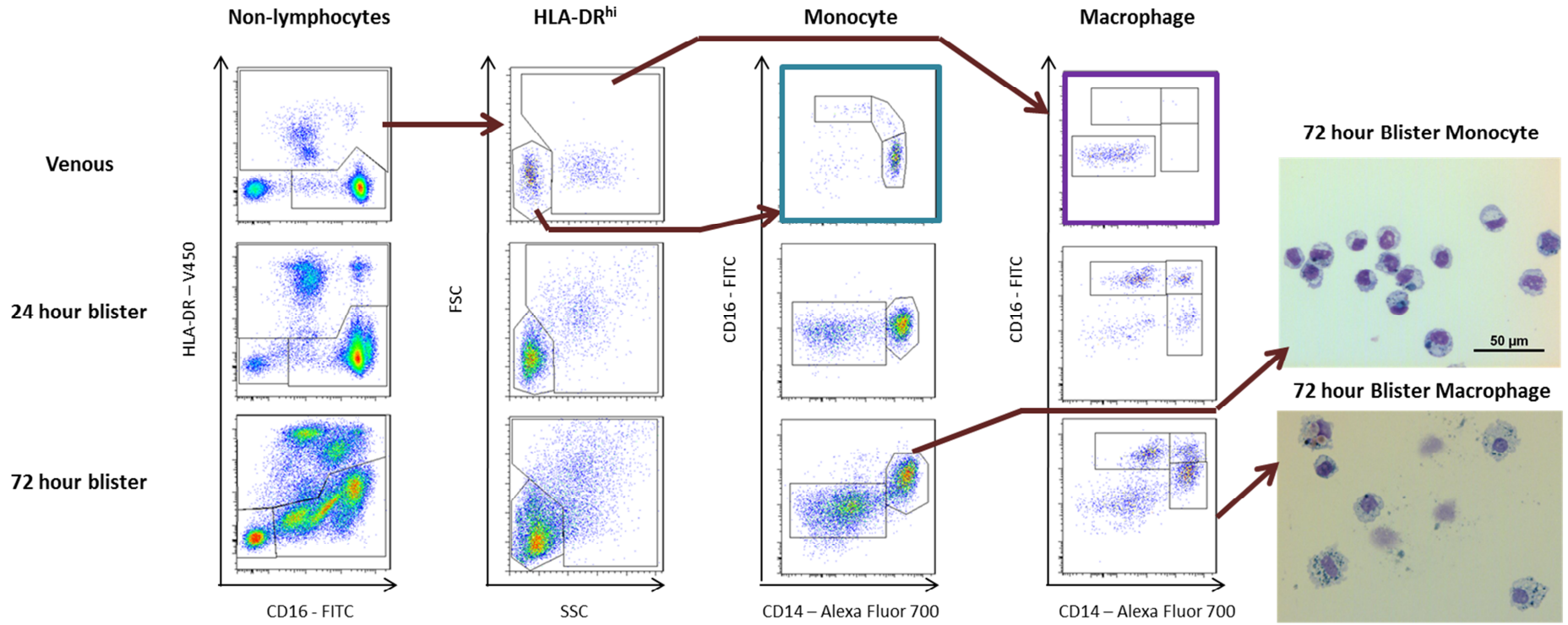

Figure 6.5 Monocyte and macrophage gating strategy for venous and inflammatory leukocytes. Above are representative dot plots for the flow cytometry gating strategy. Circulating leukocytes were obtained from venous blood and following a flash lysis to remove erythrocytes. Inflammatory leukocytes were obtained from cantharidin skin blisters in healthy males. Following removal of lymphocytes, HLA-DR^{hi} cells were differentiated into SSC^{lo} monocytes (blue box) and SSC$^{mid/hi}$ macrophages (purple box). Monocytes and macrophages were further differentiated by CD14 and CD16 expression. The strategy was almost identical for venous (top row), 24 hour blister (middle row) and the 72 hour blister (bottom row) leukocytes. Arrows indicate gating strategy.

6.3.3. Characterising the timecourse of the innate immune response

A comparison was made of leukocyte populations in the 24 and 72 hour blister.

6.3.3.1. Blister resolution is associated with an increase in fluid volume, but no change in absolute cell count

There was no change in the absolute cell count from 24 to 72 hours (24 hours 270,000 ± 271,000; 72 hours 179,000 ± 274,000; n = 17, Wilcoxon paired test, $p = 0.822$). Cell concentration was non-significantly decreased (24 hours 1,746,000 ± 1,520,000; 72 hours 796,000 ± 1,168,000; n = 17, Wilcoxon paired test, $p = 0.139$). This was most likely due to a significant increase in oedema volume from 24 to 72 hours (24 hours 0.178 ± 0.073; 72 hours 0.263 ± 0.178; n = 17, paired *t* test, $p = 0.028$). Results are shown in Figure 6.6.

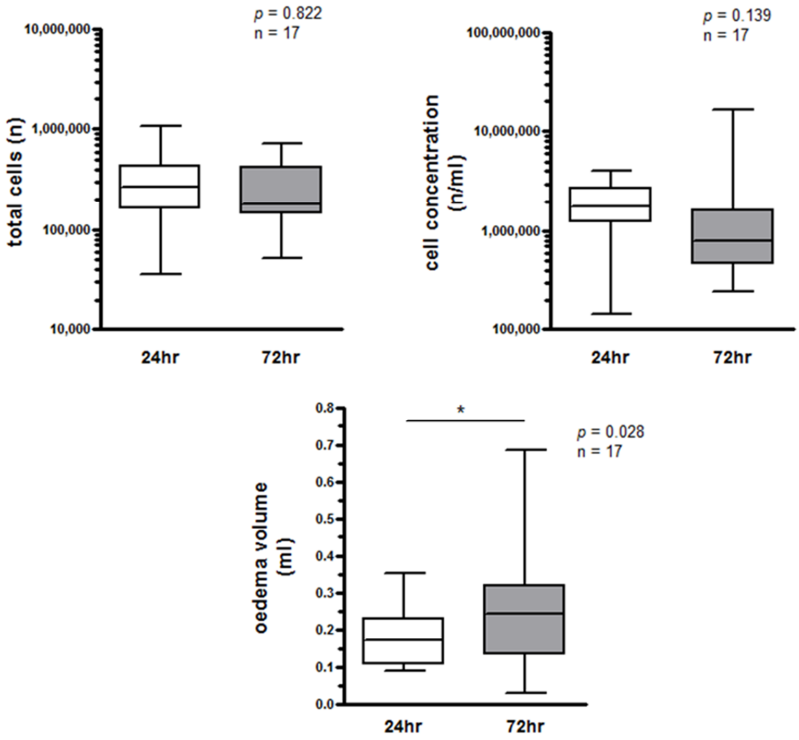

Figure 6.6 Leukocyte count and oedema volume in the 24 and 72 hour blisters. 17 healthy males received two skin blisters, with the first aspirated at 24 hours, and the second at 72 hours. Aspirates were measured for volume, and cells were isolated by centrifugation and enumerated. Results are expressed as the total cells, cell concentration, and oedema volume. There was no change in cell count from 24 to 72 hours, but oedema was increased. * denotes $p < 0.05$

6.3.3.2. Blister resolution is associated with granulocyte clearance and accumulation of MDSC-like cells

Despite a lack of change in total cell count, considerable changes occurred in the proportions of individual blister cell populations. No difference was observed in venous leukocyte populations analysed at 24 and 72 hours (no difference - data not shown).

In the blister there was an increase in the proportion of $CD3^+$ T cells, (24 hours 3.37 ± 1.83%; 72 hours 4.25 ± 2.24%; n = 17, paired *t* test, $p = 0.06$), $CD16^{hi}$ NK cells (24 hours 0.04 ± 0.04%; 72 hours 0.07 ± 0.10%; n = 17, paired *t* test, $p = 0.161$) and $CD16^{lo}$ NK cells (24 hours 0.09 ± 0.10%; 72 hours 0.16 ± 0.14%; n = 17, paired *t* test, *p*

= 0.030), with a decrease in the proportion of $CD19^{+}$ B cells (24 hours 0.04 ± 0.03%; 72 hours 0.01 ± 0.01%; n = 17, paired *t* test, $p = 0.002$) (Figure 6.7A).

There was a substantial decrease in both the proportion and absolute number of granulocytes in the blister from 24 to 72 hours consistent with resolution (Figure 6.7B); this was true for neutrophils (24 hours 38.9 ± 21.8%; 72 hours 13.7 ± 8.4%; n = 17, paired *t* test, $p < 0.001$) and eosinophils (24 hours 8.8 ± 3.7%; 72 hours 2.9 ± 1.4%; n = 17, paired *t* test, $p < 0.0001$). The reduction in the granulocyte population coincided with a substantial increase in the MDSCs (Figure 6.7C), whether they were $CD14^{hi}$ FSC^{lo} (24 hours 0.3 ± 0.2%; 72 hours 25.3 ± 11.1%; n = 17, paired *t* test, $p < 0.0001$), or $CD14^{dim/lo}$ (24 hours 4.0 ± 2.3%; 72 hours 12.7 ± 7.4%; n = 17, paired *t* test, $p < 0.0001$).

Changes in the HLA-DR^{hi} monocytes and macrophages populations, are more complex (Figure 6.8). There was a reduction in the classical monocyte population (24 hours 19.1 ± 9.5%; 72 hours 14.0 ± 5.9%; n = 17, paired *t* test, $p = 0.056$), and an increase in the HLA-DR^{hi} $CD14^{dim/lo}$ population (24 hours 5.6 ± 3.6%; 72 hours 14.2 ± 6.8%; n = 17, paired *t* test, $p < 0.001$). This coincided with an increase in the absolute $CD14^{hi}$ $CD16^{dim}$ macrophage population (24 hours 1.3 ± 2.0%; 72 hours 2.2 ± 1.3%; n = 17, paired *t* test, $p = 0.160$), no change in the $CD14^{hi}$ $CD16^{hi}$ macrophage population (24 hours 0.9 ± 1.3%; 72 hours 0.7 ± 0.5%; n = 17, paired *t* test, $p = 0.403$), and a decrease in the $CD14^{dim}$ $CD16^{hi}$ macrophage population (24 hours 1.3 ± 1.9%; 72 hours 0.6 ± 0.6%; n = 17, paired *t* test, $p = 0.157$).

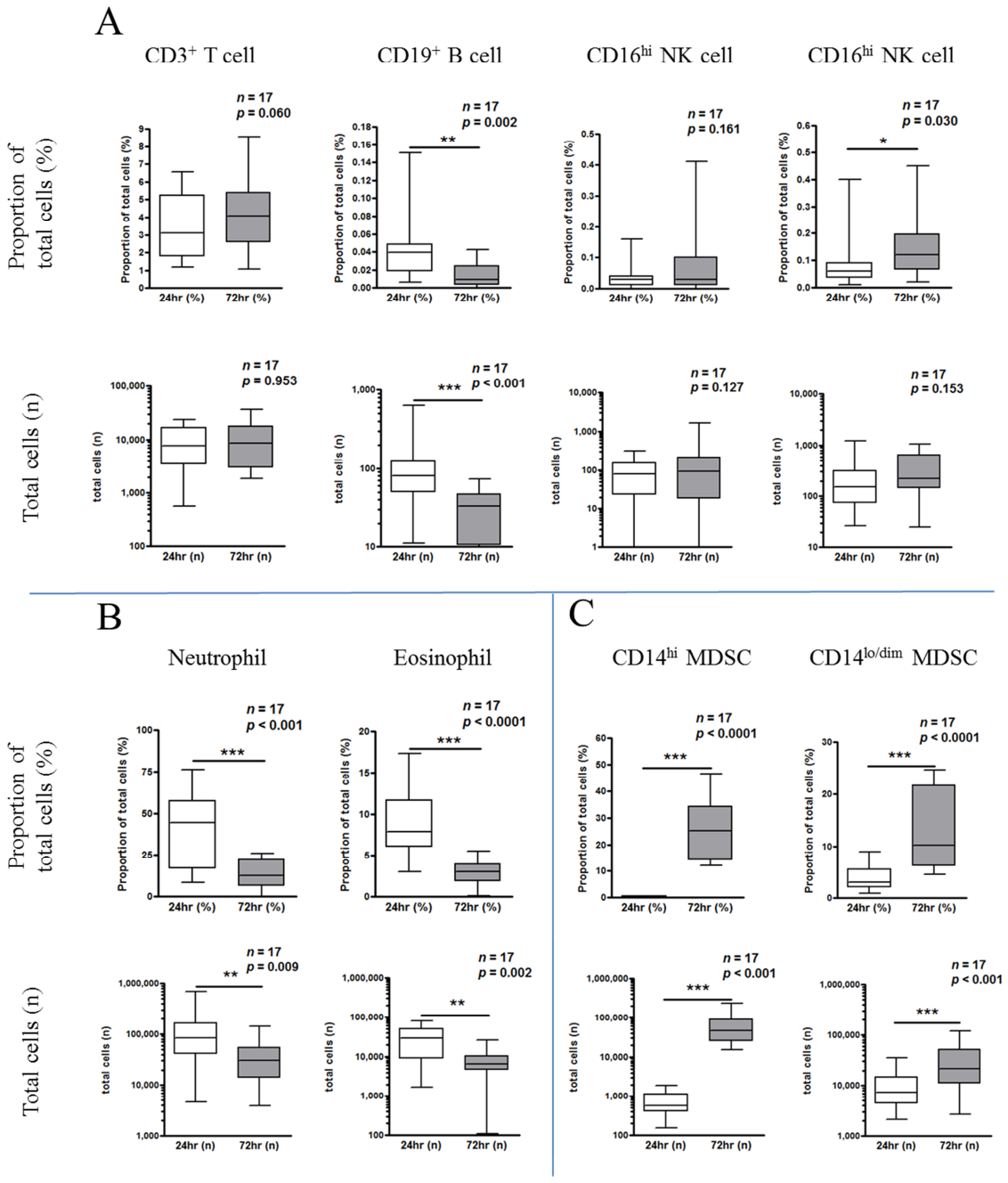

Figure 6.7 Lymphocyte, granulocyte and myeloid derived suppressor-like cell numbers in the 24 and 72 hour blister. 17 healthy males received two skin blisters, with the first aspirated at 24 hours, and the second at 72 hours. Isolated leukocytes were differentiated by flow cytometry into lymphocytes (A), granulocytes (B) and myeloid derived suppressor-like cells (MDSC) (C) according to gating in Figure 6.3 and Figure 6.4. From 24 to 72 hours there was an increase in T lymphocytes and natural killer (NK) cells, and a reduction in B lymphocytes. This coincided with a decrease in neutrophils and eosinophils and an increase in the CD14^{hi} and CD14$^{lo/dim}$ MDSCs. * denotes $p < 0.05$; ** denotes $p < 0.01$; * denotes $p < 0.001$.**

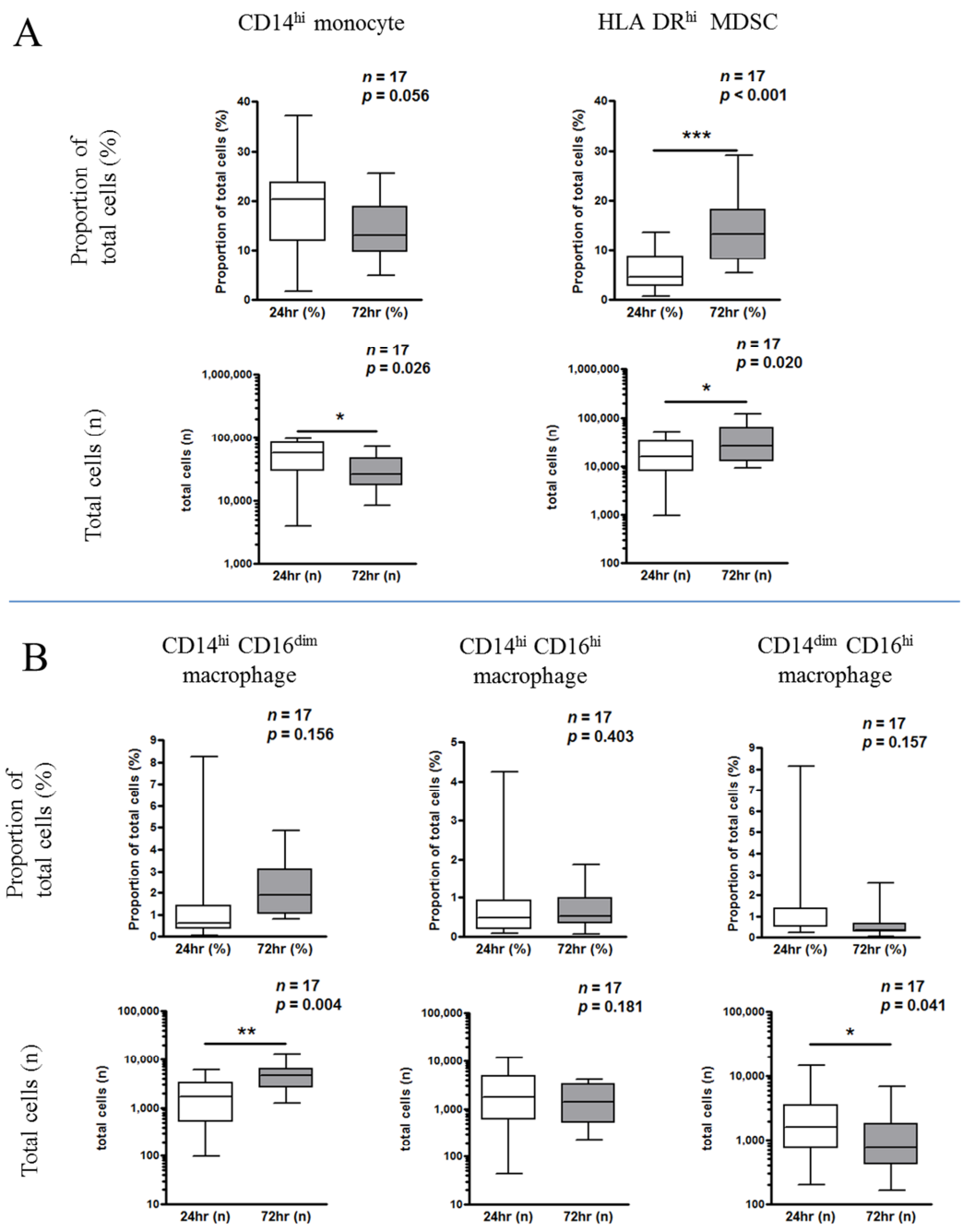

Figure 6.8 Monocyte and macrophage numbers in the 24 and 72 hour blister. 17 healthy males received two skin blisters, with the first aspirated at 24 hours, and the second at 72 hours. Isolated leukocytes were differentiated by flow cytometry into HLA-DR^{hi} cells and then SSC^{lo} cells (A) and SSC$^{mid/hi}$ macrophages (B) according to gating in Figure 6.5. Classical monocytes were significantly decreased from 24 to 72 hours, and HLA-DR^{hi} myeloid derived suppressor-like cells (MDSC) were significantly increased (A). There was an increase in CD14^{hi} CD16^{dim} macrophages, with decreases in the CD14^{hi} CD16^{hi} and CD14^{dim} CD16^{hi} macrophages (B). * denotes $p < 0.05$; ** denotes $p < 0.01$; * denotes $p < 0.001$.**

6.3.3.3. Increased HLA-DR expression during resolution

Human leukocyte antigen and its cluster (HLA-DR) form part of the major histocompatibility receptor complex (MHC) class II. MHC class II present intracellular polypeptide chains acquired from foreign antigens, to $CD4^+$ T lymphocytes that inspect and respond appropriately (228). HLA-DR is thus highly expressed on antigen presenting cells, which include monocytes, macrophages, dendritic cells, and B lymphocytes. HLA-DR expression is used as an indication of cell activation status. In the current study an increase in HLA-DR expression verified that the antigen presentation was increased in most cell populations in the blister when compared to circulating leukocytes (Figure 6.9). Furthermore HLA-DR expression was further enhanced between 24 and 72 hours within the blister. There was no change from 24 to 72 hours in HLA-DR expression in venous leukocytes (data not shown).

HLA-DR was increased in T lymphocytes (venous 155 ± 192; 24 hours 6652 ± 4468; 72 hours 25350 ± 13050; n = 16, Friedman test, $p < 0.0001$), neutrophils (venous 60 ± 135; 24 hours 149 ± 183; 72 hours 571 ± 418; n = 16, Friedman test, $p < 0.0001$), eosinophils (venous 125 ± 346; 24 hours 333 ± 657; 72 hours 1150 ± 1385; n = 16, Friedman test, $p < 0.0001$), HLA-DR^{lo} $CD14^{lo}$ MDSCs (venous 59 ± 88; 24 hours 127 ± 119; 72 hours 312 ± 343; n = 16, Friedman test, $p < 0.0001$), $CD14^{hi}$ $CD16^{dim}$ monocytes (venous 1997 ± 1576; 24 hours 15500 ± 11250; 72 hours 23650 ± 16400; n = 16, Friedman test, $p < 0.0001$), and $CD14^{hi}$ $CD16^{hi}$ macrophages (venous 2803 ± 7427; 24 hours 24300 ± 17200; 72 hours 44600 ± 32000; n = 16, Friedman test, $p < 0.0001$).

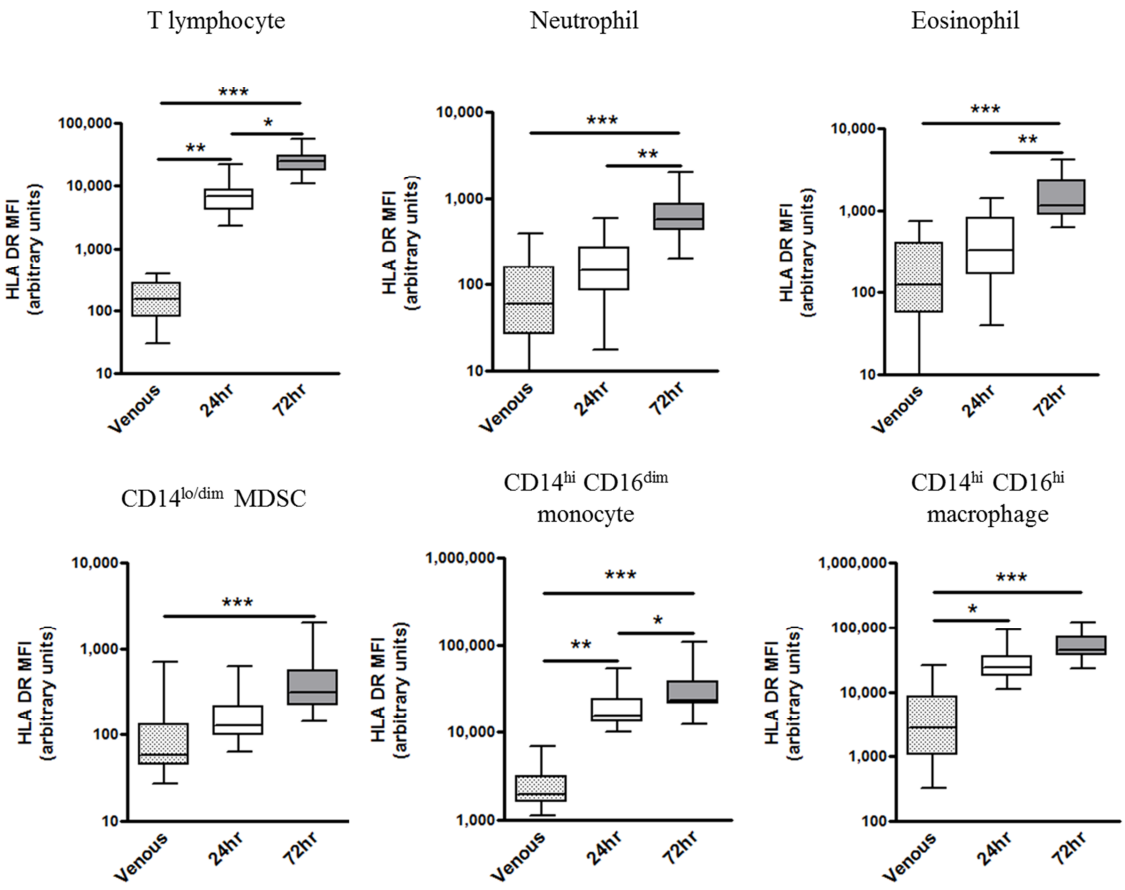

Figure 6.9 HLA-DR expression of circulating venous and blister leukocytes. 17 healthy males received two skin blisters, with the first aspirated at 24 hours, and the second at 72 hours. Circulating leukocytes were obtained from venous blood. Inflammatory leukocytes were obtained from blisters. Cells were differentiated according to gating strategy in Figure 6.3, Figure 6.4 and Figure 6.5. Individual populations were investigated for HLA-DR expression, reported in arbitrary units. Compared to venous blood, there was an increase in HLA-DR expression at 24 and 72 hours in the following blister cell types: T lymphocytes, neutrophils, eosinophils, $CD14^{lo/dim}$ MDSCs, $CD14^{hi}$ $CD16^{dim}$ monocytes, and $CD14^{hi}$ $CD16^{hi}$ macrophages. * denotes $p < 0.05$; ** denotes $p < 0.01$; * denotes $p < 0.001$.**

6.3.3.4. CD19 expression on non-lymphocytes during resolution

Unpublished work within our lab has shown that tissue-resident macrophages in the murine peritoneum can be derived from B lymphocytes, both in the steady state and during inflammation. By investigating CD19, a marker of mature B lymphocytes, I have investigated whether this phenomenon might exist in humans.

Hardly any $CD19^{+}$ B cells are present in the blisters at either 24 or 72 hours (see Figure 6.10). However an increasing CD19 expression was observed in the non-lymphocyte blister population from 24 to 72 hours. Further investigation of CD19 expression on individual populations, identified an increase in CD19 expression in HLA-$DR^{dim/lo}$ $CD14^{dim/lo}$ MDSCs (venous 19 ± 8; 24 hours 40 ± 41; 72 hours 73 ± 58; n = 16, Friedman test, $p < 0.0001$), $CD14^{hi}$ $CD16^{dim}$ monocytes (venous 84 ± 34; 24 hours 124 ± 75; 72 hours 177 ± 143; n = 16, Friedman test, $p < 0.0001$), and $CD14^{hi}$ $CD16^{hi}$ macrophages (venous 203 ± 198; 24 hours 211 ± 111; 72 hours 299 ± 167; n = 16, Friedman test, $p = 0.012$).

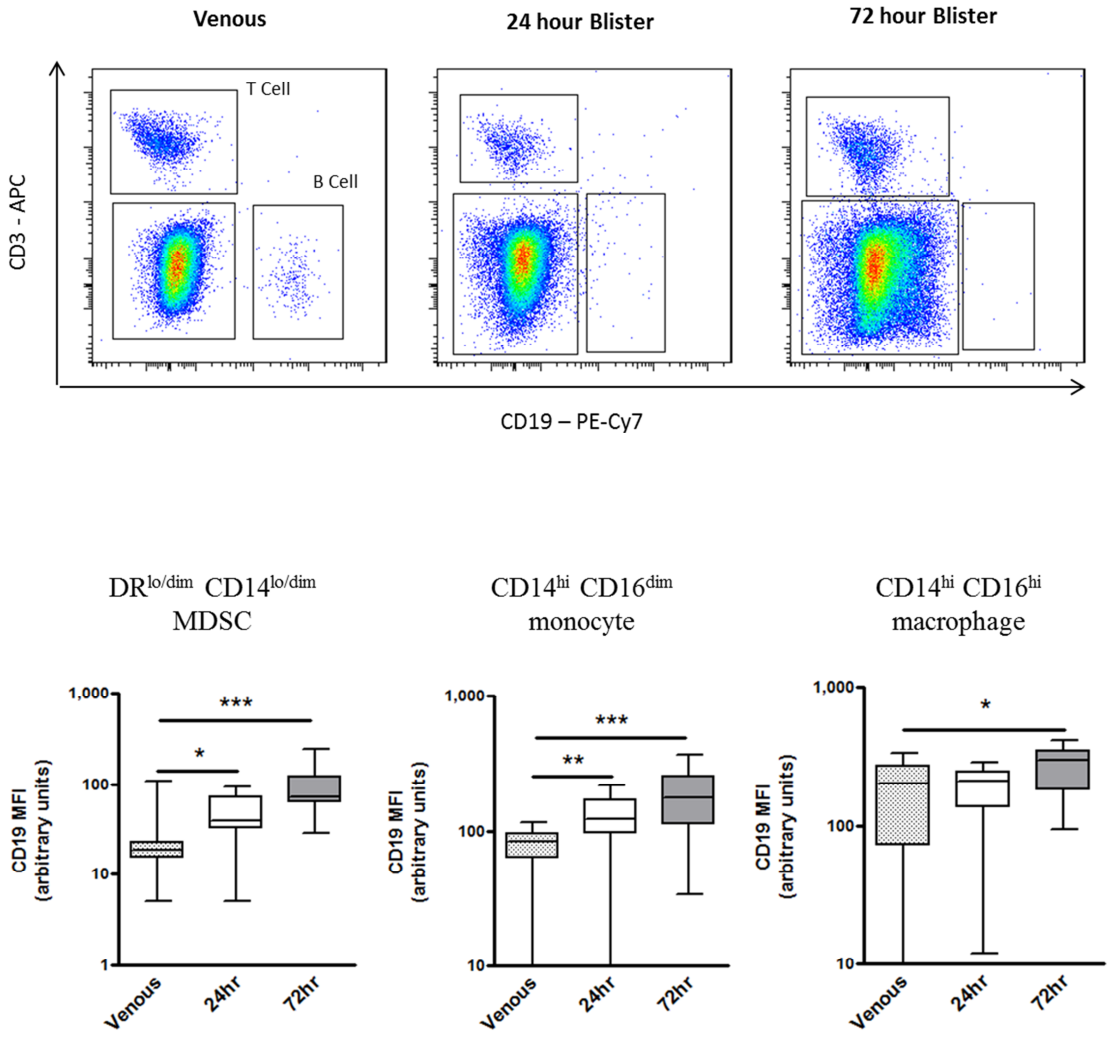

Figure 6.10 CD19 expression of circulating venous and blister leukocytes. 17 healthy males received two skin blisters, with the first aspirated at 24 hours, and the second at 72 hours. Circulating leukocytes were obtained from venous blood. Inflammatory leukocytes were obtained from blisters. Cells were differentiated according to gating strategy in Figure 6.3, Figure 6.4 and Figure 6.5. There were negligeable B lymphocytes in the blisters. However there was an increase in CD19 expression in non-lymphocyte populations at 72 hours (72 hour dot plot). Individual populations were investigated for CD19 expression, reported in arbitary units. Compared to venous blood, there was an increase in CD19 expression at 24 and 72 hours in the following blister cell types: HLA-DR$^{lo/dim}$ CD14$^{lo/dim}$ MDSCs, CD14^{hi} CD16^{dim} monocytes, and CD14^{hi} CD16^{hi} macrophages. * denotes $p < 0.05$; ** denote $p < 0.01$; * denotes $p < 0.001$.**

6.3.3.5. 72 hour blister is infiltrated by myeloid derived suppressor- like cells

Myeloid derived suppressor cells (MDSCs) are immature myeloid cells that inhibit T cell activity and are myeloid in origin. In the majority of reports, MDSCs are described as being $CD33^{hi}$ $HLA\text{-}DR^{lo}$ and $CD11b^{hi}$, but without common lineage markers (229). Section 6.3.3.2 indicates an increase in three populations from 24 to 72 hours, which might be candidates for MDSCs, due to their receptor expression. The increase at 72 hours suggests these cells may have a role in the resolution of inflammation. MDSCs have been coded to aid additional analyses: $HLA\text{-}DR^{lo/dim}$ $CD16^{dim}$ $CD14^{hi}$ cells [MDSC-α], $HLA\text{-}DR^{lo/dim}$ $CD16^{dim}$ $CD14^{lo}$ cells [MDSC-β], and $HLA\text{-}DR^{hi}$ $CD14^{lo}$ cells [MDSC-δ].

MDSCs were investigated further for their size, granularity, morphology, and expression of three typical "MDSC markers", CD33, CD11b and CD15 (see Figure 6.11). This was achieved by inducing 72 hour blisters in 3 additional subjects, and using flow assisted cell sorting (FACS) to assess morphology. Results show that MDSC-α cells are small, granular, and express $CD11b^{hi}$ $CD33^{hi}$ and $CD15^{hi}$ ($CD11b^{hi}$ $CD33^{hi}$ cells 98.7 ± 1.7%; $CD11b^{hi}$ $CD33^{hi}$ $CD15^{hi}$ cells 97.6 ± 1.6%; mean ± SD, n = 3). The MDSC-β cells were more heterogeneous, comprising primarily of $CD11b^{hi}$ $CD33^{hi}$ cells that were a mixture of $CD15^{hi}$ and $CD15^{lo}$ cells ($CD11b^{hi}$ $CD33^{hi}$ cells 68.0 ± 24.7%; $CD11b^{hi}$ $CD33^{hi}$ $CD15^{hi}$ cells 43.5 ± 24.8%; mean ± SD, n = 3). Finally, the MDSC-δ cells were fairly homogeneous, small, agranular, primarily $CD11b^{hi}$ $CD33^{hi}$ $CD15^{lo}$ cells ($CD11b^{hi}$ $CD33^{hi}$ cells 66.7 ± 2.4%; $CD11b^{hi}$ $CD33^{hi}$ $CD15^{lo}$ 57.1 ± 2.3%; mean ± SD, n = 3).

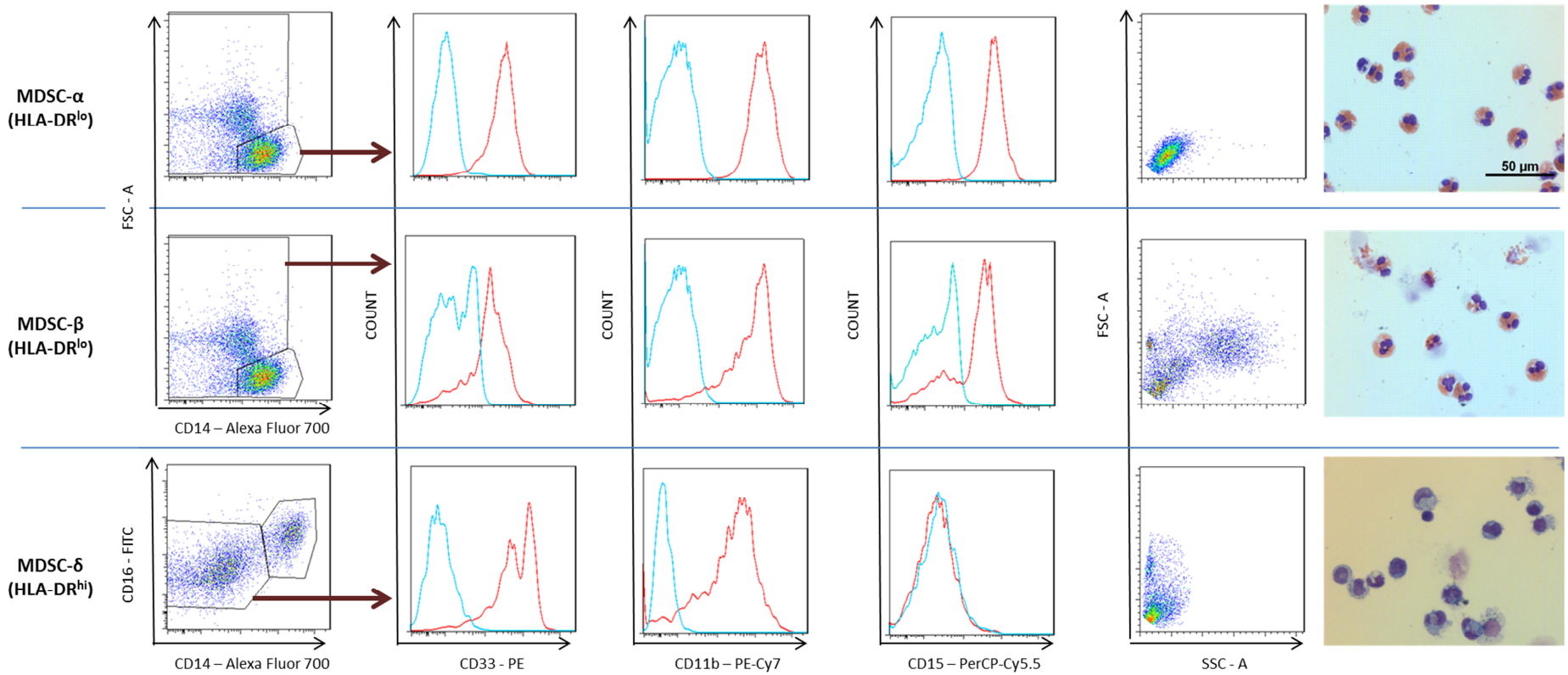

Figure 6.11 Identification of myeloid derived suppressor-like cells in the 72 hour blister. Representative plots are shown for three MDSC populations. Inflammatory leukocytes were obtained from 72 hour skin blisters in 3 subjects. MDSCs were identified by flow cytometry as described in Figure 6.4 and Figure 6.5. HLA-DR$^{lo/dim}$ CD16^{dim} CD14^{hi} (MDSC-α) cells were homogenous, small, granular, and CD33^{hi}, CD11b^{hi} and CD15^{hi}. HLA-DR$^{lo/dim}$ CD16^{dim} CD14$^{dim/lo}$ (MDSC-β) cells were heterogeneous, CD11b^{hi}, CD33^{hi} and with a split expression of CD15. HLA-DR^{hi} CD14$^{dim/lo}$ (MDSC-δ) cells were homogeneous, CD11b^{hi}, CD33^{hi} and CD15^{lo}. Red histograms show fully stained sample, blue histograms show corresponding FMO control.

6.4. Discussion

These results have described a thorough characterisation of the cantharidin skin blister. Preliminary results showed that that the blister model is repeatable, and sample size calculations showed that fewer than 10 subjects would be required to identify a 70% reduction in total cell count, and fewer than 25 for a 50% reduction. These calculations were used to design the crossover study described in chapter 7.

6.4.1. A novel gating strategy for identifying inflammatory and circulating leukocytes

The gating strategy was used to identify leukocytes both within the circulation and the blister at two time points. Using this, results showed that the granulocytes were cleared from 24 to 72 hours, as our group has previously described (181). This was not associated with a substantial increase in macrophages, but rather an increase in three other myeloid populations: 1.) HLA-DR^{lo} CD16^{dim} CD14^{hi}, 2.) HLA-DR^{lo} CD16^{dim} CD14$^{dim/lo}$, and 3.) HLA-DR^{hi} SSC^{lo} CD14^{lo}. An increase in HLA-DR expression was also observed across all major cells types, from venous to 24 hour to 72 hour blister, verifying leukocyte activation during the resolving blister.

Blisters contained few CD19^{hi} B cells, however resolution coincided with an increase in CD19 expression in non-lymphocytes. Closer examination revealed that this property was primarily observed on the HLA-DR^{hi} CD16^{dim} CD14$^{dim/lo}$ cells, CD14^{hi} CD16^{dim} classical monocytes, and CD14^{hi} CD16^{hi} macrophages. This increase in CD19 expression is corroborative with murine data from our group, which implicates that myeloid cells develop B cell receptor expression and phenotype. However, this data is only preliminary, and additional B lymphocyte markers and functional assessments are required before this phenomenon can be confirmed in humans.

6.4.2. Myeloid derived suppressor cells

In healthy participants, myeloid progenitor cells released from the bone marrow mature rapidly, and are subsequently a sparse population in circulating leukocytes. These cells are more commonly described in the blood of cancer patients, whereby malignancy invokes rapid myeloid progenitor cell production. Such myeloid progenitors are known to be immunosuppressive by inhibiting antigen-specific $CD8^+$ and $CD4^+$ T cell activation, through release of IL-10, increasing arginase and iNOS expression, ROS production, and down-regulation of IL-12 release (229–231). They are hence known as myeloid derived suppressor cells (MDSCs). MDSCs are believed to contribute to tumour progression and a reduced efficacy of cancer immunotherapy (229). MDSCs have also been described in experimental sepsis and trauma (230), suggesting that they may also complement the innate immunity.

No strict criteria exist for identifying human MDSCs, most likely due to their heterogeneous nature, malignancy-specific populations, and the sparsity in the healthy circulation. In most cases, MDSCs are $CD11b^{hi}$ HLA-DR^{lo} $CD33^{hi}$ and have a low expression of lineage markers (229). Recently $CD14^{hi}$ MDSCs have been described, which secrete TGF-ß and IL-10, and are T cell suppressive in nature (231,232). Several reviews have now characterised MDSCs into two populations: “monocytic” MDSCs ($CD14^{hi}$), and “granulocytic” MDSCs ($CD14^{lo}$) (229,233).

Results in this chapter are the first to describe the presence of MDSCs in the inflammatory skin blister. Three populations were identified that increase in number from 24 to 72 hours. Firstly, a small, granular, HLA-DR^{lo}, $CD16^{dim}$, $CD14^{hi}$, $CD33^{hi}$, $CD11b^{hi}$ and $CD15^{hi}$ population (MDSC-α). These cells had approximately a 100-fold increase from 24 to 72 hours, suggesting a function in the resolution phenotype. Secondly a granular, HLA-DR^{lo}, $CD16^{dim}$, $CD14^{lo/dim}$, $CD33^{hi}$, $CD11b^{hi}$ and $CD15^{hi}$

population (MDSC-β), which increased to a lesser extent, and was a composite of multiple cell types. Finally an agranular HLA-DR^{hi}, SSC^{lo}, CD16$^{lo/dim}$, CD14$^{lo/dim}$, CD33^{hi}, CD11b^{hi} and CD15^{lo} population, which resembled immature monocytes (MDSC-δ). Again, an increase in the 72 hour blister suggests a function during resolution.

These populations do not match exactly with known described populations. Firstly MDSC-α cells were granular, but unlike "granulocytic MDSCs" were also CD14^{hi}. Secondly MDSC-β cells were heterogeneous, including some CD15^{hi} and CD15^{lo} cells. Finally MDSCs are usually expressed as HLA-DR^{lo}, however MDSC-δ were HLA-DR^{hi} CD14^{lo} and CD16^{lo}, despite resembling immature monocytes. Studies by our group and others have observed similar MHC class II^{hi} MDSCs in murine inflammatory models (234).

Further work is required to investigate receptor expression and function of these cells, but this is beyond the scope of this thesis. Additional experiments would aim to assess the role of the cells, whether it be in mediating the innate response, or as described in cancer, mediating the adaptive response, in particular by T cell suppression. Alternatively these cells could have a more specific role in the repair and remodeling of the basement membrane between the dermis and epidermis, facilitating recovery of keratinocytes, melanocytes, and other cells present in the skin.

6.5. Conclusion

To summarise, these results describe a model for investigating the innate immune response in humans. They show for the first time in humans that resolution is characterised by an infiltration of MDSC-like cells. The model is repeatable, and can be

used to for investigate the effects of anti-inflammatory interventions on the human innate immune response.

7. THE EFFECT OF ISCHAEMIC PRECONDITIONING ON THE INNATE INFLAMMATORY RESPONSE IN HUMANS

7.1. Introduction

Preliminary evidence suggests that IPC might alter the acute, sterile inflammatory reaction that occurs during IR injury. As described in section 1.3.1.4, animal studies have demonstrated that IPC reduces leukocyte rolling, adhesion and migration following IR injury *in vivo* (66,67). These findings are consistent with human *in vitro* studies: IPC modifies circulating leukocytes by reducing neutrophil adhesion and apoptosis (72), decreasing expression of neutrophil kinin receptors (70), and reducing platelet-monocyte aggregates (71). Whilst these studies suggest that IPC modifies circulating leukocytes, this provides only limited information into how preconditioned leukocytes will respond to human IR injury. One would assume that a decrease in leukocyte adhesion is reflected in a decrease in leukocyte trafficking but this requires validation in *in vivo*.

In chapter 6 I categorised a cantharidin skin blister model, which quantified human leukocyte trafficking in response to a sterile inflammatory stimulus (cantharidin), and is thus comparable to the inflammatory response that is observed during IR injury, albeit to a different stimulus. Results show that the model is repeatable, and can be used to characterise the initiation (24 hours) and resolution (72 hours) of the innate immune response. This model has been previously been used to demonstrate the anti-inflammatory effects of TNF inhibitors (235), corticosteroids (235), trypsin inhibitors (236), and aspirin (181).

Results in chapter 5 indicate that local IPC, induced by three cycles of upper limb cuff inflations, conferred a protective effect against human endothelial IR injury. We have previously observed that ischaemic conditioning in humans is dependent on both humoral and neural pathways (79,112). To progress our understanding of the

components which govern IPC in humans, a study was performed to assess whether IPC modifies the innate immune response *in vivo*, using the skin blister model.

This chapter reports on a randomised crossover trial, designed to investigate whether IPC reduces leukocyte trafficking, with aspirin as a positive control. Cell migration into the cantharidin blister was quantified, individual cell types were identified, and the cytokine concentrations was calculated. Finally two inflammatory phenotypes are described, the early and the delayed resolvers, and how they individually respond to aspirin and IPC.

7.2. Methods

7.2.1. Study participants

Twenty healthy male subjects (age, 21 ± 4.1, mean ± SD) were recruited for this study. Participants were prepared as outlined in section 2.3.2. The sample size was based on the results in Figure 6.1.

7.2.2. Experimental protocol

The study was performed in a randomised crossover design (see Figure 7.1). Methodology for blister application and aspiration was described in section 2.3. Each subject attended the laboratory for nine visits over three weeks, to receive a total of 6 blisters. Each week represented a different arm of the study: control, IPC, or high dose aspirin. Blister application and processing protocol were consistent. At the start of each week (visit 1), a pair of blister patches were applied. After 24 hours (visit 2) subjects returned to the laboratory, a venous blood sample was taken, and one blister (24 hour blister) was aspirated with the other blister being secured and covered. After a further 48 hours (visit 3) subjects returned to the laboratory, a venous blood sample was taken, and the remaining blister (72 hour blister) was aspirated. The order of weeks was

randomised, with a washout period of at least 72 hours between the aspiration of the second blister, and the application of the next pair. Forearms were switched after each week.

Venous blood was acquired prior to blister aspiration from the antecubital vein on the contralateral arm to that with the skin blister. Plasma and leukocytes were isolated from venous blood (see section 2.3.2.4). Blister aspirates were volume assessed, and samples were centrifuged to isolate leukocytes. Cells were enumerated by haemocytometer, before being processed for antibody labeling and measurement by flow cytometry (see 2.3.2 and 2.3.3). Plasma and blister oedema were frozen at -80°C for subsequent cytokine analysis. The concentrations of tumour necrosis factor-α (TNF-α) and interleukin-10 (IL-10) were analysed using an ELISA (see section 2.3.4).

7.2.2.1. Control protocol

In the control protocol there was no intervention, with subjects performing the blister protocol as described above.

7.2.2.2. Ischaemic preconditioning protocol

On visit 1 of the IPC protocol, subjects received three IPC cycles of 5 minutes upper limb cuff inflation to 200 mmHg, followed by 5 minutes of reperfusion. Immediately after IPC skin blisters were applied to the same forearm that received the IPC stimulus. Blister aspiration at 24 and 72 hours was as above.

7.2.2.3. High dose aspirin protocol

On the aspirin protocol week, subjects were administered 3 doses of aspirin (3 x 300 mg p.o., Boots Pharmaceuticals, UK) at 8-hour intervals prior to visit 1. Immediately following blister application, a fourth dose of aspirin (300 mg p.o.) was administered. The dosing was matched to a previous study that demonstrated a reduction in leukocyte

trafficking by approximately 70% following high dose aspirin (181). Blister aspiration at 24 and 72 hours were as above.

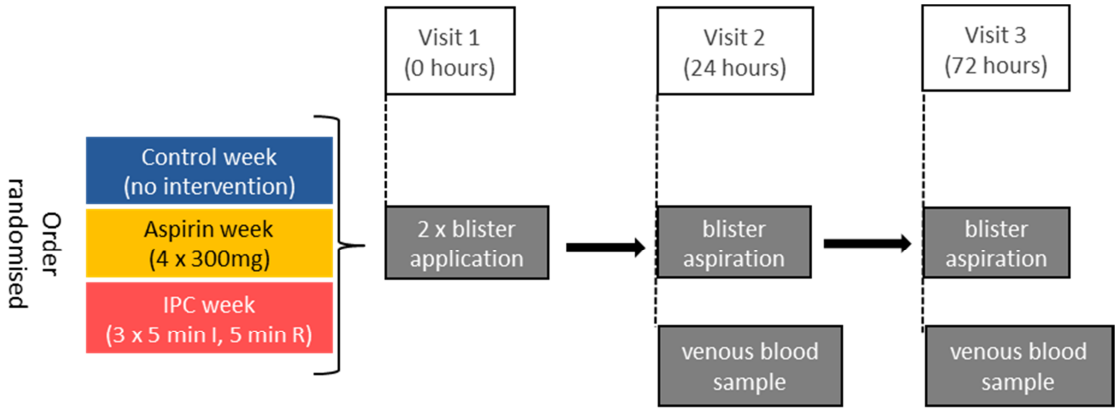

Figure 7.1 Experimental protocol for blister crossover study. 20 subjects received six blisters, two each for control, aspirin and IPC. On each week subjects received two skin blister patches (visit 1). One blister was aspirated at 24 hours (visit 2) and the other at 72 hours (visit 3). Venous samples were taken at visit 2 and visit 3 from the contralateral arm to that with the blister. In the aspirin week subjects received 4 doses of 300 mg aspirin, 3 doses at 8 hour intervals prior to blister application, and one dose immediately following application. In the IPC week subjects received 3 cycles of 5 minutes ischaemia with 5 minutes reperfusion immediately prior to blister application. Control, aspirin and IPC were performed in a random order.

7.2.3. Early and delayed resolvers of inflammation

Validation of the early and delayed resolution phenotype was made by repeating studies on six subjects at a later time point with a 24 and 72 hour blister in the control protocol conditions.

7.2.4. Statistical analysis

Data are presented as in chapter 6, using total cell count (n) and cell concentration (n/ml). Total cell count and cell concentration were non-parametric data, and hence presented on a logarithmic scale, and reported as median ± interquartile range. Oedema volume was parametric, and reported as mean ± standard deviation (SD). Given the

large number of data points and skewed distributions, results are presented as box and whisker plots, showing the median, interquartile range, and the minimum and maximum values.

Individual cell populations are given as the absolute cell count (logarithmic scale, median ± interquartile range). Between protocol differences were assessed using a repeated measures one-way ANOVA with a Bonferroni post-hoc test (parametric), or by a repeated measures Friedman test and a Dunn's post-test (non-parametric). Cytokines were non-parametric, and are reported as median ± interquartile range and displayed using a box and whisker plot. Changes from 24 to 72 hour results for cells and cytokines were assessed using Wilcoxon paired rank test.

The definition of the resolution phenotype was based upon previous work by our group (174). Subjects were retrospectively categorised using this definition from the results in their control protocol week. Missing subjects were removed by listwise deletion. Early and delayed resolver blisters are expressed as the delta change in cell count from 24 to 72 hours (mean ± SD), and comparisons between groups are made using unpaired *t* tests.

7.3. Results

There were technical issues (either blister popped or clotted) in one subject in the 24 hour blister set, and in three subjects in the 72 hour blister set. Results from remaining blisters are given below.

7.3.1. Ischaemic preconditioning has no effect on the acute and resolving inflammatory response

Results for cell number and oedema are summarised in Figure 7.2. There were no differences between groups at 24 hours whether measured as total cell count (control,

270,000 ± 278,000 cells; aspirin, 276,000 ± 178,000 cells; IPC, 285,000 ± 374,000 cells; n = 19, Friedman test, p = 0.196), cell concentration (control, 1,746,000 ± 1,707,000 cells/ml; aspirin, 1,680,000 ± 1,518,000 cells/ml; IPC, 1,651,000 ± 2,852,000 cells/ml; n = 19, Friedman test, p = 0.949) or oedema volume (control, 0.177 ± 0.068 ml; aspirin, 0.166 ± 0.075 ml; IPC, 0.181 ± 0.080 ml; n = 20, one-way ANOVA, p = 0.638).

There were no differences between groups at 72 hours whether measured as total cell count (control, 191,000 ± 261,000 cells; aspirin, 230,000 ± 268,000 cells; IPC, 336,000 ± 343,000 cells; n = 16, Friedman test, p = 0.646), cell concentration (control, 1,094,000 ± 1,168,000 cells/ml; aspirin, 814,000 ± 1,597,000 cells/ml; IPC, 1,741,000 ± 1,369,000 cells/ml; n = 16, Friedman test, p = 0.472) or oedema volume (control, 0.279 ± 0.183 ml; aspirin, 0.290 ± 0.194 ml; IPC, 0.363 ± 0.295 ml; n = 17, one-way ANOVA, p = 0.295).

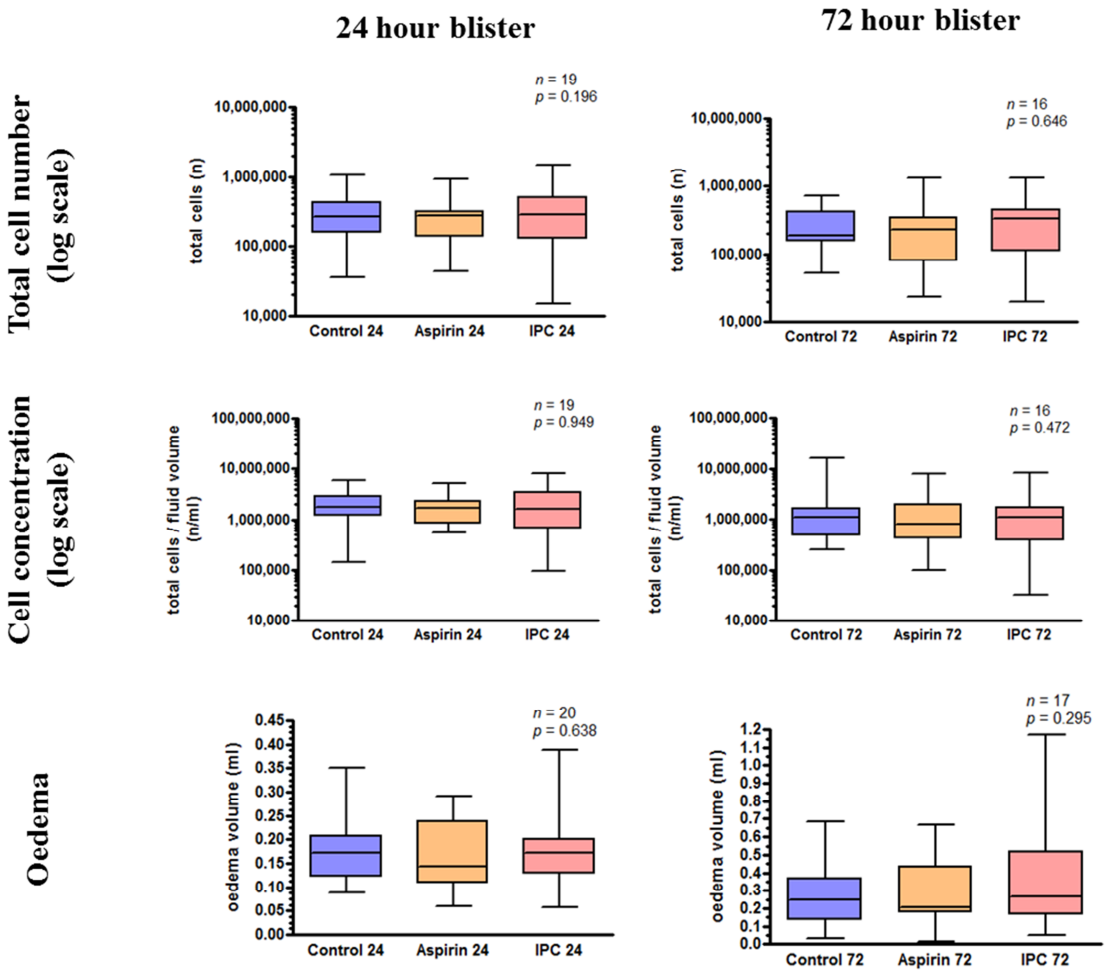

Figure 7.2 Effect of ischaemic preconditioning and aspirin and on total blister leukocyte trafficking. 20 subjects received six blisters, two each for control, aspirin, and IPC. Following aspiration, fluid volumes were measured, and cells enumerated by haemocytometer. Results are displayed for total blister cell count, cell concentration, and oedema volume alone, at 24 and 72 hours. Box and whisker plots show median, interquartile range, minimum and maximum values for control (blue), aspirin (yellow) and IPC (red). Groups were compared by Friedman test (cells) or one-way ANOVA (oedema). $p < 0.05$ was deemed statistically significant. There were no differences between the groups at either 24 or 72 hours.

There were no differences between control, aspirin or IPC in individual cell populations at either the 24 or 72 hours (Figure 7.3). Results are shown for $CD3^{hi}$ T lymphocytes (24 hours, $p = 0.854$, n = 19; 72 hours, $p = 0.607$, n = 14), neutrophils (24 hours, $p = 0.331$, n = 19; 72 hours, $p = 0.135$, n = 14), eosinophils (24 hours, $p = 0.505$, n = 19; 72 hours, $p = 0.607$, n = 14), $CD14^{hi}$ $CD16^{dim}$ classical monocytes (24 hours, $p = 0.076$, n = 19; 72 hours, $p = 0.395$, n = 14), and HLA-DR^{lo} $CD16^{dim}$ $CD14^{dim/lo}$ MDSCs (24 hours, $p = 0.949$, n = 19; 72 hours, $p = 0.931$, n = 14).

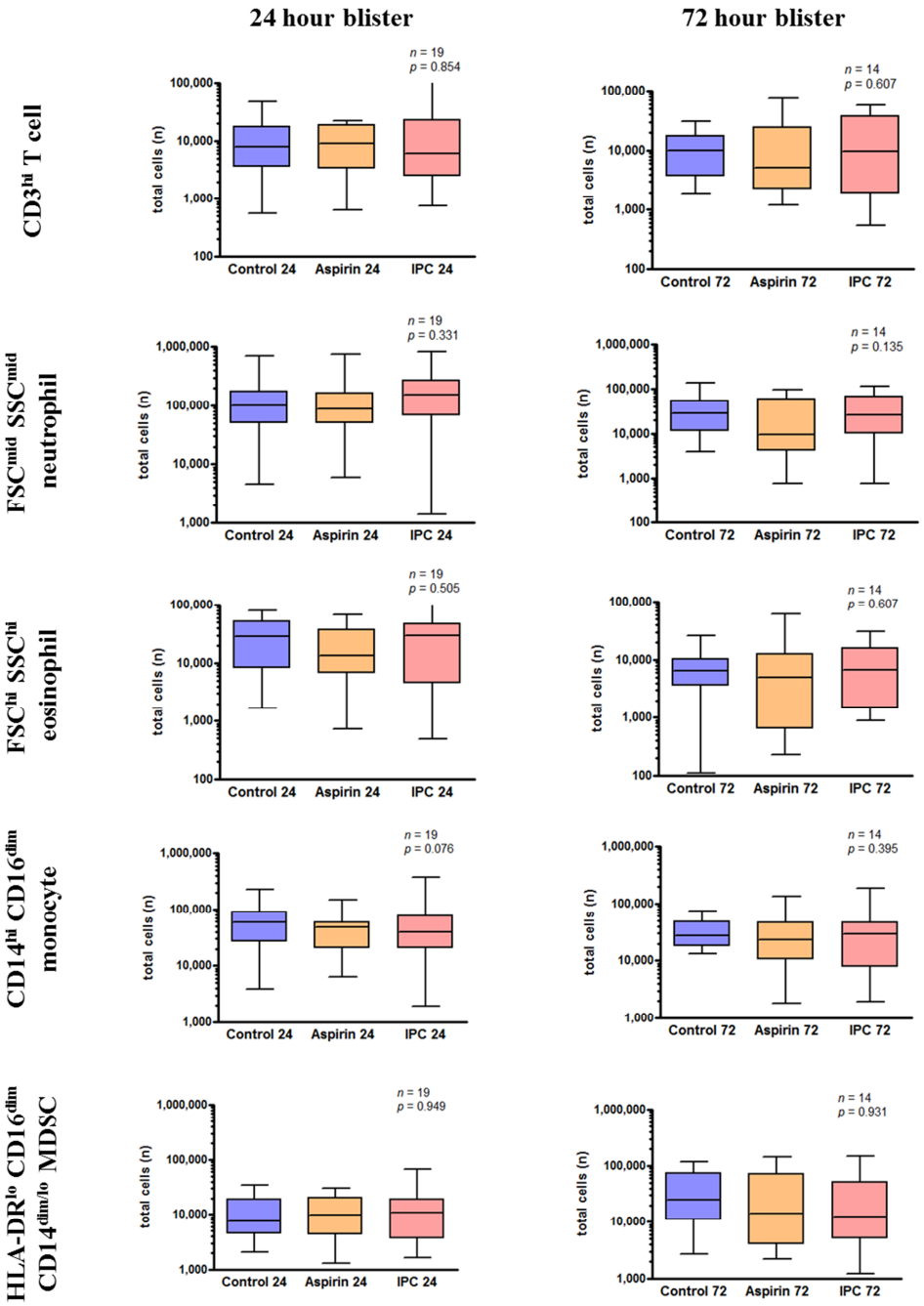

Figure 7.3 Effect of ischaemic preconditioning and aspirin on individual population blister leukocyte trafficking. 20 subjects received six blisters, two each for control, aspirin, and IPC. Following aspiration, fluid volumes were measured, cells enumerated by haemocytometer, and remaining cells stained with fluorescent antibodies and analysed by flow cytometry. Results are displayed for five major leukocytes populations present in the blister (see Figure 6.2). Box and whisker plots show median, interquartile range, minimum and maximum values for control (blue), aspirin (yellow) and IPC (red). Groups were compared by Friedman test. $p < 0.05$ was deemed statistically significant. There were no differences between the groups at either 24 or 72 hours.

From 24 to 72 hours there was no difference in the concentration of TNF-α (24 hours, 189 ± 173 pg/ml; 72 hours, 175 ± 185 pg/ml; n = 8, Wilcoxon rank test, p = 0.641) but there was an increase in the concentration of IL-10 (24 hours, 30 ± 13 pg/ml; 72 hours, 50 ± 33 pg/ml; n = 7, Wilcoxon rank test, p = 0.031). There was no difference between control, aspirin and IPC for either TNF-α (24 hours, p = 0.814, n = 9; 72 hours, p = 0.398, n = 9; Friedman test) or IL-10 (24 hours, p = 0.654, n = 8; 72 hours, p = 0.430, n = 6, Friedman test).

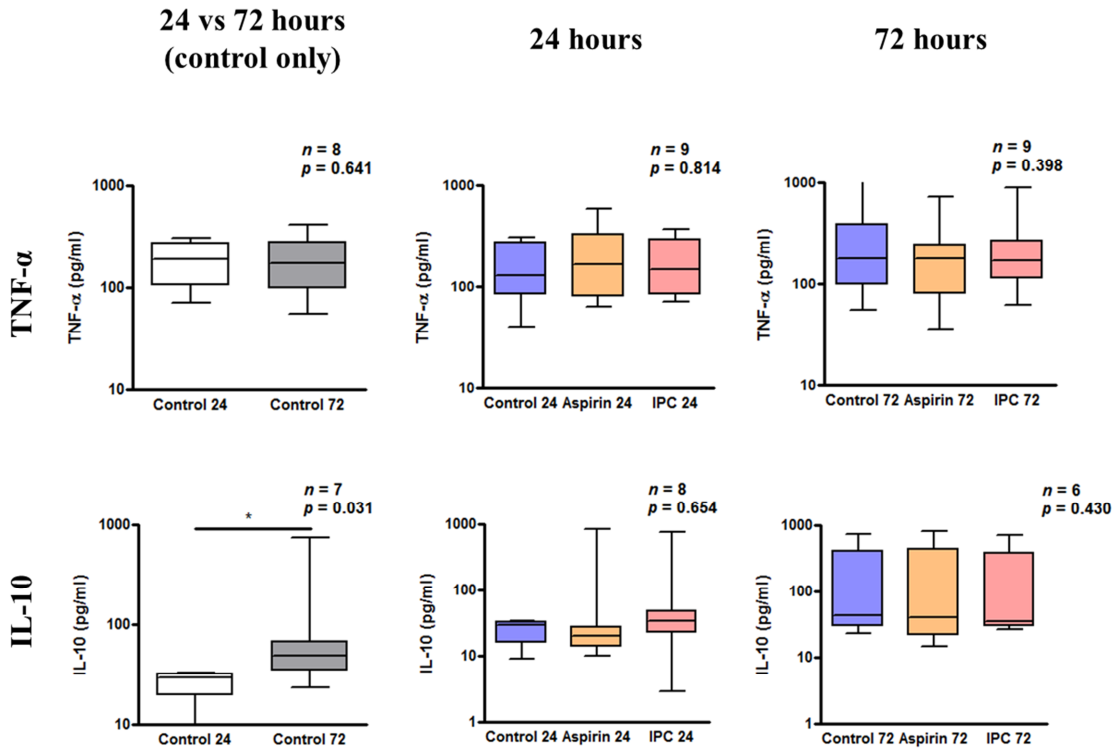

Figure 7.4 Effect of ischaemic preconditioning and aspirin on blister cytokine concentration. 20 subjects received six blisters, two each for control, aspirin, and IPC. Following aspiration, cells and fluid were separated, and fluids stored at -80°C. At a later date, samples from 9 subjects were analysed for TNF-α, and 8 subjects for IL-10, by ELISA. Results show the change in the control blisters from 24 to 72 hours, and the difference between control, aspirin and IPC at 24 and 72 hours. Box and whisker plots show median, interquartile range, minimum and maximum values. Groups were compared by non-parametric tests. $p < 0.05$ was deemed statistically significant. IL-10 but not TNF-α was increased from 24 to 72 hours. No difference existed between control, aspirin and IPC at any time point. *, $p < 0.05$

7.3.2. Early and delayed resolving inflammatory phenotype

Subjects were retrospectively divided into early (n = 8) and delayed (n = 10) resolvers of inflammation, based upon whether they increased or decreased their total cell count from 24 to 72 hours, as has been previously described (174). To confirm that this phenotype is consistent, six subjects (early, n = 4; delayed n = 2) repeated the control week, and results are shown in Table 7.1. All subjects who were early resolvers in the control week were early resolvers in the repeat week. One of the two delayed resolvers in the control week, switched to an early resolver phenotype in the repeat week (see E* in Table 7.1). However a consistent delayed resolver phenotype was obtained when results were expressed as cell concentration.

Table 7.1 Results for repeated early and delayed resolver phenotype. Six subjects (A to F) who had completed the main study, repeated the control week to confirm their resolution phenotype at a later date. A decrease from 24 to 72 hours is an early resolver (▼), an increase from 24 to 72 hours is a delayed resolver (▲). Results are given as total cell count (cells) and cell concentration (cells / ml).

		control week			repeat control week		
subject		24 hours	72 hours	delta	24 hours	72 hours	delta
A	cells	446,000	165,000	▼	1,020,000	403,000	▼
	cells / ml	4,018,000	1,542,000	▼	3,505,000	2,305,000	▼
B	cells	270,000	52,000	▼	1,483,000	146,000	▼
	cells / ml	1,849,000	494,000	▼	7,975,000	1,759,000	▼
C	cells	217,000	120,000	▼	923,000	483,000	▼
	cells / ml	1,167,000	756,000	▼	4,295,000	1,236,000	▼
D	cells	434,000	715,000	▲	203,000	1,010,000	▲
	cells / ml	2,874,000	3,505,000	▲	604,000	3,196,000	▲
E*	cells	152,000	178,000	▲	366,000	108,000	▼*
	cells / ml	1,523,000	1,633,000	▲	2,377,000	2,626,000	▲
F	cells	427,000	397,000	▼	2,255,000	317,000	▼
	cells / ml	2,481,000	1,632,000	▼	7,091,000	693,000	▼

Summarised results from the control week of blisters from 24 to 72 hours are shown in Figure 7.5. Early resolvers had a decreased total cell count from 24 to 72 hours (24 hours, 364,000 ± 197,000 cells; 72 hours, 165,000 ± 196,000 cells; n = 8, Wilcoxon rank test, $p = 0.008$). Delayed resolvers had an increased total cell count from 24 to 72 hours (24 hours, 160,000 ± 254,000 cells; 72 hours, 354,000 ± 421,000 cells; n = 10, Wilcoxon rank test, $p = 0.002$). There was a significant difference between groups in the change from 24 to 72 hours for total cell count, and the cell concentration (cells, unpaired *t* test, $p < 0.0001$; cells / ml, unpaired *t* text, $p < 0.001$). Early resolvers had an increased clearance of neutrophils from 24 to 72 hours compared to delayed resolvers (early 24 to 72 hours, -38.2 ± 25.5%; delayed 24 to 72 hours, -11.8 ± 18.7%; unpaired *t* test, $p = 0.027$).

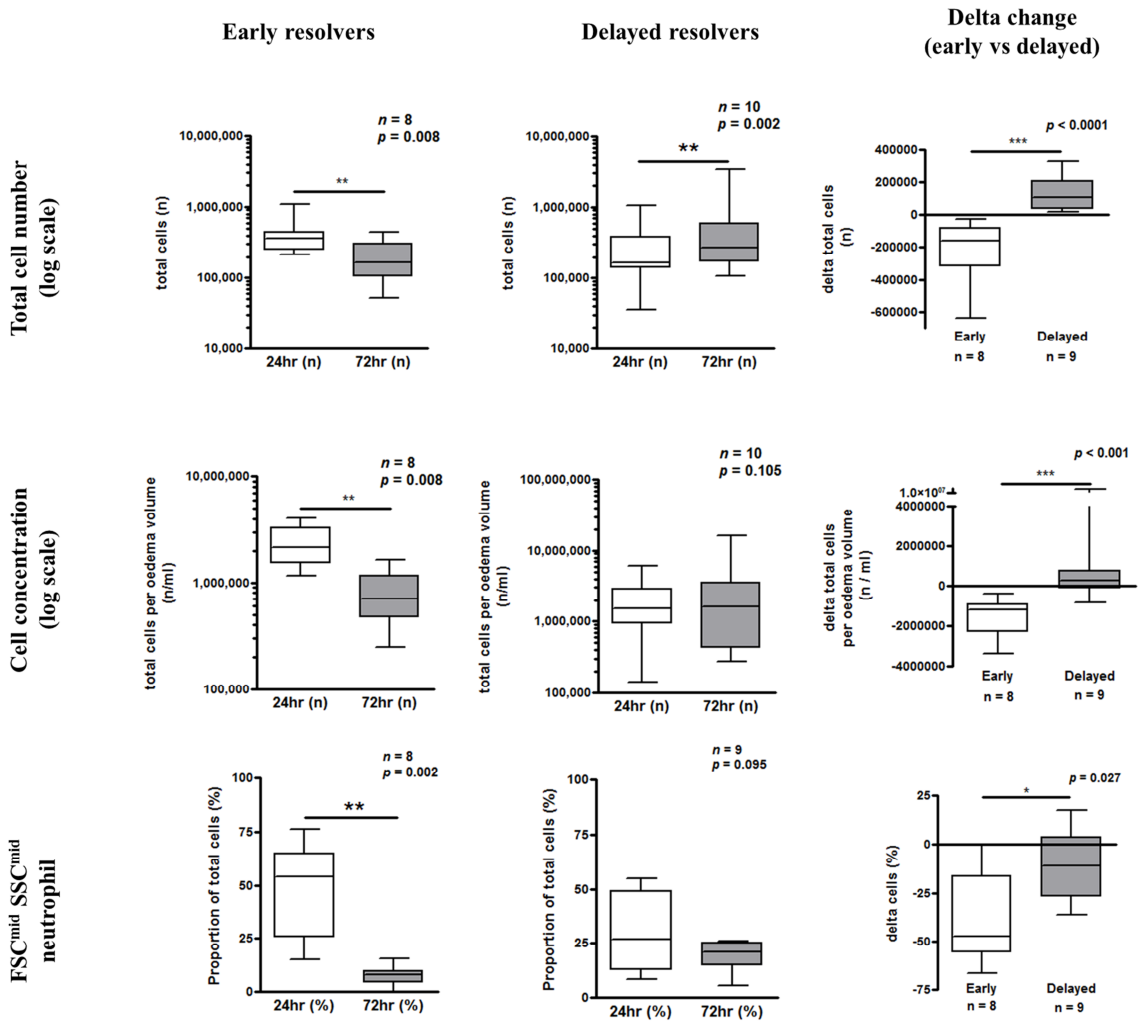

Figure 7.5 Early and delayed resolver phenotype in the 24 to 72 hour blister. 20 subjects received six blisters, two each for control, aspirin, and IPC. Following aspiration, fluid volumes were measured, and cells enumerated by haemocytometer. Control arm results allowed subjects to be subdivided into early (n = 8) or delayed (n = 10) resolvers of inflammation, according to whether they decreased (early) or increased (delayed) their total blister cell count from 24 to 72 hours. The early and delayed resolution phenotype was reflected in the change in the proportion of neutrophils from 24 to 72 hours. Results for total cell count, cell concentration, and neutrophil proportion are shown as box and whisker plots, with the median, interquartile range, minimum, and maximum values. *, $p < 0.05$; **, $p < 0.01$; ***, $p < 0.001$

7.3.3. Aspirin, but not IPC, reduces leukocyte trafficking in the early resolvers of inflammation

Early and delayed resolvers were assessed for their response to aspirin and IPC (Figure 7.6). Early resolvers had a significantly lower total cell count at 24 hours following administration of aspirin compared to control (control, 364,000 ± 197,000 cells; aspirin, 286,000 ± 161,000 cells; n = 8, Wilcoxon pairs, $p = 0.016$). There was no difference between control and aspirin in the delayed resolvers (control, 160,000 ± 254,000 cells; aspirin, 167,000 ± 198,000 cells; n = 10, Wilcoxon pairs, $p = 0.922$).

There was no difference in leukocyte trafficking between control and IPC in either the early (control, 364,000 ± 197,000 cells; IPC, 318,000 ± 456,000 cells; n = 8, Wilcoxon pairs, $p = 0.547$) or delayed resolvers (control, 160,000 ± 254,000 cells; IPC, 276,500 ± 290,000 cells; n = 10, Wilcoxon pairs, $p = 0.846$).

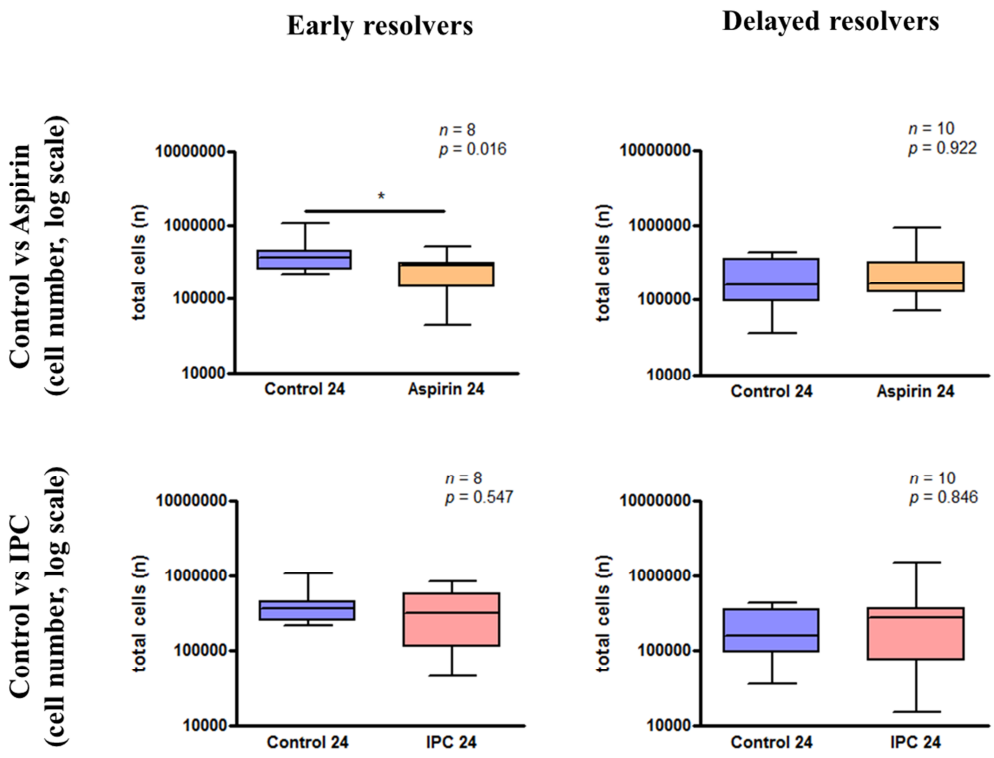

Figure 7.6 Effect of ischaemic preconditioning and aspirin on total cell trafficking in early and delayed resolvers. 20 subjects received six blisters, two each for control, aspirin, and IPC. Following aspiration, fluid volumes were measured, and cells enumerated by haemocytometer. Subjects were subdivided into early (n = 8) and delayed (n = 10) resolvers of inflammation, and then assessed for their response to aspirin and IPC. Results for total cell count are shown as box and whisker plots, with the median, interquartile range, minimum, and maximum values. $p < 0.05$ was deemed statistically significant. Early resolvers had a reduced leukocyte trafficking with aspirin compared to control at 24 hours. There was no difference in delayed resolvers, or with IPC in either group. * , $p < 0.05$

The reduction in leukocyte trafficking by aspirin in the early resolvers was attributable to the granulocyte population. In early resolvers aspirin administration was associated with a reduction in neutrophils (control, 145,000 ± 120,000 cells; aspirin, 91,000 ± 120,000 cells; n = 8, Wilcoxon rank test, $p = 0.109$) and eosinophils (control, 40,000 ± 32,000 cells; aspirin, 18,000 ± 29,000 cells; n = 8, Wilcoxon rank test, $p = 0.008$). There was no difference in delayed resolvers for neutrophils (control, 71,000 ± 99,000 cells; aspirin, 75,000 ± 107,000 cells; n = 10, Wilcoxon rank test, $p = 0.557$) or eosinophils

(control, 9,000 ± 27,000 cells; aspirin, 13,000 ± 29,000 cells; n = 10, Wilcoxon rank test, p = 1.000).

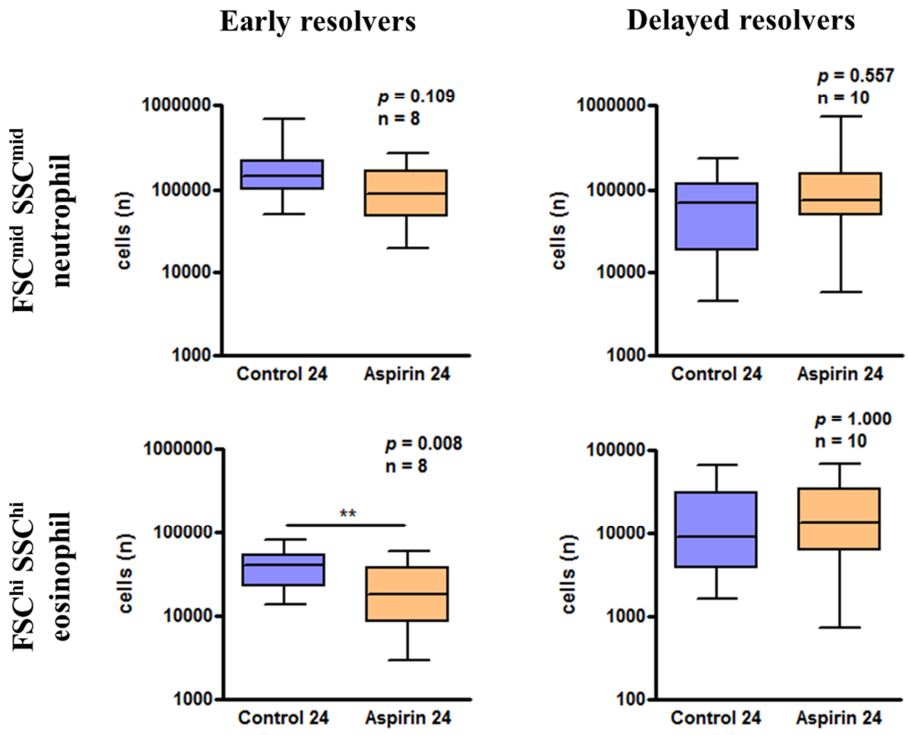

Figure 7.7 Effect of ischaemic preconditioning and aspirin on granulocyte trafficking in early and delayed resolvers. 20 subjects received six blisters, two each for control, aspirin, and IPC. Following aspiration, cells were enumerated, stained with fluorescent antibodies, and analysed by flow cytometry. Subjects were subdivided into early (n = 8) and delayed (n = 10) resolvers of inflammation, and then assessed for their response to aspirin and IPC. Granulocyte results in response to aspirin for the early and delayed resolvers are shown as box and whisker plots, with the median, interquartile range, minimum, and maximum values. p < 0.05 was deemed statistically significant. Granulocyte populations in the early resolvers were lower following aspirin and control at 24 hours. There was no difference in the delayed resolvers. ** , p < 0.01.

7.4. Discussion

7.4.1. Ischaemic preconditioning does not reduce leukocyte trafficking in an in vivo skin blister model

Results from the study observed no difference in leukocyte trafficking between IPC and control, irrespective of whether total cells or individual populations were investigated. Two plausible reasons might explain this null effect: 1.) IPC does not reduce the IR-induced innate immune response, 2.) model limitations prevented the detection of an immune modifying effect. There are several arguments in support of each.

Firstly, as described, the evidence supporting a role for a reduced leukocyte trafficking in IPC is primarily based upon evidence from animal *in vivo* studies (66,67) and human *in vitro* experiments (15,70,72). Animal experiments have demonstrated that IPC reduces leukocyte rolling, migration, expression of CD11b, selectins, and ICAM-1 expression (66–68). However, there are numerous examples of therapeutic interventions that have shown protection against experimental IR in animals, but have failed to transfer into clinically useful effects, including antioxidants (237), and erythropoietin (238).

Shimizu et al. observed that following IPC stimulation, circulating neutrophils have a decreased adhesion and an increased cytokine secretion *in vitro* (72). However these are only two elements of the inflammatory pathway, and no differences were seen for phagocytic activity, NADPH oxidase production, and apoptosis in neutrophils at 24 hours. Our group has previously observed that IPC abolishes the increase in neutrophil CD11b expression following IR (15).

Unfortunately, it is not uncommon for *in vitro* observations to fail to materialise in effects *in vivo*, and recently two studies did not observe an IPC-induced alteration in the systemic inflammatory response to IR. Karuppasamy et al. randomised 54 patients to

RIPC or sham prior to coronary artery bypass graft surgery (239). They observed no difference in the post-surgical increase in circulating cytokines (including IL-6, IL-8, monocyte chemotactic protein-1) between the groups. Furthermore Memtsoudis et al. measured the increase in circulating inflammatory markers post-operatively following a total knee arthroplasty (240). They observed no difference in IL-6, C-reactive protein, TNF-α and white blood cell count between patients who received preconditioning prior to surgery, and matched controls.

If IPC does not dampen acute inflammation, this might be attributed to the role of immunity in reperfusion injury itself. Section 1.2.2.2 described a substantial leukocyte migration into reperfused tissue, and how leukocyte activity contributes to the pathogenesis of reperfusion injury by enzymatic and ROS release within the interstitial tissue. However, this theory is controversial, and the arguments for and against a role of inflammation in the pathogenesis of reperfusion injury have been summarised by Vinten-Johansen (36).

The argument against a role for inflammation is supported by a number of observations. Firstly a substantial infarction can be obtained from isolated heart preparations submitted to IR injury, despite reperfusion with a neutrophil-free buffer (241). In addition the superoxide anion burst during reperfusion has been largely attributed to NADPH oxidase activity by neutrophils in the tissue. However Kevin et al. observed that this superoxide anion burst can still occur in isolated hearts supplied by a neutrophil-free buffer (241).

Secondly a number of clinical trials have investigated whether anti-inflammatory therapies can protect against IR injury. Baran et al. randomised 394 patients who presented with ST-segment elevation consistent with acute myocardial infarction, to either a monoclonal antibody for CD18 (part of the CD11b/CD18 glycoprotein complex

on neutrophils) or placebo (242). No differences were observed between groups for any clinically relevant outcome. If IR injury itself is not dependent on the innate immunity, it is unlikely that IPC activates an anti-inflammatory pathway. However, as has been described, the pathogenesis of IR is complex, and the exact role of inflammation in IR may depend on the site and type of injury, and may vary between species.

Despite these arguments, section 1.3.1.4 described strong evidence supporting an anti-inflammatory role for IPC. An alternative hypothesis for the null effect is that inherent limitations of the experimental technique prevented the detection of an anti-inflammatory effect, such as 1.) powering of the study, 2.) differences in inflammatory phenotype, 3.) windows of preconditioning activity.

The sample size in this study was powered to detect at least a 50% reduction in leukocyte trafficking at 24 hours. It was anticipated that this would be sufficient to detect a clinically relevant anti-inflammatory effect. However, the mechanism of IPC is multifactorial, believed to include a reduction in necrotic and apoptotic cell death, an improved glucose uptake, and a reduced Ca^{2+} overload (see Figure 1.3). Given this, the mechanistic component of modulating the inflammatory response could be small, and as such the study might be underpowered to detect an effect.

Another factor is the fundamental differences in the vascular beds between this study and experiments to date. *In vivo* experiments by Szabo et al. and Erling et al. reported a reduction in leukocyte migration in periosteal and mesenteric post-capillary venules respectively (66,67). Leukocyte trafficking into the blister primarily occurs from the vasculature supplying the dermis of the skin, and it is plausible that differences exist between endothelial cells in the dermis, and the periosteum or mesentery. In particular, the blood flow to these tissues is likely to be significantly greater than the skin.

In addition this study has assumed that the innate immune response in the blister is similar to that occurring during IR. It is likely that the balance of cytokines, chemokines, complement, lipid mediators and ROS which are known to activate the immune response, may vary between IR and in response to cantharidin. This may also be attributable to differences in local tissue metabolic requirements, given that cells in the dermis and epidermis, including keratinocytes, melanocytes, fibroblasts and adipocytes, have a low metabolic requirement when compared to cardiomyocytes and neurons.

IPC exerts its protective effects in an initial window lasting 1-2 hours, and a second window, present from 12 hours and lasting to 72 hours (55). This study has characterised skin blisters which were aspirated at 24 and 72 hours, consistent with the second window of protection. These time points were chosen because they match with previous studies in this field (181), and aspirating prior to 24 hours is limited by the requirement of several hours for the blister itself to form. The timing of blister aspiration is in contrast with the *in vitro* human leukocyte studies, whereby circulating neutrophils were isolated within an hour of IPC application, therefore in the first window of protection (15,72). It is plausible that the anti-inflammatory property of IPC occurs in the early, but not the second window of protection.

Several reasons have been speculated that might account for the null effect of this study. Further research aims to investigate whether RIPC reduces circulating inflammatory mediators in a clinical trial of live-donor kidney transplant, which is currently being carried out by our research group.

7.4.1. Aspirin, and the resolution phenotype in humans

In contrast to previous studies, my results did not show a substantial reduction in leukocyte trafficking following administration of high-dose aspirin. This result was

surprising; Morris et al. noted a 70% reduction in total leukocyte trafficking with aspirin at a similar dose (181). One reason for this could be methodological differences in the assessment of leukocyte trafficking. Morris et al. observed a substantially larger leukocyte infiltration at 24 hour control blisters in comparison to my study (W Jenner, total cell count = 270,000 ± 271,000 cells [median ± interquartile range]; T Morris, total cell count ≈ 700,000 ± 150,000 [mean ± standard error]). This difference could be attributable to aspects of the experimental set up, including size of paper, film and dressing. A more substantial inflammatory response may be is required to observe a robust anti-inflammatory effect of aspirin.

Our group has previously shown that those with a heightened early immune activity (early resolvers), exhibit a robust response to administration of aspirin (174). Those with a more tempered profile (delayed resolvers) are refractory to aspirin. This response is reflected in differences in blister IL-1β and 15-epi-lipoxin concentration, and by neutrophil clearance. Subjects in my study were also subdivided according to early and delayed resolver phenotype. Early resolvers had a greater reduction in total leukocyte trafficking from 24 to 72 hours, and this was reflected in an increase in neutrophil clearance. Furthermore the early resolvers were responsive to aspirin administration at 24 hours, unlike the delayed resolvers, consistent with previous observations (174). Neither the early nor delayed resolvers exhibited an anti-inflammatory response to IPC.

7.4.2. Study limitations

The study population was a homogenous group of young males, and results may not be reflected in female or older subjects. This study has investigated TNF-α and IL-10 concentration, but further experiments are required to assess whether other mediators, such as IL-6, IL-8 and interferon-γ are altered between the groups, and whether the

differences in early and delayed resolvers are matched by a modulation of their cytokine profile.

7.5. Conclusion

To summarise, this study has, for the first time in humans, observed that IPC does not influence the human innate immune response to an *in vivo* skin blister model. As previously described, aspirin reduces leukocyte trafficking in subjects with the early, but not delayed resolver phenotype. Further experiments aim to investigate alternative mechanistic properties of IPC.

8. THE EFFECT OF ISCHAEMIC PRECONDITIONING ON INCREMENTAL EXERCISE IN HUMANS

8.1. Introduction

Improving exercise performance is of vital importance to elite athletes, coaches and sponsors across the world. Months, even years of training are required to improve competitive performance, often by a small margin. In the 21st century sport scientists regularly investigate novel interventions which can aid training and performance in competition. Recent studies have included nitrate (186), bicarbonate (187), polyphenols, (243) and ischaemic preconditioning (IPC) (126), to the list of methods able to acutely influence exercise performance.

Several studies have shown that IPC improves sporting performance (see section 1.3.5.). Groot et al. observed that 3 IPC cycles of 5 minutes ischaemia and 5 minutes reperfusion cycles applied to each leg, improves intense exercise tolerance, resulting in an increased maximal power output of 1.6% and an increased maximal oxygen delivery ($\dot{V}_{O_2\ max}$) of 3% (126). IPC may also increase the time to exhaustion and maximal heart rate during a standardised cycling test (127). Another study has suggested that IPC can improve swimming performance over 100 m by 1% (128).

High-flow ischaemia and the subsequent resaturation known to occur during high-intensity exercise have been suggested as a model for low-flow ischaemia-reperfusion (IR) following arterial occlusion (see section 1.2.1.2). The mechanisms attributable to the improvement in exercise performance by IPC have been hypothesised, but this area of research remains in its infancy. Establishing the mechanisms by which IPC influences exercise could implicate the pathways conferred by IPC against IR injury in humans.

Based upon the evidence in chapter 5 that IPC protects the endothelium from IR injury, and published data showing that IPC can alter skeletal muscle function (244), the current study was designed to investigate whether IPC alters a number of physiological

parameters associated with incremental exercise. These principally included measurements of cardiorespiratory fitness, metabolic function and blood gases during exercise and recovery. In addition to the above skeletal muscle oxygenation was measured by near-infrared spectroscopy (NIRS) throughout. This study aimed to provide a mechanistic insight into the effects of IPC on incremental exercise, in addition to complementing results from other studies (126,127).

In summary, a randomised crossover study was designed to investigate the effects of local IPC on exercise physiology using an incremental cycling test.

8.2. Methods

8.2.1. Study participants

Twenty-one healthy male amateur club cyclists and triathletes were recruited for this study. The sample size was calculated using the expected change in $\dot{V}_{O_2\ max}$ (126), and the standard deviation of $\dot{V}_{O_2\ max}$ from preliminary data in our laboratory. Well-trained subjects were recruited due to their low thigh skinfold thicknesses to improve accuracy of NIRS measurement (see 2.4.5.3), and aid the applicability to elite athletes. Subject characteristics are described in Table 8.1.

Table 8.1 Exercise testing subject characteristics. Results are reported for 21 healthy male subject characteristics during the familiarisation study. Results are given as mean ± SD.

subject characteristics	mean	±	SD
age (years)	35.0	±	6.1
height (cm)	180.0	±	6.5
weight (kg)	75.4	±	7.7
body mass index (kg/m^2)	23.3	±	2.3
resting systolic blood pressure (mmHg)	134	±	12
resting diastolic blood pressure (mmHg)	80	±	8
resting heart rate (bpm)	60	±	7
sum of 7 skinfolds (mm)	75.4	±	32.7
front thigh skinfold (mm)	13.7	±	6.3
body fat (%)	13.3	±	7.6
$\dot{V}_{O_2\ max}$ (ml/min/kg)	64.0	±	9.0

8.2.2. Experimental set up and subject preparation

All experimental procedures were performed as described in detail in section 2.4. Subjects were prepared as outlined in section 2.4.2.

8.2.3. Experimental protocol

A schematic of the testing protocol is given in Figure 8.1. Subjects attended the laboratory in the British Olympic Medical Institute on three occasions. The first visit was a familiarisation study. The remaining two visits were experimental studies, either "preconditioning" or "sham" and performed in a random order. Subjects were not informed of the rationale behind the differences between the preconditioning and sham visits until the end of all testing.

8.2.3.1. Familiarisation study

Subjects were briefed and consented for the study. This was followed by baseline measurements of height, weight and blood pressure, and followed by baseline venous

and capillary blood samples. Blood samples were assessed for blood gases (pO_2, pCO_2, HCO_3^-), pH, lactate, electrolytes (Na^+, K^+, Ca^{2+}) and haemoglobin.

Subjects then rested in a supine position, the NIRS probe was applied to the thigh and the pressure required to occlude the femoral artery was obtained. Participants then performed an incremental exercise test on a cycle ergometer until physical exhaustion (see protocol in Figure 2.15). The exercise test started with 4 minutes of submaximal cycling at a power output of 150W at a constant, self-selected cadence (80-100 rpm). This was followed by cycling against an increasing resistance of 50 W/min increments until volitional exhaustion (T_{MAX}), as judged by an inability to maintain a cadence within 5 rpm of selected cadence despite encouragement. Oxygen delivery ($\dot{V}_{O_2}$), carbon dioxide elimination ($\dot{V}_{CO_2}$), ventilation (V_E), heart rate (HR), perceived exertion (RPE), power output (WR) and skeletal muscle oxygenation (StO_2) were measured continuously throughout the test.

Following T_{MAX} subjects stopped pedalling but remained stationary on the bike. A capillary sample was immediately taken to measure gases, lactate, and electrolytes. After 2 minutes subjects moved to lie supine on a couch. During recovery sequential measurements were made of blood pressure (at 1, 4, 10, 15, 20, 25 and 30 minutes post-T_{MAX}) and lactate (at 3, 4.5, 15 and 30 minutes post-T_{MAX}). In addition a venous blood sample was taken at 5 minutes of recovery to assess haemoglobin and haematocrit. Heart rate and respiratory measurements were continually measured for 30 minutes of recovery.

8.2.3.2. Experimental study

Subjects underwent baseline measurements and blood sampling. The NIRS probe was attached over the vastus lateralis, and cuffs were applied to the upper thigh of both legs. Cuffs were inflated 3 cycles of 5 minutes occlusion and recovery, with inflations

alternating between legs. Inflation pressures were suprasystolic for IPC (20 mmHg above occlusion pressure in the familiarisation study) and subdiastolic for sham study (20 mmHg below resting diastolic pressure) (see 2.4.4.2). Capillary and venous blood samples were taken immediately following cuff inflations and measured for lactate and haemoglobin. Subjects then performed the exercise test and subsequent recovery as described in the familiarisation study.

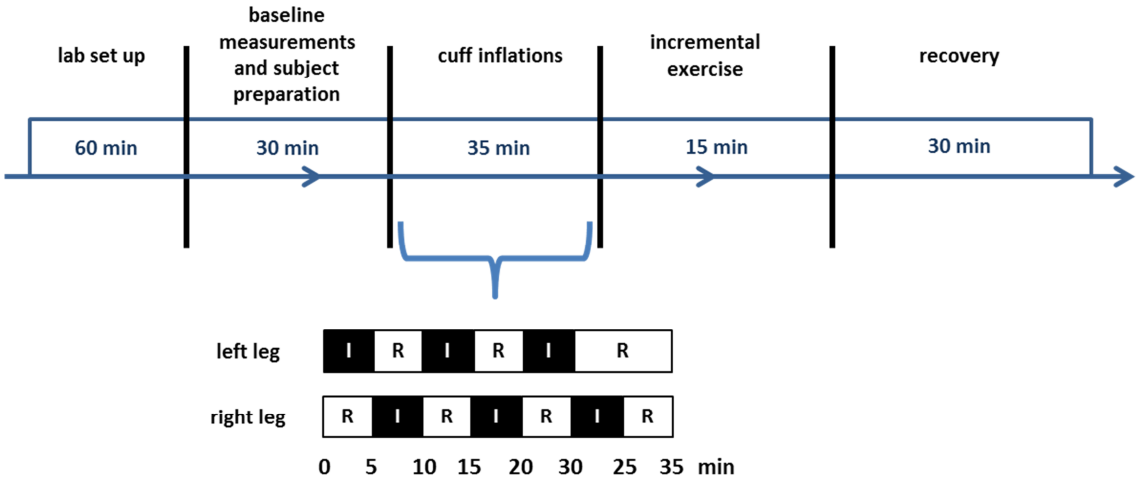

Figure 8.1 Schematic for experimental study. After one hour of laboratory set up, subjects attended the laboratory and underwent baseline measurements. This was followed by cuff inflation on the thigh: 3 cycles of 5 minutes occlusion followed by five minutes reperfusion, alternating legs. Cuff inflation was to a suprasystolic pressure for IPC, or a subdiastolic pressure for sham. This was followed by an incremental exercise protocol (see Figure 2.15), and subsequent recovery.

8.2.4. Statistical analysis

Submaximal results were calculated as the mean value attained over the final minute of pedalling at 150W (T_{SUBMAX}). HR $_{max}$ was calculated as the mean HR in the final 20 seconds prior to T_{MAX}. $\dot{V}_{O_2\,max}$, $\dot{V}_{CO_2\,max}$ and $\dot{V}_{E\,max}$ were estimated by extrapolation from submaximal values. StO_2 and THI are expressed as percentage change from baseline, and were measured prior to and at the end of each cuff inflation, immediately before

starting exercise, at 10% increments (deciles) between T_{SUBMAX} and T_{MAX}, and at 0.5, 1 and 5 minutes of recovery. Differences between the IPC and sham trials at specific time points were assessed using paired *t* tests. Differences in StO_2, blood pressure and lactate during cuff inflations, exercise testing and recovery were assessed using 2-way ANOVA, accounting for time and treatment.

Complete data sets were achieved in all subjects for time to exhaustion (TTE), WR_{max} and StO_2/THI. A high percentage of data points were complete for the other variables: heart rate (60/63, 95.2%), iSTAT (109/126, 86.5%), lactates (454/483, 94.0%), blood pressures (488/504, 96.8%), and haemoglobin (161/168, 95.8%). In cases of missing data, multiple imputations were applied as others have used (245), according to the multiple imputation function in SPSS (IBM SPSS® statistics version 20, IBM, USA). Data were assumed missing at random, and 5 imputations were applied to all data, with pooled results used for subsequent statistics. $p < 0.05$ was deemed statistically significant.

8.3. Results

Participants completed all exercise protocols with no adverse events. First are described the changes in StO_2 during IPC and sham cuff inflations, and during exercise. Secondly full physiological results are reported for T_{SUBMAX} and T_{MAX}, and finally for measurements observed during recovery.

8.3.1. Skeletal muscle oxygenation is decreased during the ischaemic preconditioning protocol

Cuff inflations caused a reduction in StO_2, and reductions were more profound during IPC than sham cuff inflations (IPC, 55 ± 10%; sham, 79 ± 5%; n = 21, two-way ANOVA, $p < 0.0001$; Figure 8.2A). IPC reduced THI, whereas THI was increased by

sham cuff inflations (IPC, 93 ± 29%; sham, 122 ± 15%, two-way ANOVA, $p = 0.002$; Figure 8.2B). Lactate assessed at the end of the three cuff inflation cycles was increased following IPC compared to sham (IPC, 1.4 ± 0.6 mmol/l; sham 1.0 ± 0.4 mmol/l; n = 21, paired *t* test, $p = 0.014$, Figure 8.2C).

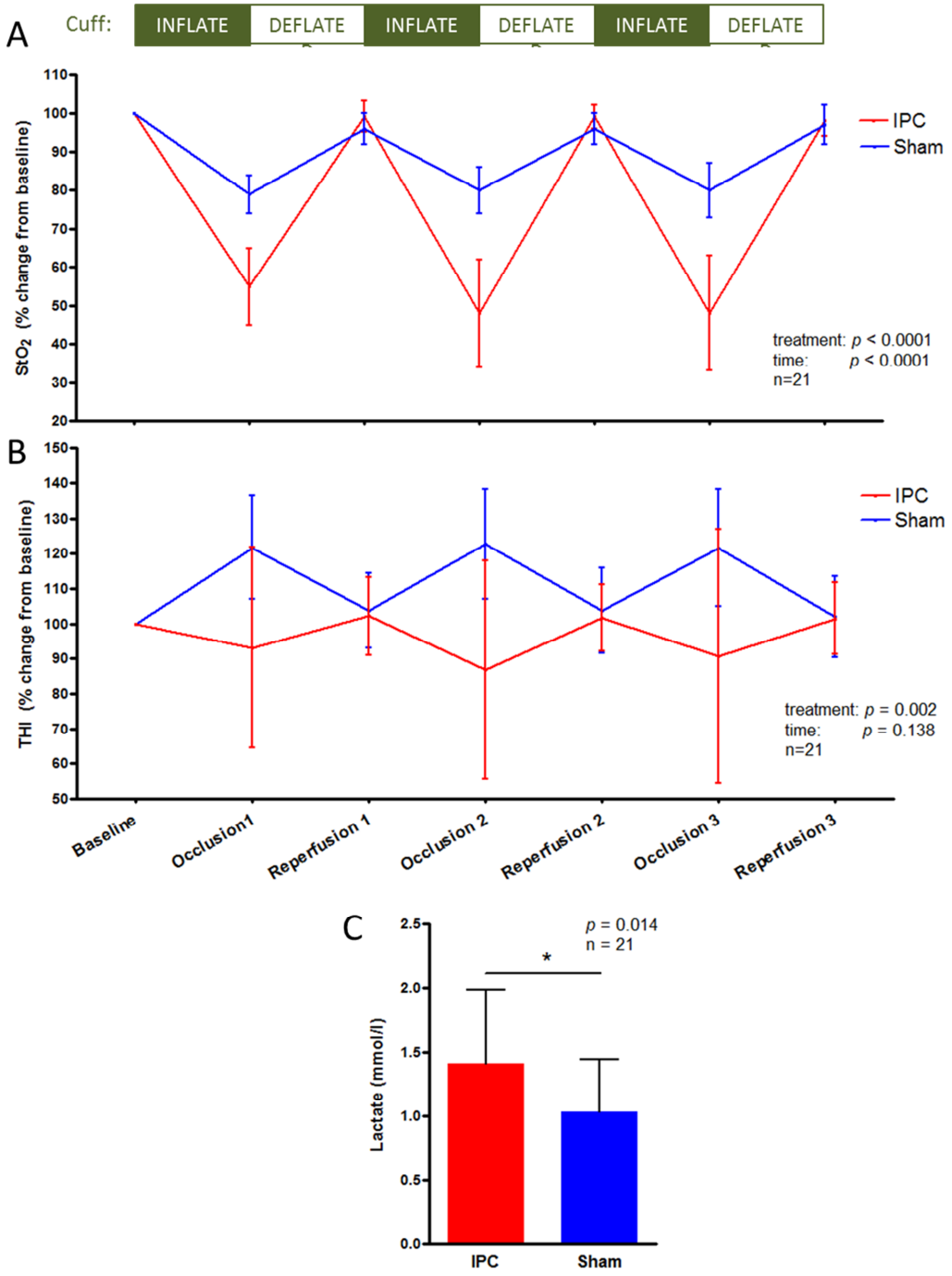

Figure 8.2 Effect of ischaemic preconditioning on skeletal muscle oxygenation and circulating lactate during cuff inflations. 21 healthy male subjects attended the laboratory on three occasions. On the IPC and sham visits, subjects received intermittent cuff inflations to either suprasystolic or subdiastolic pressures respectively. IPC caused a greater reduction in oxygenation than sham (A). IPC caused a small reduction in THI, whereas sham inflations caused an increase in THI (B). IPC increased circulating lactate concentration (C). Red lines/bar show IPC, blue lines/bar show sham results. StO_2 and THI were calculated as the percentage change from baseline (%). Results are presented as mean ± SD. * , $p < 0.05$.

8.3.2. Ischaemic preconditioning improves skeletal muscle oxygenation during exercise

IPC had no overall effect on StO_2 (n = 21, two way ANOVA, p = 0.44, Figure 8.3A). However, closer examination of specific time points observed that IPC improved exercise during the submaximal, aerobic phase of exercise and during the immediate recovery. At the 1st decile (10%) between T_{SUBMAX} and T_{MAX}, StO_2 was greater in the IPC group than the sham group (IPC, 89 ± 8%; sham 84 ± 9%; n = 21, paired t test, p = 0.034, Figure 8.3B). There was no difference at T_{MAX} (IPC, 51 ± 15%; sham, 51 ± 13%; n = 21, paired t test, p = 0.923, Figure 8.3C). IPC improved reoxygenation during the initial 30 seconds of recovery with subjects at rest (IPC, 90 ± 14%; sham, 84 ± 12%; n = 21, paired t test, p = 0.013, Figure 8.3D).

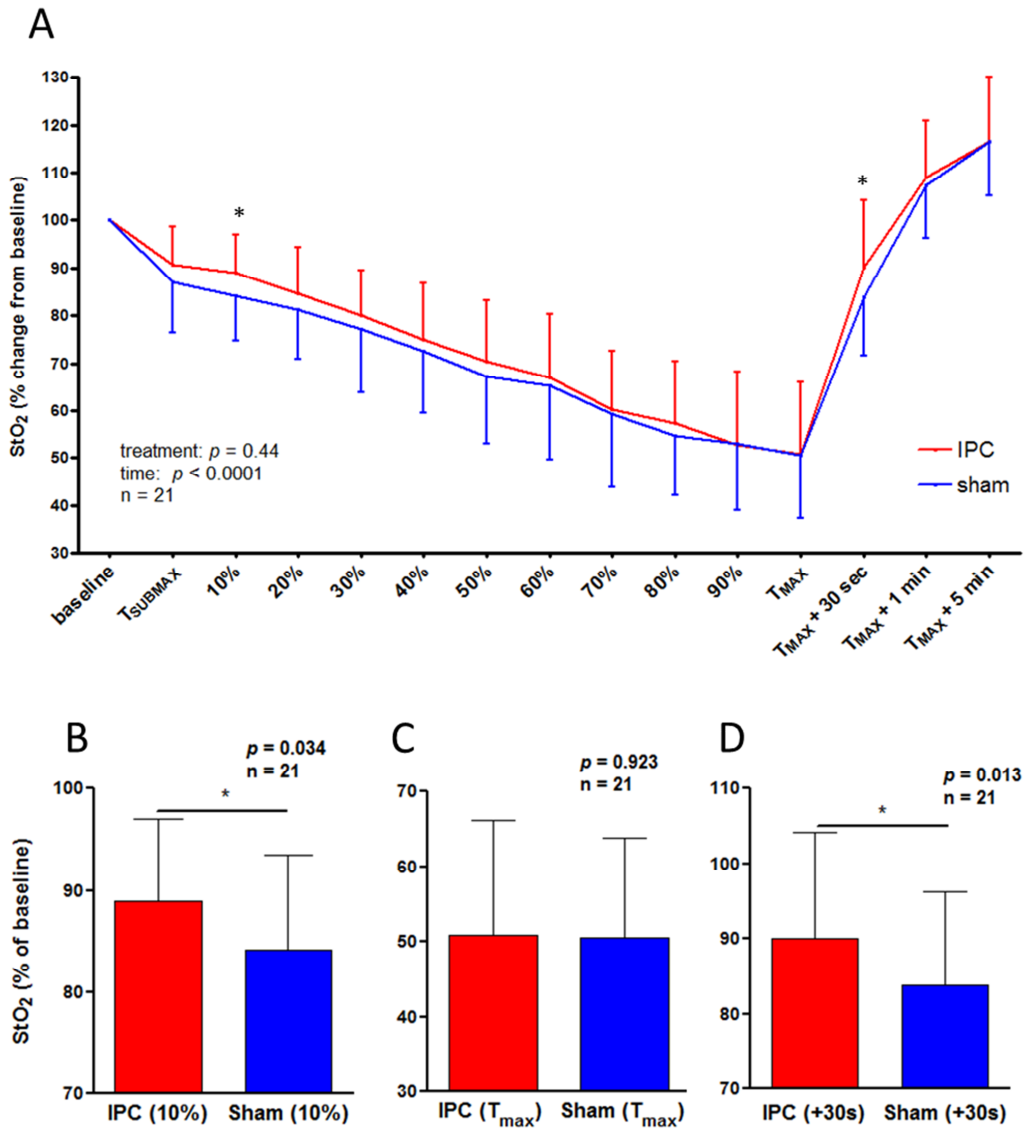

Figure 8.3 Effect of ischaemic preconditioning on skeletal muscle oxygenation during exercise. 21 healthy male subjects attended the laboratory on three occasions. On the IPC and sham visits, subjects received intermittent cuff inflations to a suprasystolic or subdiastolic pressure respectively. Following cuff inflations subjects performed an incremental exercise test to physical exhaustion, with StO_2 recorded throughout. IPC tended towards preserving StO_2 during exercise and recovery (A). A difference was evident during the early aerobic phase of exercise (B), but no difference existed at maximal exercise (C). IPC improved reoxygenation during recovery (D). Graphs show mean and SD. * , $p < 0.05$.

8.3.3. Ischaemic preconditioning has no effect on cardiorespiratory factors and perceived exertion during submaximal exercise

There were no differences in cardiorespiratory parameters between IPC and sham for at T_{SUBMAX} (n = 21, paired *t* test, $p > 0.05$, Figure 8.4).

	Preliminary	IPC	Sham	IPC vs Sham
	mean ± SD	mean ± SD	mean ± SD	*p* value
$\dot{V}_{O2}$ (ml / min)	2199 ± 221	2134 ± 144	2177 ± 258	0.275
$\dot{V}_{CO2}$ (ml / min)	1986 ± 256	1975 ± 227	1990 ± 274	0.723
$\dot{V}_{E}$ (l / min)	51.5 ± 7.9	50.9 ± 8.0	51.5 ± 8.9	0.530
HR (bpm)	124 ± 13	121 ± 14	121 ± 13	0.862
Lactate (mmol/l)	2.1 ± 0.7	2.1 ± 0.6	2.1 ± 0.8	0.848
StO_2 (% baseline)	86 ± 7	91 ± 8	87 ± 10	0.092
RPE (OMNI scale)	2 ± 1	2 ± 1	2 ± 1	0.666

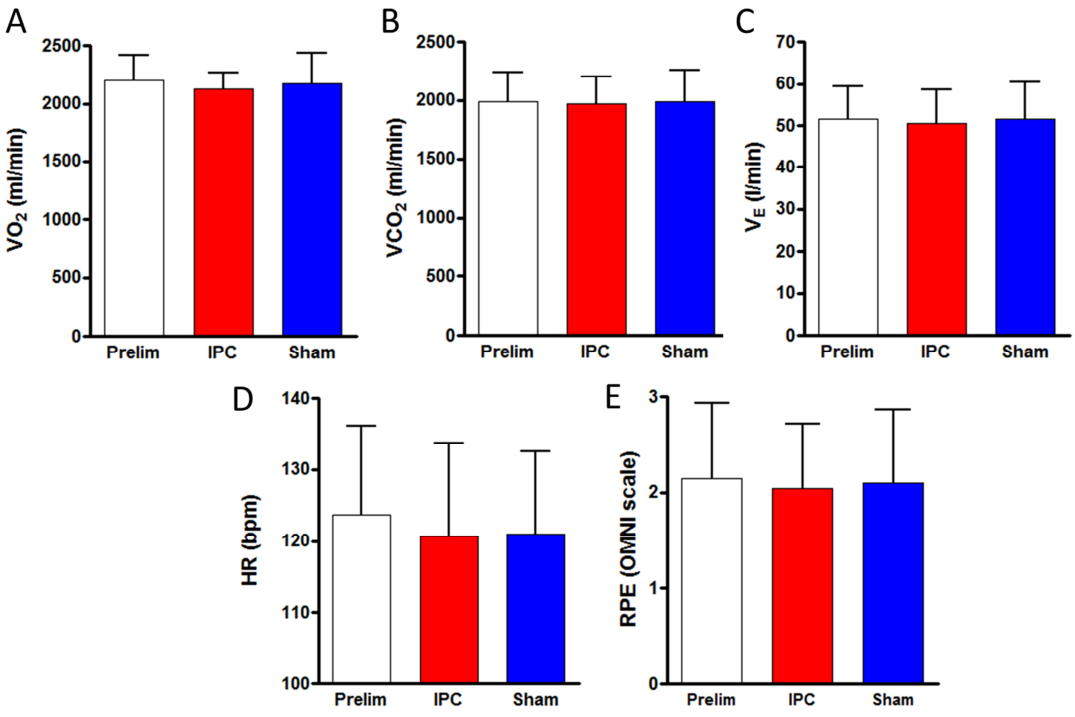

Figure 8.4 Effect of ischaemic preconditioning on respiratory parameters during submaximal exercise. 21 healthy male subjects attended the laboratory on three occasions. Following cuff inflations subjects performed an incremental exercise test to physical exhaustion, with respiratory parameters measured throughout. Table summarises results calculated at T_{submax}. Bars show the mean and SD from the familiarisation (white), IPC (red) and sham (blue) studies. There was no difference between IPC and sham for $\dot{V}_{O_2}$ (A), $\dot{V}_{CO_2}$ (B), $\dot{V}_{E}$ (C), HR (D), lactate, and RPE (E).

8.3.4. Ischaemic preconditioning has no effect on cardiorespiratory factors, perceived exertion or blood gases during maximal exercise

There were no differences in cardiorespiratory parameters or blood gases between IPC and sham at T_{MAX} (n = 21, paired *t* test, $p > 0.05$, Figure 8.5, Table 8.2).

	Preliminary	IPC	Sham	IPC vs Sham
	mean ± SD	mean ± SD	mean ± SD	*p* value
$\dot{V}_{O2}$ (ml / min)	4827 ± 675	4504 ± 652	4675 ± 778	0.211
$\dot{V}_{CO2}$ (ml / min)	5472 ± 669	5540 ± 838	5478 ± 791	0.530
$\dot{V}_{E}$ (l / min)	211.5 ± 34.0	213.7 ± 31.1	214.5 ± 32.8	0.686
HR (bpm)	178 ± 7	180 ± 12	178 ± 10	0.302
Lactate (mmol/l)	8.3 ± 2.9	7.6 ± 2.4	7.9 ± 2.7	0.526
StO_2 (% baseline)	47 ± 15	51 ± 15	51 ± 13	0.922
RPE (OMNI scale)	8 ± 2	8 ± 2	8 ± 2	0.566
TTE (s)	565 ± 45	570 ± 42	569 ± 45	0.523

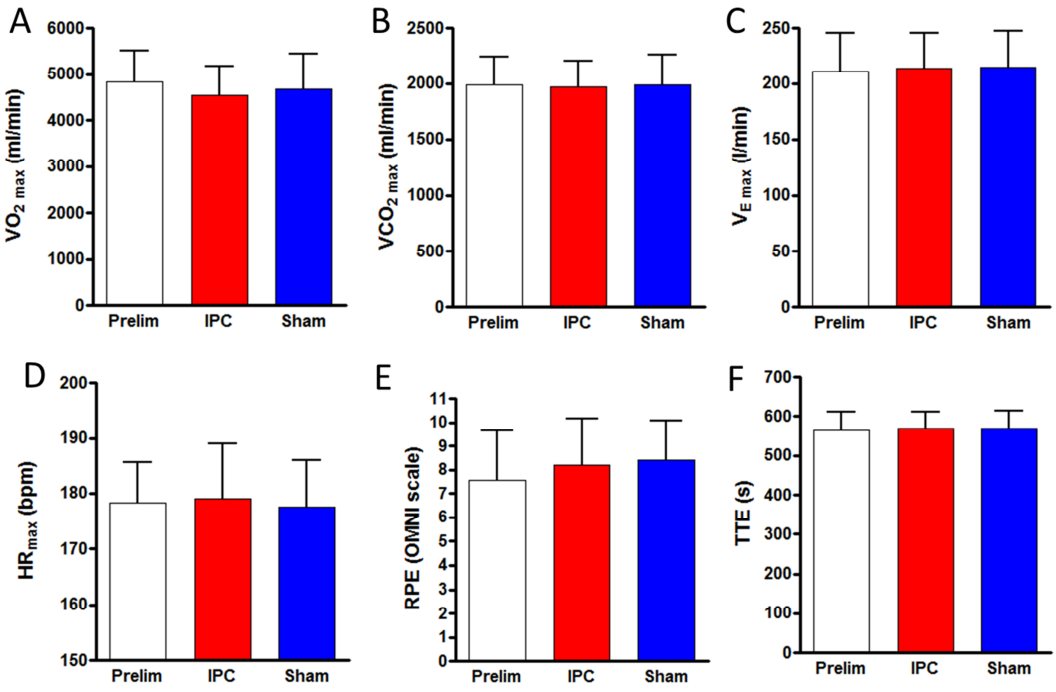

Figure 8.5 Effect of ischaemic preconditioning on physiological parameters at maximal exercise. 21 healthy male subjects attended the laboratory on three occasions. Following cuff inflations, subjects performed an incremental exercise test to physical exhaustion, with respiratory parameters measured throughout. Table summarises results calculated at T_{MAX}. Bars show the mean and SD from the familiarisation (white), IPC (red) and sham (blue) studies. There were no differences between IPC and sham for $\dot{V}_{O_2}$ (A), $\dot{V}_{CO_2}$ (B), $\dot{V}_{E}$ (C), HR (D), lactate, StO_2, RPE (E) and TTE (F).

Table 8.2 Effect of ischaemic preconditioning on blood gas and electrolytes during incremental exercise. 21 healthy male subjects attended the laboratory on three occasions. Following cuff inflations subjects performed an incremental exercise test to physical exhaustion, with respiratory parameters measured throughout. Table summarises results from capillary and venous blood samples taken at baseline and immediately following peak exercise. Exercise alone caused a decrease in pH, HCO_3^-, BE, TCO_2, SO_2, and an increase in pO_2, Na^+, K^+, Ca^{2+}, haemoglobin, haematocrit and lactate. There were no observed differences between IPC and sham. $p > 0.05$, n = 21.

	Familiarisation			IPC			sham			
	baseline	T_{MAX}	BL vs Ex	baseline	T_{MAX}	BL vs Ex	baseline	T_{MAX}	BL vs Ex	IPC vs sham
	mean ± s.d.	mean ± s.d.	*p* value	mean ± s.d.	mean ± s.d.	*p* value	mean ± s.d.	mean ± s.d.	*p* value	*p* value
pH	7.4 ± 0.1	7.2 ± 0.2	<0.001	7.4 ± 0.1	7.2 ± 0.2	< 0.001	7.4 ± 0.1	7.2 ± 0.2	< 0.001	0.759
pCO2 (kPa)	5.3 ± 0.4	5.2 ± 0.7	0.186	5.4 ± 0.3	5.4 ± 0.8	0.991	5.3 ± 0.3	5.3 ± 0.5	0.937	0.845
HCO3 (mEq/l)	26.0 ± 1.5	15.9 ± 2.4	< 0.001	26.1 ± 1.2	16.2 ± 3.1	< 0.001	26.0 ± 1.3	16.1 ± 2.2	< 0.001	0.508
BE (mmol/l)	2 ± 1	-12 ± 2	< 0.001	2 ± 1	-12 ± 3	< 0.001	2 ± 1	-12 ± 3	< 0.001	0.927
TCO2 (mmol/l)	27 ± 2	17 ± 2	< 0.001	27 ± 1	17 ± 3	< 0.001	27 ± 1	17 ± 2	< 0.001	0.711
pO2 (kPa)	9.3 ± 1.5	11.4 ± 2.9	< 0.001	9.3 ± 1.2	10.5 ± 2.2	0.005	9.8 ± 1.1	11.1 ± 2.8	0.032	0.379
sO2 (%)	94 ± 3	94 ± 3	0.878	94 ± 2	92 ± 4	0.028	95 ± 3	93 ± 4	0.073	0.661
Na^+ (mmol/l)	141 ± 2	144 ± 2	< 0.001	141 ± 2	144 ± 2	< 0.001	141 ± 1	144 ± 2	< 0.001	0.056
K^+ (mmol/l)	4.3 ± 0.3	5.7 ± 0.5	< 0.001	4.3 ± 0.3	5.5 ± 0.8	< 0.001	4.2 ± 0.2	5.6 ± 0.4	< 0.001	0.419
Ca^{2+} (mmol/l)	1.13 ± 0.75	1.18 ± 0.83	0.004	1.11 ± 0.04	1.16 ± 0.04	< 0.001	1.10 ± 0.04	1.16 ± 0.05	< 0.001	0.791
Glucose (mmol/l)	5.4 ± 3.6	6.0 ± 0.9	0.002	5.4 ± 0.4	5.9 ± 1.0	0.017	5.4 ± 0.4	6.0 ± 0.9	< 0.001	0.650
Haemoglobin (g/l)	150 ± 15	162 ± 11	< 0.001	141 ± 17	161 ± 11	< 0.001	141 ± 14	158 ± 11	< 0.001	0.559
Haematocrit (%)	45 ± 4	49 ± 3	< 0.001	42 ± 6	49 ± 3	< 0.001	41 ± 6	47 ± 4	< 0.001	0.479
Lactate (mmol/l)	0.9 ± 0.3	8.3 ± 2.8	< 0.001	0.9 ± 0.2	7.6 ± 2.4	< 0.001	0.8 ± 0.6	7.9 ± 2.7	< 0.001	0.992

8.3.5. Ischaemic preconditioning has no effect on lactate and blood pressure recovery following an incremental exercise test

Lactate and blood pressure were transiently increased during exercise and recovery, but there were no differences between IPC and sham (lactate, n = 21, two-way ANOVA, $p = 0.924$; systolic blood pressure, n = 21, two-way ANOVA, $p = 0.504$; diastolic blood pressure, n = 21, two-way ANOVA, $p = 0.658$; Figure 8.6).

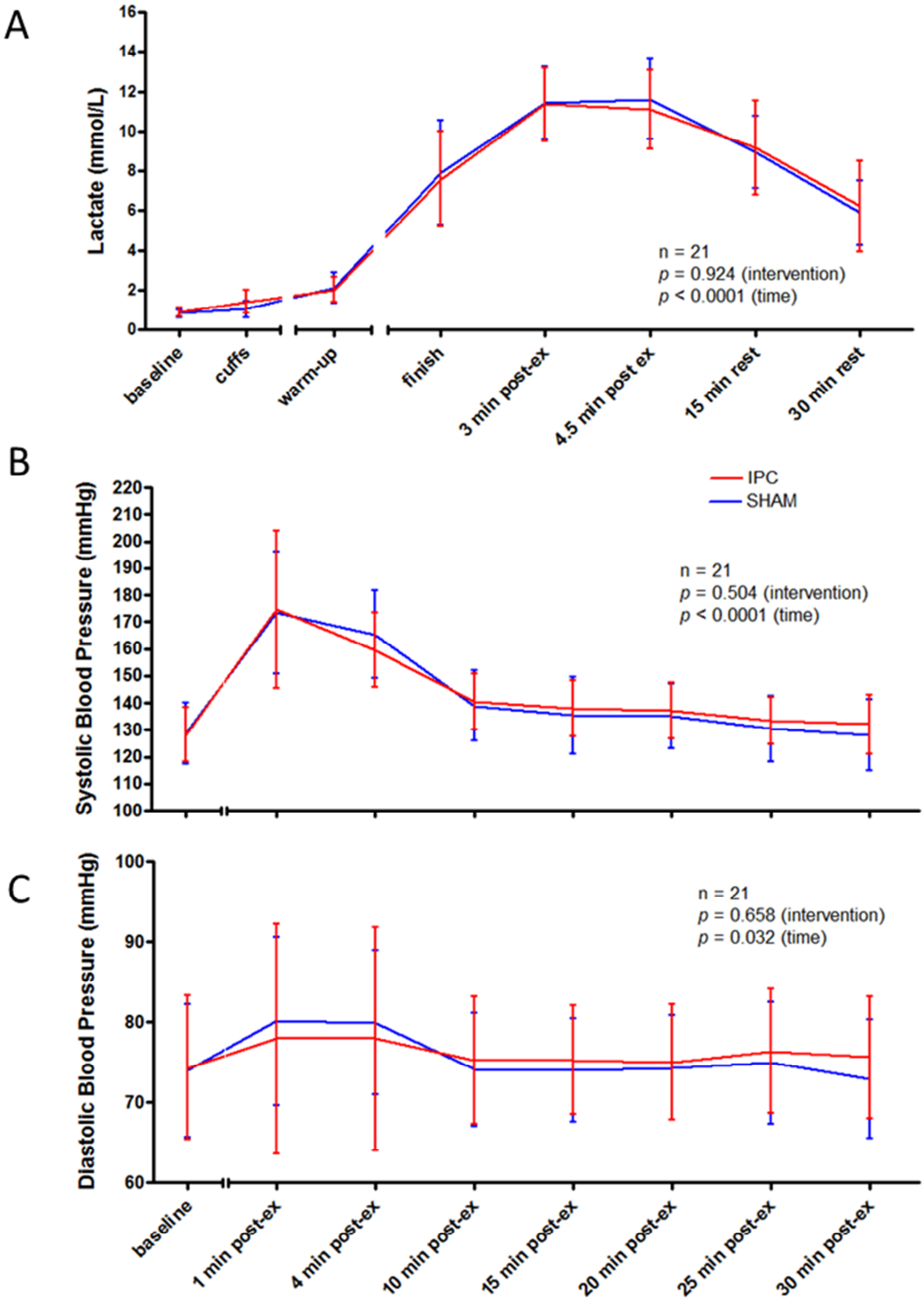

Figure 8.6 Lactate and blood pressure during recovery. 21 healthy male subjects attended the laboratory on three occasions. Following cuff inflations subjects performed an incremental exercise test to physical exhaustion, followed by recovery. Graphs summarise results for 30 minutes of recovery. Exercise caused an increase in lactate (A) systolic blood pressure (B) and diastolic blood pressure (C). There were no differences between IPC (red) and sham (blue). Lines represent group mean ± SD.

8.4. Discussion

8.4.1. Ischaemic preconditioning improves skeletal muscle oxygenation during aerobic exercise and resaturation

A substantial deoxygenation occurred during IPC (45%) as observed by NIRS, consistent with results made during arterial occlusion by others (198). Subdiastolic cuff inflation caused a small reduction in StO_2 (21%) and an increase in haemoglobin (22%), attributed to blood pooling within the interstitium, second to venous but not arterial occlusion (199). IPC improved skeletal muscle oxygenation by 6% during early aerobic exercise, but there was no difference at maximal exercise. This is a post hoc observation and requires demonstration in a validation cohort.

The reason for improved oxygenation during aerobic exercise is uncertain. In one of the seminal IPC papers, Murry et al. observed that IPC reduced cardiomyocyte ATP utilisation during early ischaemia, but differences were lost as ischaemia was prolonged, suggesting that IPC lowers ATP demand during early ischaemia (54). A similar effect has been identified in humans: an *in vitro* study suggested that aerobic metabolism of human skeletal muscle was improved by simulated IPC (246). These results suggest that IPC alters myocyte function at a molecular level to improve efficiency, and hence reduces requirement for oxygen extraction from capillaries. It is unlikely that IPC has any effect on anaerobic metabolism during exercise given that no difference in lactate production was observed in the current study, and others have reported that IPC has no effect on performance in an anaerobic exercise test (127).

IPC is now believed to be more closely associated with treating reperfusion over ischaemic injury (section 1.3.1). Indeed the current study showed an improved post-exercise tissue resaturation of 7% by IPC, consistent with results observed in animal studies (122). Saito et al. observed that IR injury induced by clamping of the abdominal

aorta and iliac artery in rats, impaired subsequent oxygen uptake within the musculature, assessed by an increase in half-resaturation time following stimulation gastrocnemius (122). IPC applied prior to IR injury prevented this impairment, suggesting that IPC improves the oxygen delivery pathway during reperfusion. Another study has shown by functional MRI that post-ischaemic phosphocreatine is increased by IPC in humans (124).

The mechanism of improved oxygenation resaturation can be attributed to either a reduced cellular oxygen uptake, or an improved oxygen delivery. Firstly, IPC is known to reduce the reperfusion-induced cellular reactive oxygen species (56), and if this is due to limiting oxidative phosphorylation, it is possible this may feedback to a reduced oxygen uptake, and subsequent increase in interstitial oxygen saturation. Further work is required on isolated human skeletal myocytes to investigate their response to reperfusion following IPC.

Alternatively the improved resaturation may be attributable to an increase in delivery. My results did not identify an increase in systemic oxygen delivery during submaximal or maximal exercise, however if IPC induced vasodilatation within the muscle vasculature this could increase blood flow. Increased flow will improve muscle oxygen saturation, given that resaturation time is positively correlated with the severity of arterial occlusion in patients with peripheral arterial disease (247). However the results in chapter 5, in conjunction with previous work (15), have shown that IPC improves endothelial response to IR in a manner that is independent of changes in vessel diameter. Further work is required to confirm this is the case during exercise.

The increase in reoxygenation due to IPC might be reflected in an improved post-ischaemic muscular function. Mattei et al. took groups of rats and either exposed them to 2.5 hours of hindlimb ischaemia, or ischaemia that was preceded by IPC (244). IPC

improved post-ischaemic function of both fast and slow-twitch muscle fibres. To investigate this in humans, specific testing can be performed to investigate changes in muscular force following limb IPC and IR.

8.4.2. Ischaemic preconditioning does not alter systemic physiological measures of performance

In the current study IPC had no effect on systemic cardiorespiratory outcomes, power output, or time to exhaustion. There were no differences between IPC and sham for $\dot{V}_{O_2}$, $\dot{V}_{CO_2}$, $\dot{V}_E$, RPE and HR during submaximal exercise, consistent with two previous studies (126,129). This suggests that despite an increased oxygenation, this did not reflect in a systemic improvement in metabolic efficiency. There were also no differences between IPC and sham at maximal exercise, in contrast with two previous studies (126,127). Groot et al. observed an increase in $\dot{V}_{O_2\ max}$ and WR $_{max}$ (126), and Crisafulli et al. observed an increase in WR $_{max}$, HR $_{max}$ and TTE (≈ 6%) (127). However in a similar study, Clevidence et al. recently did not observe an improvement in any physiological outcomes following IPC, other than a small change in submaximal heart rate (129).

There are several reasons which may account for differences. Firstly, whilst the current study was matched closely with Groot et al., some methodological difference did exist. The ramp protocol of my study was steeper (50 W/min) than the three other studies (20-30 W/min). Varying durations at which subjects were metabolising aerobically or anaerobically might alter the potential benefit from IPC, and as such it is possible that these differences did exist but were hidden by protocol design. Secondly, population differences may explain response to IPC. The current experiment consisted of well-trained, male subjects, unlike the mixed-sex population studied by Groot et al, and the physically active, but not trained population by Crisafulli et al. Finally it is possible that differences at maximal exercise may be attributable to subjective factors. As described

previously, maximal performance is dependent on both physical and mental attributes, and communication between athletes and investigators regarding the testing and the intervention might cause subjective bias. The aim in our investigation was to avoid bias by randomising between sham and IPC cuff inflations, and maintaining blinding by not discussing the rationale between high and low pressures until all visits were completed.

8.4.3. Study limitations

The results in this study might be attributable to IPC increasing muscle blood flow during exercise, however this could not be detected in the current protocol design. Proof of this requires additional investigations of flow such as by plethysmography. In addition, NIRS as a technique has several limitations. It is likely that there is some contribution to the signal by adipose tissue. However adipose tissue has a low blood flow in comparison to skeletal muscle, and the desaturations during brief cuff inflations closely match results from the thenar eminence (198). Furthermore the well-trained study population had low a skinfold thickness compared to a sample from the general population (75 ± 33 vs 123 ± 52 respectively; mean ± SD) (190), resulting in a haemoglobin index that was within the acceptable range, and consistent with muscle and not adipose tissue recordings. A general limitation of NIRS is the contribution to the results by myoglobin and cytochrome C, which requires further investigation to assess the contribution during exercise.

Despite an improvement in oxygenation, this was not reflected in an improvement in power output. Specific testing is required to identify whether IPC improves oxygen delivery or muscle efficiency and must be done using protocols that maintain blinding, to offset the effect of assessment bias on subjective outcomes. This could be achieved by greater analysis of $\dot{V}_{O_2}$ kinetics at a variety of exercise intensities, or by performing muscle biopsies to investigate myocytes function and mitochondrial activity. Whilst an

incremental exercise test is useful in detecting respiratory thresholds, ventilatory efficiency and $\dot{V}_{O_2\ max}$, there is only limited benefit in detecting exercise performance. Performance in specific exercise tasks is related to numerous factors, and whilst aerobic fitness is important, this does not account for techniques required to succeed in sport. Specific performance directed tests, such as time trials, may be required to further understand underlying processes and potential benefits of IPC. Furthermore, the study investigated a homogeneous population of young, trained males, and is it unknown whether the same effects would be observed in a group of elite athletes, in women, or of younger or older subjects. The exact IPC protocol necessary to induce an effect is also uncertain, and a dose-response study is required.

8.4.4. Application to clinical science and elite sport

The increase in oxygenation during exercise and recovery observed in the current study suggests that IPC modifies oxygenation during IR injury. Further studies are required to investigate whether local IPC improves oxygenation during experimental IR injury using the vascular model characterised in chapter 4. In addition it is important to assess whether this phenotype is observed in postconditioning and in remote ischaemic preconditioning. Further studies using the current model could assess this.

These results could be of value in elite sport. Jacobs et al. performed a detailed examination of physiological factors that contribute to time-trial performance in a group of highly-trained cyclists (248). They observed that two of the factors most closely associated with sustained power output during a cycling time trial included oxidative phosphorylation capacity of the vastus lateralis, and maximal leg oxygenation. Given this, an increase in oxygenation may improve sustained power output, despite being unable to improve TTE in the current incremental exercise study. Given that marginal

increases in performance can be the difference between success and failure in elite sport, an investigation of the effect of IPC on time trial performance may be of value. However, ischaemic cuff inflations as a method to improve performance should be viewed with skepticism at present. Association between StO_2 and power output may not mean that they are causal, and current results did not show an improvement in maximal power output during incremental exercise. Prospective studies are required to investigate whether muscle oxygenation is reflected in performance over varying exercise intensities. Furthermore, no evidence exists reporting the safety of repeated high pressure cuff inflations for athletes. Given the volume of muscle bulk being compressed at high pressure it is possible that tourniquet-induced neuromuscular damage could occur, and as with any intervention, rigorous safety checks are required.

8.5. Conclusion

This study is the first to show that IPC might increase skeletal muscle oxygenation during aerobic exercise and recovery but without a measureable increase in performance and in contradiction with some of the published literature. Further work is needed to understand the effects, if any, of IPC on exercise performance and the associated underlying mechanisms.

9. SUMMARY OF FINDINGS

This thesis has described four *in vivo* models of ischaemia-reperfusion, which facilitated investigations of the protective ischaemic preconditioning phenomenon. I first investigated the effect of RIPC on cerebral IR using a transient rodent stroke model. Secondly I characterised a human endothelial IR injury model, and investigated the protective effect of IPC, RIPC and ExPC upon this. Thirdly I characterised a human inflammatory blister model, and investigated the anti-inflammatory properties of IPC. Finally I investigated the effect of IPC on muscle oxygenation and metabolism during an incremental exercise test.

9.1. Remote ischaemic preconditioning as a treatment for cerebral ischaemia-reperfusion injury

Chapter 3 investigated rodent cerebral IR injury. Manipulation of the surgical and analysis techniques allowed for the definition of a robust, transient middle cerebral artery occlusion model. In this model RIPC reduced infarct size, but only when using inhaled anaesthesia. It was thus hypothesised that injectable anaesthesia inhibited RIPC, the mechanism of which has been speculated.

Evidence of neuroprotection by RIPC from the experimental results in this thesis complement findings in the literature (73,90), and suggest that RIPC could offer a therapeutic potential against human stroke. Recently Jensen et al. furthered this evidence by showing that RIPC can induce neuroprotection using a porcine model (249). Given that this phenomenon exists in two mammalian species, it is plausible that RIPC can protect the human brain from IR. Substantial interest in this has developed, and recently a phase I clinical trial reported acceptable safety of RIPC in subarachnoid haemorrhage, which indicates that larger trials will be undertaken to assess efficacy

(250). Further studies in this thesis aimed to investigate the efficacy of RIPC in a human IR injury model.

9.2. Ischaemic preconditioning as a treatment for IR injury in humans

Human *in vivo* models are often used as a bridge between animal studies and clinical trials, to validate efficacy and safety of novel therapies. Chapter 4 characterised an IR injury model, which our group has used for a number of years. Results demonstrated that L-FMC correlates with FMD, baseline diameter and the reduction in flow. This suggests that L-FMC might be an additional component of vascular function, complementing the work of others (154). Consistent with previous work, IR injury reduced flow mediated dilatation (FMD), and the novel finding was made that IR increases low-flow mediated constriction (L-FMC). Further experiments are required to reveal whether L-FMC is dependent on the endothelium, and how it could complement interventional or epidemiological studies.

In chapter 5 this model was then used to investigate IPC, RIPC and ExPC on human IR injury. RIPC did not protect the endothelium from IR injury, contradicting findings from previous studies (79,111). This inconsistency cannot be explained by results in this thesis alone, but raises questions as to the robustness of RIPC as a protective phenotype in humans. Whether or not RIPC attenuated IR injury in humans will depend on forthcoming results from randomised phase III clinical trials that are adequately powered to detect a clinically relevant effect (251).

In contrast to RIPC, IPC conferred protection in the brachial artery, yet this was not complemented by observations in the radial artery. This was attributed to variation in

the control of endothelial function between the two vessels. Additional chapters in this thesis explored mechanism of IPC using alternative *in vivo* models.

9.3. Ischaemic preconditioning and inflammation

Experimental data has speculated an anti-inflammatory role for IPC. Chapters 6 & 7 reported a study aimed at determining whether IPC can reduce leukocyte trafficking using an *in vivo* skin blister model. Chapter 6 characterised the blister model, and observed that from 24 to 72 hours there was a clearance of granulocytes, and an increase in three types of leukocyte that resembled myeloid-derived suppressor cells. Furthermore receptor expression indicated an increase in cell activation, and the possible adoption of a B cell phenotype by myeloid cells. These novel findings, in combination with previous work by our group (174), have also identified two resolution phenotypes in humans. Further work in this area aims to explore the function of myeloid derived suppressor cells within the 72 hour blister, and in particular whether they show specific suppressive features that contribute to the resolution of inflammation.

In chapter 7 this model was used to investigate the effects of aspirin and IPC on inflammation. Aspirin attenuated the inflammatory response, but only in subjects with an early resolver phenotype. There were no differences between control and IPC for leukocyte trafficking, or for cytokine release in the collective group or in each group of resolvers. The reported effects of IPC on leukocytes *in vitro*, were not replicated by observations *in vivo* (15,72), and therefore it is unlikely that IPC modulates the inflammatory response during IR. Further work aims to investigate whether IPC reduces systemic mediators of inflammation during human IR injury, and to explore the humoral and neural pathways of preconditioning in more depth.

9.4. Ischaemic preconditioning and muscle oxygenation during exercise

Chapter 8 investigated whether IPC can be used to alter skeletal muscle oxygenation and subsequent exercise performance in humans. This was achieved in a randomised cross-over trial, using an incremental exhaustive cycling test to investigate the effect of IPC on muscle oxygenation, the cardiorespiratory, and metabolic response. Results showed that muscle oxygen saturation was improved during aerobic low-intensity exercise and during recovery. This was however, not reflected in a modulation of other factors, either during submaximal or maximal exercise. However, given the discrepancies evident in the literature, this observation is unsurprising (126–129).

Further studies are required to understand how IPC influences oxygen delivery or utilisation in humans, and whether this is also the case during IR injury. It has been reported that muscle oxygenation is correlated with power output in a cycling time trial (248). Thus an IPC-induced increase in skeletal muscle oxygenation might improve a steady state power output. Further studies are required to investigate whether this exists by performing specific exercise tests that are more reflective on performance than an incremental test, such as a time trial.

9.5. Conclusion

This thesis has made novel investigations into the properties of ischaemic preconditioning in rodents and humans. It suggests that local, but not remote ischaemic preconditioning might offer potential therapy for the treatment of human ischaemia-reperfusion injury. The mechanism of ischaemic preconditioning in humans appears unlikely to be due to the inflammatory response, but may relate to modifications in oxygen supply and utilisation.

10. APPENDIX

10.1. Gating strategy for lymphocytes in venous blood.

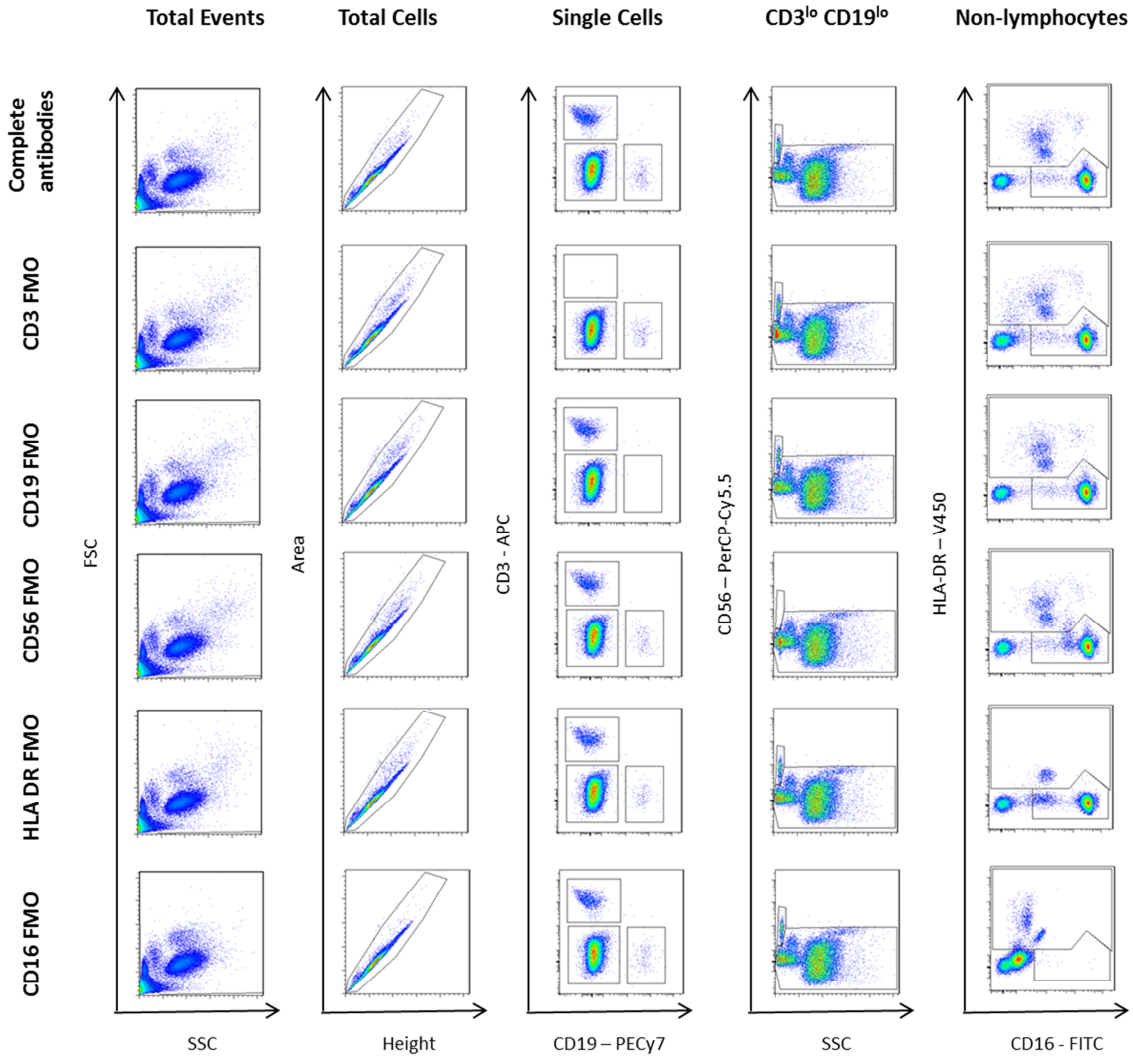

Figure 10.1 Lymphocyte gating strategy and fluorescence-minus-one controls for venous leukocytes. Firstly single cells were isolated by the forward scatter / side scatter, and then an area / height plot. Secondly T and B lymphocytes were isolated as CD3^{hi} and CD19^{hi} respectively, and then NK cells as CD56^{hi}. Remaining cells were separated into HLA-DR^{hi}, or HLA-DR^{lo} CD16$^{hi/dim}$. The remainder, mainly erythrocytes and debris were excluded.

10.2. Gating strategy for non-lymphocytes and natural killer cells in venous blood.

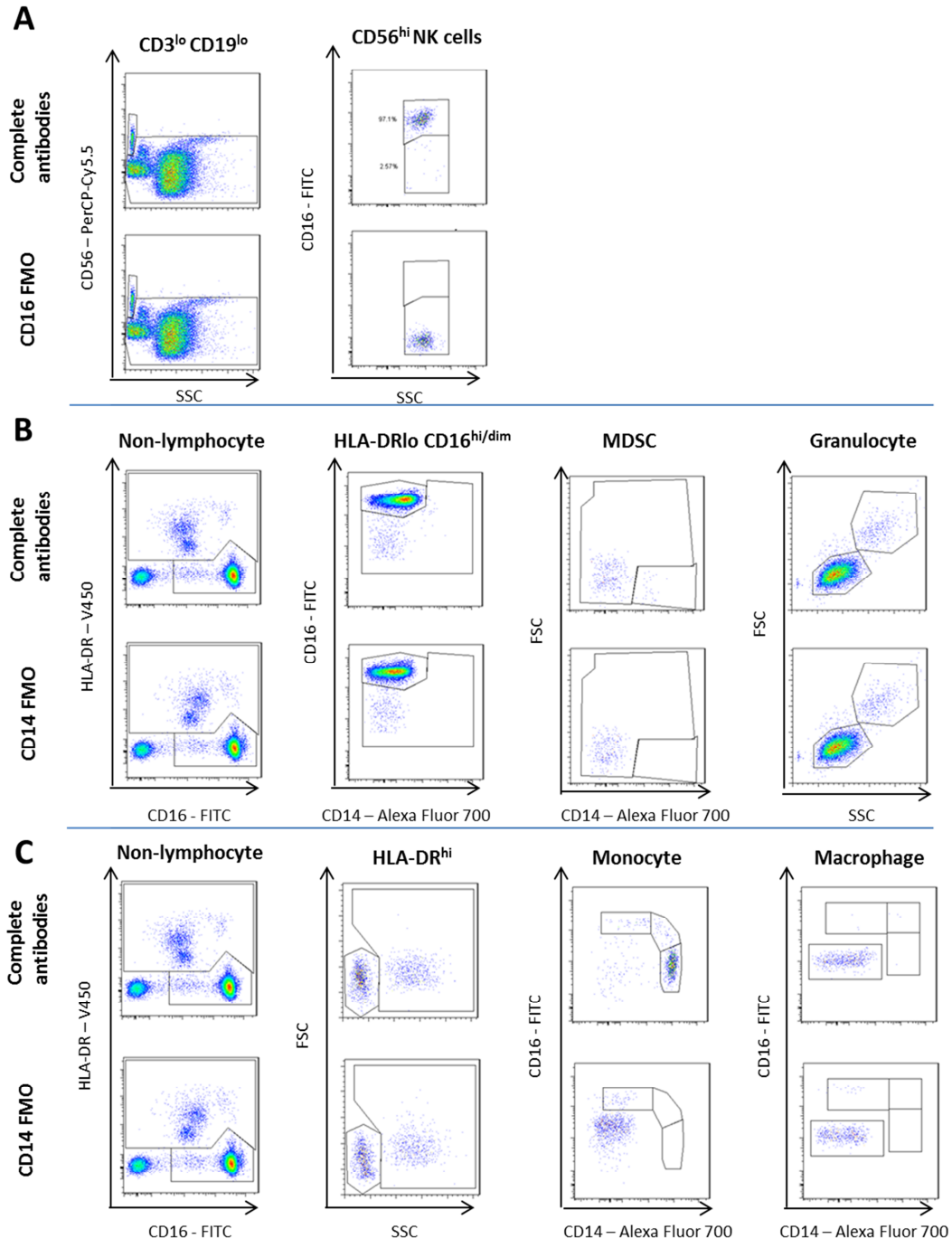

Figure 10.2 Non-lymphocyte and natural killer cell gating strategy and fluorescence-minus-one controls for venous leukocytes. Continuation from Figure 10.1. CD56^{hi} NK cells were differentiated into CD16^{hi} and CD16^{lo} cells (A). HLA-DR^{lo} CD16$^{hi/dim}$ cells were then differentiated into MDSCs (CD16^{dim}) and granulocytes (CD16^{hi} CD14^{lo}) (B). MDSCs were differentiated as FSC^{lo} CD14^{hi} and CD14$^{lo/dim}$. Granulocytes, were separated into neutrophils (FSC^{mid} SSC^{mid}) and eosinophils (FSC^{hi} SSC^{hi}). HLA-DR^{hi} cells were differentiated into monocytes (FSC$^{lo/mid}$ SSC^{lo}) and macrophages (remainder) and then by expression of CD14 and CD16 (C).

10.3. Gating strategy for lymphocytes in 24 hr blisters.

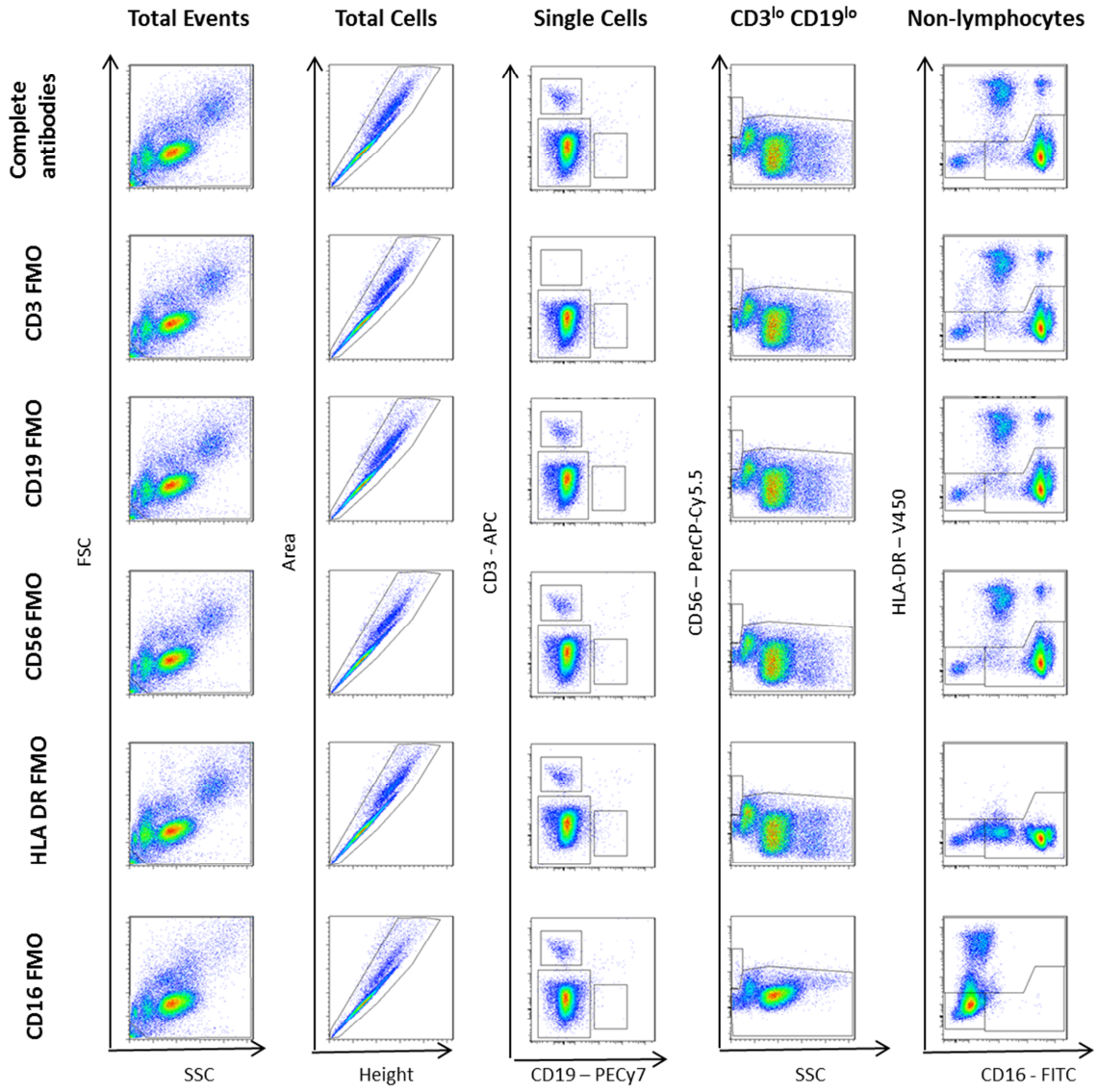

Figure 10.3 Lymphocyte gating strategy and fluorescence-minus-one controls for 24 hour blister leukocytes. Firstly single cells were isolated by the forward scatter / side scatter, and then an area / height plot. Secondly T and B lymphocytes were isolated as $CD3^{hi}$ and $CD19^{hi}$ respectively, and then NK cells as $CD56^{hi}$. Remaining cells were separated as HLA-DR^{hi}, or HLA-DR^{lo} $CD16^{hi/dim}$. The remainder, mainly erythrocytes and debris were excluded.

10.4. Gating strategy for non-lymphocytes and natural killer cells in 24 hr blisters.

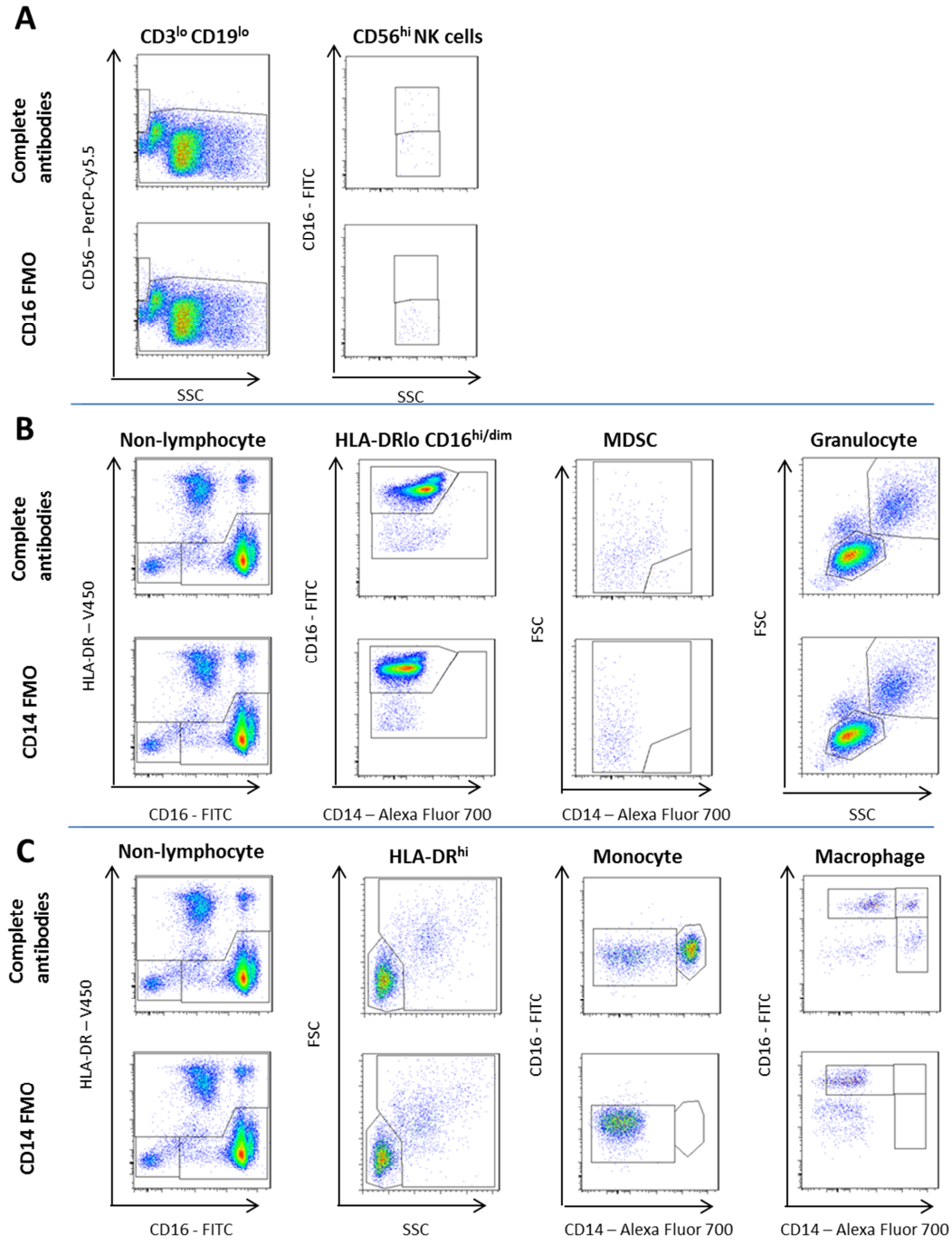

Figure 10.4 Non-lymphocyte and natural killer cell gating strategy and fluorescence-minus-one controls for 24 hour blister leukocytes. Continuation from Figure 10.3. $CD56^{hi}$ NK cells were differentiated into $CD16^{hi}$ and $CD16^{lo}$ cells (A). HLA-DR^{lo} $CD16^{hi/dim}$ cells were then differentiated into MDSCs ($CD16^{dim}$) and granulocytes ($CD16^{hi}$ $CD14^{lo}$) (B). MDSCs were differentiated as FSC^{lo} $CD14^{hi}$ and $CD14^{lo/dim}$. Granulocytes, were separated into neutrophils (FSC^{mid} SSC^{mid}) and eosinophils (FSC^{hi} SSC^{hi}). HLA-DR^{hi} cells were differentiated into monocytes ($FSC^{lo/mid}$ SSC^{lo}) and macrophages (remainder) and then by expression of CD14 and CD16 (C).

PUBLICATIONS

Review

Jenner WJ and Gilroy DW. Assessment of leukocyte trafficking in humans using the cantharidin blister model. JRSM Cardiovascular Disease. 2012; 1(1), 1-5

Abstracts

Jenner WJ, Gyori A, Fallan C, Cunniffe B, Montgomery H, MacAllister RJ, Cardinale M. The effects of ischemic preconditioning on skeletal muscle deoxygenation during an exhaustive cycling test. European College of Sport Science Congress. Bruges - Belgium, July 2012

Jenner WJ, Rayner CS, Okorie MI, Loukogeorgakis SP, MacAllister RJ. Ischaemia-reperfusion injury increases low-flow mediated constriction in humans. UCL Experimental Medicine Symposium 2011, London – UK, 24th May 2011

REFERENCES

1. Lloyd-Jones D, Adams RJ, Brown TM, Carnethon M, Dai S, De Simone G, et al. Heart disease and stroke statistics--2010 update: a report from the American Heart Association. Circulation. 2010;121(7):46–215.

2. British Heart Foundation. Mortality from Coronary Heart Disease Statistics. 2010;

3. British Heart Foundation. Morbidity from Coronary Heart Disease Statistics. 2010;

4. Yellon DM, Hausenloy DJ. Myocardial reperfusion injury. New Engl J Med. 2007;357(11):1121.

5. Murry CE, Jennings RB, Reimer KA. Preconditioning with ischemia: a delay of lethal cell injury in ischemic myocardium. Circulation. 1986;74(5):1124.

6. Przyklenk K, Bauer B, Ovize M, Kloner RA, Whittaker P. Regional ischemic preconditioning protects remote virgin myocardium from subsequent sustained coronary occlusion. Circulation. 1993;87(3):893.

7. Walsh SR, Tang TY, Kullar P, Jenkins DP, Dutka DP, Gaunt ME. Ischaemic preconditioning during cardiac surgery: systematic review and meta-analysis of perioperative outcomes in randomised clinical trials. Eur J Cardiothorac Surg. 2008;34(5):985.

8. Ludman AJ, Yellon DM, Hausenloy DJ. Cardiac preconditioning for ischaemia: lost in translation. Disease Models & Mechanisms. 2010 Jan;3(1-2):35–8.

9. Jennings RB, Reimer KA. Factors involved in salvaging ischemic myocardium: effect of reperfusion of arterial blood. Circulation. 1983;68(2 Pt 2):25–36.

10. Jennings RB, Reimer KA. The cell biology of acute myocardial ischemia. Annu. Rev. Med. 1991;42:225–46.

11. Jennings RB, Reimer KA, Hill ML, Mayer SE. Total ischemia in dog hearts, in vitro. Comparison of high energy phosphate production, utilization, and depletion, and of adenine nucleotide catabolism in total ischemia in vitro vs. severe ischemia in vivo. Circ. Res. 1981;49(4):892–900.

12. Kübler W, Spieckermann PG. Regulation of glycolysis in the ischemic and the anoxic myocardium. J Mol Cell Cardiol. 1970;1(4):351–77.

13. Shao Q, Matsubara T, Bhatt SK, Dhalla NS. Inhibition of cardiac sarcolemma Na+/K+ ATPase by oxyradical generating systems. Mol. Cell. Biochem. 1995;147(1):139–44.

14. Tani M, Neely JR. Na+ accumulation increases Ca2+ overload and impairs function in anoxic rat heart. J. Mol. Cell. Cardiol. 1990;22(1):57–72.

15. Kharbanda RK, Peters M, Walton B, Kattenhorn M, Mullen M, Klein N, et al. Ischemic preconditioning prevents endothelial injury and systemic neutrophil activation during ischemia-reperfusion in humans in vivo. Circulation. 2001;103(12):1624–30.

16. Carden DL, Granger DN. Pathophysiology of ischaemia-reperfusion injury. J Pathol. 2000;190(3):255–66.

17. Niccoli G, Burzotta F, Galiuto L, Crea F. Myocardial no-reflow in humans. J. Am. Coll. Cardiol. 2009;54(4):281–92.

18. Mergenthaler P, Dirnagl U, Meisel A. Pathophysiology of stroke: lessons from animal models. Metab Brain Dis. 2004;19(3):151–67.

19. Meldrum B, Evans M, Griffiths T, Simon R. Ischaemic Brain Damage: The Role of Excitatory Activity and of Calcium Entry. Br. J. Anaesth. 1985;57(1):44–6.

20. Wasserman K, Hansen JE, Sue DY, Stringer WW, Whipp BJ. Principles of Exercise Testing and Interpretation. Philadelphia, PA: Lipincott Williams and Wilkins; 2005.

21. Place N, Yamada T, Bruton J, Westerblad H. Muscle fatigue: from observations in humans to underlying mechanisms studied in intact single muscle fibres. Eur J Appl Physiol. 2010;110(1):1–15.

22. Wagner PD. New ideas on limitations to VO2max. Exerc Sport Sci Rev. 2000;28(1):10–4.

23. Jennings RB, Sommers HM, Smyth GA, Flack HA, Linn H. Myocardial necrosis induced by temporary occlusion of a coronary artery in the dog. Arch Pathol. 1960;70:68–78.

24. Zhao Z-Q, Corvera JS, Halkos ME, Kerendi F, Wang N-P, Guyton RA, et al. Inhibition of myocardial injury by ischemic postconditioning during reperfusion: comparison with ischemic preconditioning. Am. J. Physiol. Heart Circ. Physiol. 2003;285(2):579–88.

25. Kolh P, Danchin N, Di Mario C, Falk V, Folliguet T, Garg S, et al. Guidelines on myocardial revascularization: The Task Force on Myocardial Revascularization of the European Society of Cardiology (ESC) and the European Association for Cardio-Thoracic Surgery (EACTS). Eur Heart J. 2010;31(20):2501–55.

26. Piot C, Croisille P, Staat P, Thibault H, Rioufol G, Mewton N, et al. Effect of cyclosporine on reperfusion injury in acute myocardial infarction. N Engl J Med. 2008;359(5):473.

27. Bates E, Bode C, Costa M, Gibson CM, Granger C, Green C, et al. Intracoronary KAI-9803 as an adjunct to primary percutaneous coronary intervention for acute ST-segment elevation myocardial infarction. Circulation. 2008;117(7):886–96.

28. Ibanez B, Fuster V, Jiménez-Borreguero J, Badimon JJ. Lethal myocardial reperfusion injury: A necessary evil? Int. J. Cardiol. 2011;151(1):3–11.

29. Coetzee WA, Opie LH. Effects of oxygen free radicals on isolated cardiac myocytes from guinea-pig ventricle: electrophysiological studies. J. Mol. Cell. Cardiol. 1992;24(6):651–63.

30. Bell RM, Yellon DM. There is More to Life than Revascularization: Therapeutic Targeting of Myocardial Ischemia/Reperfusion Injury. Cardiovasc Ther. 2011;29(6):67–79.

31. Halestrap AP, Connern CP, Griffiths EJ, Kerr PM. Cyclosporin A binding to mitochondrial cyclophilin inhibits the permeability transition pore and protects hearts from ischaemia/reperfusion injury. Mol. Cell. Biochem. 1997;174(1-2):167–72.

32. Mocanu MM, Baxter GF, Yellon DM. Caspase inhibition and limitation of myocardial infarct size: protection against lethal reperfusion injury. Br. J. Pharmacol. 2000;130(2):197–200.

33. Yan L, Vatner DE, Kim S-J, Ge H, Masurekar M, Massover WH, et al. Autophagy in chronically ischemic myocardium. Proc. Natl. Acad. Sci. U.S.A. 2005;102(39):107–12.

34. Kloner RA, Ganote CE, Jennings RB. The “no-reflow” phenomenon after temporary coronary occlusion in the dog. J. Clin. Invest. 1974;54(6):1496–508.

35. Elgebaly SA, Hashmi FH, Houser SL, Allam ME, Doyle K. Cardiac-derived neutrophil chemotactic factors: detection in coronary sinus effluents of patients undergoing myocardial revascularization. J. Thorac. Cardiovasc. Surg. 1992;103(5):952–9.

36. Vinten-Johansen J. Involvement of neutrophils in the pathogenesis of lethal myocardial reperfusion injury. Cardiovasc. Res. 2004;61(3):481–97.

37. Baines CP. How and When Do Myocytes Die During Ischemia and Reperfusion The Late Phase. J Cardiovasc Pharmacol Ther. 2011;16(3-4):239–43.

38. Kawaguchi M, Takahashi M, Hata T, Kashima Y, Usui F, Morimoto H, et al. Inflammasome Activation of Cardiac Fibroblasts Is Essential for Myocardial Ischemia/Reperfusion Injury. Circulation. 2011;123(6):594–604.

39. Pearson PJ, Schaff HV, Vanhoutte PM. Long-term impairment of endothelium-dependent relaxations to aggregating platelets after reperfusion injury in canine coronary arteries. Circulation. 1990;81(6):1921–7.

40. Quillen JE, Sellke FW, Brooks LA, Harrison DG. Ischemia-reperfusion impairs endothelium-dependent relaxation of coronary microvessels but does not affect large arteries. Circulation. 1990;82(2):586–94.

41. Kharbanda RK, Mortensen, U.M., White, P.A. Transient Limb Ischemia Induces Remote Ischemic Preconditioning In Vivo. Circulation. 2002;106(23):2881–3.

42. Horwitz LD, Kaufman D, Keller MW, Kong Y. Time course of coronary endothelial healing after injury due to ischemia and reperfusion. Circulation. 1994;90(5):2439–47.

43. Nakanishi K, Vinten-Johansen J, Lefer DJ, Zhao Z, Fowler WC 3rd, McGee DS, et al. Intracoronary L-arginine during reperfusion improves endothelial function and reduces infarct size. Am. J. Physiol. 1992;263(6):1650–8.

44. Ma XL, Tsao PS, Viehman GE, Lefer AM. Neutrophil-mediated vasoconstriction and endothelial dysfunction in low-flow perfusion-reperfused cat coronary artery. Circ. Res. 1991;69(1):95–106.

45. Tsao PS, Lefer AM. Time course and mechanism of endothelial dysfunction in isolated ischemic- and hypoxic-perfused rat hearts. Am. J. Physiol. 1990;259(6):1660–6.

46. Loukogeorgakis SP, van den Berg MJ, Sofat R, Nitsch D, Charakida M, Haiyee B, et al. Role of NADPH Oxidase in Endothelial Ischemia/Reperfusion Injury in Humans. Circulation. 2010;121(21):2310–6.

47. Nawashiro H, Martin D, Hallenbeck JM. Neuroprotective effects of TNF binding protein in focal cerebral ischemia. Brain Res. 1997;778(2):265–71.

48. Brouns R, De Deyn PP. The complexity of neurobiological processes in acute ischemic stroke. Clin Neurol Neurosurg. 2009;111(6):483–95.

49. Dutka TL, Verburg E, Larkins N, Hortemo KH, Lunde PK, Sejersted OM, et al. ROS-mediated decline in maximum Ca2+-activated force in rat skeletal muscle fibers following in vitro and in vivo stimulation. PLoS ONE. 2012;7(5):e35226.

50. Edwards RH, Hill DK, Jones DA, Merton PA. Fatigue of long duration in human skeletal muscle after exercise. J. Physiol. 1977;272(3):769–78.

51. Bruton JD, Place N, Yamada T, Silva JP, Andrade FH, Dahlstedt AJ, et al. Reactive oxygen species and fatigue-induced prolonged low-frequency force depression in skeletal muscle fibres of rats, mice and SOD2 overexpressing mice. J. Physiol. (Lond.). 2008;586(1):175–84.

52. Zeymer U, Suryapranata H, Monassier JP, Opolski G, Davies J, Rasmanis G, et al. The Na(+)/H(+) exchange inhibitor eniporide as an adjunct to early reperfusion therapy for acute myocardial infarction. Results of the evaluation of the safety and cardioprotective effects of eniporide in acute myocardial infarction (ESCAMI) trial. J. Am. Coll. Cardiol. 2001;38(6):1644–50.

53. Kitakaze M, Asakura M, Kim J, Shintani Y, Asanuma H, Hamasaki T, et al. Human atrial natriuretic peptide and nicorandil as adjuncts to reperfusion treatment for acute myocardial infarction (J-WIND): two randomised trials. Lancet. 2007;370(9597):1483–93.

54. Murry CE, Richard VJ, Reimer KA, Jennings RB. Ischemic preconditioning slows energy metabolism and delays ultrastructural damage during a sustained ischemic episode. Circ. Res. 1990;66(4):913–31.

55. Marber MS, Latchman DS, Walker JM, Yellon DM. Cardiac stress protein elevation 24 hours after brief ischemia or heat stress is associated with resistance to myocardial infarction. Circulation. 1993;88(3):1264–72.

56. Yang X, Cohen MV, Downey JM. Mechanism of cardioprotection by early ischemic preconditioning. Cardiovasc Drugs Ther. 2010;24(3):225–34.

57. Tsuchida A, Liu Y, Liu GS, Cohen MV, Downey JM. alpha 1-adrenergic agonists precondition rabbit ischemic myocardium independent of adenosine by direct activation of protein kinase C. Circ. Res. 1994;75(3):576–85.

58. Costa ADT, Garlid KD, West IC, Lincoln TM, Downey JM, Cohen MV, et al. Protein kinase G transmits the cardioprotective signal from cytosol to mitochondria. Circ. Res. 2005;97(4):329–36.

59. Hausenloy DJ, Tsang A, Yellon DM. The reperfusion injury salvage kinase pathway: a common target for both ischemic preconditioning and postconditioning. Trends Cardiovasc. Med. 2005;15(2):69–75.

60. Hausenloy DJ, Tsang A, Mocanu MM, Yellon DM. Ischemic preconditioning protects by activating prosurvival kinases at reperfusion. Am. J. Physiol. Heart Circ. Physiol. 2005;288(2):971–6.

61. Hausenloy DJ, Yellon DM. Reperfusion injury salvage kinase signalling: taking a RISK for cardioprotection. Heart Fail Rev. 2007;12(3-4):217–34.

62. Argaud L, Gateau-Roesch O, Augeul L, Couture-Lepetit E, Loufouat J, Gomez L, et al. Increased mitochondrial calcium coexists with decreased reperfusion injury in postconditioned (but not preconditioned) hearts. Am. J. Physiol. Heart Circ. Physiol. 2008;294(1):386–91.

63. Juhaszova M, Zorov DB, Yaniv Y, Nuss HB, Wang S, Sollott SJ. Role of glycogen synthase kinase-3beta in cardioprotection. Circ. Res. 2009;104(11):1240–52.

64. Burwell LS, Brookes PS. Mitochondria as a target for the cardioprotective effects of nitric oxide in ischemia-reperfusion injury. Antioxid. Redox Signal. 2008;10(3):579–99.

65. Sanada S, Komuro I, Kitakaze M. Pathophysiology of myocardial reperfusion injury: preconditioning, postconditioning, and translational aspects of protective measures. Am J Physiol Heart Circ Physiol. 2011;301(5):1723–41.

66. Szabó A, Varga R, Keresztes M, Vízler C, Németh I, Rázga Z, et al. Ischemic limb preconditioning downregulates systemic inflammatory activation. J. Orthop. Res. 2009;27(7):897–902.

67. Erling N Jr, Nakagawa NK, Costa Cruz JWM, Zanoni FL, Baptista-Silva JCC, Sannomiya P, et al. Microcirculatory effects of local and remote ischemic preconditioning in supraceliac aortic clamping. J. Vasc. Surg. 2010;52(5):1321–9.

68. Hartmann P, Varga R, Zobolyák Z, Héger J, Csosz B, Németh I, et al. Anti-inflammatory effects of limb ischaemic preconditioning are mediated by sensory

nerve activation in rats. Naunyn Schmiedebergs Arch. Pharmacol. 2011;383(2):179–89.

69. Weber C. Far from the heart: Receptor cross-talk in remote conditioning. Nat. Med. 2010;16(7):760–2.

70. Saxena P, Shaw OM, Misso NL, Naran A, Shehatha J, Newman MAJ, et al. Remote Ischemic Preconditioning Stimulus Decreases the Expression of Kinin Receptors in Human Neutrophils. J Surg Res. 2011;171(1):311–6.

71. Pedersen CM, Cruden NL, Schmidt MR, Lau C, Bøtker HE, Kharbanda RK, et al. Remote ischaemic preconditioning prevents systemic platelet activation associated with ischaemia-reperfusion injury in man. J Thromb Haemost. 2011;9(2):404–7.

72. Shimizu M, Saxena P, Konstantinov IE, Cherepanov V, Cheung MMH, Wearden P, et al. Remote ischemic preconditioning decreases adhesion and selectively modifies functional responses of human neutrophils. J. Surg. Res. 2010;158(1):155–61.

73. Ren C, Gao X, Steinberg GK, Zhao H. Limb remote-preconditioning protects against focal ischemia in rats and contradicts the dogma of therapeutic time windows for preconditioning. Neuroscience. 2008;151(4):1099–103.

74. Ates E, Genç E, Erkasap N, Erkasap S, Akman S, Firat P, et al. Renal protection by brief liver ischemia in rats1. Transplantation. 2002;74(9):1247.

75. Addison PD, Neligan PC, Ashrafpour H, Khan A, Zhong A, Moses M, et al. Noninvasive remote ischemic preconditioning for global protection of skeletal muscle against infarction. Am J Physiol Heart Circ Physiol. 2003;285(4):1435.

76. Abu-Amara M, Yang SY, Quaglia A, Rowley P, Tapuria N, Seifalian AM, et al. Effect of remote ischemic preconditioning on liver ischemia/reperfusion injury using a new mouse model. Liver Transpl. 2011;17(1):70–82.

77. Birnbaum Y, Hale SL, Kloner RA. Ischemic preconditioning at a distance: A reduction of myocardial infarct size by partial reduction of blood supply combined with rapid stimulation of the gastrocnemius muscle in the rabbit. Circulation. 1997;96(5):1641–6.

78. Heidbreder M, Naumann A, Tempel K, Dominiak P, Dendorfer A. Remote vs. ischaemic preconditioning: the differential role of mitogen-activated protein kinase pathways. Cardiovasc. Res. 2008;78(1):108–15.

79. Loukogeorgakis SP, Panagiotidou AT, Broadhead MW, Donald A, Deanfield JE, MacAllister RJ. Remote ischemic preconditioning provides early and late protection against endothelial ischemia-reperfusion injury in humans: role of the autonomic nervous system. J Am Coll Cardiol. 2005;46(3):450.

80. Mastitskaya S, Marina N, Gourine A, Gilbey MP, Spyer KM, Teschemacher AG, et al. Cardioprotection evoked by remote ischaemic preconditioning is critically dependent on the activity of vagal pre-ganglionic neurones. Cardiovasc Res. 2012;95(4):487–94.

81. Steensrud T, Li J, Dai X, Manlhiot C, Kharbanda R, Tropak MB, et al. Pretreatment with the nitric oxide donor SNAP or nerve transection blocks humoral preconditioning by remote limb ischemia or intra-arterial adenosine. Am J Physiol Heart Circ Physiol. 2010;299(5):1598–603.

82. Dickson EW, Reinhardt CP, Renzi FP, Becker RC, Porcaro WA, Heard SO. Ischemic preconditioning may be transferable via whole blood transfusion: preliminary evidence. J Thromb Thrombolys. 1999;8(2):123–9.

83. Shimizu M, Tropak M, Diaz RJ, Suto F, Surendra H, Kuzmin E, et al. Transient limb ischaemia remotely preconditions through a humoral mechanism acting directly on the myocardium: evidence suggesting cross-species protection. Clin. Sci. 2009;117(5):191–200.

84. Cai ZP, Parajuli N, Zheng X, Becker L. Remote ischemic preconditioning confers late protection against myocardial ischemia-reperfusion injury in mice by upregulating interleukin-10. Basic Res. Cardiol. 2012;107(4):277.

85. Brzozowski T, Konturek PC, Konturek SJ, Pajdo R, Kwiecien S, Pawlik M, et al. Ischemic preconditioning of remote organs attenuates gastric ischemia-reperfusion injury through involvement of prostaglandins and sensory nerves. Eur. J. Pharmacol. 2004;499(1-2):201–13.

86. Atochin DN, Clark J, Demchenko IT, Moskowitz MA, Huang PL. Rapid cerebral ischemic preconditioning in mice deficient in endothelial and neuronal nitric oxide synthases. Stroke. 2003;34(5):1299–303.

87. Belayev L, Ginsberg MD, Alonso OF, Singer JT, Zhao W, Busto R. Bilateral ischemic tolerance of rat hippocampus induced by prior unilateral transient focal ischemia: relationship to c-fos mRNA expression. Neuroreport. 1996;8(1):55.

88. Zhao H-G, Sun X-C, Xian X-H, Li W-B, Zhang M, Li Q-J. The role of nitric oxide in the neuroprotection of limb ischemic preconditioning in rats. Neurochem. Res. 2007;32(11):1919–26.

89. Mori T, Muramatsu H, Matsui T, McKee A, Asano T. Possible role of the superoxide anion in the development of neuronal tolerance following ischaemic preconditioning in rats. Neuropathol. Appl. Neurobiol. 2000;26(1):31–40.

90. Malhotra S, Naggar I, Stewart M, Rosenbaum DM. Neurogenic pathway mediated remote preconditioning protects the brain from transient focal ischemic injury. Brain Res. 2011;1386:184–90.

91. Lee CD, Folsom AR, Blair SN. Physical activity and stroke risk: a meta-analysis. Stroke. 2003;34(10):2475–81.

92. Morris JN, Pollard R, Everitt MG, Chave SPW, Semmence AM. Vigorous exercise in leisure-time: protection against coronary heart disease. Lancet. 1980;316(8206):1207–10.

93. McElroy CL, Gissen SA, Fishbein MC. Exercise-induced reduction in myocardial infarct size after coronary artery occlusion in the rat. Circulation. 1978;57(5):958.

94. Ding YH, Luan XD, Li J, Rafols JA, Guthinkonda M, Diaz FG, et al. Exercise-induced overexpression of angiogenic factors and reduction of ischemia/reperfusion injury in stroke. Curr Neurovasc Res. 2004;1(5):411–20.

95. Libonati JR. Sprint training improves postischemic, left ventricular diastolic performance. J Appl Physiol. 2005;99(6):2121–7.

96. Kavazis AN. Exercise Preconditioning of the Myocardium. Sports Med. 2009;39(11):923–35.

97. Powers SK, Quindry JC, Kavazis AN. Exercise-induced cardioprotection against myocardial ischemia-reperfusion injury. Free Radic. Biol. Med. 2008;44(2):193–201.

98. Demirel HA, Powers S, Zergeroglu, Murat A., Shanely, R. Andrew, Hamilton KL, Coombes, Jeff, et al. Short-term exercise improves myocardial tolerance to in vivo ischemia-reperfusion in the rat. J Appl Physiol. 2001;91(5):2205–12.

99. Domenech R, Macho P, Schwarze H, Sánchez G. Exercise induces early and late myocardial preconditioning in dogs. Cardiovasc Res. 2002;55(3):561.

100. Yamashita N, Baxter GF, Yellon DM. Exercise directly enhances myocardial tolerance to ischaemia–reperfusion injury in the rat through a protein kinase C mediated mechanism. Heart. 2001;85(3):331.

101. Quindry JC, Schreiber L, Hosick P, Wrieden J, Irwin JM, Hoyt E. Mitochondrial KATP channel inhibition blunts arrhythmia protection in ischemic exercised hearts. Am. J. Physiol. Heart Circ. Physiol. 2010;299(1):175–83.

102. Tomai F. Warm up phenomenon and preconditioning in clinical practice. Heart. 2002;87(2):99.

103. Macalpin R, Kattus A. Adaptation to exercise in angina pectoris: the electrocardiogram during treatmill walking and coronary angiographic findings. Circulation. 1966;33(2):183–201.

104. Lambiase PD, Edwards RJ, Cusack MR, Bucknall CA, Redwood SR, Marber MS. Exercise-induced ischemia initiates the second window of protection in humans independent of collateral recruitment. J Am Coll Cardiol. 2003;41(7):1174–82.

105. Paraskevaidis IA, Iliodromitis EK, Mavrogeni S, Karavolias GK, Theodorakis GN, Georgiadis M, et al. Repeated exercise stress testing identifies early and late preconditioning. Int J Cardiol. 2005;98(2):221–6.

106. Wisløff U, Nilsen TIL, Drøyvold WB, Mørkved S, Slørdahl SA, Vatten LJ. A single weekly bout of exercise may reduce cardiovascular mortality: how little pain for cardiac gain? “The HUNT study, Norway.”Eur J Cardiovasc Prev Rehabil. 2006;13(5):798–804.

107. Gibala MJ, Little JP, MacDonald MJ, Hawley JA. Physiological adaptations to low-volume, high-intensity interval training in health and disease. J Physiol. 2012;590(5):1077–84.

108. Jia J, Hu YS, Wu Y, Liu G, Yu HX, Zheng QP, et al. Pre-ischemic treadmill training affects glutamate and gamma aminobutyric acid levels in the striatal dialysate of a rat model of cerebral ischemia. Life sciences. 2009;84(15-16):505–11.

109. Tyldum GA, Schjerve IE, Tjonna AE, Kirkeby-Garstad I, Stolen TO, Richardson RS, et al. Endothelial dysfunction induced by post-prandial lipemia: complete protection afforded by high-intensity aerobic interval exercise. J Am Coll Cardiol. 2009;53(2):200.

110. Loukogeorgakis SP, Panagiotidou AT, Yellon DM, Deanfield JE, MacAllister RJ. Postconditioning protects against endothelial ischemia-reperfusion injury in the human forearm. Circulation. 2006;113(7):1015–9.

111. Loukogeorgakis SP, Williams R, Panagiotidou AT, Kolvekar SK, Donald A, Cole TJ, et al. Transient limb ischemia induces remote preconditioning and remote postconditioning in humans by a KATP channel dependent mechanism. Circulation. 2007;116(12):1386.

112. Okorie MI, Bhavsar DD, Ridout D, Charakida M, Deanfield JE, Loukogeorgakis SP, et al. Postconditioning protects against human endothelial ischaemia-reperfusion injury via subtype-specific KATP channel activation and is mimicked by inhibition of the mitochondrial permeability transition pore. Eur Heart J. 2011;32(10):1266–74.

113. Gori T, Sicuro S, Dragoni S, Donati G, Forconi S, Parker JD. Sildenafil prevents endothelial dysfunction induced by ischemia and reperfusion via opening of adenosine triphosphate-sensitive potassium channels: a human in vivo study. Circulation. 2005;111(6):742–6.

114. Liuni A, Luca MC, Gori T, Parker JD. Rosuvastatin Prevents Conduit Artery Endothelial Dysfunction Induced by Ischemia and Reperfusion by a Cyclooxygenase-2-Dependent Mechanism. J Am Coll Cardiol. 2010;55(10):1002–6.

115. Andreani P, Hoti E, de la Serna S, Degli Esposti D, Sebagh M, Lemoine A, et al. Ischaemic preconditioning of the graft in adult living related right lobe liver transplantation: impact on ischaemia-reperfusion injury and clinical relevance. HPB (Oxford). 2010;12(7):439–46.

116. Lin L, Wang L, Wang W, Jin L, Zhao X, Zheng L, et al. Ischemic preconditioning attenuates pulmonary dysfunction after unilateral thigh tourniquet-induced ischemia-reperfusion. Anesth. Analg. 2010;111(2):539–43.

117. Gurusamy KS, Kumar Y, Pamecha V, Sharma D, Davidson BR. Ischaemic pre-conditioning for elective liver resections performed under vascular occlusion. Cochrane Database of Systematic Reviews. 2009.

118. Hausenloy DJ, Mwamure PK, Venugopal V, Harris J, Barnard M, Grundy E, et al. Effect of remote ischaemic preconditioning on myocardial injury in patients

undergoing coronary artery bypass graft surgery: a randomised controlled trial. Lancet. 2007;370(9587):575–9.

119. Ali ZA, Callaghan CJ, Lim E, Ali AA, Reza Nouraei SA, Akthar AM, et al. Remote Ischemic Preconditioning Reduces Myocardial and Renal Injury After Elective Abdominal Aortic Aneurysm Repair: A Randomized Controlled Trial. Circulation. 2007;116(11):98–105.

120. Er F, Nia AM, Dopp H, Hellmich M, Dahlem KM, Caglayan E, et al. Ischemic Preconditioning for Prevention of Contrast Medium-Induced Nephropathy: Randomized Pilot RenPro Trial (Renal Protection Trial). Circulation. 2012;126(3):296–303.

121. Desai M, Gurusamy KS, Ghanbari H, Hamilton G, Seifalian AM. Remote ischaemic preconditioning versus no remote ischaemic preconditioning for vascular and endovascular surgical procedures. Cochrane Database Syst Rev. 2011;(12):8472.

122. Saito T, Komiyama T, Aramoto H, Miyata T, Shigematsu H. Ischemic preconditioning improves oxygenation of exercising muscle in vivo. J Surg Res. 2004;120(1):111–8.

123. Attkiss KJ, Suski M, Hunt TK, Buncke HJ. Ischemic preconditioning of skeletal muscle improves tissue oxygenation during reperfusion. J Reconstr Microsurg. 1999;15(3):223–8.

124. Andreas M, Schmid AI, Keilani M, Doberer D, Bartko J, Crevenna R, et al. Effect of ischemic preconditioning in skeletal muscle measured by functional magnetic resonance imaging and spectroscopy: a randomized crossover trial. J Cardiovasc Magn Reson. 2011;13(1):32.

125. Takarada Y, Takazawa H, Sato Y, Takebayashi S, Tanaka Y, Ishii N. Effects of resistance exercise combined with moderate vascular occlusion on muscular function in humans. J. Appl. Physiol. 2000;88(6):2097–106.

126. Groot PCE, Thijssen DHJ, Sanchez M, Ellenkamp R, Hopman MTE. Ischemic preconditioning improves maximal performance in humans. Eur J Appl Physiol. 2009;108(1):141–6.

127. Crisafulli A, Tangianu F, Tocco F, Concu A, Mameli O, Mulliri G, et al. Ischemic preconditioning of the muscle improves maximal exercise performance but not maximal oxygen uptake in humans. J Appl Physiol. 2011;111(2):530–6.

128. Jean-St-Michel E, Manlhiot C, Li J, Tropak M, Michelsen MM, Schmidt MR, et al. Remote Preconditioning Improves Maximal Performance in Highly-Trained Athletes. Med Sci Sports Exerc. 2011;43(7):1280–6.

129. Clevidence MW, Mowery RE, Kushnick MR. The effects of ischemic preconditioning on aerobic and anaerobic variables associated with submaximal cycling performance. Eur J Appl Physiol. 2012;In Press.

130. NICE. NICE clinical guidelines. Stroke: Diagnosis and initial management of acute stroke and transient ischaemic attack (TIA). 2008.

131. Molina CA, Montaner J, Abilleira S, Arenillas JF, Ribó M, Huertas R, et al. Time course of tissue plasminogen activator-induced recanalization in acute cardioembolic stroke: a case-control study. Stroke. 2001;32(12):2821–7.

132. Bisschops RHC, Klijn CJM, Kappelle LJ, van Huffelen AC, van der Grond J. Collateral flow and ischemic brain lesions in patients with unilateral carotid artery occlusion. Neurology. 2003;60(9):1435–41.

133. Carmichael ST. Rodent models of focal stroke: size, mechanism, and purpose. NeuroRx. 2005;2(3):396–409.

134. Durukan A, Tatlisumak T. Acute ischemic stroke: overview of major experimental rodent models, pathophysiology, and therapy of focal cerebral ischemia. Pharmacol. Biochem. Behav. 2007;87(1):179–97.

135. Liu F, McCullough LD. Middle cerebral artery occlusion model in rodents: methods and potential pitfalls. J. Biomed. Biotechnol. 2012;In Press.

136. Koizumi J, Yoshida Y, Nakazawa T, Ooneda G. Experimental studies of ischemic brain edema. I. A new experimental model of cerebral embolism in which recirculation can introduced into the ischemic area. Jpn J Stroke. 1986;8(108).

137. Huttner HB, Schwab S. Malignant middle cerebral artery infarction: clinical characteristics, treatment strategies, and future perspectives. Lancet Neurol. 2009;8(10):949–58.

138. Lin T, He Y, Wu G, Khan M, Hsu C. Effect of brain edema on infarct volume in a focal cerebral ischemia model in rats. Stroke. 1993;24(1):117 –121.

139. Belayev L, Khoutorova L, Deisher TA, Belayev A, Busto R, Zhang Y, et al. Neuroprotective effect of SolCD39, a novel platelet aggregation inhibitor, on transient middle cerebral artery occlusion in rats. Stroke. 2003;34(3):758–63.

140. Yang G, Chan PH, Chen SF, Babuna OA, Simon RP, Weinstein PR. Reduction of vasogenic edema and infarction by MK-801 in rats after temporary focal cerebral ischemia. Neurosurgery. 1994;34(2):339–45.

141. Margaill I, Parmentier S, Callebert J, Allix M, Boulu RG, Plotkine M. Short therapeutic window for MK-801 in transient focal cerebral ischemia in normotensive rats. J. Cereb. Blood Flow Metab. 1996;16(1):107–13.

142. Ryang Y-M, Fahlenkamp AV, Rossaint R, Wesp D, Loetscher PD, Beyer C, et al. Neuroprotective effects of argon in an in vivo model of transient middle cerebral artery occlusion in rats. Crit. Care Med. 2011;39(6):1448–53.

143. Wu Y, Wang Y-P, Guo P, Ye X-H, Wang J, Yuan S-Y, et al. A Lipoxin A(4) Analog Ameliorates Blood-Brain Barrier Dysfunction and Reduces MMP-9 Expression in a Rat Model of Focal Cerebral Ischemia-Reperfusion Injury. J Mol Neurosci. 2012;46(3):483–91.

144. Dupont WD, Plummer WD Jr. Power and sample size calculations. A review and computer program. Control Clin Trials. 1990;11(2):116–28.

145. Halcox JPJ, Donald AE, Ellins E, Witte DR, Shipley MJ, Brunner EJ, et al. Endothelial function predicts progression of carotid intima-media thickness. Circulation. 2009;119(7):1005–12.

146. Gokce N, Keaney JF, Hunter LM, Watkins MT, Menzoian JO, Vita JA. Risk Stratification for Postoperative Cardiovascular Events Via Noninvasive Assessment of Endothelial Function A Prospective Study. Circulation. 2002;105(13):1567–72.

147. Gokce N, Keaney Jr JF, Hunter LM, Watkins MT, Nedeljkovic ZS, Menzoian JO, et al. Predictive value of noninvasivelydetermined endothelial dysfunction for long-term cardiovascular events inpatients with peripheral vascular disease. Journal of the American College of Cardiology. 2003;41(10):1769–75.

148. Petrie JR, Ueda S, Morris AD, Murray LS, Elliott HL, Connell JM. How reproducible is bilateral forearm plethysmography? Br J Clin Pharmacol. 1998;45(2):131–9.

149. Quyyumi AA, Dakak N, Diodati JG, Gilligan DM, Panza JA, Cannon III RO. Effect of l-Arginine on Human Coronary Endothelium-Dependent and Physiologic Vasodilation. J Am Coll Cardiol. 1997;30(5):1220–7.

150. Celermajer DS, Sorensen KE, Gooch VM, Spiegelhalter DJ, Miller OI, Sullivan ID, et al. Non-invasive detection of endothelial dysfunction in children and adults at risk of atherosclerosis. Lancet. 1992;340(8828):1111–5.

151. Kuvin JT, Patel AR, Sliney KA, Pandian NG, Sheffy J, Schnall RP, et al. Assessment of peripheral vascular endothelial function with finger arterial pulse wave amplitude. American Heart Journal. 2003;146(1):168–74.

152. Hansell J, Henareh L, Agewall S, Norman M. Non-invasive assessment of endothelial function - relation between vasodilatory responses in skin microcirculation and brachial artery. Clin Physiol Funct Imaging. 2004;24(6):317–22.

153. Naka KK, Tweddel AC, Doshi SN, Goodfellow J, Henderson AH. Flow-Mediated Changes in Pulse Wave Velocity: A New Clinical Measure of Endothelial Function. Eur Heart J. 2006;27(3):302–9.

154. Gori T, Dragoni S, Lisi M, Di Stolfo G, Sonnati S, Fineschi M, et al. Conduit Artery Constriction Mediated by Low Flow: A Novel Noninvasive Method for the Assessment of Vascular Function. J Am Coll Cardiol. 2008;51(20):1953–8.

155. Mullen MJ, Kharbanda RK, Cross J, Donald AE, Taylor M, Vallance P, et al. Heterogenous nature of flow-mediated dilatation in human conduit arteries in vivo: relevance to endothelial dysfunction in hypercholesterolemia. Circ. Res. 2001;88(2):145.

156. Bellien J, Iacob M, Gutierrez L, Isabelle M, Lahary A, Thuillez C, et al. Crucial role of NO and endothelium-derived hyperpolarizing factor in human sustained conduit artery flow-mediated dilatation. Hypertension. 2006;48(6):1088–94.

157. Corretti MC, Anderson TJ, Benjamin EJ, Celermajer D, Charbonneau F, Creager MA, et al. Guidelines for the ultrasound assessment of endothelial-dependent flow-mediated vasodilation of the brachial artery: A report of the International Brachial Artery Reactivity Task Force. J Am Coll Cardiol. 2002;39(2):257–65.

158. Korkmaz H, Onalan O. Evaluation of Endothelial Dysfunction: Flow-Mediated Dilation. Endothelium. 2008;15(4):157–63.

159. Thijssen DHJ, Black MA, Pyke KE, Padilla J, Atkinson G, Harris RA, et al. Assessment of flow-mediated dilation in humans: a methodological and physiological guideline. Am. J. Physiol. Heart Circ. Physiol. 2011;300(1):H2–12.

160. Simova I, Nossikoff A, Denchev S. Interobserver and intraobserver variability of flow-mediated vasodilatation of the brachial artery. Echocardiography. 2008;25(1):77–83.

161. Donald AE, Halcox JP, Charakida M, Storry C, Wallace SML, Cole TJ, et al. Methodological approaches to optimize reproducibility and power in clinical studies of flow-mediated dilation. J. Am. Coll. Cardiol. 2008;51(20):1959–64.

162. Anderson TJ, Charbonneau F, Title LM, Buithieu J, Rose MS, Conradson H, et al. Microvascular function predicts cardiovascular events in primary prevention: long-term results from the Firefighters and Their Endothelium (FATE) study. Circulation. 2011;123(2):163–9.

163. Fathi R, Haluska B, Isbel N, Short L, Marwick TH. The relative importance of vascular structure and function in predicting cardiovascular events. J. Am. Coll. Cardiol. 2004;43(4):616–23.

164. Caballero AE, Arora S, Saouaf R, Lim SC, Smakowski P, Park JY, et al. Microvascular and Macrovascular Reactivity Is Reduced in Subjects at Risk for Type 2 Diabetes. Diabetes. 1999;48(9):1856–62.

165. Charakida M, Masi S, Lüscher TF, Kastelein JJP, Deanfield JE. Assessment of atherosclerosis: the role of flow-mediated dilatation. Eur Heart J. 2010;31(23):2854–61.

166. Filitti V, Giral P, Simon A, Merli I, Del Pino M, Levenson J. Enhanced constriction of the peripheral large artery in response to acute induction of a low-flow state in human hypercholesterolemia. Arterioscler. Thromb. 1991;11(1):161–6.

167. Spieker LE, Lüscher TF, Noll G. ETA receptors mediate vasoconstriction of large conduit arteries during reduced flow in humans. J. Cardiovasc. Pharmacol. 2003;42(3):315–8.

168. Spiro JR, Digby JE, Ghimire G, Mason M, Mitchell AG, Ilsley C, et al. Brachial artery low-flow-mediated constriction is increased early after coronary

intervention and reduces during recovery after acute coronary syndrome: characterization of a recently described index of vascular function. Eur Heart J. 2011;32(7):856–66.

169. Weissgerber TL, Davies GAL, Tschakovsky ME. Low flow-mediated constriction occurs in the radial but not the brachial artery in healthy pregnant and nonpregnant women. J. Appl. Physiol. 2010;108(5):1097–105.

170. Hashimoto M, Akishita M, Eto M, Ishikawa M, Kozaki K, Toba K, et al. Modulation of endothelium-dependent flow-mediated dilatation of the brachial artery by sex and menstrual cycle. Circulation. 1995;92(12):3431–5.

171. Kenney RT, Rangdaeng S, Scollard DM. Skin blister immunocytology. A new method to quantify cellular kinetics in vivo. J. Immunol. Methods. 1987;97(1):101–10.

172. Michel O, Nagy AM, Schroeven M, Duchateau J, Nève J, Fondu P, et al. Dose-response relationship to inhaled endotoxin in normal subjects. Am. J. Respir. Crit. Care Med. 1997;156(4):1157–64.

173. Maglio D, Nightingale CH, Nicolau DP. Production and resolution of cantharidin-induced inflammatory blisters. Int. J. Antimicrob. Agents. 2003;22(1):77–80.

174. Morris T, Stables M, Colville-Nash P, Newson J, Bellingan G, de Souza PM, et al. Dichotomy in duration and severity of acute inflammatory responses in humans arising from differentially expressed proresolution pathways. Proc. Natl. Acad. Sci. U.S.A. 2010;107(19):8842–7.

175. Silverberg NB, Sidbury R, Mancini AJ. Childhood molluscum contagiosum: experience with cantharidin therapy in 300 patients. J. Am. Acad. Dermatol. 2000;43(3):503–7.

176. Moed L, Shwayder TA, Chang MW. Cantharidin revisited: a blistering defense of an ancient medicine. Arch Dermatol. 2001;137(10):1357–60.

177. Karras DJ, Farrell SE, Harrigan RA, Henretig FM, Gealt L. Poisoning from “Spanish fly” (cantharidin). Am J Emerg Med. 1996;14(5):478–83.

178. Kaçar N, Taşlı L, Korkmaz S, Ergin Ş, Erdoğan BŞ. Cantharidin–podophylotoxin–salicylic acid versus cryotherapy in the treatment of plantar warts: a randomized prospective study. J Eur Acad Dermatol Venereol. 2012;26(7):889–93.

179. Wong J, Phelps R, Levitt J. Treatment of Acquired Perforating Dermatosis With Cantharidin. Arch Dermatol. 2012;148(2):160–2.

180. Piérard-Franchimont C, Piérard GE. Cantharidin-induced acantholysis. Am J Dermatopathol. 1988;10(5):419–23.

181. Morris T, Stables M, Hobbs A, de Souza P, Colville-Nash P, Warner T, et al. Effects of low-dose aspirin on acute inflammatory responses in humans. J. Immunol. 2009;183(3):2089–96.

182. Jenner WJ, Gilroy DW. Assessment of Leukocyte Trafficking in Humans Using the Cantharidin Blister Model. J R Soc Med Cardiovasc Dis. 2012;1(1):1–5.

183. Hristov M, Schmitz S, Nauwelaers F, Weber C. A flow cytometric protocol for enumeration of endothelial progenitor cells and monocyte subsets in human blood. J. Immunol. Methods. 2012;381(1-2):9–13.

184. Dilaimy M. Letter: Lymphangitis caused by cantharidin. Arch Dermatol. 1975;111(8):1073.

185. Stazzone AM, Borgs P, Witte CL, Witte MH. Lymphangitis and Refractory Lymphedema After Treatment With Topical Cantharidin. Arch Dermatol. 1998;134(1):104–6.

186. Bailey SJ, Winyard P, Vanhatalo A, Blackwell JR, Dimenna FJ, Wilkerson DP, et al. Dietary nitrate supplementation reduces the O2 cost of low-intensity exercise and enhances tolerance to high-intensity exercise in humans. J. Appl. Physiol. 2009;107(4):1144–55.

187. Sale C, Saunders B, Hudson S, Wise JA, Harris RC, Sunderland CD. Effect of β-Alanine plus Sodium Bicarbonate on High-Intensity Cycling Capacity. Med Sci Sports Exerc. 2011;43(10):1972–8.

188. Larsen FJ, Weitzberg E, Lundberg JO, Ekblom B. Dietary nitrate reduces maximal oxygen consumption while maintaining work performance in maximal exercise. Free Radic. Biol. Med. 2010;48(2):342–7.

189. Medicine AC of S. ACSM's Guidelines for Exercise Testing and Prescription. Franklin BA, editor. Lippincott Williams & Wilkins; 2000.

190. Jackson A, Pollock M. Practical assessment of body composition. Physician Sport Med. 1985;13:76–90.

191. Grassi B, Pogliaghi S, Rampichini S, Quaresima V, Ferrari M, Marconi C, et al. Muscle oxygenation and pulmonary gas exchange kinetics during cycling exercise on-transitions in humans. J. Appl. Physiol. 2003;95(1):149–58.

192. Horecker BL. The Absorption Spectra of Hemoglobin and Its Derivatives in the Visible and Near Infra-Red Regions. J. Biol. Chem. 1943;148(1):173–83.

193. Chance B, Wang NG, Maris M, Nioka S, Sevick E. Quantitation of tissue optical characteristics and hemoglobin desaturation by time- and frequency-resolved multi-wavelength spectrophotometry. Adv. Exp. Med. Biol. 1992;317:297–304.

194. Smith KJ, Billaut F. Influence of cerebral and muscle oxygenation on repeated-sprint ability. Eur. J. Appl. Physiol. 2010;109(5):989–99.

195. Hesford CM, Laing SJ, Cardinale M, Cooper CE. Asymmetry of quadriceps muscle oxygenation during elite short-track speed skating. Med Sci Sports Exerc. 2012;44(3):501–8.

196. Vogiatzis I, Tzineris D, Athanasopoulos D, Georgiadou O, Geladas N. Quadriceps oxygenation during isometric exercise in sailing. Int J Sports Med. 2008;29(1):11–5.

197. Rao R, Danduran M, Loomba R, Dixon J, Hoffman G. Near-Infrared Spectroscopic Monitoring During Cardiopulmonary Exercise Testing Detects Anaerobic Threshold. Pediatr Cardiol. 2012;33(5):791–6.

198. Myers DE, Anderson LD, Seifert RP, Ortner JP, Cooper CE, Beilman GJ, et al. Noninvasive method for measuring local hemoglobin oxygen saturation in tissue using wide gap second derivative near-infrared spectroscopy. J Biomed Opt. 2005;10(3):034017–034017–18.

199. Myers D, McGraw M, George M, Mulier K, Beilman G. Tissue hemoglobin index: a non-invasive optical measure of total tissue hemoglobin. Crit Care. 2009;13 Suppl 5:S2.

200. McLaughlin JE, King GA, Howley ET, Bassett DR Jr, Ainsworth BE. Validation of the COSMED K4 b2 portable metabolic system. Int J Sports Med. 2001;22(4):280–4.

201. Robertson RJ, Goss FL, Boer NF, Peoples JA, Foreman AJ, Dabayebeh IM, et al. Children's OMNI scale of perceived exertion: mixed gender and race validation. Med Sci Sports Exerc. 2000;32(2):452–8.

202. Pyne DB, Boston T, Martin DT, Logan A. Evaluation of the Lactate Pro blood lactate analyser. Eur J Appl Physiol. 2000;82(1):112–6.

203. Baldari C, Bonavolontà V, Emerenziani GP, Gallotta MC, Silva AJ, Guidetti L. Accuracy, reliability, linearity of Accutrend and Lactate Pro versus EBIO plus analyzer. Eur J Appl Physiol. 2009;107(1):105–11.

204. Abbott Laboratories. Cartridge and Test Information Sheets, www.abbottpointofcare.com. 2011.

205. Jung T, Korotzer B, Stringer W, Jones A, Wasserman K. Lactate concentration increase and transcellular fluid flux during exercise. Am. J. Respir. Crit. Care Med. 1996;153:A647.

206. von Schenck H, Falkensson M, Lundberg B. Evaluation of "HemoCue," a new device for determining hemoglobin. Clin. Chem. 1986;32(3):526–9.

207. Morris LD, Pont A, Lewis SM. Use of a new HemoCue system for measuring haemoglobin at low concentrations. Clin Lab Haematol. 2001;23(2):91–6.

208. British Heart Foundation. Stroke Statistics. 2009.

209. Wardlaw JM, Murray V, Berge E, del Zoppo G, Sandercock P, Lindley RL, et al. Recombinant tissue plasminogen activator for acute ischaemic stroke: an updated systematic review and meta-analysis. Lancet. 2012;379(9834):2364–72.

210. Ren C, Gao X, Steinberg GK, Zhao H. Limb remote-preconditioning protects against focal ischemia in rats and contradicts the dogma of therapeutic time windows for preconditioning. Neuroscience. 2008;151(4):1099–103.

211. Oliff HS, Weber E, Miyazaki B, Marek P. Infarct volume varies with rat strain and vendor in focal cerebral ischemia induced by transcranial middle cerebral artery occlusion. Brain Res. 1995;699(2):329–31.

212. Hahn CD, Manlhiot C, Schmidt MR, Nielsen TT, Redington AN. Remote Ischemic Per-Conditioning: A Novel Therapy for Acute Stroke? Stroke. 2011;42(10):2960–2.

213. Hu S, Dong H, Zhang H, Wang S, Hou L, Chen S, et al. Noninvasive limb remote ischemic preconditioning contributes neuroprotective effects via activation of adenosine A1 receptor and redox status after transient focal cerebral ischemia in rats. Brain Research. 2012;In Press.

214. Rentoukas I, Giannopoulos G, Kaoukis A, Kossyvakis C, Raisakis K, Driva M, et al. Cardioprotective Role of Remote Ischemic Periconditioning in Primary Percutaneous Coronary Intervention: Enhancement by Opioid Action. JACC Interventions. 2010;3(1):49.

215. Wei D, Ren C, Chen X, Zhao H. The chronic protective effects of limb remote preconditioning and the underlying mechanisms involved in inflammatory factors in rat stroke. PLoS ONE. 2012;7(2):e30892.

216. Ren C, Yan Z, Wei D, Gao X, Chen X, Zhao H. Limb remote ischemic postconditioning protects against focal ischemia in rats. Brain Res. 2009;1288:88–94.

217. Hougaard KD, Hjort N, Zeidler D, Sørensen L, Nørgaard A, Thomsen RB, et al. Remote ischemic perconditioning in thrombolysed stroke patients: Randomized study of activating endogenous neuroprotection - design and MRI measurements. Int J Stroke. 2012;In Press.

218. Botker HE, Kharbanda R, Schmidt MR, B\ottcher M, Kaltoft AK, Terkelsen CJ, et al. Remote ischaemic conditioning before hospital admission, as a complement to angioplasty, and effect on myocardial salvage in patients with acute myocardial infarction: a randomised trial. Lancet. 2010;375(9716):727–34.

219. De Roos NM, Bots ML, Schouten EG, Katan MB. Within-subject variability of flow-mediated vasodilation of the brachial artery in healthy men and women: implications for experimental studies. Ultrasound Med Biol. 2003;29(3):401–6.

220. Dragoni S, Gori T, Lisi M, Di Stolfo G, Pautz A, Kleinert H, et al. Pentaerythrityl tetranitrate and nitroglycerin, but not isosorbide mononitrate, prevent endothelial dysfunction induced by ischemia and reperfusion. Arterioscler. Thromb. Vasc. Biol. 2007;27(9):1955–9.

221. Brook R, Grau M, Kehrer C, Dellegrottaglie S, Khan B, Rajagopalan S. Intrasubject variability of radial artery flow-mediated dilatation in healthy subjects

and implications for use in prospective clinical trials. Am. J. Cardiol. 2005;96(9):1345–8.

222. Hijmering M. Variability of flow mediated dilation: consequences for clinical application. Atherosclerosis. 2001;157(2):369–73.

223. Gori T, Grotti S, Dragoni S, Lisi M, Di Stolfo G, Sonnati S, et al. Assessment of vascular function: flow-mediated constriction complements the information of flow-mediated dilatation. Heart. 2010;96(2):141 –147.

224. Harrison M, Parkhurst K, Tarumi T, Lin H-F, Tanaka H. Low flow-mediated constriction: prevalence, impact and physiological determinant. Clin Physiol Funct Imaging. 2011;31(5):394–8.

225. Roussel M, Davis BH, Fest T, Wood BL. Toward a reference method for leukocyte differential counts in blood: Comparison of three flow cytometric candidate methods. Cytometry A. 2012;In Press.

226. Ziegler-Heitbrock L, Ancuta P, Crowe S, Dalod M, Grau V, Hart DN, et al. Nomenclature of monocytes and dendritic cells in blood. Blood. 2010;116(16):e74–80.

227. Abeles RD, McPhail MJ, Sowter D, Antoniades CG, Vergis N, Vijay GKM, et al. CD14, CD16 and HLA-DR reliably identifies human monocytes and their subsets in the context of pathologically reduced HLA-DR expression by CD14(hi) /CD16(neg) monocytes: Expansion of CD14(hi) /CD16(pos) and contraction of CD14(lo) /CD16(pos) monocytes in acute liver failure. Cytometry A. 2012;In Press.

228. Sant A. Endogenous antigen presentation by MHC class II molecules. Immunol Res. 1994;13(4):253–67.

229. Nagaraj S, Gabrilovich DI. Myeloid-derived suppressor cells in human cancer. Cancer J. 2010;16(4):348–53.

230. Makarenkova VP, Bansal V, Matta BM, Perez LA, Ochoa JB. CD11b+/Gr-1+ myeloid suppressor cells cause T cell dysfunction after traumatic stress. J. Immunol. 2006;176(4):2085–94.

231. Filipazzi P, Valenti R, Huber V, Pilla L, Canese P, Iero M, et al. Identification of a new subset of myeloid suppressor cells in peripheral blood of melanoma patients with modulation by a granulocyte-macrophage colony-stimulation factor-based antitumor vaccine. J. Clin. Oncol. 2007;25(18):2546–53.

232. Vuk-Pavlović S, Bulur PA, Lin Y, Qin R, Szumlanski CL, Zhao X, et al. Immunosuppressive CD14+HLA-DRlow/- monocytes in prostate cancer. Prostate. 2010;70(4):443–55.

233. Greten TF, Manns MP, Korangy F. Myeloid derived suppressor cells in human diseases. Int. Immunopharmacol. 2011;11(7):802–7.

234. Cuenca AG, Delano MJ, Kelly-Scumpia KM, Moreno C, Scumpia PO, Laface DM, et al. A paradoxical role for myeloid-derived suppressor cells in sepsis and trauma. Mol. Med. 2011;17(3-4):281–92.

235. Dinh PHD, Corraza F, Mestdagh K, Kassengera Z, Doyen V, Michel O. Validation of the cantharidin-induced skin blister as an in vivo model of inflammation. Br J Clin Pharmacol. 2011;72(6):912–20.

236. Evans BJ, Haskard DO, Finch JR, Hambleton IR, Landis RC, Taylor KM. The inflammatory effect of cardiopulmonary bypass on leukocyte extravasation in vivo. J. Thorac. Cardiovasc. Surg. 2008;135(5):999–1006.

237. Thiele H, Hildebrand L, Schirdewahn C, Eitel I, Adams V, Fuernau G, et al. Impact of High-Dose N-Acetylcysteine Versus Placebo on Contrast-Induced Nephropathy and Myocardial Reperfusion Injury in Unselected Patients With ST-Segment Elevation Myocardial Infarction Undergoing Primary Percutaneous Coronary Intervention:: The LIPSIA-N-ACC (Prospective, Single-Blind, Placebo-Controlled, Randomized Leipzig Immediate PercutaneouS Coronary Intervention Acute Myocardial Infarction N-ACC) Trial. Journal of the American College of Cardiology. 2010;55(20):2201–9.

238. Ludman AJ, Yellon DM, Hasleton J, Ariti C, Babu GG, Boston-Griffiths E, et al. Effect of erythropoietin as an adjunct to primary percutaneous coronary intervention: a randomised controlled clinical trial. Heart. 2011;97(19):1560–5.

239. Karuppasamy P, Chaubey S, Dew T, Musto R, Sherwood R, Desai J, et al. Remote intermittent ischemia before coronary artery bypass graft surgery: a strategy to reduce injury and inflammation? Basic Res. Cardiol. 2011;106(4):511–9.

240. Memtsoudis SG, Valle AGD, Jules-Elysse K, Poultsides L, Reid S, Starcher B, et al. Perioperative inflammatory response in total knee arthroplasty patients: impact of limb preconditioning. Reg Anesth Pain Med. 2010;35(5):412–6.

241. Kevin LG, Camara AKS, Riess ML, Novalija E, Stowe DF. Ischemic preconditioning alters real-time measure of O2 radicals in intact hearts with ischemia and reperfusion. Am. J. Physiol. Heart Circ. Physiol. 2003;284(2):H566–574.

242. Baran KW, Nguyen M, McKendall GR, Lambrew CT, Dykstra G, Palmeri ST, et al. Double-blind, randomized trial of an anti-CD18 antibody in conjunction with recombinant tissue plasminogen activator for acute myocardial infarction: limitation of myocardial infarction following thrombolysis in acute myocardial infarction (LIMIT AMI) study. Circulation. 2001;104(23):2778–83.

243. Jówko E, Sacharuk J, Balasińska B, Ostaszewski P, Charmas M, Charmas R. Green tea extract supplementation gives protection against exercise-induced oxidative damage in healthy men. Nutr Res. 2011;31(11):813–21.

244. Mattei A, Sutter PM, Marx A, Stierli P, Heberer M, Gürke L. Preconditioning with short cycles improves ischemic tolerance in rat fast- and slow-twitch skeletal muscle. Eur Surg Res. 2000;32(5):297–304.

245. Catellier DJ, Hannan PJ, Murray DM, Addy CL, Conway TL, Yang S, et al. Imputation of missing data when measuring physical activity by accelerometry. Med Sci Sports Exerc. 2005;37(11 Suppl):S555–562.

246. Martou G, O'Blenes CA, Huang N, McAllister SE, Neligan PC, Ashrafpour H, et al. Development of an in vitro model for study of the efficacy of ischemic preconditioning in human skeletal muscle against ischemia-reperfusion injury. J. Appl. Physiol. 2006;101(5):1335–42.

247. McCully KK, Halber C, Posner JD. Exercise-induced changes in oxygen saturation in the calf muscles of elderly subjects with peripheral vascular disease. J Gerontol. 1994;49(3):B128–134.

248. Jacobs RA, Rasmussen P, Siebenmann C, Díaz V, Gassmann M, Pesta D, et al. Determinants of time trial performance and maximal incremental exercise in highly trained endurance athletes. J. Appl. Physiol. 2011;111(5):1422–30.

249. Jensen HA, Loukogeorgakis S, Yannopoulos F, Rimpiläinen E, Petzold A, Tuominen H, et al. Remote Ischemic Preconditioning Protects the Brain Against Injury After Hypothermic Circulatory Arrest. Circulation. 2011;123(7):714–21.

250. Koch S, Katsnelson M, Dong C, Perez-Pinzon M. Remote Ischemic Limb Preconditioning After Subarachnoid Hemorrhage: A Phase Ib Study of Safety and Feasibility. Stroke. 2011;42(5):1387–91.

251. Hausenloy DJ, Candilio L, Laing C, Kunst G, Pepper J, Kolvekar S, et al. Effect of remote ischemic preconditioning on clinical outcomes in patients undergoing coronary artery bypass graft surgery (ERICCA): rationale and study design of a multi-centre randomized double-blinded controlled clinical trial. Clin Res Cardiol. 2012;101(5):339–48.